Applications of Layer-by-Layer (LbL) films in Electrochromic Devices and Bending Actuators

Vaibhav Jain

Dissertation submitted to the Faculty of the Virginia Polytechnic Institute and State University in partial fulfillment of the requirements for the degree of

Doctor of Philosophy
In
Macromolecular Science and Engineering

Dr James R. Heflin
(Committee Chairman)
Dr Victoria Soghomonian
Dr Richey M. Davis
Dr Harry W. Gibson

September 2, 2009
Blacksburg, VA 24060

Keywords: Layer-by-Layer (LbL), Electrochromic (EC), Switching speed, Polyviologen, PEDOT, actuators, Ionic Polymer Metal Composite (IPMC)

Abstract

Applications of Layer-by-Layer (LbL) films in Electrochromic Devices and Bending Actuators
Vaibhav Jain

This thesis presents work done to improve the switching speed and contrast performance of electrochromic devices. Layer-by-Layer (LbL) assembly was used to deposit thin films of electrochromic materials ranging from organic, inorganic, conducting polymers, etc. The focus was on developing new materials with high contrast and long lifecycles. A detailed switching-speed study of solid-state EC devices of already-developed materials (PEDOT (Poly(3,4-ethylenedioxythiophene)), polyviologen, inorganic) and some new materials (Prodot-Sultone) was performed to achieve the optimum thickness and number of bilayers in LbL films resulting in high-contrast and fast switching. Device sizes were varied for comparison of the performance of the lab-made prototype device with the commercially available "small pixel" size displays. Symmetrical EC devices were fabricated and tested whenever conducting polymers were used as an EC material. This symmetrical configuration utilized conducting polymers as an electroactive layer on each of two ITO-coated substrates; potential was applied to the two layers of similar conducting polymers and the device changed color from one redox state to another. This method, along with LbL film assembly,were the main factors in the improvement of switching speed results over already-published work in the literature. PEDOT results showed that EC devices fabricated by LbL assembly with a switching speed of less than 30 ms make EC flat-panel displays possible by adjusting film thickness, device size, and type of material. The high contrast value (84%) for RuP suggests that its LbL films can be used for low-power consumption displays where contrast, not fastest switching, is of prime importance.

In addition to the electrochromic work, this thesis also includes a section on the application of LbL assembly in fabricating electromechanical bending actuators. For bending actuators based on ionic polymer metal composites (IPMCs), a new class of conductive network composite (CNC) electrodes was investigated, based on LbL self-assembled multilayers of conductive gold (Au) nanoparticles. The CNC of an electromechanical actuator fabricated with 100 bilayers of poly(allylamine hydrochloride) (PAH)/Au NPs exhibited a high strain value of 6.8% with an actuation speed of 0.18 seconds for a 26 μm thick IPMC with 0.4 μm thick LbL CNCs under 4 volts.

This Thesis is devoted to my later father S. P. Jain, my mother Usha Jain & my wife Deirdre Jain

Acknowledgements

I would like to express my sincere gratitude and appreciation to my advisor, Dr. Randy Heflin, for supporting me all the way through the PhD. He provided me the freedom to work, which brought out the best in me. It was his constant belief in my ideas that made it possible to for me to grow and think scientifically.

Thanks also to my committee members: Dr. Victoria Soghomonian, Dr. Richey M. Davis, and Dr. Harry Gibson for their generous motivation and encouragement.

I would also like to thank my family, especially my mother, Usha Jain, and my sisters, Archana, Prachi, and Ruchi Jain. They have been my constant support and cheerleading section from back home in India. They were always confident that I'd go far, and I hope that I can continue to make them proud.

This wouldn't have been possible without the help of my soul mate, Deirdre, as she is always there to help me with everything whether it is stress in academia or personal life. She has been a constant source of encouragement and I would like to thank her from the bottom of my heart for being a true companion.

I am appreciative to many of my group members: Reza Montazami, Dong Wang, Manpreet Kaur, Cemil Durak, and Akhilesh Garg, without whose efforts in film fabrication and characterization this research would not have been possible. Steve McCartney also deserves special mention as he taught me several tricks in imaging, analysis and sample preparation for SEM, TEM and AFM.

I would like to thank Dr Rabindra Sahoo, IIT Mumbai for his help in making me a better electrochemist and for being there to answer my questions.

Thanks also go to Dr. Hank Yochum, from Sweet Briar College, who was a valuable research partner while he was on sabbatical at Virginia Tech. His advice and ideas were important in moving forward some parts of my research.

Thanks to my buddies, Sayan Naha, Ashok Sinha, and Jason Ridley for providing much-needed stress relief and fun.

Special thanks go to my collaborators, including Prof. Anil Kumar (IIT Mumbai), Prof Ken Shea UC- Irvine), Dr Liangbing Hu (UCLA), Prof Qiming Zhang (Penn State), Sheng Liu (Penn State).

I would like to acknowledge the support of National Science Foundation Grant CTS-0610213, U.S. Army Research Office Grant - W911NF-07-1-0452 Ionic Liquids in Electro-Active Devices (ILEAD) MURI and Macromolecular Interface Institute (MII) for travel grants and research fellowship for Spring 2006.

Table of Contents

List of Figures:

CHAPTER ONE

CHAPTER TWO

CHAPTER THREE

CHAPTER FOUR

CHAPTER FIVE

CHAPTER SIX

CHAPTER SEVEN

List of Tables:

Chapter 1

Motivation and Outline

This thesis presents work on a number of different applications of self-assembled nanoscale films. The overarching goal is to make use of the ability to fabricate exceptionally thin films with finely tuned composition and properties to improve the performance parameters in potential device applications. Two of the application areas investigated here (electrochromics (EC) and electromechanical actuators) require mass transport of ions through the films, which can be optimized through nanoscale control of the thickness and composition. The primary project of the thesis is to improve the switching speed and contrast performance of electrochromic devices. Layer-by-Layer (LbL) assembly has been used to deposit thin electrochromic films of various materials ranging from organic, inorganic, conducting polymers, etc. Electrochromic devices were developed as long ago as the nineteenth century, but it has only been in the last two decades that their study has gained significant growth. A primary focus of this thesis is on the development of new materials that have high contrast and long lifecycles. However, the development of fast-switching solid-state electrochromic devices still needs significant attention. A detailed switching-speed study of the solid-state EC devices of already-developed (PEDOT (poly(3,4-ethylenedioxythiophene)), polyviologen, inorganic materials) and some new materials (Prodot-Sultone) has been performed. Work was done to achieve the optimum thickness of the number of bilayers of the LbL films that results in high-contrast and fast switching. Device sizes were varied to bring the realization and comparison of the performance of the lab-made prototype device with the commercially available “small pixel” size display devices.

In addition to the electrochromic work, this thesis also includes sections on the application of LbL assembly for fabricating bending actuators. This work is a unique, new area of research that is enabled by nanoscale thin films fabricated by LbL. In the work on bending actuators, a new class of conductive composite network (CNC) electrodes was investigated, which is based on LbL self-assembled conductive gold nanoparticle composites, which achieve very high strain.

1.1 Motivation

The last three decades have seen exponential growth of the use of LCDs in the display market. LCDs, which are used in thin, flat panels used for displaying information, moving images and pictures have completely taken over the display market from CRTs (Cathode Ray Tube), which was the display industry leader merely a decade back. According to some sources, in 2008, LCD displays currently had about 50% of the overall market share of all kinds of displays.[1] Thin and lightweight LCDs have several definite advantages over CRTs such as low power consumption, higher contrast, and quicker response, among others. However, they have several drawbacks: LCDs have lower contrast ratios when displaying black, which results in blacks that look grey or bluish.[2] The limited viewing angle in LCDs is another major problem, the solution to which industry and scientists still have not discovered. LCDs consist of liquid crystals and their inability to be used in flexible displays or paper technology is hindering their growth and applications for future technologies. In contrast to this, EC displays should not have any issues with the viewing angle for laptops, TVs, computers etc. Hence, there is a need to find an alternative to LCDs for next generation flat-panel display devices, and EC displays are a very good candidate for this.

Recent work at Ntera Inc. has shown that their Nanochromic Displays need low driving voltage (-1.3 V) to switch and exhibit a high contrast ratio along with excellent readability that is independent of the viewing angle. Scientists at Ntera have further improved their approach and demonstrated that multi-color displays (Figure 1.1) can be possible by selective patterning of different electrochromophores onto different areas of conductive working electrodes.[3] Another important aspect of flat-panel displays that should be noted here is that for any display to be used for the application of moving images, it should be able to switch at least 24 frames/s, i.e. a maximum switching time of 40 ms or lower. This has not been possible through the displays and work presented by Ntera Inc. in several patents and exhibitions, and there is therefore a need to look for an alternate approach to EC devices than that adopted by Ntera.

Figure 1.1 Nanochromics displays.

There are a few examples in the literature of attempts to fabricate fast-switching EC displays. Schoot et al. were the first to start working on this technology and developed a solution-phase hexylviologen device in the early 70s.[4] A much more sophisticated device based on the concept was developed by IBM in the mid 1980s, which features an array of 96,000 micron-scale devices integrated as a dynamic flat-panel display.[5]

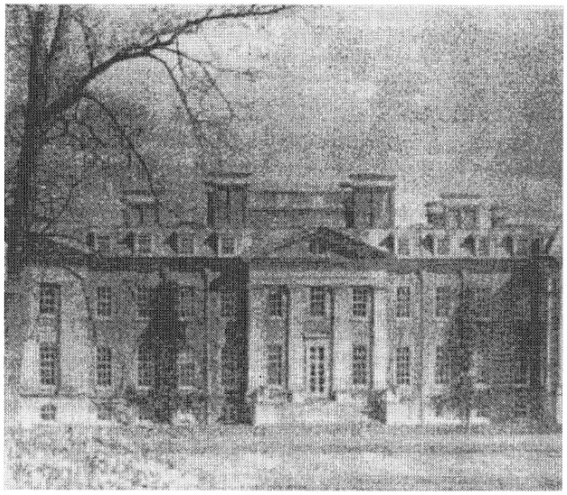

Figure 1.2 Reproduction of an IBM electrochromic image display on a 64 x 64 pixel integrated ECD device with eight levels of 'grey tone' of heptyl viologen.

Although work on adopting electrochromic devices in displays has been going on for the last 30 years, durability (long-term life cycle) and low switching speed issues have kept the industry from focusing on displays based on EC devices. The research group of Dr. Sang Bok Lee at the University of Maryland has shown some interesting findings in the field of fast-switching EC displays.[6,7,8,9] The synthesis of PEDOT nanotubes through a porous alumina template (Figure 1.3) in between two electrodes (usually gold) resulted in displays with a switching time of less than 20 ms (Figure 1.4) for both coloration and decoloration. The approach was interesting, but the process was limited to only a few types (reductive) of conductive polymers with the requirement of an expensive conductive substrate such as gold. In addition, it is very difficult to adapt this method for industrial applications due to the cumbersome approach, cost, minimal adaptability, use of liquid electrolyte at all times etc. But this has provided the motivation to work towards an approach to achieve fast-switching time for EC devices while still maintaining other necessary features like high contrast, compatibility, long-term life cycle etc.

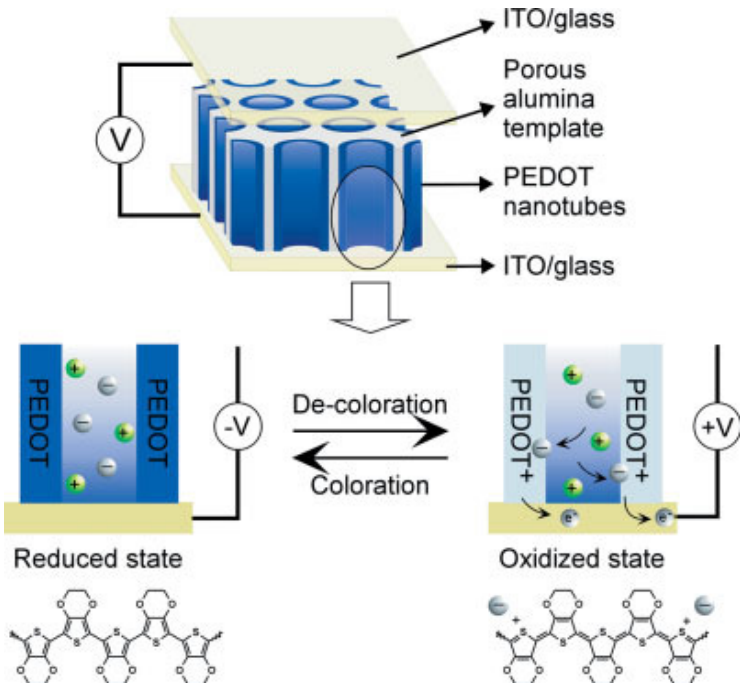

Figure 1.3 Schematic representation of the ultrafast electrochromic device based on PEDOT nanotube arrays. Counter-anion (negatively charged gray balls) diffuse into the thin layer of the PEDOT nanotube wall when PEDOT nanotubes are oxidized by applying positive potential on the ITO glass electrode. The color of PEDOT changes from a deep blue to a transparent pale blue. [S. I. Cho , W. J. Kwon , S.-J. Choi , P. Kim , S.-A. Park , J. Kim [2], S. J. Son , R. Xiao , S.-H.

Kim , S. B. Lee, Nanotube-Based Ultrafast Electrochromic Display, Advanced Materials 2005, 2, 171-175. Copyright Wiley-VCH Verlag GmbH & Co. KGaA. Reproduced with permission].[7]

To achieve the goal of creating a fast-switching EC device, it is quite important to deposit thin-films in which nanoscale control of thickness is possible. Major approaches to thin-film deposition include Langmuir-Blodgett, spin coating, Layer-by-Layer (LbL), sputtering, sol-gel etc. Out of these, sputtering is not an option as it is quite difficult to deposit a compound or organic material powder with it. Spin coating provides relatively uneven film thickness with high surface roughness, which is unacceptable if fast-charge transfer between the two electrodes is required. LbL is an excellent choice because it provides flexibility in choosing the material components and number of bilayers, while still maintaining nanoscale control of the thickness. One of the important advantages of the LbL film assembly is that it is very easy to use without

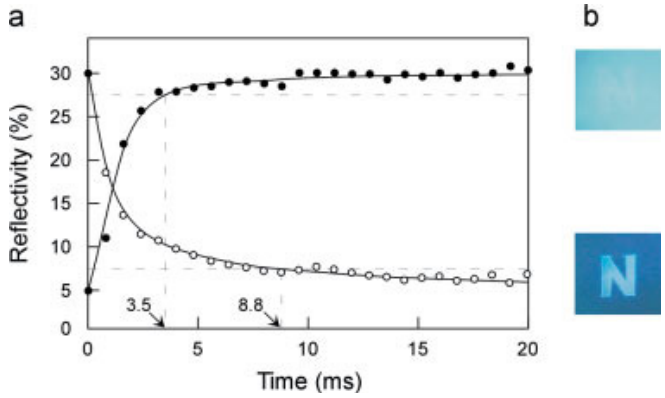

Figure 1.4 Plots of reflectivity of electrochromic window (1cm^2) monitored at 530 nm for coloration (open circles) and de-coloration (solid circles) upon potential switching between -1.0 V to +1.0 V, respectively. (b) Patterned letter 'N'on the PEDOT nanotube arrayed film. The alternate square potentials between -1.0V (lower images) and 1.0V (upper image) were applied on the background area after 1.0V was applied to letter 'N' (de-colored state). [S. I. Cho , W. J. Kwon , S.-J. Choi, P. Kim , S.-A. Park, J. Kim, S. J. Son, R. Xiao, S.-H. Kim, S. B. Lee, Nanotube-Based Ultrafast Electrochromic Display, Advanced Materials 2005, 2, 171-175. Copyright Wiley-VCH Verlag GmbH & Co. KGaA. Reproduced with permission].[7]

the need of any kind of expensive or special apparatus. The combination of various electrochromic materials that could be either water-soluble or dispersed materials, such as

polymers or nanoparticles, has made LbL assembly a strong candidate for thin-film EC devices. Other techniques, such as the Langmuir-Blodgett (LB)[10,11] and sol-gel processing[12,13] methods of fabrication have also been used in depositing EC films. Of these, LB has not gained much attention because of the difficulty in forming highly oriented, thin, homogeneous and robust films. The main advantage of adopting the LbL technique over LB multilayers is that the electroactivity decreases quickly as the number of layers is increased, disappearing after three to four layers in the case of LB films, whereas the films deposited by the LbL method remain highly electroactive even after deposition of 80 layers.[12] However, the sol-gel process of fabrication has gained some attention because of its better compatibility for commercial production. But it is primarily useful for depositing thick films on a large area since the deposition of thin films requires smooth and homogenous coverage, which is not possible with this technique.

Use of LbL for depositing films for EC devices have been exploited by the research group of Prof Hammond at MIT.[14,15,16,17,18,19] The focus of that research was more towards proving applicability of this technique for EC devices, rather than fabricating fast-switching EC devices. Prof Hammond's group was heavily focused on fabricating unsymmetrical EC devices, which is not the best way to fabricate fast EC devices due to mismatching oxidation and reduction potential of materials on two electrodes. In our research, symmetrical EC devices were fabricated and tested whenever conducting polymers were used as EC materials. This symmetrical configuration utilizes conducting polymers as an electroactive layer on each of the two ITO-coated substrates and the potential is applied to the two layers of similar conducting polymers and the device changes color from one redox state to another. The change in color occurs because of the change in redox state of only one of the conducting polymer layers, while the other layer remains in the original redox state and does not contribute to the color change. The device goes back to the original color once the potential is switched back to 0 V, showing no degradation or memory effect. An important thing to note here is that a conjugated polymer can form symmetrical devices and hence does not need a reduction partner for switching. This also results in much faster switching of the symmetrical solid-state devices as compared to unsymmetrical solid-state devices in which both cathodically and anodically coloring material are used for device switching. A very detailed discussion of symmetrical and unsymmetrical EC devices

along with the work done in the past on both them is given in sections 2.4.1 and 2.4.2.

In addition to working on LbL assembly of EC devices and achieving the fastest switching times of coloration and decolaration of 31 ms and 6 ms, respectively, for an active device area of 0.6 cm^2 of PEDOT, research focus was also devoted in this thesis towards the application of LbL in fabricating ionic polymer metal composite (IPMC) actuators.

1.2 Outline

Chapter Two gives a review of the basic principles of electrochromism in visible, near infra-red (NIR)[20,21] thermal infra-red[22], and microwave regions[3]. Its wide application in smart windows, rearview mirrors, goggles and displays is also presented as well. This is followed by a detailed discussion of the basic concept of LbL assembly, the deposition conditions, materials and its applications in various fields from organic optoelectronics, optics, electrocatalysis, coatings etc along with its compatibility with a large range of materials. This chapter also consists of various examples of EC devices that have been demonstrated in the literature in the past few decades followed by a clear distinction between symmetrical and unsymmetrical devices. Various important techniques used in this thesis for characterizing the EC devices are explained and also an important analysis of the use of these techniques in characterizing LbL EC films in recent literature. Various electrochromic materials are sub-divided into organic (primarily polyviologens and derivatives), inorganic (tungsten oxide, Prussian Blue and Ruthenium Purple), conducting polymers (PEDOT, PANI and their derivatives), quantum dots, and Polyoxymetalates (POMs) sections to present the wide range of materials that show the phenomenon of electrochromism.

Chapter Three describes the fabrication of EC devices from a polyviologen (PV) synthesized by polymerization of N,N'-bis(-δ aminopropyl)-4,4'-bipyridinium bromide hydrobromide (APD) and isophthaloyl chloride (ISP). This PV was fully soluble in water as well as in organic solvents and is an ideal candidate for LbL assembly. The spectroelectrochemical and electrochromic properties of the resulting LbL films of PV/poly(2-acrylamido 2-methylpropanesulfonic acid) (PAMPS) were examined by cyclic voltammetry, Fourier transform infrared (FTIR)

spectroscopy, UV–vis spectroscopy, optical switching, and current density measurements. Solid state devices made of PV films sandwiched with polyaniline (PANI) as a counter electrode have switching times of 100-250 ms. 40-bilayer films of PV/PAMPs show high contrast ($\Delta T = 61\%$) in 0.1 M $NaClO_4$ liquid electrolyte solution and coloration efficiency (CE) as high as 57 cm^2/C, one of the highest reported so far for any bipyridinium salt system.

The fastest reported switching time for any electrochromic devices so far is presented in Chapter Four. The EC devices are solid-state conducting polymer symmetrical devices fabricated by the LbL technique. The devices were composed of bilayers of poly(3, 4-ethylenedioxythiophene): poly(styrenesulfonate) and poly(allylamine hydrochloride) on indium tin oxide substrates. Devices fabricated from 40-bilayer-thick films have coloration and decolaration switching times of 31 ms and 6 ms, respectively, with low applied voltage (1.4 V) for an active area of 0.6 cm^2. The switching times have been shown to decrease with the active area of the electrochromic device suggesting that even faster electrochromic switching times are possible for devices with smaller areas. This is an important comparison to show because the "pixel-size" of standard commercial displays is much smaller and a further reduction in device size through commercially available techniques has the possibility of reducing the switching time from milliseconds to microseconds.

Chapter Five presents the results on a new regiosymmetric water-soluble sulfonated monomer based on 3,4-propylenedioxythiophene (ProDOT-Sultone), via the *O*-alkylation of the corresponding unreactive *β,β*-disubstituted hydroxyl group with propane sultone in presence of catalytic amount of a 1,4-diazabicyclo[2.2.2]octane (DABCO). This new monomer was oxidatively polymerized to form a regiosymmetric water-soluble conjugated anionic polyelectrolyte, which was then used for the fabrication of solid-state electrochromic devices using LbL deposition method. A comparison of EC devices fabricated through the LbL method and the cast film technique was made and the superior performance of the former further shows the usefulness of LbL in this field. The LbL solid state devices were found to exhibit better electrochromic properties in terms of color contrast, switching time, coloration efficiency (CE), surface control electroactivity and conductivity in thin films compared to the corresponding water soluble regiorandom 3,4-ethylenedioxythiophene (EDOT) derivative. For the 40 and 80-

bilayer solid-state electrochromic devices, the electrochemical contrast was measured to be 31% and 40% at 570 nm with fast solid-state switching times of 100 and 220 ms, respectively, indicating faster movement of the ions in and out of the films. Furthermore, the coloration efficiency was found to be as high as 250 cm^2/C for 80 bilayer device, and independent of device thickness, indicating the full accessibility of all the ionic sites even in thicker films. Four-point probe conductivity of the LbL and *in situ* conductivity of solution cast films was found to be in the range of 10^{-4} S/cm and 10^{-3} S/cm, respectively.

Chapter Six presents the synthesis of Ruthenium Purple (RuP) nanocolloids, their deposition through the LbL technique and characterization of EC films and devices. RuP is an analog of Prussian Blue (PB) that goes from dark purple to colorless and shows a very high contrast capability. Electrochromic RuP/polymer nanocomposite films, fabricated by multilayer assembly, were found to exhibit sub-second switching speed and the highest electrochromic contrast reported to date for any inorganic material.

Research was done on various EC materials to study the materials with the specific application towards EC performance such as high contrast, fast-switching speed, cost etc. In summary of these four chapters, we have found that RuP shows the best contrast of 84%, PEDOT shows the best switching-speed (31 ms and 6 ms for coloration and decolaration, respectively) and polyviologen is the one of the cheapest to synthesize, also shows high contrast, and is very easy to use because of its water-soluble nature.

Chapter Seven relates to applications other than EC devices. To create a high strain and large force in a bending actuator, a high concentration of the excess ions near the electrodes is necessary. To realize these goals, various porous electrodes in the forms of conductive network-ionomer composites have been investigated in the past decades in order to increase the electrode surface area and optimize the morphology of the porous conductive network composite (CNC) electrodes. The results presented here for the bending actuators are of a completely new approach to fabricating CNCs of the actuator with the LbL assembly method. The process makes it possible for CNCs to be fabricated at sub-micron thickness with high precision and quality. This CNCs exhibits high strain ~6.8% under 4 volts, whereas a comparative study on the well-

established composite Ruthenium Oxide (RuO_2)/Nafion CNCs exhibit a strain ~ 3.3%. The high strain and sub-micron thickness of the LbL layers in an ionic polymer metal composite (IPMC) yield large and fast actuation. The response time of a 26 μm thick IPMC with 0.4 μm thick LbL CNCs to a step voltage of 4 volts is 0.18 seconds.

The thesis ends with a chapter on the conclusions reached from the individual studies of different electrochromic materials for the devices as well as the application of the LbL films in electromechanical bending actuators. Suggestions are made for future work that can be done to further improve the switching speed in EC devices while still maintaining the high contrast and quality of actuation in IPMC actuators.

References

[1] http://www.displaybank.com/eng/info/news/press_show.php?id=2996

[2] http://en.wikipedia.org/wiki/Liquid_crystal_display#cite_note-14

[3] N. Vlachopoulos, J. Nissfolk, M. Moller, A, Briancon, D. Corr, M. Ryan, A. Hagfeldt, *Electrochim. Acta*, **2008**, 53, 4065.

[4] C. J. Schoot, J. J. Ponjee, H. T. van Dam, R. A. van Doorn, P. T. Bolwjin, *Appl. Phys. Letter.,* **1973**, 23, 64.

[5] D. J. Barclay, D.H. Martin, In *Technology of Chemicals and Materials for Electronics*: E. R.Howells, Ed.: John Wiley and Sons: New York, **1984**, 266.

[6] S. Cho, S. B. Lee, *Acc. Chem. Res*. **2007**, 6, 699.

[7] S. Cho, W. J. Kwon, S. Choi, P. Kim, *Adv. Mater.* **2005**, 17, 2, 171.

[8] S. Cho, D. Choi, S. Kim, S. Lee, *Chem. Mater*. **2005** 17, 4564.

[9] S. Cho, R. Xiao, S. Lee, *Nanotechnology* **2007** 18, 405705

[10] S. Ravaine, C. Lafuente, C. Mingtoaud, *Langmuir* **1998**, 14, 6347.

[11] H. Q. Xiang, K. Tanaka, A. Takahara, T. Kajiyama, *Langmuir* **2002**, *18*, 2223.

[12] J. Livage, *Chem. Mater*.**1991**, 3,578.

[13] A. E. Aliev, H. W. Shin, *Solid State Ion.* **2002**, *154*, 425.

[14] D. M. DelongChamp, M. Kastantin, P. T. Hammond, *Chem. Mater*. **2003**, *15,* 1575.

[15] D. M. Delongchamp, P. T. Hammond, *Adv. Funct. Mater.*. **2004**, *14*, 224.

[16] D. M. Delongchamp, PhD Thesis, MIT, **2003.**

[17] D. M. Delongchamp, P. T. Hammond, *Adv. Mater*. **2001**, *13*, 1455.

[18]D. M. Delongchamp, P. T. Hammond, *Chem. Mater*. **2003**, *15*, 1165.

[19] D. M. DeLongchamp P.T. Hammond, *Chem. Mater*. **2004**, *16*, 4799.

[20] R. J. Mortimer, N. M. Rowley, in J. A. McCleverty, T.J. Meyer, eds., *Comprehensive Coordination Chemistry – II : From Biology to Nanotechnology*, Elsevier, Oxford, **2004**, Volume 9.2, M. D. ward., pp. 581.

[21] M. D. Ward, J. A. McCleverty, *H. Chem. Soc. Dalton Trans*., **2002**, 275.

[22] Z. C. Wu, Z. H. Chen, X. Du, J. M. Logan, J. Sippel, M. Nikolou, J. R. Reynolds, D. B. Tanner, A. F. Hebard, A. G. Rinzler, *Science*, **2004**, *305*, 1273.

Chapter 2

Theoretical and Historical Background of Layer-by-Layer (LbL) films in Electrochromic Devices

This review describes the technique of using Layer-by-Layer (LbL) films in the development of electrochromic (EC) devices with both new and previously developed electroactive materials. Electrochromism is the phenomenon of an electroactive species to exhibit new optical absorption bands (a new color) when it undergoes either oxidation or reduction. The major thrust towards the development of these devices is their low cost as well as their exceptional ability for multiple colors, fast switching speeds and long lifetimes, which makes them suitable for flexible displays and "smart windows[1]."

Each electroactive species contains a different number of electrons before and after the change in redox state takes place; these redox states have different spectroscopic properties and therefore have different energies for electron movement between the ground and the excited states.[2] Usually, materials that change color in the visible spectrum are considered electrochromic, but recent interest in electrochromic devices (ECDs) for multispectral energy modulation by reflectance and absorbance has extended the parameters.[2,3,4] Studies have been done to determine the effect of chemical species to the modulation of radiation in the near infra-red (NIR)[5,6] thermal infra-red[7], and microwave regions[3]. This is just to clarify that the 'color' can be a response by detectors to these electromagnetic regions and not just to the human eye.

LbL films formed by both organic and inorganic EC materials have shown their performance to be in general superior to the EC films formed by other methods. The strong influence of LbL deposition conditions such as ionic strength, pH, and salt concentration provides an option to vary and optimize the films according to the desired application and uses. Work related to depositing EC materials in LbL films has helped in exploring the electrochemical behavior, which aids in creating an ever-expanding library of these electroactive materials. LbL is an ideal

processing tool in the deposition of EC materials, as it allows precise control for designing EC films with high uniformity and thickness control, higher contrast by combination of multiple EC materials, and an increase in ionic conductivity for faster switching speeds.

The aim of this review is to highlight the development of EC devices, specifically those fabricated with the film-forming technique known as LbL. Interest has developed in EC devices for use as an inexpensive flat-panel display alternative to liquid crystal, light emitting diode, and cathode ray tube displays[8]. EC films can be fabricated by many methods, e.g. electropolymerization, spin coating or surface polymerization by chemical means, but the LbL film fabrication method gives a fine degree of control to optimize the capabilities of EC films. The thickness control and robustness of the films with nano-scale roughness gives LbL films significant advantages over conventional EC film fabrication methods. Along with a detailed explanation on the background for LbL process and electrochromism, this chapter covers a large range of EC materials (e.g. organic, organometallics, inorganic and semiconductor materials) with the detailed description of a few of them forming LbL films.

2.1 Layer-by-Layer (LbL)

LbL deposition of polymeric thin films (also known as Ionic Self-Assembled Multilayers (ISAMs) of polyelectrolytes) is a technique developed by Decher et al.[9,10] which uses the attractive forces between the molecules of opposite charges to form the films.[11,12] Figure 2.1 shows the steps of the fabrication process along with its brief description. In this technique, a high concentration of polyelectrolytes is deposited on the substrate that was carrying a negative charge. These highly concentrated solutions lead to excess adsorption, which means that there is complete charge neutralization and resaturation bringing charge reversal.[13] Brent et al. proved this phenomenon by adopting a surface force measurement technique.[14] Alternate deposition of these highly concentrated polyelectrolytes of positive and negative charge increases the thickness of the film and also provides flexibility in choosing the number of bilayers while still maintaining nanoscale control of the thickness. One of the important advantages of the LbL film assembly is that it is very easy to use without the need of any kind of expensive or special

apparatus. Various combinations of polyelectrolytes with other materials such as gold colloids,[15] silica,[16,17] clay minerals,[18] proteins,[19,20] viruses,[21] dendrimers[22] etc, have also proven that the LbL technique is very flexible and easy to use.

Soon after Decher's work, Rubner et al. showed the ability to deposit thin uniform LbL films of conductive materials (polymers like polyaniline, polypyrrole etc.) on substrates of different shapes and sizes.[23,24,25] Thin film formation by molecular self-assembly of p-type-doped electrically conductive polymers with either a conjugated or non-conjugated polyanion was demonstrated. Partially doped conjugated polymers have delocalized defect sites along the polymer backbone that carry positive charges (polarons and bipolarons) and that charge has been used with the negative charge of the polyanion to deposit the multilayers.[25] The solution preparation of polyaniline from its emeraldine base form to provide sufficient positive charge in a particular pH range has in fact become quite standard now. An important thing to note here is that the commercially available polyaniline does not usually dissolve in water, but this technique helps it dissolve in water even at very high concentrations. Briefly, Rubner et al. dissolve polyaniline (emeraldine base form) in dimethylacetamide (DMAc), followed by rigourous stirring and ultrasonication to ensure complete dissolution. This highly concentrated solution is then slowly added to water at pH 3.5 to decrease the overall concentration level to 10-fold times the initial. Polypyrrole solutions were also prepared in a similar fashion by using low pH (1.0) aqueous solution and the multilayer thin films deposited with polystyrene sulfonic acid (PSS) display conductivity as high as 40 S/cm for as low as four deposited bilayers. The range of the applications of LbLs is very broad, but a few of the most common ones that have been demonstrated in last 15 years are: thin films for non-linear optics,[26,27] selective area patterning,[28] sensors,[29] electrochromic films,[30,31] electrocatalysis,[32] thin films for light emitting diodes,[33] anti-reflection coatings,[34] and active enzymes[35].

A change in pH, ionic strength and salt concentration of the polyelectrolyte (PE) solution results in changing the thickness of the LbL film bilayers. Rubner et al. have explained the influence of changing pH of the solution on the film morphology, physical properties and composition.[36,37] Variation in the charge density of a weak polyelectrolyte (eg. poly(allylamine hydrochloride) and poly(acrylic acid)) can result in a change in the adsorption behavior, that finally results in a

change in the behavior of the films resulting in very thick to very thin films over a narrow pH range.[37] At low pHs, positively charged polyelectrolytes (polycations) are highly ionized, but lose protons as the pH goes higher than a characteristic pH known as the pK_a, hence resulting in more deposition of material to neutralize the same amount of charge from the prior layer. This results in thicker film deposition at higher pH for polycations with globular (loops and tails) morphology. The opposite happens in the case of a negatively charged polyelectrolyte (polyanion), which forms thicker films at lower pH and thinner at higher. In brief, the film thickness of an adsorbed layer is dependent on the charge density (or pH) of the adsorbing polyelectrolyte and remains relatively independent of the morphology of the previously deposited polyelectrolyte or bilayers. However, in some cases at neutral pH for one of the polyelectrolytes it was observed that the thickness also depends on whether the layers deposited before are above or below the value of that polyelectrolyte's pKa.[36] Lvov[38] et al. first introduced the idea of changing the ionic strength of the PE solution to adjust the desired layer thickness; later this idea was further developed by many scientists[39,40]. Screening enhanced adsorption[41] explains the increase in the thickness of adsorbed PE layer by the addition of a small amount of the salt, but needs to be carefully used because higher salt concentration can result in delamination of films from the substrates and also surface defects by increased surface roughness. [42] Schlenoff et al. have explained in detail the effects of surface charge and mass balance in the polyelectrolyte multilayers and how the salt content within the multilayers can be controlled easily by using electrochemically active multilayers.[43] There are also secondary interactions (H bonding) that occur between opposite charged PE layers, but they are weak interactions and are excluded from the focus of this review. Rubner et al.[44] and Garnick et al.[45] have discussed the presence of secondary interactions in weak PE, which can be used to fabricate films by inkjet printing water of controlled pH.

A principal advantage of water-soluble polymers is that they can be processed using a wide range of deposition techniques such spin coating,[46] solution casting,[47] thermal evaporation,[48] surface polymerization by chemical means[49] electropolymerization[50], and Langmuir-Blodgett (LB),[51] but the LbL film fabrication method gives a fine degree of control to optimize the properties of EC films.[30,52]

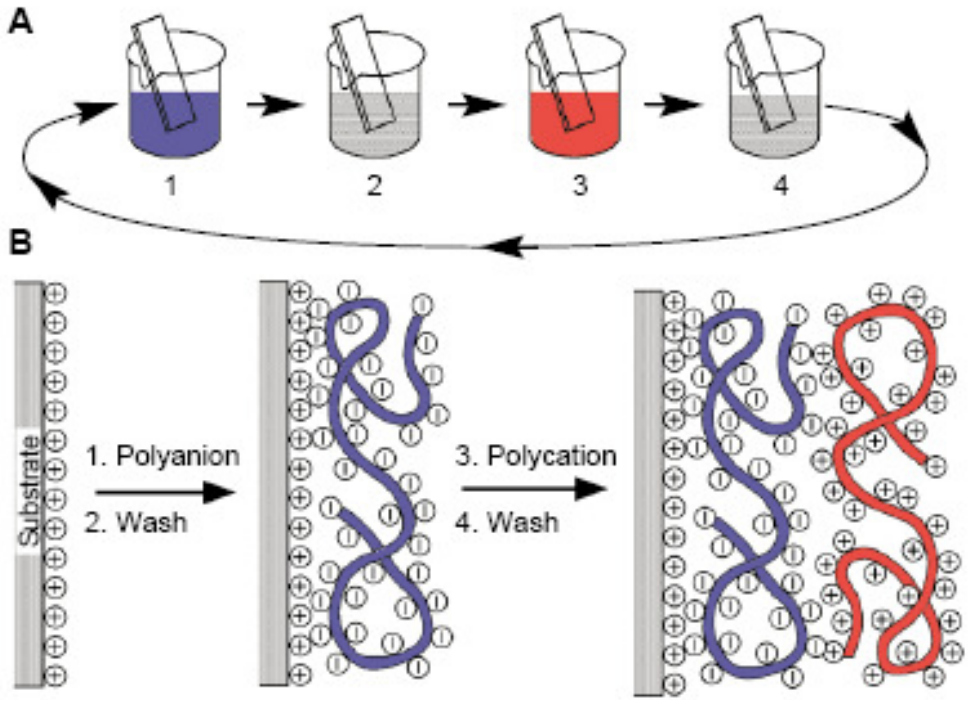

Figure 2.1(A) Schematic of the film deposition process using slides and beakers. Steps 1 and 3 represent the adsorption of a polyanion and polycation, respectively, and steps 2 and 4 are washing steps. The four steps are the basic buildup sequence for the simplest film architecture, (A/B)*n*. The construction of more complex film architectures requires only additional beakers and a different deposition sequence. (B) Simplified molecular picture of the first two adsorption steps, depicting film deposition starting with a positively charged substrate. Counterions are omitted for clarity. The polyion conformation and layer interpenetration are an idealization of the surface charge reversal with each adsorption step. [From G. Decher, Fuzzy Nanoassemblies: Toward Layered Polymeric Multicomposites, *Science*, **1997**, 277, 1232. Reprinted with permission from AAAS.][12]

Kotov et al.[53] were the first to introduce nanoparticles in the LbL fashion (Figure 2.2). Successful LbL film deposition of a polycation (poly-(diallylmethylammonium chloride (PDDA)) with cadmium sulfide (CdS), lead sulfide (PbS) and titanium dioxide (TiO_2) nanoparticles was demonstrated. To confirm the uniform deposition of NPs, ultrathin films were characterized by spectroscopic (absorption and emission), microscopic (transmission electron and atomic force), X-ray diffraction and photocurrent measurements techniques. Formation of LbL film assembly by NPs has led Kotov et al. to assemble a free-standing LbL film of NPs as well; bilayers were deposited on cellulose acetate that was easily dissolved in acetone leaving behind stable free-standing thin films.[54] Working on the same stategy, Tsukruk and coworkers assembled freely

suspended, multi-layered nanocomposite membrane of gold nanoparticles for highly sensitive pressure sensors.[55,56] Several other groups have also done pioneering work in studying various aspects of nanoparticle LbL assembly, making it one of the most promising new methods of thin film deposition of nanoparticles.[57,58,59]

One of the other important areas where the LbL film fabrication technique is most exploited is in forming films of water-soluble conducting polyelectrolytes. We mentioned above that the LbL film assembly of water-insoluble conducting polymers can be done by using the charges created by the defect sites on the polymer backbones. This section describes the usage of ionic charge from groups ($-SO_3^-Na^+$, NH_3^+, COO^-Na^+, etc.) that exist either on the polymer backbone or side chain. These kinds of polymers are water-soluble and exhibit high conjugation length both in solution and solid-state. Zotti et al.[60] were the first to introduce the water-soluble derivatives of conducting polymers, especially polythiophenes in the LbL film fabrication. The thin film deposition of polythiophene-based multilayers which were then characterized in aqueous media was also reported by Lukkari et al. in 2001.[61] The first set of multilayer films were formed of inactive polycation, poly(diallyldimethylammonium chloride) (PDDA) and conductive polyanion, poly-[3-(3-thienyloxy)propanesulfonate] (P3TOPS) and the film properties were found to be similar to polythiophene films prepared in organic media. The in-plane conductivity of these films is rather low (~1.6×10^{-5} S cm^{-1}), but improved by about 40 times by replacing PDDA with conductive polycation, poly-[3-(3-thienyloxy) propyltriethylammonium] (P3TOPA). By measuring the charge-transfer ratio, the authors have also shown that the interpenetration of layers is very important for conductive films and hence LbL film assembly is an important tool to achieve that.[61] Recently Reynolds et al. and others[62,63] reported the LbL deposition studies on a polymer based on 3-4-ethylenedioxythiophene-sultone (PEDOT-Sultone) for electrochromic devices and also as hole transport layers in OLEDs. PEDOT-S is a self-doping water-soluble conducting polymer, and the availability of the dopant ion in the polymer backbone increases the water-solubility and is also expected to initiate faster switching within the polymer film. The LbL films of PAH/PEDOT-S show faster switching, highly reversible color change and better redox properties in aqueous media as compared to electrochemically deposited or cast films.[63]

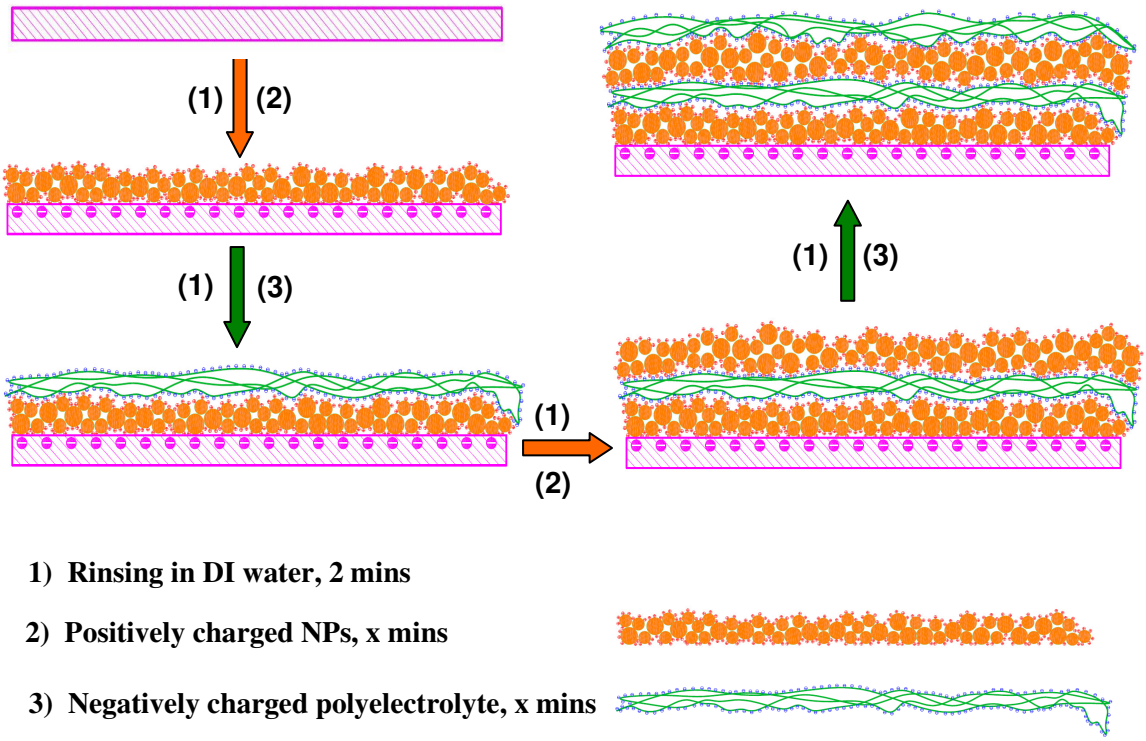

Figure 2.2 LbL deposition of nanoparticles (positively charged in this case) and negatively charged polyelectrolyte.

The Langmuir- Blodgett (LB)[64,65] and sol-gel processing[66,67] methods of fabrication have also been used in depositing EC films. Of these, LB has not gained much attention because of the difficulty in forming highly oriented, thin, homogeneous and robust films. The main advantage of adopting the LbL technique over LB multilayers is that the electroactivity decreases quickly as the number of layers is increased, disappearing after three to four layers, in the case of LB films, whereas the films deposited by the LbL method remain highly electroactive even after deposition of 80 layers.[12] However, the sol-gel process of fabrication has gained some attention because of its better compatibility for commercial production. But it is primarily useful for depositing thick films on a large area since the deposition of thin films requires smooth and homogenous coverage, which is not possible with the sol-gel process.

2.2 Electrochromism

An electroactive species often exhibits new optical absorption bands (i.e. shows a new color) in accompaniment with an electron-transfer or redox reaction in which it either gains or loses an electron; that is to say, it undergoes reduction or oxidation.[3,8] In order for any material to appear colored, it must absorb a part of the visible spectrum. This absorbed energy causes an electronic transition between the highest occupied molecular orbital (HOMO) and lowest unoccupied molecular orbital (LUMO). Conjugated molecular structures generally possess lower bandgaps between HOMO and LUMO, and electrons in low energy π orbitals can easily be excited to higher energy π^* orbitals in a $\pi \rightarrow \pi^*$ transition. The "donor-acceptor" system in organic molecules leads to a lower energy transition in transferring electrons from HOMO to LUMO. An electron "donor" group (eg. NH_2), if linked directly to the conjugated double bond structure, can enhance transfer of electrons to an "acceptor" group (eg. NO_2); this intermolecular charge transfer increases the charge transfer rate and switching speed. The location of the "donor-acceptor" is important in deciding the charge transfer mechanism and to obtain fast switching speed at low applied potentials. Reversible electrochromic materials are typically used on an optically transparent electrode (OTE), e.g., tin doped indium oxide (ITO) into the form of thin films; this work has been extensively reviewed by Granquist et al [68].

Contrast ratio is typically defined as the change in transmittance at a specific wavelength during EC switching and is directly related to the logarithimic change in the absolute number of photons absorbed by the film and thus is closely related to contrast perception in the human eye and is one of the important parameters for EC films. Switching speed, which corresponds to how fast a device chnages color between its reduced and oxidized states, is another important performance parameter and depends on the size of the device as well as the material properties. EC films should be able to quickly change color on the application of voltage and lose the color (bleach) on the removal of the voltage or, in some cases, application of a reverse voltage. Ion movement in and out of the film and the film thickness are a couple of factors that control the switching speed of the EC polymers.

Some of the most commonly studied electrochromic materials include transition metal oxides (e.g., tungsten oxide, WO_3),[3] organic molecules (e.g., viologens), [4,8] inorganic complexes (e.g., Prussian Blue [PB]),[3,8] and conducting polymers. [3,69,70] With many of these materials, the electrochromic effect is reversible and also can occur not only in the visible region but also in the ultraviolet (UV), infrared (IR), and even microwave regions of the spectrum.

2.3 Multi-color Electrochromic Materials

The materials that exhibit multi-hued coloration effects have various (more than 2) redox states that display colors other than the colorless or the bleached state. For organic materials, polyviologen falls into this category as they usually have three redox states that show color changes from colorless to dark violet to yellow at dicationic, monocationic and completely reduced states, respectively. In inorganic electrochromic materials, Prussian Blue (PB) exhibits about four colored states that go from blue to clear to green to yellow depending on the amount and polarity of the voltage that corresponds to different redox states. A detailed description of the color range with redox states is given in the later part of this chapter. Work on modifying the structure of these materials and adjusting the color change has been going on for last couple of decades, but the response towards achieving different colored state from one material is nowhere near to that provided by conjugated polymers. Even after modifying the structure and shape of the polyviologens and PB materials, the color change is more or less similar to that exhibited by the original compound. It is observed that sometimes one of the colored states is also unstable that cannot sustain the same color after a few cycles. In contrast, conjugated polymers provide us the flexibility of controlling the color by adjusting the band gap control. Polyaniline in its original state shows at least three different states (yellow, green and blue) and all of these are very stable.

Taking this work a step further, the Reynolds group showed that by simply modifying the main chain or pendant group, a control over the band gap can be achieved and the material can easily switch two to four states at different potentials.[71] Plenty of work has been done in the field of conjugated polymers showing numerous synthetic strategies for tuning the band gap.[72] Figure

2.3 shows about 15 polymers as examples of how the novel monomers can be designed to tune the band gap and achieve multicolor electrochromic polymers. Other than showing standard modifications in PANI, Polythiophene, polypyrrole materials, the authors explained in detail the modifications and the respective color chain effect that can be possible by introducing various aromatic groups in these EC materials. Significant change in EC properties can occur by introducing aromatic groups such as carbazoles, [58] biphenyls, [73] and alkoxybenzenes[74] in the EDOT backbone. Changes in pyrrole monomers were made by either introducing a chain at the electron-rich N-atom or by introducing alkoxybenzenes at the standard compound.

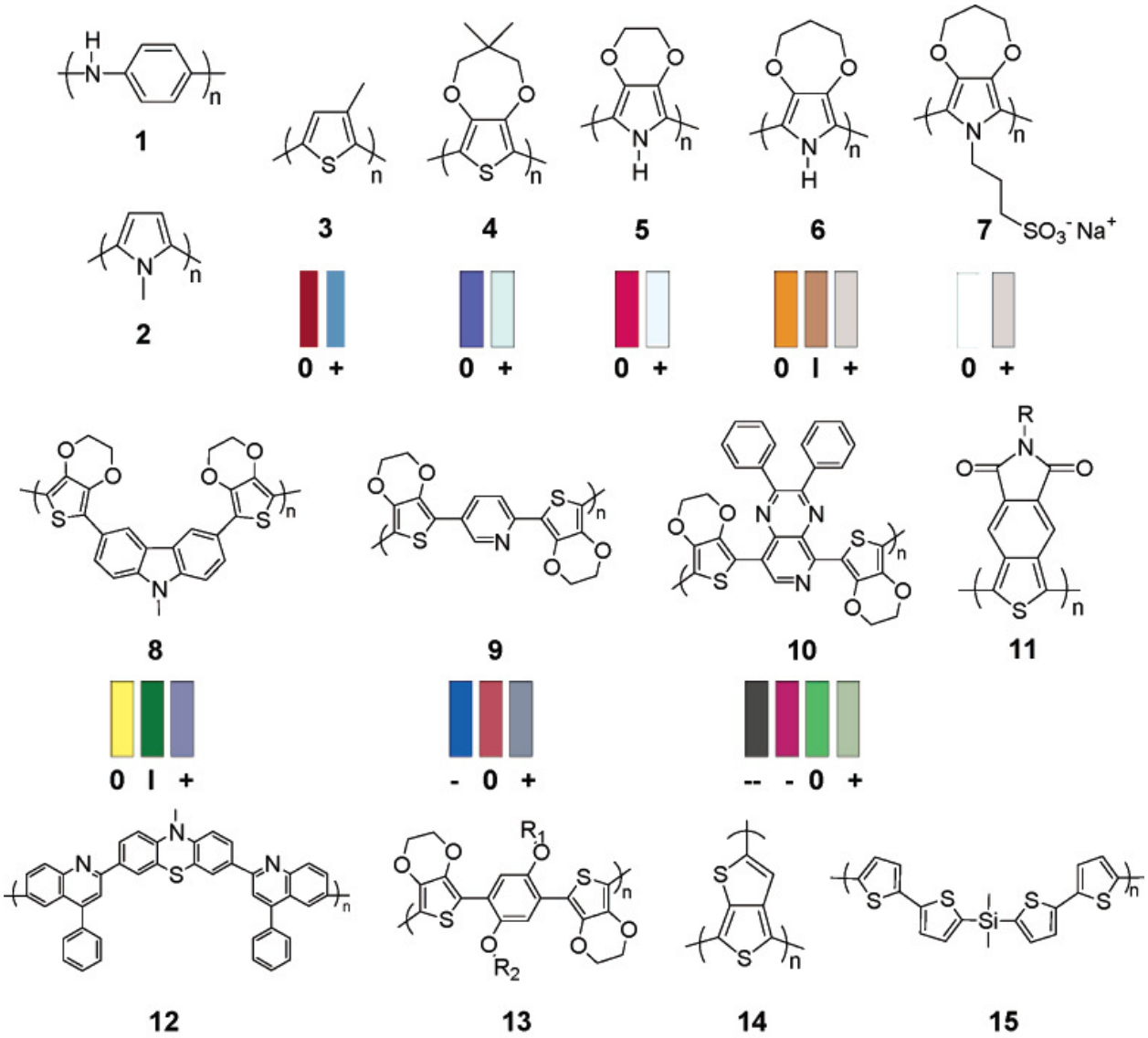

Figure 2.3 Representation of different electrochromic states of various conducting polymers in their 0, neutral; I, partially oxidized; +, oxidized; and – and --, reduced states. Color swatches are

representations of thin films based on measured CIE 1931Yxy color coordinates. [Reprinted with permission from A. A. Argun, P. H. Aubert, B. C. Thompson, I. Schwendeman, C. L. Gaupp, J. Hwang, N. J. Pinto, D. B. Tanner, A. G. MacDiarmid, J. R. Reynolds, *Chem. Mater.* **2004**, *16*, 4401. Copyright 2004 American Chemical Society] [71]

Other than working on modifying the structures, Reynolds et al. also introduced a technique to obtain multi-color films by varying the concentrations of the monomers (bis-EDOT(BEDOT) and BEDOT-NMeCz (bis-EDOT-*N*-methylcarbazole)) in electrochemical copolymerization.[75] This technique is rather limited as it only works well for monomers with nearby oxidation potential. Figure 2.4 shows as how a random copolymer is formed when a potential is applied and both the monomers at different concentrations are oxidized.

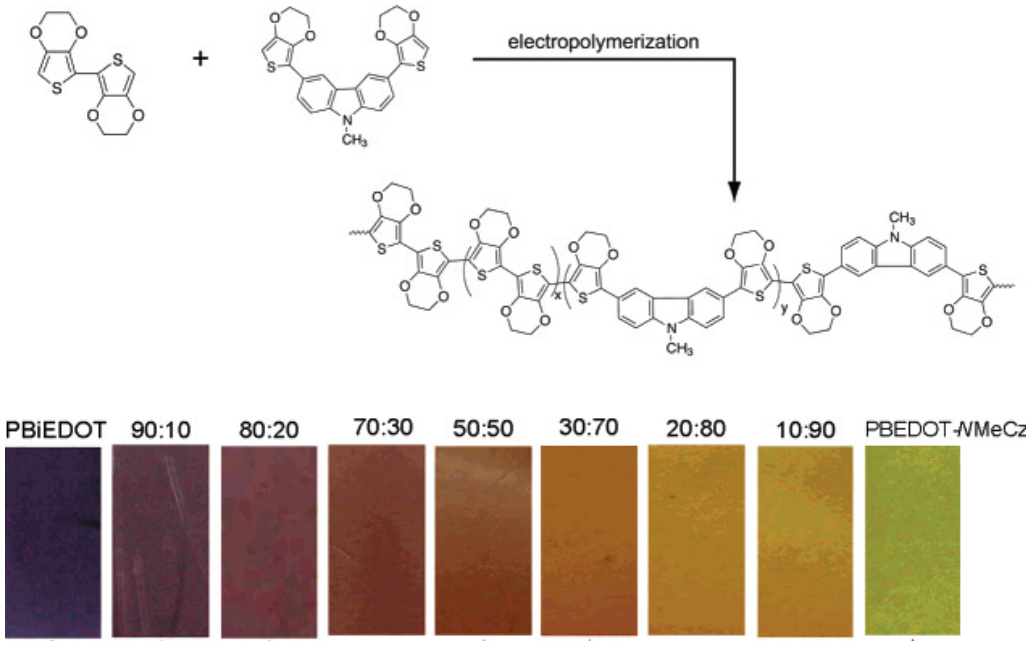

Figure 2.4 Top: Chemical scheme of the electropolymerization of BiEDOT (left) and BEDOT-NMeCz (right) to yield a representative random copolymer structure. Bottom: Photographs of neutral copolymer films on ITO/glass ranging from pure PBiEDOT on the left to pure PBEDOT-*N*MeCz on the right. [Reprinted with permission from C. L. Gaupp, J. R. Reynolds, *Macromolecules* **2003**, 36, 6305. Copyright 2003 American Chemical Society] [75]

2.4 Construction of Electrochromic Devices (ECD)

This section explains the different kinds of designs of electrochromic devices and also lists some important parameters related with their ability to modulate optical properties. Granqvist et al. did a good job in understanding and explaining the phenomenon from charge transfer, use of appropriate materials, electrolyte, to conductor coating for EC devices.[76] In the last 20 years, Dr. Granqvist and his group did a large amount of work on the different basic details of electrochromic devices and materials.

Before discussing the different kinds of electrochromic devices, it is important to explain the main principles behind different applications of these devices. Figure 2.5 summarizes a number of applications for electrochromic devices. The first one is mostly used for information displays. Schoot et al. were the first to start working on this technology and developed a solution-phase hexylviologen device in the early 70s.[77] A much more sophisticated device based on the concept was developed by IBM in the mid 1980s, which featured an array of 96,000 micron-scale devices integrated as a dynamic flat-panel display.[78] Although work on adopting electrochromic devices in displays has been going on for the last 30 years, durability (long-term life cycle) issues along with the progress in the area of liquid-crystal based devices have made the industry move its focus to the latter. However, recent applications of these electrochromic- based devices are reappearing in contemporary contexts such as "electronic paper"[79,80] and "printed or painted"[81,82] displays.

The second concept of electrochromic devices is used in a variable-reflectance (anti-dazzling) mirror; electrochromic rear-view mirrors used in some automobiles fall into this category. One of the most widely explored electrochromic devices is the 'smart window', which controls the solar radiation. Such windows are of great use in building architecture[83,84,85] in that they can allow a user to control the amount of light and heat inside the building.[86,87] A window can easily turn transparent to opaque or somewhere in between, just by the press of a button, partially or completely blocking the light from coming in while still maintaining a clear view of what lies behind the window. Finally, the fourth type of electrochromic device is used for a surface that needs variable thermal emittance and they are mainly used for temperature control of space vehicles. [88,89]

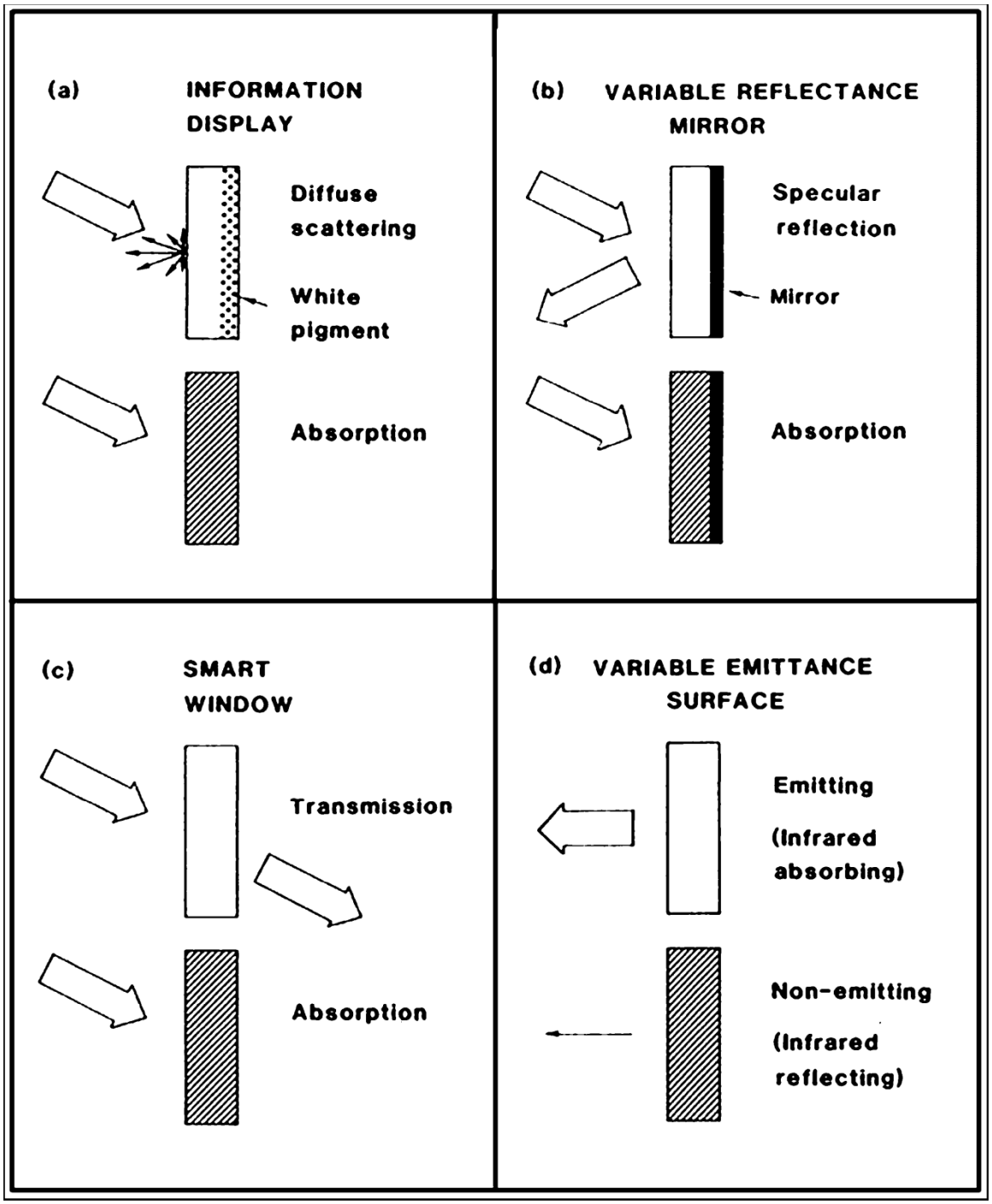

Figure 2.5 Principles for four different applications of electrochromic devices. Arrows indicate incoming and outgoing electromagnetic radiation; the thickness of the arrow signifies radiation intensity. [Reprinted with permission from J. Roncali, Chem. Rev. 1997, 97, 173. Copyright 1997 American Chemical Society [72]

The basic design/configuration and operating principle of EC devices can be understood from either of the images in Figure 2.6. These kinds of devices are the most commonly used and consist of five layers on one substrate or in between two substrates in a sandwiched/laminated form. The best known commercially available conducting material that forms transparent films is of SnO_2: F, which is commonly known as Tin Oxide. The electrochromic materials are usually deposited onto tin oxide or indium tin oxide (ITO) coated glass slides[90], or a flexible polyester foil such as was demonstrated by Reynolds et al. in depositing a layer of PEDOT-PSS to give the first all-polymer electrochromic device.[91] The central part of the device is a pure conducting gel electrolyte that can be either inorganic (made of salts of either Li^+, Na^+ etc) or organic (poly(2-acrylamido 2-methylpropane sulfonic acid) (PAMPS) which contains mobile H^+ ions). For faster transport mobility between the two layers, it is important that the transporting ions are small, which is why protons (H^+) or lithium ions (Li^+) are usually preferred.

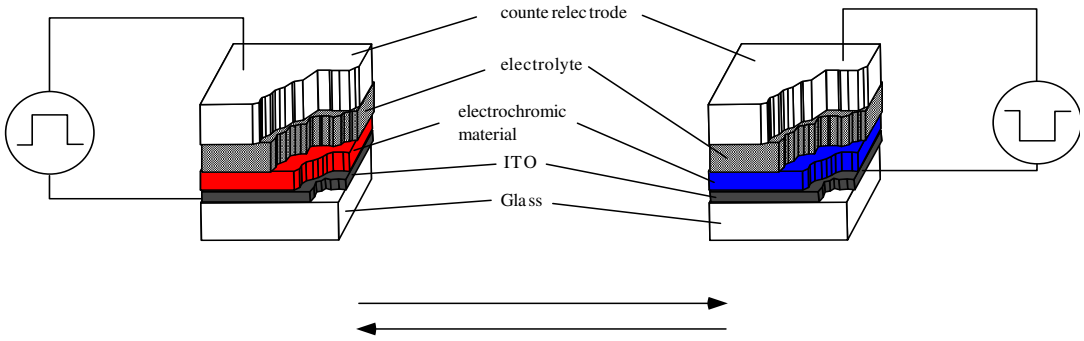

Figure 2.6(a) Schematic configuration for a solid state Electrochromic Device (ECD) [16]

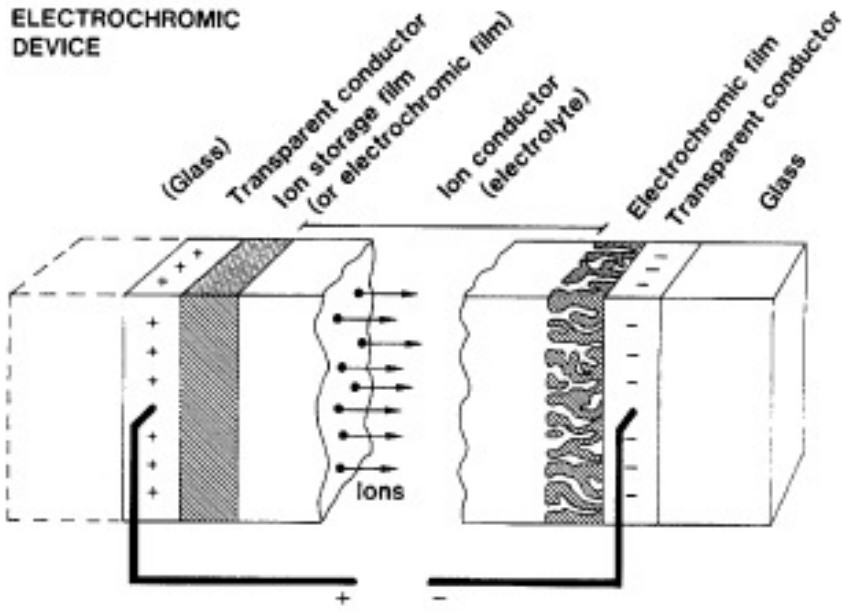

Figure 2.6(b) Basic design of an electrochromic device, indicating the transport of positive ions under the electric field. [Reprinted with permission from J. Roncali, Chem. Rev. 1997, 97, 173. Copyright 1997 American Chemical Society] [72]

When the voltage is applied between two transparent conducting layers such as ITO, ions shuttle between the two electroactive layers (either electrochromic or ion storage film) sandwiched between the two electrodes, which then changes the redox state and finally the color. Any kind of disconnection or elimination of the voltage brings back the device to its original color. The flexibility of the EC devices is that the color can be quickly changed or stopped at any moment just by a slight alteration in the supply voltage.

Next, the separate topic of an electrochromic device and its arrangement is explained in detail. The main electrochromic material is deposited on the conducting, transparent film (ITO) and is capable of conducting both electrons as well as ions. A similar film on the opposite ITO surface could either be a film of the same electrochromic material or could be an ion storage material with complementary properties to those of the first electrochromic film. This divides the description of quasi solid-state EC (Figure 2.7) devices into two sections: (a) symmetrical solid-state devices and (b) unsymmetrical solid-state devices and the configuration of these devices can be understood from Figure 2.8.

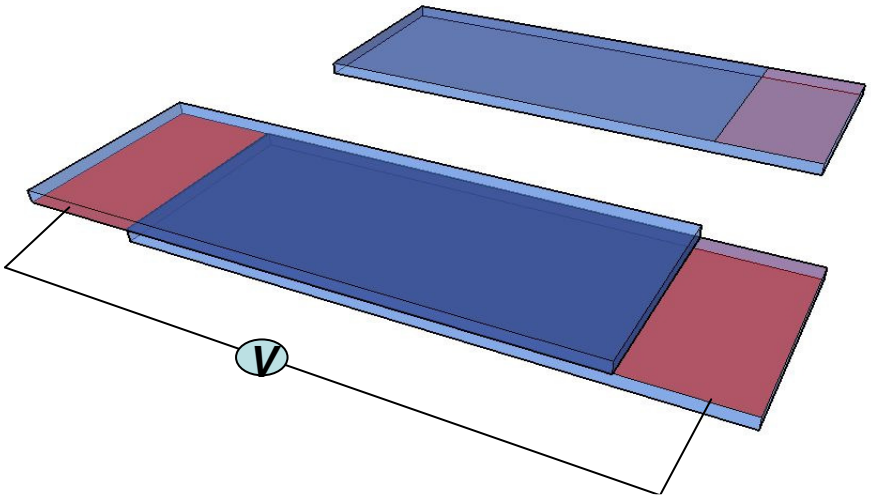

Figure 2.7 3-D description of the quasi solid-state electrochromic device showing that a little area on top of the ITO should stay uncovered by the electrochromic material and used for electrical connections.

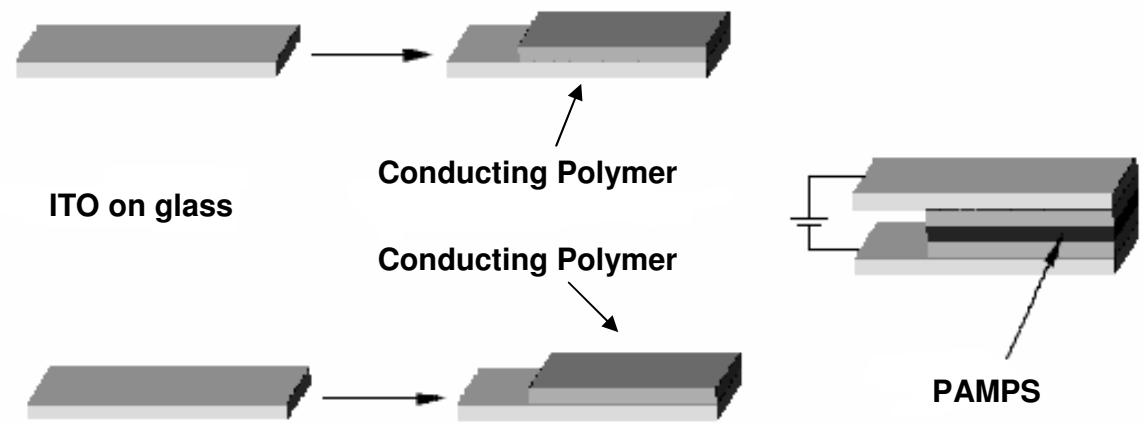

Figure 2.8(a) Symmetrical Solid-State device

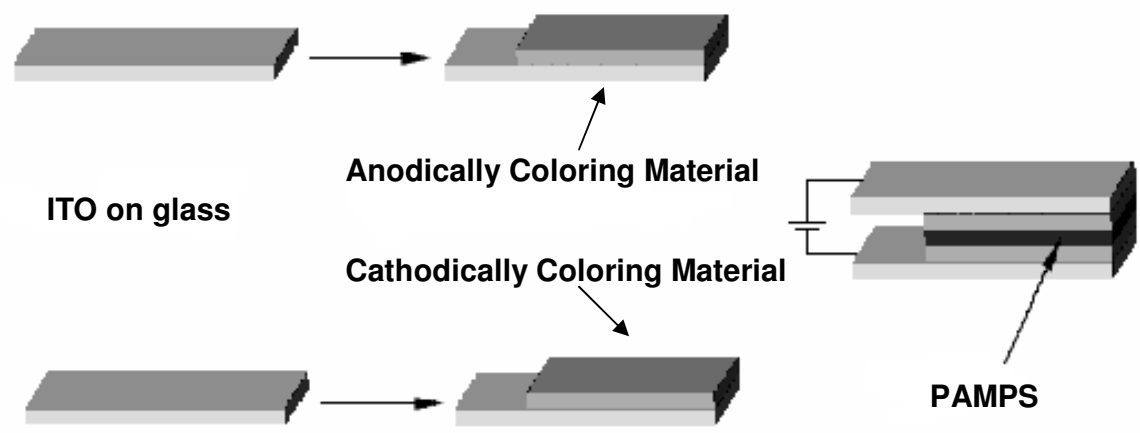

Figure 2.8(b) Un-symmetrical Solid-State device

2.4.1. Symmetrical Solid-state Devices

Fabrication of symmetrical solid-state devices made up from the conducting electrochromic polymer, PEDOT, was shown previously by Mecerreyes et al.[92] This symmetrical configuration utilizes conducting polymers as electroactive layers on each of the two ITO-coated substrates. In brief, the potential was applied to the two layers of similar conducting polymer and the device changed color from one redox state to another. The change in color occured because of the change in redox state of only one of the conducting polymer layers, while the other layer remained in the original redox state and did not contribute to the color change. The device went back to the original color once the potential was switched back to 0 V, showing no degradation or memory effect. An important thing to note here is that a conjugated polymer can form symmetrical devices and hence does not need a reduction partner for switching. This also results in fast switching of the symmetrical solid-state devices as compared to non-symmetrical solid-state devices in which both cathodically and anodically coloring material are used for device switching. Meccereyes et al. (Figure 2.9 (a & b) successfully showed the performance of symmetrical solid-state device of PEDOT. In addition, Heflin et al. successfully demonstrated this approach with a response time as low as 50 ms on the application of 1.0 V with a life cycle of more than 50000 cycles[93,94].

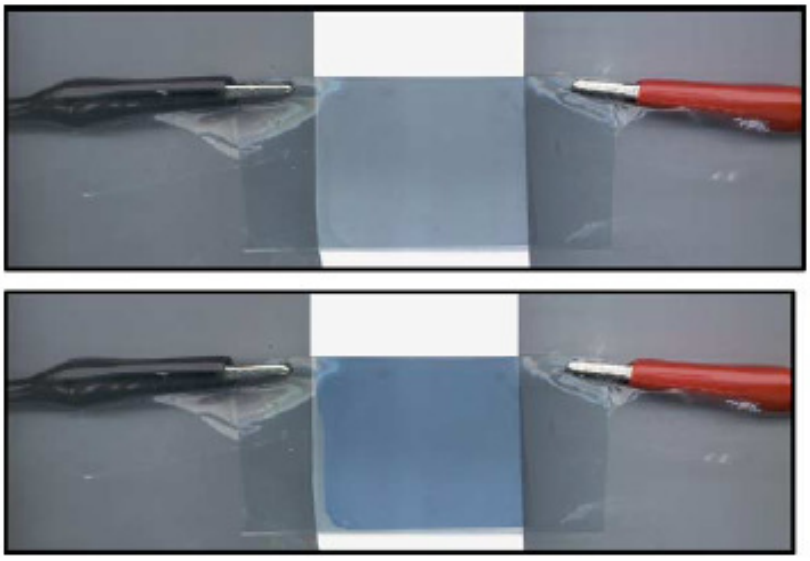

Figure 2.9(a) Photograph of a symmetrical 5 cm × 5 cm electrochromic device in the transparent state (0 V) and dark blue state (3 V). [Reprinted from D. Mercerryes, P. Marcilla, E. Ochoteco, H. Grande, J. P. Pomposa, R. Vergaz, J. M. S. Pena, A simplified all-polymer flexible electrochromic device, *Electrochim. Acta* **2004**, *49*, 3555 with with permission from Elsevier] [92]

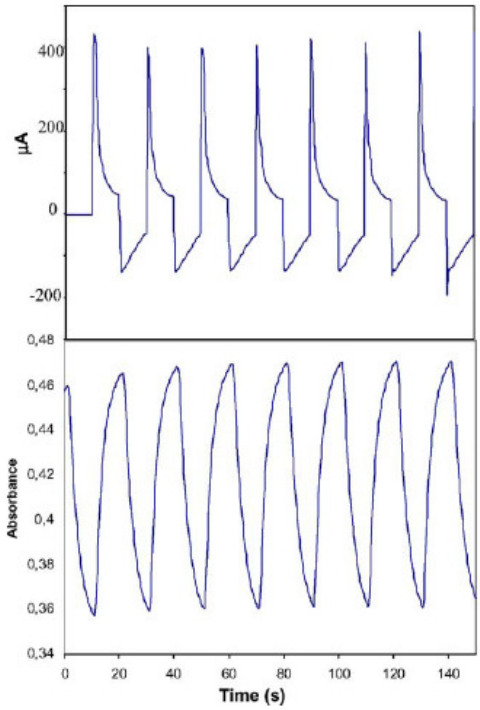

Figure 2.9(b) Electric current and absorbance at 650 nm of the electrochromic device under subsequent double potential steps between 0 and 3V. [Reprinted from D. Mercerryes, P.

Marcilla, E. Ochoteco, H. Grande, J. P. Pomposa, R. Vergaz, J. M. S. Pena, A simplified all-polymer flexible electrochromic device, *Electrochim. Acta* **2004**, *49*, 3555 with with permission from Elsevier] [92]

2.4.2. Unsymmetrical Solid-State Devices

For unsymmetrical solid-state EC devices, the two active layers are usually complementary to one another, for example, one is cathodically coloring polymer such as Poly(3,3-dimethyl-3,4-dihydro-2*H*-thieno[3,4-*b*]dioxepine) (PProDOT-Me_2) switching from a dark blue neutral state to a transmissive sky blue oxidized state, while the other polymer is anodically coloring such as (N-substituted poly(3,4-propylenedioxypyrrole)s *(N*-PrS-PProDOP), switching from a transmissive neutral form to a blue-gray oxidized form.[95] The device then switches between a colored state and a transmissive state, potentially useful as an electrochromic window. This particular device exhibited good stability, retaining 86% of its optical contrast after 20,000 switches. Reynolds et al. showed the synthesis, electrochromic and unsymmetrical device behavior for a series of anodically coloring N-substituted poly(3,4-propylenedioxy pyrroles)(PProDOPs). The devices fabricated from these N-PProDOPs have very well defined cyclic voltammograms with long lifetimes for switching and changes in transmittance in near infrared (NIR) of up to 97%.

Reflective devices have also been constructed by electrodepositing and assembling an unsymmetrical solid-state device using an electrochromic polymer such as PProDOT-Me_2 on a reflective surface such as gold.[96] Slits were formed to allow ion transport from a gel electrolyte as the polymer is oxidized by applying a bias between the gold surface and the counter electrode. The surface of the gold changes from colored to highly reflective with a change in reflectance of 55% at 600 nm.

2.4.3. Liquid Electrolyte Cell Devices

The last kind of EC device that has been very commonly studied for the last 40-50 years is the liquid electrolyte cell device. An important thing to note here is that these kinds of devices are no longer preferred in either academia or industry, because of their poor performance and the need

of a liquid electrolyte for the color change. Figure 2.10 explains the basic principal and schematic of this liquid cell device, in which a low concentration electrolyte (NaCl, KBr, $NaClO_4$, HCl

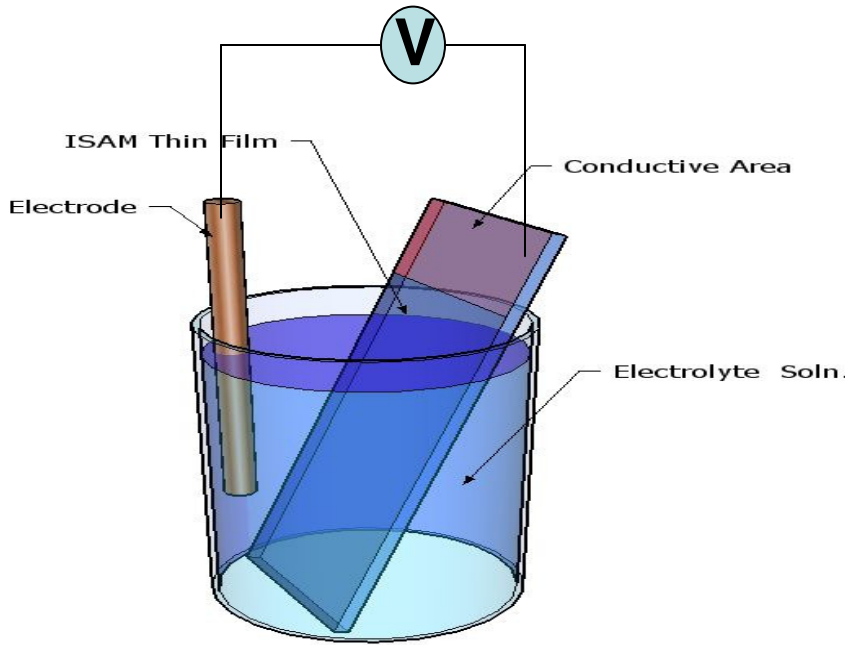

Figure 2.10 Liquid electrolyte cell electrochromic device.

etc) is required to transfer the ions. The overall size of these devices is rather large; leakage, easy degradation or drying of the electrolyte are a few of the problems that these devices have, so they have never had a serious impact in the EC industry. Still, a few of the results with these kinds of devices will be discussed in this thesis. Mostly, synthetic chemists use these types of devices to understand the electrochromic properties of a newly synthesized material. Kumar et al. (Figure 2.11) showed some very good results in the past,[97] along with reporting one of the fastest switching speeds (Figure 2.12) to date of 300 ms with the liquid electrolyte cell device for 95% of full contrast.[98] In addition, the coloration efficiency values (CE) of these devices calculated at various film thicknesses came out to be in the range of 200 cm^2/C. These are not as high (~500-1000 cm^2/C) as expected from polymer-based EC devices, but certainly much higher (10-100 cm^2/C) than the EC devices fabricated from metal oxides. The authors also showed a comparison of the device properties for Poly(3,4-dihydro-2*H*-thieno[3,4-*b*]dioxythiophene)(Prodot), which is the slowest, followed by Poly(3-methyl-3,4-dihydro-2*H*-thieno[3,4-*b*]dioxythiophene)(Prodot – Me), and then Prodot-Me_2 as the fastest reported. This is to be expected as highly substituted

polymers support the faster ion movement due to more open morphology; the same was also confirmed by Doblhofer et al.[99]

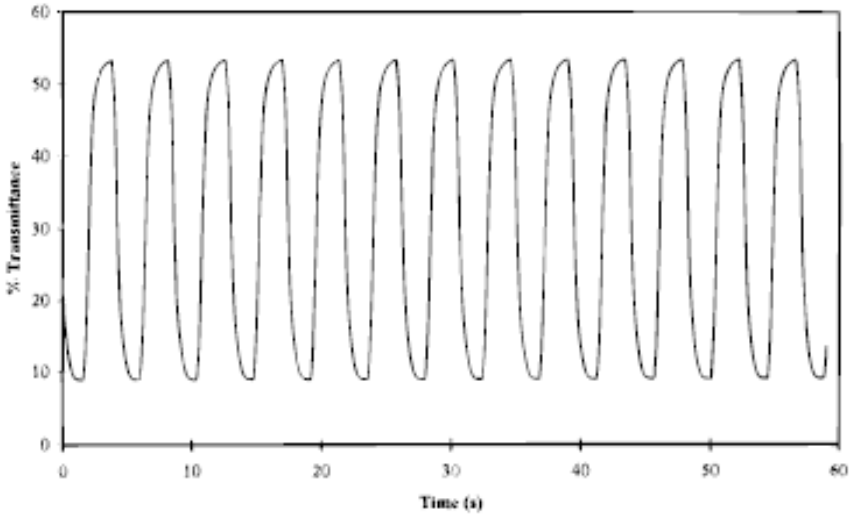

Figure 2.11 Electrochromic switching, optical absorbance change monitored at 590 nm for PEDOT in 0.1 M TBAP/ACN. [Reprinted with permission from A. Kumar, D. M.Welsh, M. C. Morvant, F. Piroux, K. A. Abboud, and J.R. Reynolds, *Chem. Mater*. 1998, 10, 896.Copyright 1997 American Chemical Society] [97]

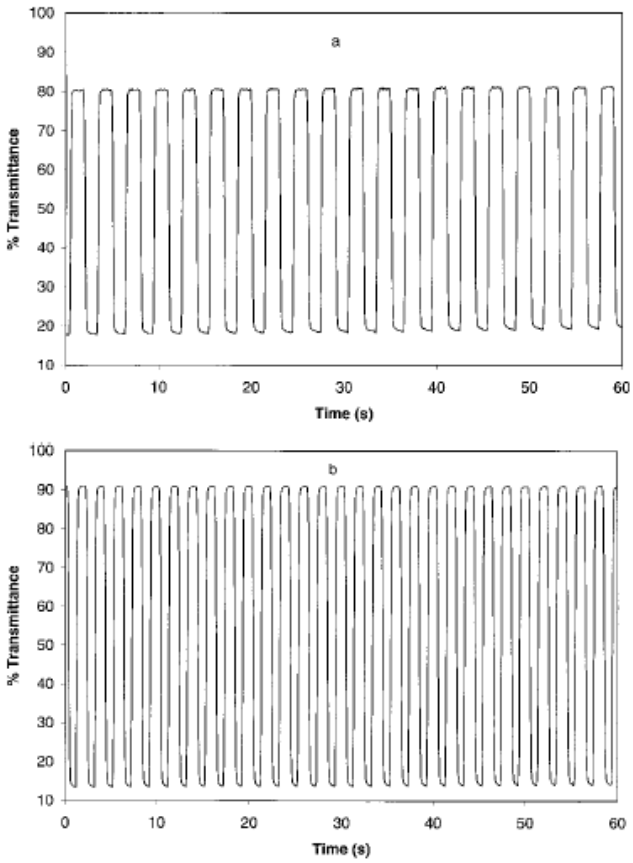

Figure 2.12 Optical switching for PProDOT (a) at 100 nm film thickness and PProDOT ± Me2 (b) at 150 nm film thickness monitored at 578 nm. [D. M. Welsh, A. Kumar, E. W. Meijer, and J. R. Reynolds, Enhanced Contrast Ratios and Rapid Switching in Electrochromics Based on Poly(3,4-propylenedioxythiophene) Derivatives, *Adv. Mater.* **1999**, 11, 1379. Copyright Wiley-VCH Verlag GmbH & Co. KGaA. Reproduced with permission.][98]

This section has contained the discussion of the many ways by which EC devices can be assembled, but the most important and extensively studied is the solid-state or sandwich approach as it provides fast switching speeds with high contrast ratio. The construction of solid-state EC devices will be the same whether a large area cell or one small element (pixel) of a multi-electrode array is required.[100]

While different kinds of EC devices can be distinguished according to their construction pattern, they can also be categorized on the basis of the number of EC materials changing color. That is, it is possible to have either a ***single*** or ***dual*** electrochrome in which either one or both of the materials in the device are electrochromic, respectively. The use of this terminology for the

description of the EC devices is very limited, however, and will not be discussed in detail in this literature review.

Concerning the electrolytes, solid polymer electrolytes are classified into two main categories: *Salt host*, which consists of anhydrous employed polymer electrolytes with a host matrix polymer such as polyethyleneoxide (PEO), polyacrylonitrile (PAN) etc., while the other is *Polyelectrolytes,* which have high ion conductivity and mechanical flexibility during hydration, eg. PAMPS, Nafion etc. High electrical conduction of hydrated polyelectrolyes in thick films makes them an obvious choice for solid polymer electrolytes.

2.5 Analysis Techniques

There are a few analysis techniques that are necessary in order to discern key information concerning the electrochemical process. Modern analytic electrochemistry techniques have been developed to measure very small responses of a vast array of properties. Some of the most important techniques employed for electrochromic materials are discussed here.

2.5.1 Cyclic Voltammetry (CV)

The use of various kinds of electrochemical methods that can be applied to electrochromic materials deposited on a conductive substrate is fairly broad and for conducting polymers it was covered in detail by Doblhofer et al.[101] Of all the electrochemical methods, cyclic voltammetry (CV) is one of the easiest ways to study the redox states of a material due its to simple and versatile approach. In CV, current entering or exiting an electrode is monitored and the potential of the working electrode is cycled between upper and lower limits. Current peaks versus voltage are plotted to obtain the oxidation and reduction potentials during the complete cycle. In other words, the current is measured while the potential is increased linearly from an initial potential to a peak potential and back to the initial potential again.[102] Resistance in the electrodes makes it possible to distinguish between different degrees of irreversibility. In addition to this,

information regarding the stability of the product can be easily revealed during multiple redox cycles. Both fast and slow reactions can be followed as the rate of potential scan can be easily varied. The peak current can be calculated by the Randles-Sevcik equation[103], which is

$$i_p = (2.69 \times 10^5)\, n^{3/2} A D^{1/2} C^b \nu^{1/2} \qquad (1)$$

where n is the number of electrons, A is the surface area of the electrode (cm^2), D is the diffusion constant (cm^2/s), C^b is the concentration of the electrolyte (mol/cm^3), and ν is the scan rate (V/s). Hence, when the reaction is diffusion-controlled, the peak current should be proportional to the square root of the scan rate. If the process is non-diffusion controlled (i.e. surface controlled) then it cannot be described using the Randles-Sevcik equation discussed above and the peak current is represented by[104,105] :

$$i_p = n^2 F^2 \Gamma \nu / 4RT \qquad (2)$$

where Γ is the concentration of the surface bound electroactive species (mol/cm^2) and F is the Faradays constant (96,485 C/mol). Hence, in the case of species to be surface bound, both the anodic and cathodic peak current will be linearly proportional to the scan rates.

One of the recent papers by Reynolds et al. explained in detail the electrochemical characterization of different number of bilayers for an LbL film of PAH/PEDOT-S.[63a] Figure 2.13 shows that the peak current value of the oxidation and reduction peak increase with an increase in number of bilayers from 3 to 12, which means that the current needed to oxidize the film linearly increased as the number of bilayers increased, but achieves a saturation at approximately 20 bilayers. Figure 2.14 shows the linear relationship of peak current with scan rate (not square root of scan rate) for LbL films containing 10 to 50 bilayers for scan rates as high as 1000 mV/s This shows that the electrochemical reaction wasn't diffusion controlled but surface controlled. Sometimes, it has been observed that the films formed by LbL fabrication technique are quite thin and display an increase in redox potentials (peak skewing) for both cathodic and anodic peaks due to an increase in the internal resistance of the bulk film.

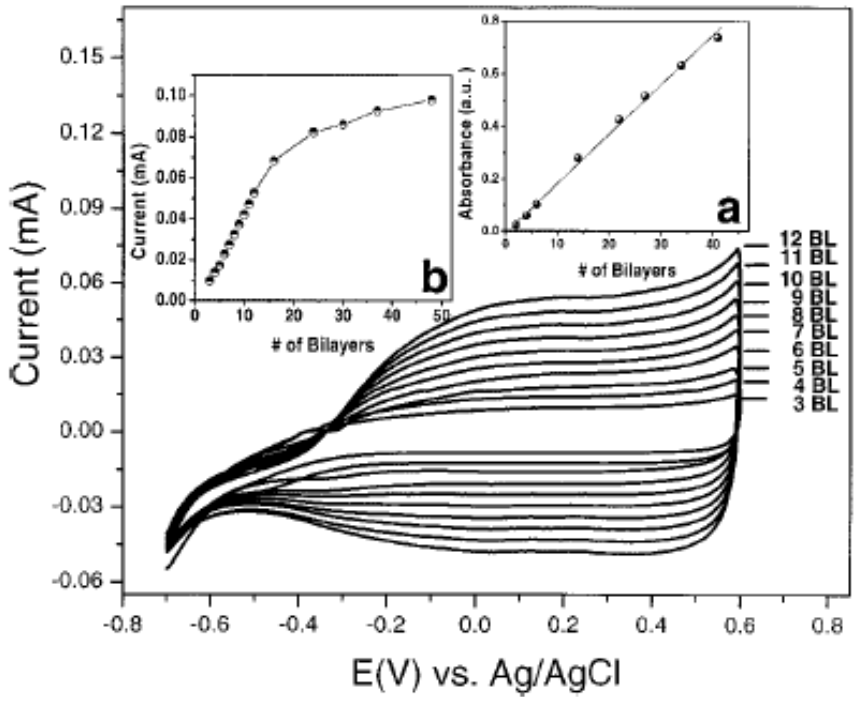

Figure 2.13 CVs of sequential bilayer deposition, from 3-12 BLs at a scan rate of 50mV/s, between -0.8V to + 0.6V. Inset [a] The absorbance of PAH/PEDOT-S films v/s the number of bilayers deposited on ITO-coated glass. [b] peak current v/s number of bilayers deposited. [C. A. Cutler, M. Bouguettaya, J. R. Reynolds, PEDOT Polyelectrolyte Based Electrochromic Films via Electrostatic Adsorption, *Adv. Mater.* **2002**, *14*, 684.Copyright Wiley-VCH Verlag GmbH & Co. KGaA. Reproduced with permission.] [63(a)]

2.5.2. Square wave switching

The number of redox centers present in the film can be calculated through the Faradic charge density by square wave switching. In this technique, the electrode potential is continuously switched between the potential where the electrochromic material on the device goes from completely reduced to oxidized and vice-versa. It is a multiple-step process, which is monitored during the square wave switching. Electrodes containing capacitive charges can be easily determined by switching experiments. This means that the speed of color change of the film can be directly observed by the speed of current decay, which is also the speed that the Columbic integration approaches a limiting value.[106] Electrochromic switching speed measurements of the

films are usually performed both in liquid electrolyte solution as well as in solid state. Here, we explain the principle for solid-state switching, as the basic concept is the same behind both.

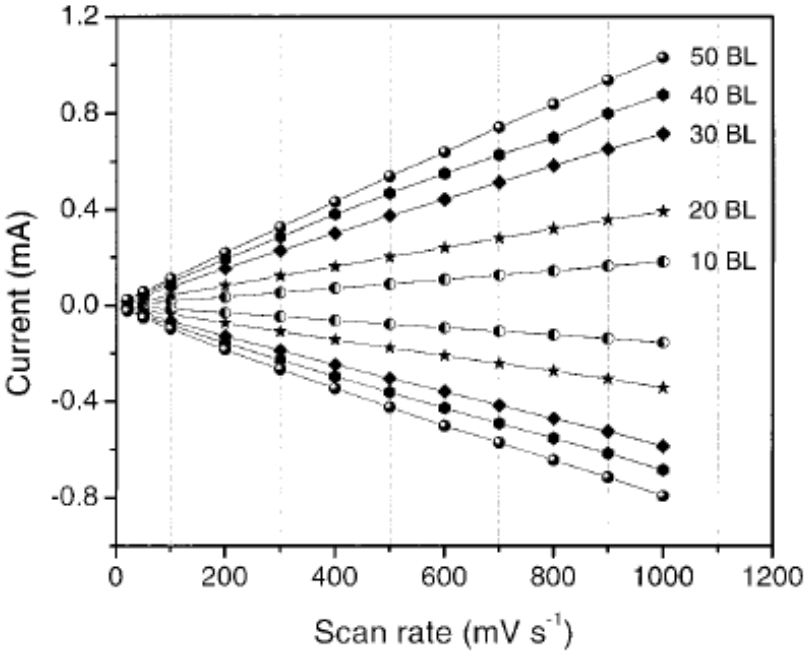

Figure 2.14 Scan rate dependence of PAH/PEDOT-S multilayer films of 10-50 BLs CVs were scanned between -0.7V and +0.6V (vs Ag/AgCl) at scan rate ranges from 200-1000mV/s. [C. A. Cutler, M. Bouguettaya, J. R. Reynolds, PEDOT Polyelectrolyte Based Electrochromic Films via Electrostatic Adsorption, *Adv. Mater.* **2002**, *14*, 684.Copyright Wiley-VCH Verlag GmbH & Co. KGaA. Reproduced with permission.] [63(a)]

Switching speed measurements of solid-state devices (or device in liquid electrolyte) were done as shown in Figure 2.15. The set-up consisted of a laser (the most common one is He-Ne (633 nm) laser, but there are examples of usage of other lasers in the literature as well), which was passed through optical density filters which were in contact (to reduce stray light background) with a photodiode. The sample electrodes were connected to an HP Pulse Generator. The signal of the pulse generator was monitored on Ch1 of a Tektronix Digital Oscilloscope, and the signal of the photodiode was sent to Ch2. A square wave pulse was sent to the EC device that subsequently caused a decrease in the amount of light detected by the photodiode. Usually, the

maximum spectral change was not in the region of the wavelength of the laser, but since the goal of the switching experiments was simply to measure the response time (which should be independent of wavelength), the spectral change observed at the wavelength of the laser was sufficient for that purpose.

In a similar way, the switching speed measurement for a liquid electrolyte cell device can be performed by applying the voltage between an ITO electrode and a platinum counter electrode and keeping rest of the parameters similar to the switching speed measurement of solid-state device. The important thing to note in the case of liquid electrolyte cell is that the device is kept in a special cell cuvette that can hold liquid salt solution.

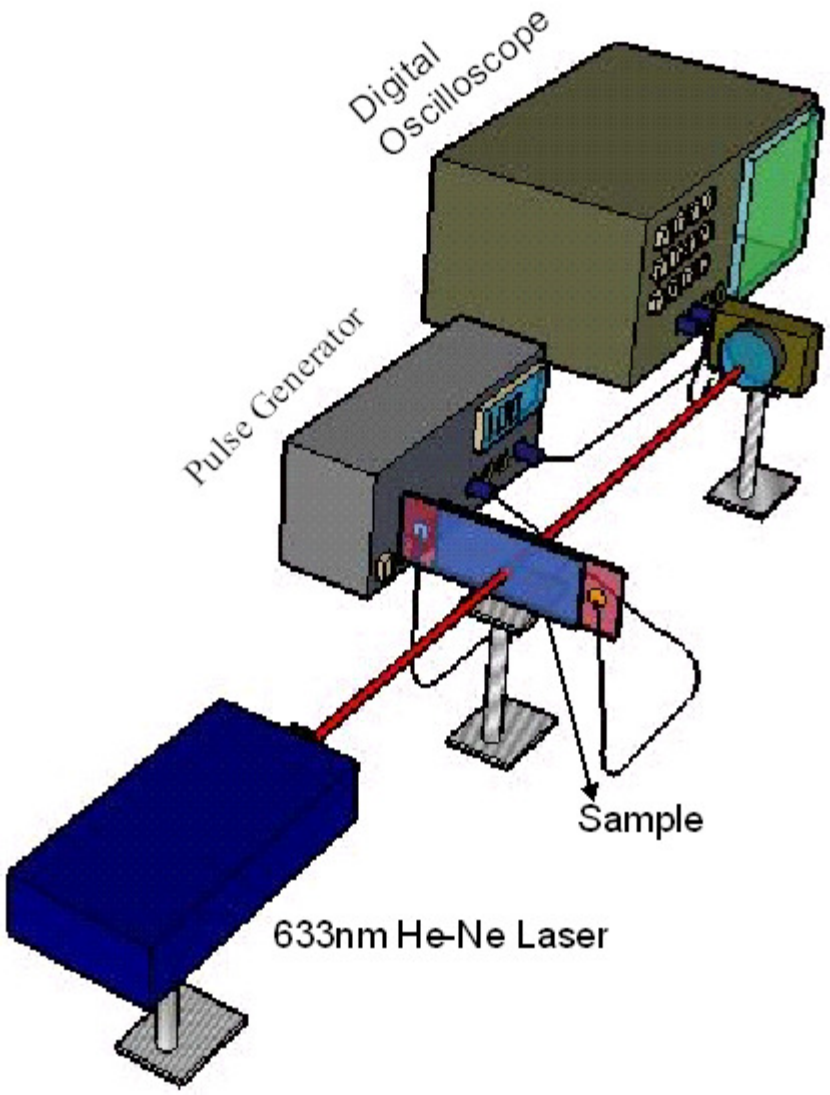

Figure 2.15 Switching speed experiment on a solid-state electrochromic device. [*Diagram courtesy of Reza Montazami, Physics, Virginia Tech*]

Measurement of the lifespan of an electrochromic device can be done easily by leaving the device at a particular frequency on the voltage needed for the color change. Any degradation in the color or spectral change can be noticed by a change in the value of the photodiode response, which is the raw data for the spectral change. The photodiode response can be represented in terms of absorption or transmittance, by calibrating the laser through a known filter of absorbance value and recording the change in the photodiode value.

Figure 2.16 shows the switching curve (Figure 2.16.a) as well as the degradation (Figure 2.16.b) in the device with the number of cycles. The literature has been divided as to how to quantify the switching time. For example in the figure shown below[107], the authors have taken that the response time is indicated as the time needed to reach 2/3 of the total transmittance change at a given switching cycle; however, our research group and many others have taken it to be 90% of the overall transmittance/absorbance change.

2.5.3. Spectroelectrochemistry

The measurement of the spectral change of an electrochromic device, both in a liquid electrolyte cell and in solid-state is known as spectroelectrochemistry. It was performed using a spectrophotometer by passing a collimated UV-Vis light beam through an electrode placed in an electrochemical cell[108] (in the case of liquid electrolyte device; solid-state devices don't need one) and measurements were taken while the electrode is at different potentials, i.e. colored or dis-colored (Figure 2.17). Optical absorbance data of the electrochromic device are usually presented as either transmittance (%T) or absorbance units versus wavelength of light or photon energy. The absorption spectrum of a substance represents the relative intensity (relative number of photons) absorbed at each wavelength.[8]

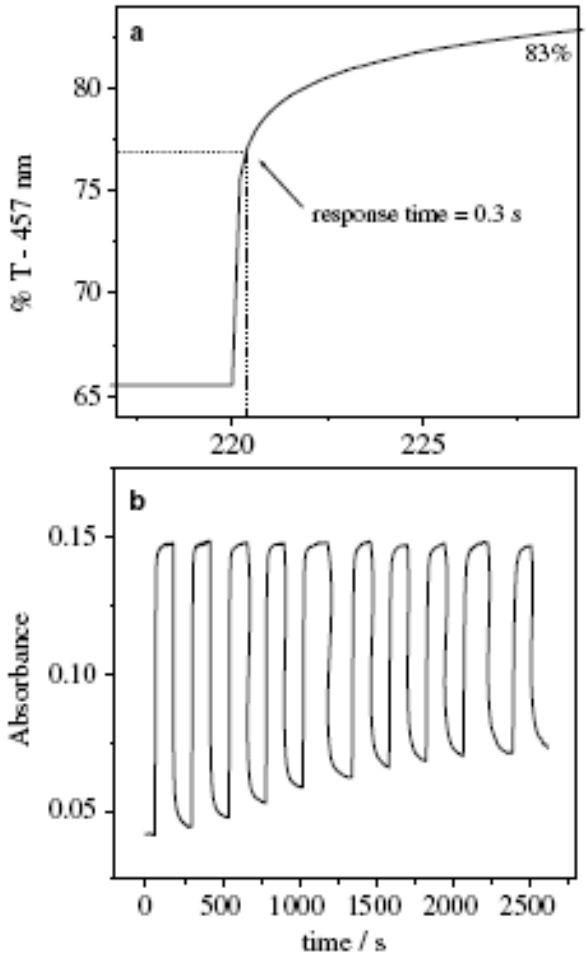

Figure 2.16(a) %T/t chronoamperometric profile for a 3-bilayers $Ni(OH)_2$ nanoparticles electrode. The response time is indicated as the time needed to reach 2/3 of the total transmittance change. (b) Absorbance as a function of time profile recorded by switching the potential between 0.0 and 0.55 V for a 3-bilayers $Ni(OH)_2$ nanoparticles electrode. Electrolytic solution: KOH 0.1 mol/l. [Reprinted from M. Vidotti, C. Greco, E. A. Ponzio, S. I. C. de Torresi, Sonochemically synthesized Ni(OH)2 and Co(OH)2 nanoparticles and their application in electrochromic electrodes, *Electrochemistry Communications*, **2006**, 8, 554 with permission from Elsevier] [107]

The Beer-Lambert law for optical absorption relates the absorbance, expressed as the log of the ratio of the intensities, to the concentration *c* of chromophore and optical pathlength *l* through the sample[3,8,109] :

$$A = Log\ (Io/I) = \varepsilon cl \quad \text{---} \qquad (3)$$

The molar extinction coefficient (ε) of the absorbing species being evaluated, along with path length and concentration, determines the percent transmittance (%T = I/I_0). In the case of electrochromic films, the path length *l* is the film thickness and the *c* is the concentration of solid chromophore. In the case of the actual spectral measurement (see Figure 2.18), the first tramsmittance/absorbance scan was usually done in the neutral state before any potential is applied. After this, a stepwise (+0.1V) increase in the voltage was done over the desired range while recording an absorbance scan each time the potential is changed. A change in the absorbance value of the electrochromic device at a particular wavelength showed that the color had changed because of a change in the redox state of the electrochromic device.

Figure 2.17 Digital photographs of bleached (colorless) and colored state (dark violet) of a polyviologen electrochromic device in an electrochemical cell. The alligator clip on the left hand side of both images acts as a counter-electrode.

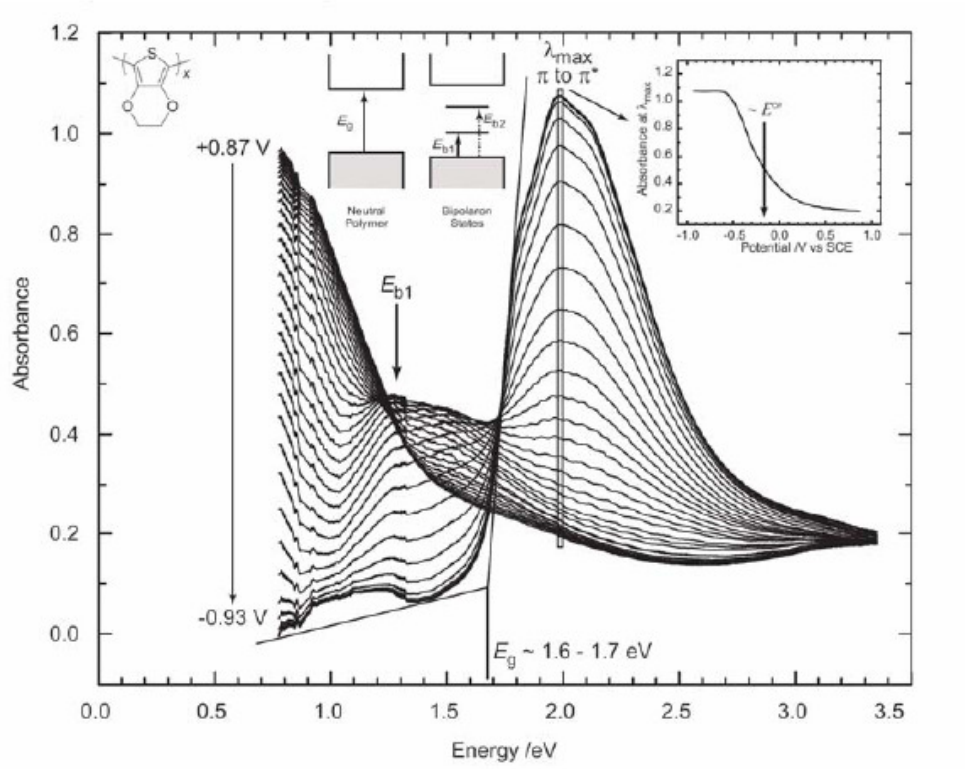

Figure 2.18 Spectroelectrochemistry of a PEDOT film on an ITO slide.[110]

Similar measurements were also done in the case of transmittance scans for the solid-state devices, but no electrochemical cells were used in this case. Neither water nor any other solvent is involved in this latter case. Instead, a gel polyelectrolyte was used. In our labs, the spectral changes were recorded with an optical fiber instrument known as Filmetrics. A conventional style uv-Vis spectrophotometer can also be used in this case, but results with the Filmetrics instrument were found to be more accurate.

2.5.4. Coloration efficiency (η)

Coloration efficiency is a very common terminology (rather than a technique) used in the field of electrochromics. It is determined from the spectroelectrochemistry and CV. It is thus included here after the topic "Spectroelectrochemistry." For the electrochromic devices, the color change

is better expressed in terms of coloration efficiency (η), which is determined at the wavelength maximum λ_{max}; in other words η is defined as the relationship between the changes in optical density to the total injected/ejected charge as a function of the electrode area.[111] For electrochromic materials to be employed in fast-switching and efficient display operations, the value of η should be as high as possible. There has been a report of η as high as 1400 $cm^2.C^{-1}$ in the case of a conducting polymer-based electrochromic device.[112,113] The best coloration efficiency value of any polyviologen system reported to date is 170 $cm^2.C^{-1}$.[114] Here, an example (taken from reference 108) on how to calculate the coloration efficiency will help in providing better understanding to the reader. The change in the transmittance state from colorless to dark violet gives an optical density of

$$\Delta OD\ (\lambda) = \log [T_b\ (\lambda)/ T_c\ (\lambda)] \quad (4)$$

$$= 0.49$$

$$\text{where } \eta\ (\lambda) = \Delta OD\ (\lambda)/Q_d \quad (5)$$

in which Q_d = 8.8 $mC.cm^{-2}$ for the reduction step and is calculated as the area under the CV curve for the reduction peak for the scan rate of 100 mV/s. The active working area of the film on the ITO electrode was 10 cm^2.

$$\eta\ (\lambda) = 57\ cm^2.C^{-1}$$

The absence of a second reduction peak in the CV curve, even at low scan rates, makes it difficult to calculate the charge required for the second reduction step from monocationic to the completely reduced state. As explained by Cinnsealach et al., [109] the extinction coefficient (ε) of the reduced PV, assuming that every electron injected into the ITO electrode reduces a viologen moiety, can be expressed as:

$$\varepsilon\ (\lambda) = \eta\ (\lambda)\ F/1000 = 96.5\ \eta\ (\lambda) \quad (6)$$

in which F is the Faraday constant (96.5 x 10^3 C.mol^{-1}).

The value of ε for the reduced PV film at 515 nm was 5.3 x 10^3 $M^{-1}cm^{-1}$, which falls within the range of values reported by Monk et al. [8] for bipyridinium systems.

2.5.5. Impedance analysis

RC or AC impedance is a voltammetric technique to calculate the Faradic contribution employed in electrochemical reactions. However, the work related with the EC polymers deals with small potentials so impedance analysis is used to determine ionic motion in the solid electrolytes as a non-Faradic contribution.
The impedance Z is comprised of two components, real and imaginary ($Z^{'}$ and $Z^{''}$ respectively)

$$Z = Z^{'} - j\,Z^{''} \qquad (7)$$

Where $j = (-1)^{½}$

This technique has not been used much in studying the electrochemical properties of EC films fabricated by LbL process and hence its explanation is very limited in this review.

2.6 Electrochromic (EC) Materials

The classes of EC materials are divided into several subcategories.

2.6.1. Organic Systems

2.6.1.1. Viologens

Since the first major report on electrochromism, there has been much work done in the field of inorganic[115] and phthalocyanine[116,117] compounds as possible electrochromic materials, while

work with conducting polymeric[118,119] electrochromic devices has gained significant attention in last decade or so. Other electrochromic materials have been studied, but polyviologens (which are bipyridinium systems) and their derivatives have been widely investigated for more than thirty-five years because of their electrical and electrochromic properties and good environmental stability.[120] Viologens are some of the most important materials in the EC materials library, and were the first ones to be studied through the LbL film fabrication method by Schlenoff et al.[30] Multilayers of electrochemically active viologen units in the form of poly(butanyl viologen)(PBV) were deposited with poly(styrene sulfonate)(PSS) by LbL deposition technique. This was the first time a redox active polyelectrolyte has been deposited using this approach and the films showed stable reversible electrochemical behavior, although no electrochromic properties of PBV were discussed. The authors also made efforts to explain the internal morphology of the multilayer films by measuring the extent of interpenetration of one layer in the adjacent layers; this is confirmed by variable-angle XPS.[30] Small molecule viologens are the largest family of chemical compounds that have been investigated for EC properties.[8] A great amount of work has been done for dialkyl bipyridinium units, but significant efforts have also been made from time to time on the modification of their chemical structures to improve the electrochromic properties[121] and film-forming abilities. Out of all the states, the colorless dication is the most stable, followed by the radical cation, whose stability depends upon the delocalization of the radical electron in the π-framework and then the unstable neutral state Electrochromism in bipyridinium species occurs due to the interconverison of these three species. Manipulation of the substituents at N and N' modifies the color by attaining the appropriate molecular orbital energy levels. Suitable substitution not only results in fine color tuning of the polyviologen system, but also results in the alteration of the redox and other physical properties without disturbing the electroactivity. Attached groups (aryl or alkyl) influence the reduction potential (E°), but further substitution of the aromatic system helps in tuning the rate of electron transfer between the redox species and influences the contrast, switching speed and coloration efficiency. Recently polyviologens have been applied in liquid crystal devices, [122] light emitting diodes, [123] printing [124] and frozen food monitoring.

There are three common bipyridinium redox states: a dication ($bipm2^{+}$), which is colorless; a radical cation ($bipm^{+\bullet}$), which is of intense color; and a di-reduced neutral compound ($bipm^{\circ}$), which is of weak color. The reductive electron transfers take place as follows [8]:

$$\underset{\text{(Colorless)}}{bipm^{2+}} + e^{-} \rightarrow \underset{\text{(Intense color)}}{bipm^{+\bullet}} \qquad (8)$$

Little is known about the third redox form, as it is not of primary importance because of its tendency to show weak contrast. However, the reduction takes place as:

$$\underset{\text{(Intense Color)}}{bipm^{+\bullet}} + e^{-} \rightarrow \underset{\text{(Weak Color)}}{bipm^{\circ}} \qquad (9)$$

The main reasons these systems are not used in displays are their slow switching speeds and inability to work in solid-state form. Being an important member of the EC materials library, it is important to synthesize several different PVs, substituted by various groups at branches, for faster ionic motion and high contrast. Lee et al.[125,126] studied the electrochromic properties of polythiophene and polycarbazole derivatives with a viologen as a pendant unit by electropolymerization, but the whole process was tedious and expensive and there is no report of the device stability, which has been one of the main drawbacks of polyviologen-based electrochromic devices.

The electrochromic properties of viologens are well documented and have received significant attention for the past thirty-five years because of their electrical and electrochromic properties and good environmental stability[127,128,129,4], but with the exception of TiO_2 microparticles modified with viologen pendants,[130] all of these reports describe electrodeposited or polymeric thin films of 1, 1'-substituted-4,4'-bipyridinium salts. Suh[131] and Neoh[132] et al. were the first to have shown the fabrication of viologen functionalized polymeric micro and nanospheres, respectively. In addition, Suh et al. also showed the application of the mono-dispersed, micrometer-size range poly(styrene-co-crylonitrile) microspheres with different lengths of the viologen pendant group in reflective EC devices as well.[133] Improvement in switching speed

(<1s) with a significant drop in contrast (< 30%) was observed, but the overall device fabrication is tedious and thin film device with long-term stability (>10000 cycles) is a distant possibility.[134] The switching speed of 270 ms was the best performance shown by this kind of device and by doing so the authors significantly sacrificed the contrast. In addition, porous polymeric microspheres are fairly big (>20 μm) in size and it is very difficult to imagine the possibility of a display containing these microparticles also having < 10 μm^2 pixel size. Along the same lines, Shea et al. were the first to show synthesis of viologen-bridged polysilsesquioxane spherical nanoparticles[135] The nanoparticles described were prepared by inverse water-in-oil microemulsion polymerization.[136,137] Briefly, the emulsions were prepared using NP-5 as the surfactant and 1-hexanol as the co-surfactant to disperse 0.4 M aqueous 1, 1'-bis [3-(trimethoxysilyl)propyl]-4,4'-bipyridinium iodide solutions in cyclohexane. 1,1'-bis[3-(trimethoxysilyl)propyl]-4,4'-bipyridinium iodide was prepared from 3-iodopropyltrimethoxysilane and bipyridyl according to published procedure by Bookbinder et al.[138] Here, each microemulsion droplet acts as a "container" where the sol-gel reaction takes place (Figure 2.19).

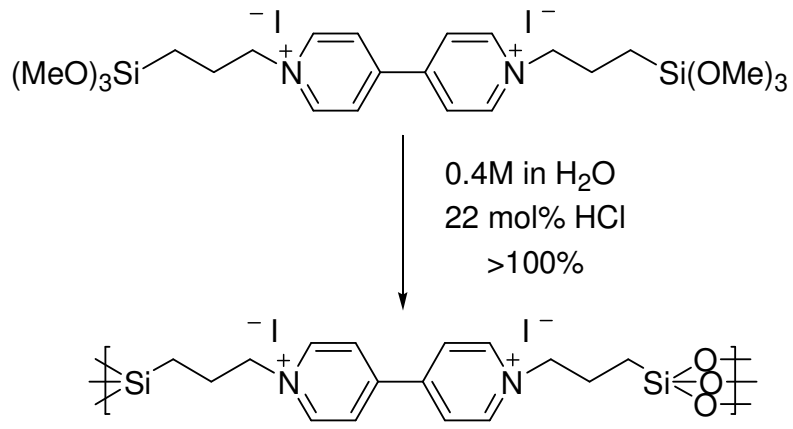

Figure 2.19 Sol-gel polymerization of 1,1'-bis[3-(trimethoxysilyl)propyl]-4,4'-bipyridinium iodide. [Reprinted with permission from M. Khiterer, K. J. Shea, *Nano Lett* 2007, 7, 2684.Copyright 2007 American Chemical Society] [135]

After addition of the catalyst (HCl), the emulsions were allowed to age for 48 h to provide time for the formation of stable, solid BPS gel particles. The particles were precipitated with ethanol

and washed with water to remove residual surfactant. To determine particle size and distribution, wet gel particle microemulsions were analyzed by dynamic light scattering. The samples were also drop deposited onto Si wafer substrates, allowed to dry over a period of 24 h, then analyzed by scanning electron microscopy (Figure 2.20). The internal structure of the BPS nanoparticles was also investigated using transmission electron microscopy (Figure 2.20). The material was found to be uniform and featureless with no apparent phase separation or long-range order.

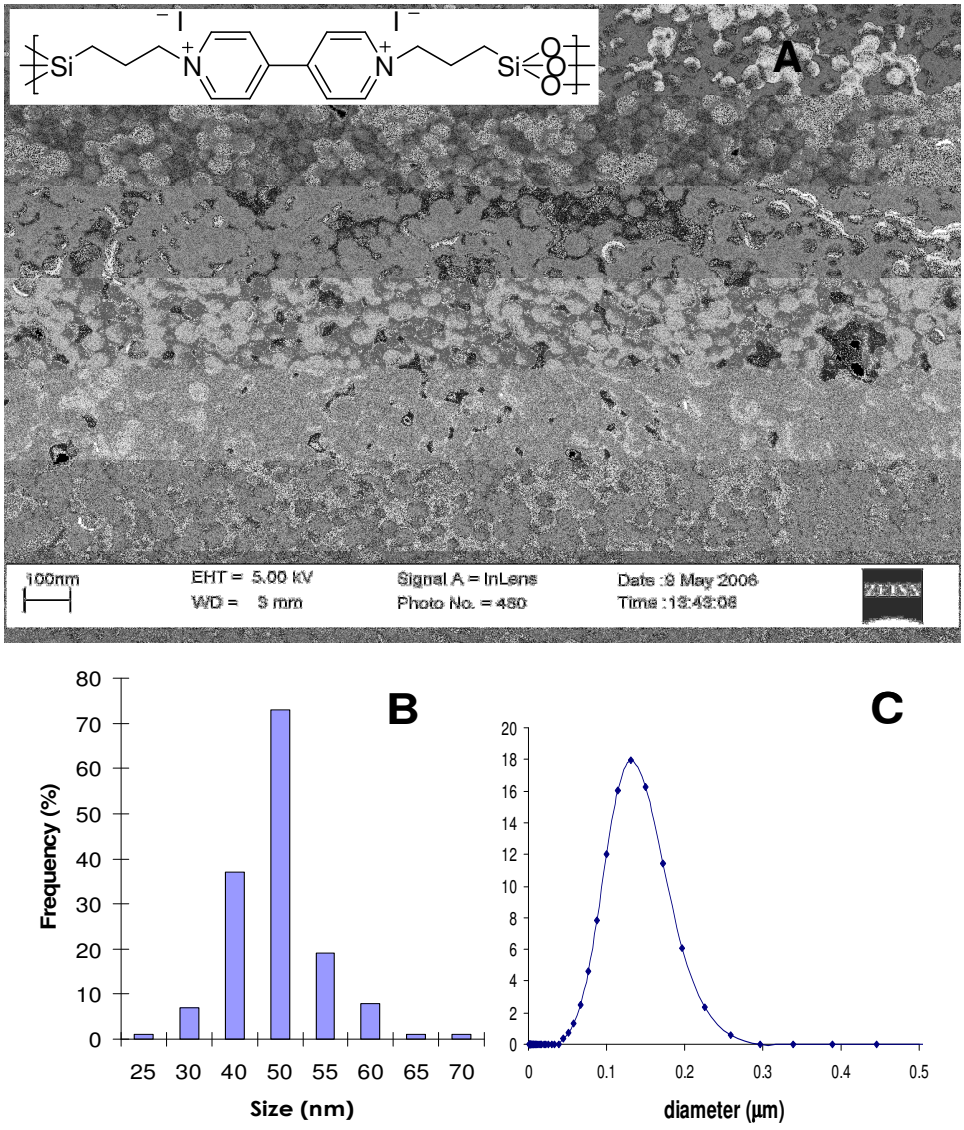

Figure 2.20 1,1'-Bis[3-(trimethoxysilyl)propyl]-4,4'-bipyridinium iodide BPS nanoparticles A). Scanning Electron Micrograph of dried xerogel, B). Size distribution of the particles in A). C)

Size distribution of wet gel particles in microemulsion. [Reprinted with permission from M. Khiterer, K. J. Shea, *Nano Lett* 2007, 7, 2684.Copyright 2007 American Chemical Society][135]

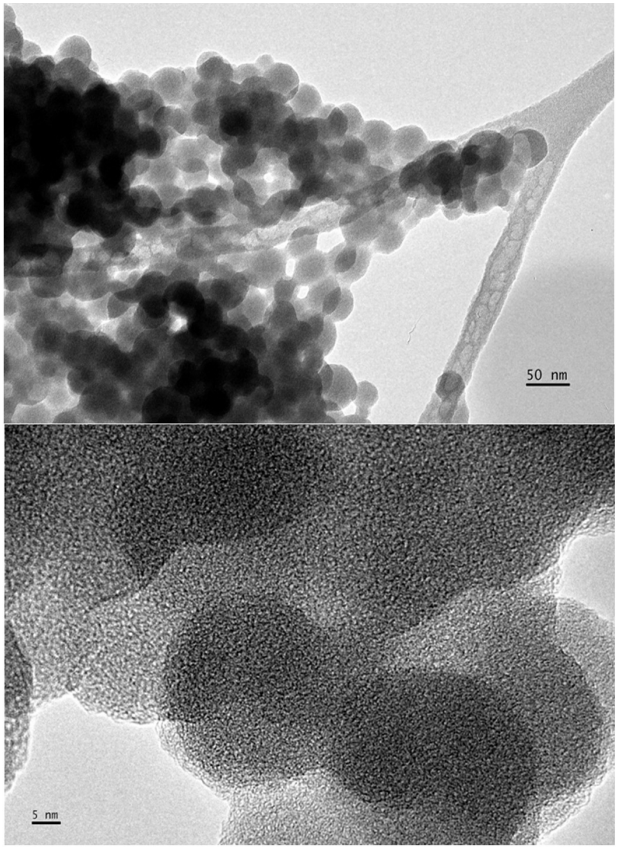

Figure 2.21 Transmission Electron Microscopy of BPS nanoparticles prepared from 1,1'-bis[3-(trimethoxysilyl)propyl]-4,4'-Bipyridinium iodide. [Reprinted with permission from M. Khiterer, K. J. Shea, *Nano Lett* 2007, 7, 2684.Copyright 2007 American Chemical Society] [135]

Bridged polysilsesquioxanes (BPS) are hybrid network materials that have organic and inorganic domains dispersed at the molecular level.[139,140,141] Since the organic group remains an integral component of the material, this variability provides an opportunity to modulate bulk properties such as porosity, thermal stability, refractive index, optical clarity, chemical function, hydrophobicity and dielectric constant. The organic component not only strongly contributes to the bulk physical properties, but also provides functionality to the materials. The fine degree of

control over the bulk chemical and physical properties has made these materials candidates for applications in optical devices,[142,143,144,145,146] as high capacity absorbents,[147,148,149] 3D information storage media,[150] and proton conducting media for fuel cells.[151,152] Work related to polysilsesquioxane (POSS) in EC devices is quite new. Lu et al. showed the importance of porosity and facile ion diffusion of POSS.[153] Although the results were interesting, the nanosized POSS in their work was not water-soluble, had a long switching time with low coloration efficiency and resulted in significant red/blue shift during spectro-electrochemical measurements. POSS-PANI have shown improved contrast as compared to PANI, but still the work is in preliminary stages and even the films fabricated with a high concentration (1 mol%) of POSS-PANI have low ionic (3.29×10^{-5} Scm^{-1}) and electrical (1.7×10^{-4} Scm^{-1}) conductivity, making the overall device switch very slow.

Several groups have previously reported [154,155,156,157] polyviologen electrochromic devices on mesoporous electrodes for display purposes, but the major breakthrough in this field came from the work done by Ntera Inc. [158] Moller et al. (Ntera Inc) showed low-power-consuming EC displays, in which switching in the millisecond or second range was possible, and the technology was based on the combination of top-down (inkject technology) and bottom-up ideas (molecular trapping of electrochromophores in mesorpores).[160] The authors showed that the large to small area coloring electrodes was possible by exposing the conductive glass surface to sub-millimolar solution of phosphoric acid functionalized-viologens attached to TiO_2 nanoparticles. Scientists at Ntera further improved their approach and demonstrated that multi-color displays (figure 2.22) were possible by selective patterning of different electrochromophores onto different areas of conductive working electrode.[159] In this work, they showed that nanochromic displays need low driving voltage (-1.3V) to switch and exhibit a high contrast ratio along with excellent readability that is independent to the viewing angle.

Hammond et al. showed various combinations of Poly hexyl viologen (PXV) and Poly butylviologen (PBV) with nafion, PAMPS, PEDOT: SPS by LbL film fabrication technique. The best response was received by a 45-layer pair of PXV/ PEDOT: SPS, which exhibited a transmittance change of 82.1 % at 525 nm and a color change time of 1-4 s.[52] This was the best-reported transmittance change to date from any kind of EC formation technique. Due to the

Figure 2.22 Nanochromics displays. [Reprinted from N. Vlachopoulos, J. Nissfolk, M. Moller, A, Briancon, D. Corr, M. Ryan, A. Hagfeldt, Electrochemical aspects of display technology based on nanostructured titanium dioxide with attached viologen chromophores, *Electrochim. Acta*, **2008**, 53, 4065 with permission from Elsevier] [159]

unusual film architecture and complex interaction between PXV and PEDOT, a charge trapping system was formed with the layers; resulting in a type of electrochemical rectification.[30] Trapping between the layers showed an incomplete bleached state in a 50-bilayer film but it is complete in 40 bilayers. To overcome this problem, Hammond et al. optimized the above-mentioned best result at 45 bilayers. Effective potentials at which coloration occurs in PXV/ PEDOT: SPS from sky-blue color when oxidized, to a deep blue coloration when reduced, are -0.9 V, -0.4 V and 0.5 V. One unusual effect that was seen with this dual EC polymer was the exponential increase in the thickness with increasing layer-pair number. The authors showed that high contrast fast-switching multi-chromic displays was possible with the LbL technique along with the easy fabrication of complex nano-composites in a simple processing platform.

2.6.2. Inorganic Materials

Transition metal oxides and transition metal hexacyanometallates are two important classes of inorganic EC materials. Inorganic materials have the advantage of having multiple

electrochemical transitions because of the availability of multiple oxidation states for transition metal chromphores.

2.6.2.1. Tungsten Oxide (WO_3)

Tungsten oxide is by far the most widely studied inorganic EC material and was first reported in 1969.[3] Granqvist et al.[160] did extensive research on WO_3 and explained the redox chemistry, electrical, optical properties, and color efficiency characteristics involved with it in detail. Tungsten trioxides, with tungsten in the oxidation state W^{VI}, is in the transparent form, but changes to a blue color on first reduction, with W^{V} state gives the electrochromic effect (Figure 2.23).[161]

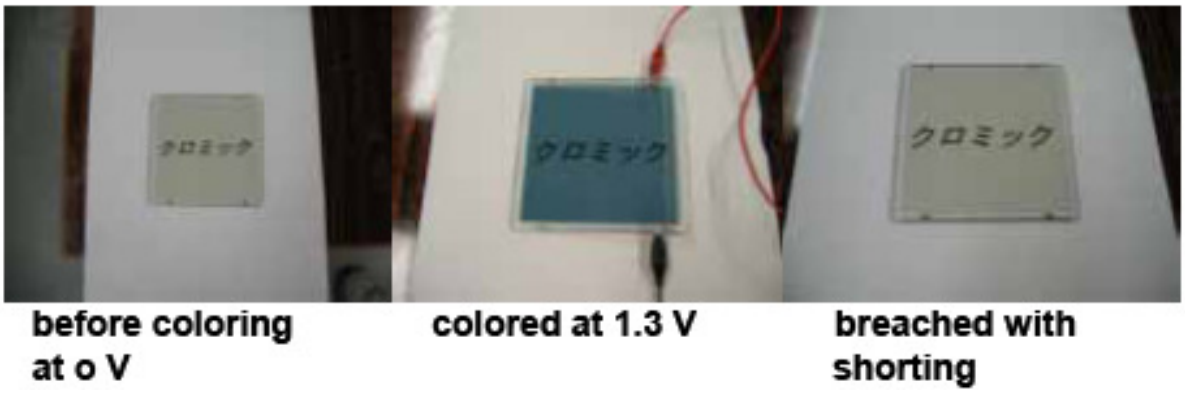

Figure 2.23 Bleaching and coloring states in a transparent WO_3 EC cell.[162]

Although the detailed coloration mechanism is still controversial, it is generally accepted that intercalation, which is the insertion of protons or alkali metal cations from the electrolyte into the metal oxide film, is responsible for the coloration in WO_3. If the electrolyte contains Li^+ cations the color changing reaction can be written as

$$\underset{\text{(transparent)}}{WO_3} + x(Li^+ + e^-) \rightarrow \underset{\text{(blue)}}{Li_xW^{VI}_{(1-x)}W^{V}_{x}O_3} \qquad (10)$$

Lower x brings the intense blue color, which is caused by the photoeffected intervalence charge transfer (CT) and that happens with the adjacent W^{V} and W^{VI} sites.[3,8] It was also observed that at higher x, irreversible insertion forms a metallic "bronze" which is red or golden in color.

In addition, Granquist et al. also explained various techniques of depositing WO_3 on ITO, which were done by evaporation in *vacuo*, sputter-deposition, electrochemical oxidation of tungsten metal, sol-gel methods and chemical vapor deposition (CVD).[76] One of the first commercial applications of the WO_3 in smart windows for temperature control inside a building, thus reducing the winter heating and summer cooling requirements, was demonstrated by a glass manufacturer, Pilkington Technology.[162]

As discussed before, the above-mentioned techniques can form thin films of WO_3, but most of these techniques form highly disordered films. These films might be suitable for laboratory studies but the inhomogeneous, rough and weak films are not yet considered suitable for fast-switching display applications. The LbL film fabrication method gives a variety of advantages that are not possible with other film fabrication processes. LbL film fabrication of WO_3 have been shown before by Oliveira et al.,[163] but only once the electrochromic properties of LbL films of WO_3 were studied by Fendler et al.[164] The electrochromic study of these LbL films showed poor performance of a contrast of less than 25% and switching response time of 100 s for both colored and bleached cycles and that too when the switching time was obtained from 80% absorbance change. The insoluble nature of WO_3 makes it difficult to have a uniform dispersion in solution.

2.6.2.2. Prussian Blue (PB)

In the last two decades, the only inorganic non-oxide materials that have attracted significant attention for incorporation in low power electrochromic displays are those belonging to the metal hexacyanoferrate (HCNF) family.[3] Prussian Blue belongs to a very important family of mixed insoluble transition metal hexacyanoferrates which were extensively used as a pigment in the

formulation of paints, lacquers, and printing inks[1]. The chemical formula for insoluble and soluble PB is $Fe_4^{3+}[Fe^{2+}(CN)_6]_3$ and $KFe^{3+}[Fe^{2+}(CN)_6]_3$ respectively, and both of these forms possess a brilliant blue color-"cyan". A valence change of the component metal centers in the crystal causes a contributing change in the energy of charge transfer oscillation and brings electrochromism.

Table 2.1. Some of the important PB redox states:

State	Name	Acronym
$Fe(III)[Fe(III)(CN)_6]$	Prussian Brown	PX
$Fe(III)[Fe(III(CN)_6]/KFe(II)[Fe(III)(CN)_6]$-intermediate	Berlin Green	BG
$KFe(II)[Fe(III)(CN)_6]$	Prussian Blue	PB
$K2Fe(II)[Fe(II)(CN)_6]$	Prussian White	PW

The reactions and coloration can be schematically illustrated by only looking at the valence states of the iron ions, as

$$\underset{\text{Clear}}{(2+, 2+)} \leftrightarrow \underset{\text{Blue}}{(3+, 2+)} \leftrightarrow$$

$$\underset{\text{Green}}{[(1-\delta)(3+, 2+)+\delta(3+,3+)]} \leftrightarrow \underset{\text{Yellow}}{(3+, 3+)}$$

The general effect of PB as an effective high contrast[1,165,166] EC material opens the possibility of the fabrication of metal hexacyanoferrate thin films for a wide variety of device applications. Hammond et al.[52,167] showed the high ordered LbL film fabrication of PB with linear

poly(ethylene imine)(LPEI). The choice of LPEI rather than other weak polyelectrolytes was due to LPEI's ability to increase the conductivity by two orders of magnitude[168]. They showed that higher ionic conductivity can be achieved by carefully designing a unique assembly mechanism and have demonstrated the highest reported ionic conductivity (10^{-5}S/cm) for LbL films of LPEI and PAMPS of low concentrations. The LbL approach allows the fabrication of flexible film composites with practically unlimited compositional variation that possess a film architecture that can be controlled by manipulating nanoparticle size as well as varying LbL processing conditions.[30] PB is not completely soluble in water and most common solvents, so assembling high contrast and fast switching EC polymer/inorganic composites by depositing PB nanoparticles in the form of LbL films is a challenge. This is one of the reasons that work on forming PB nanoparticle LbL films had not been previously explored. Hammond et al.[52,167] did an excellent job in uniformly dispersing the "PB" nanoparticle; synthesis of these particles was done with $FeCl_2$ by step growth mechanism, rather than by a conventional controlled condensation method. The EC color change of LPEI/PB LbL films was indicated by spectroelectrochemistry. Figure 2.24 shows the color change from PW at -0.2V to cyan at 0.6 V; further potential increase gives green and yellow color at 1.0V and 1.5 V respectively. Switching time and contrast of the different bilayers of LPEI/PB are illustrated in Table 2.2. The switching speed is taken as the time required to attain 90% of the maximum absorbance change. The switching time is not fast

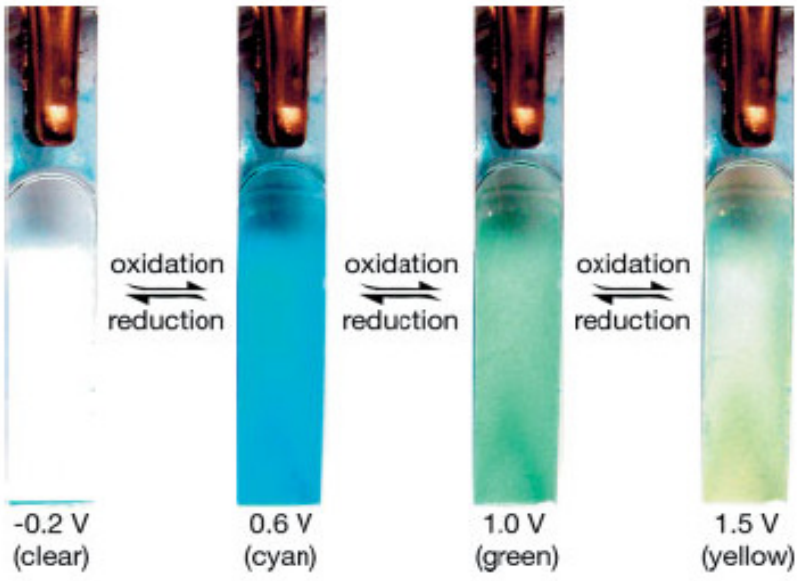

Figure 2.24 Photograph of extended potential range electrochromism of a 50 layer pair LPEI/PB film. The film was photographed immersed in an electrochemical cell after 30s equilibrium at the noted potential. [D. M. Delongchamp, P. T. Hammond, High-Contrast Electrochromism and Controllable Dissolution of Assembled Prussian Blue/Polymer Nanocomposites**,** *Adv. Funct. Mater.* **2004**, *14*, 224.Copyright Wiley-VCH Verlag GmbH & Co. KGaA. Reproduced with permission.][167]

Table 2.2: Switching time and contrast of the LPEI/PB series [D. M. Delongchamp, P. T. Hammond, High-Contrast Electrochromism and Controllable Dissolution of Assembled Prussian Blue/Polymer Nanocomposites**,** *Adv. Funct. Mater.* **2004**, *14*, 224.Copyright Wiley-VCH Verlag GmbH & Co. KGaA. Reproduced with permission.][167]

Layer pairs	Color time (s)	Bleach time (s)	ΔT % (λ=700nm)
10	0.63	0.83	16.5
20	1.55	2.15	37.6
30	2.84	2.78	54.0
40	3.98	4.98	63.3
50	4.60	5.10	72.4
60	5.48	5.88	77.4

enough to allow incorporation of these polymer/inorganic composite film commercially, but the work definitely gives a clear path for future work in this field.

2.6.2.3. Ruthenium Purple

In the HCNF family, Prussian Blue (PB) is by far the most studied electrochromic material. In contrast, Ruthenium Purple (RuP) has not been explored for electrochromic displays because the neutral form is insoluble in aqueous solution. Though nanocomposites incorporating polymer and inorganic materials have shown improved performance as compared to the separate constituents for mechanical stability, electrochemical activity, and solar energy conversion,[169] their use in electrochromic devices has not been well studied. RuP belongs to the class of well-defined zeolite-like poly nuclear inorganic materials with fixed metal ionic redox centers (e.g., Ru (II) and Fe (III)) (Figure 2.25) wherein the electroneutrality is maintained during the redox process by the movement of freely diffusing cations in and out of the lattice structure.[170]

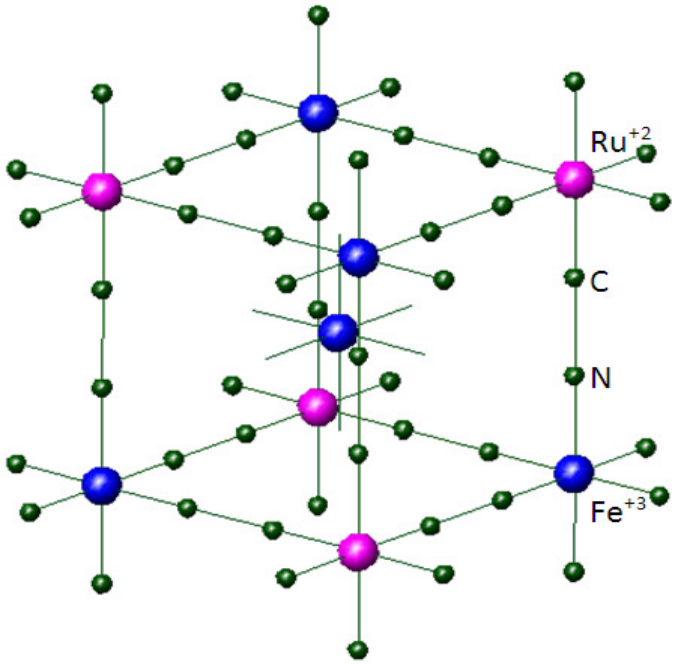

Figure 2.25 The unit cell of Ruthenium Purple, $Fe_4[Ru(CN)_6]_3$.

As discussed by several groups and similar to PB, RuP is present *in two forms*: ionized water-soluble KFe^{III} $[Ru^{II}$ $(CN)_6]$. xH_2O and a neutral insoluble compound, $Fe^{III}{}_4[Ru^{II}(CN)_6]_3$.

[167,171,172,173] The soluble RuP is present in a colloidal form and the inclusion of potassium makes it stable in aqueous media, bringing an overall negative charge, which allows LbL film growth using RuP colloids as the anions. As explained by Rosseinsky et al.,[174] the incorporation of K^+ as a 'supernumerary' cation in $Fe^{III}[Ru^{II}(CN)_6]$ makes it water-soluble. RuP ($Fe^{III}_4[Ru^{II}(CN)_6]_3$ / $KFe^{III}[Ru^{II}(CN)_6].xH_2O$) is present in its natural form as a deep purple color which changes to colorless ruthenium white (RW), $Fe^{II}_3[Ru^{II}(CN)_6]_2$ upon reduction. Although the LbL approach has been used in the formation of (all-inorganic) PB onto electrode surfaces.[172] Jaiswal et al. showed the synthesis of PB colloids and the film fabrication of these colloids by using the negative charge on them with positively charged polyethyleneimine (PEI) for LbL assembly.[172] The reported results were not very exciting, as even after depositing more than 45 bilayers the absorbance and lamination is poor and is attributed to the high surface roughness of the deposited LbL films. The application of this technique in the production of hybrid polymer/inorganic nanocomposites films has been so far reported only for PB combined with either LPEI[167] or polyaniline (PANI)[175] as the polymeric materials, but none has been reported for RuP. The overall reaction mechanism does not change for different electrolytes but as reported by Chen et al[176], the E° values of the RuP seem to be affected by the type of cation (H^+, Li^+, Na^+, K^+, Rb^+) in the electrolytic solutions. This could be due to the size of the cation, which plays an important role in the electrochemical behavior of the RuP films due to its inclusion and expulsion in the crystal lattice during potential cycling. According to the above discussion, the redox reaction of the RuP in the case of Li^+ cations can be written as:

$$KFe^{III}[Ru^{II}(CN)_6] + Li^+ + e^- \leftrightarrow LiKFe^{II}[Ru^{II}(CN)_6] \quad (11)$$

Other transition metal oxides which show intercalation similar to WO_3, PB and RuP are MoO_3, V_2O_5, IrO_2 , $Ni(OH)_2$, and Nb_2O_5. Granqvist et al.[3] explained in detail about all these inorganic materials which are electrochromic. The coloration in MoO_3, V_2O_5, and Nb_2O_5 turns to blue upon reduction, but they can't be commercially adopted because of the small light extinction coefficient as compared to WO_3. IrO_2 and $Ni(OH)_2$ show coloration on oxidation, and the coloration mechanism has not been well-explained both with the H^+ and anion insertion approaches.[2,3,8] Oxides such as V_2O_5 and $Ni(OH)_2$ are also known as transparent EC materials because the color change upon reduction (V_2O_5) and oxidation ($Ni(OH)_2$) is very faint.

2.6.3. Conducting Polymers

Conducting polymers are long chains of conjugated carbon (alternate single and double bonds), that are formed along with other kinds of atoms such as hydrogen, nitrogen, sulphur, oxygen, selenium etc. Before the famous discovery done by Shirakawa et al.[177], polymers were thought of and used as insulators. In their work, it was shown that the conductivity of the polymers like poly-(acetylene) (PAc, **1**) can be increased by several orders of magnitude by doping with iodine. This work was continued and explored by three collaborating scientists, Alan J. Heeger, Alan G. MacDiarmid, and Heidi Shirkawa, who established a niche in this field and later received a Nobel Prize in Chemistry in 2000 "for the discovery and development of electronically conductive polymers".[178,179,180] Further, other conjugated polymers like poly(aniline) (PANI, **3**), poly(pyrrole) (PPy, **4**), poly(thiophene) (PT, **5**) and its derivatives like poly(3,4-ethylenedioxythiophene) (PEDOT, **6**) (Figure 2.26) have been widely studied and the work has been presented in several books and reviews.[181,182] These materials are so-called "first-generation" conducting materials.

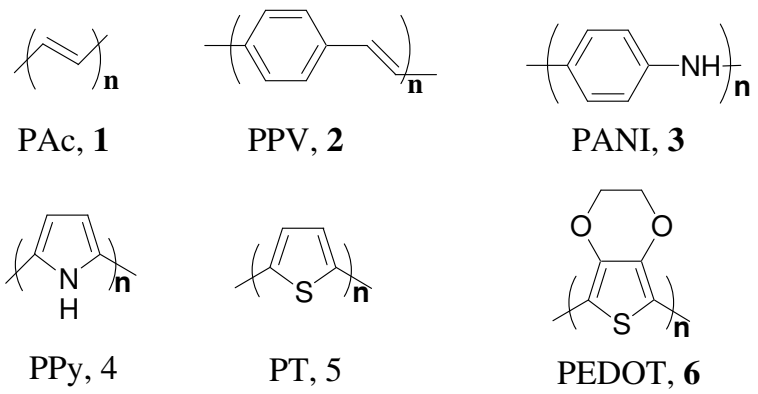

Figure 2.26 Common conjugated polymers [Figure adapted from Sahoo et.al][183]

The intellectual curiosity of scientists in this field has made it possible to generally understand the fundamental nature of the charge propagation in the conducting polymers. Electron exchange reaction (electron hopping) between neighbouring redox sites in redox polymers is assumed to be the reason for the transport of electrons, and in the case of intrinsically conducting polymers (e.g.

polyaniline, polypyrrole), it happens because of the movement of the delocalized electrons through the conjugated systems. [184]

Much work has been done in the past couple of decades in modifying the structural properties and making these materials applicable for commercial industry. The conductivity of these polymers, i.e. the ease with which the materials can be reversibly switched between their insulating and conducting forms, can be easily tuned either by modifying their structures or the extent of doping.[183]

Oxidative electropolymerization of aniline in acidic media[185,186,187] or chemical oxidation by $FeClO_4$, $K_2S_2O_8$ [188,189] was performed and it was also shown that some of the other derivatives of **PANI (3)** (e.g. poly (o-toulidine)[190] or poly (o-ethoxyaniline)[191]) can also be prepared in a similar monomers by their respective monomers. Polypyrrole is one of the other classes of conjugated polymer that has been heavily worked, due to its low oxidation potential and easy processability. Diaz et al. were the first to show that the synthesis of free-standing poly(pyrrole) (**PPy**, **4**) can be obtained via oxidative electropolymerization[192] and a similar electropolymerization technique was extended to other aromatic compounds such as thiophene, furan, indole, carbazole, indole, azulene, and fluorine.[193,194] The main areas of applications for the conducting polymers so far have been in batteries,[195] antistatic coatings, sensors,[196] photovoltaics,[197] organic light emitting diodes (OLEDs), [198] supercapacitors,[199] molecular electronics, [200] etc.

But among all these different classes of conjugated polymers, Polythiophene (**PT, 5**) is the one that is most widely studied, due to its environmental stability in the neutral form and also the flexibility that structural versatility of the thiophene ring provides by making the synthetic modification straight-forward and simple.[201] Garnier et al. in 1983 were the first to show the electrochemical polymerization and electrochromic switching of both substituted and unsubstituted PTs.[202,203] Shirkawa et al. showed that the films, being red in the neutral state, can be easily switched to blue upon oxidation and black-green on reduction.[204] Solution processability was an important aspect to be considered, so significant efforts were devoted towards developing and modifying the monomers, and second generation PT derivatives were

developed. Much attention was given towards adding the substituents at 3- and 4- position of the thiophene ring to avoid hinderance at the sulphur atom, resulting in a whole new class of materials. Of these, PEDOT has been the most successful so far because of its high stability in the oxidized state. Figure 2.27 shows the monomeric structures of thiophene (**10**) based analogues including EDOT (**11**), 3,4-ethylenedithiathiophene EDTT (**12**) [both oxygen atoms were replaced by sulfur], thieno[3,4-b]-l,4-oxathiane (**13**)[one oxygen atom replaced by sulfur], respectively and the selenium derivative EDOS (14)[sulfur atoms replaced by selenium in EDOT (**11**)] and the polymerization of these monomers were performed by various groups during the past decade.[182,205,206,207]

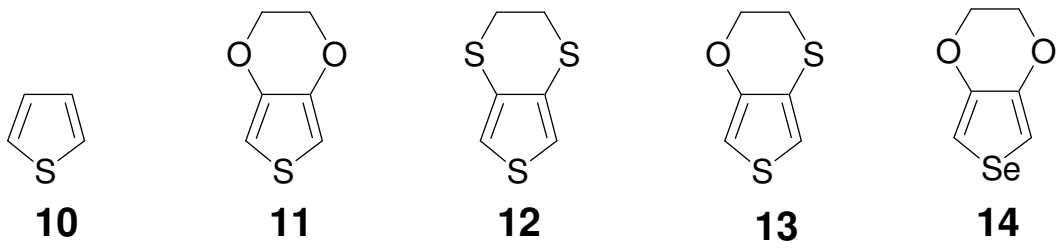

Figure 2.27 Thiophene based analogues [Figure adapted from Sahoo et.al] [183]

PEDOT was first synthesized by Jonas et al. via 3, 4-ethylenedioxythiophene (EDOT) in the late 1980s. [208,209] The structural synthesis of PEDOT has been very carefully done. On the one hand, the ether oxygen linked to thiophene decreases the oxidation potential, but on the other the ethyl bridge that connects the two oxygens minimizes the steric hindrance. It exhibits a very high conductivity of 300 S/cm and was found to be almost transparent in thin film form. Even after showing several advantageous properties, it was not suitable to be used because of its insolubility. This issue was later resolved by using a water-soluble polyelectrolyte, poly(styrene sulfonic acid)(PSS) as a charge-balancing dopant during polymerization to yield PEDOT/PSS. The resulting product has all the exceptional qualities of PEDOT or even better on the expense of slight decrease in conductivity (10 S/cm).[210,211] PEDOT has a bandgap of ~1.6 eV, which is much lower than the unsubstituted and alkyl-substituted PTs, bringing down the much lower

oxidation potential and causing its oxidation and conducting forms to be more stable under ambient conditions.

Reynolds et al. were the first to show the synthesis of PProdot and its other derivatives by increasing the ring size of the alkylenedioxy bridge on the PEDOT.[201] It was shown that while an increase in the ring size from ethylene (PEDOT) to propylene (PProdot) to butylene (Poly (3,4-butylenedioxythiophene)(PBuDOT) also increases the oxidation potential of the polymers as compared to PEDOT, but it also increases the switching speed. The increase in the oxidation potential is due to a decrease in the electron donating ability of the oxygens, which results in a larger degrees of freedom of movement of the oxygen lone pair.[201]

The two most heavily studied electrochromic conjugated polymers that are discussed in detail in this chapter are PANI and PEDOT, while a complete chapter is devoted to the synthesis and electrochromic properties of one of the water-soluble derivative of PProdot.

2.6.3. 1. Poly (3, 4- ethylene dioxythiopene) - PEDOT

PEDOT, which falls into the class of polythiopene electrochromes, has a high conductivity of 300 S/cm. PEDOT is commercially available in the form of PEDOT: SPS under the trade name Baytron® P; the excess of SPS helps in charge stabilizing the colloid by providing negative polyvalency. A few of the main examples of antistatic coating applications of PEDOT:PSS are photographic films,[212] electronics packaging, cathode-ray tube (CRT) screens, and LCD polarizer films.[213] In the industry, in situ PEDOT is used as a polymeric cathode material for solid aluminum, tantantalum, and niobium capacitors, and also as a conductive template for copper-through-hole plating of printing writing boards.[201] Much work has been done in proving the importance of PEDOT as an electrochromic material. [63(a),214,215] Reynolds et al. have shown that sulfonated-PEDOT can be deposited in a similar way as PEDOT, but in this compound the LbL fabrication is happening because of the sulfonate ionic group in the sidegroup of the polymer, rather than from PSS as is the case with PEDOT. 10-20 BLs films of PAH/PEDOT-S switched within 2.5 s and have reached 82% of the maximum contrast value. An important property that

the authors reported is the saturation limit of higher numbers (50) of bilayers in terms of coloration efficiency. The highest coloration efficency (434 cm^2/C) reported was in the case of 10 BL PAH/PEDOT-S films as compared to value of 200-250 cm^2/C for the 20-40BL films; this was attributed to inability of ions to access all the sites in case of thicker films. Kumar et al.[97] have reported the best response time of 300 ms with PEDOT EC films deposited on the ITO; the deposition method used is electropolymerization, but there is not enough evidence that the EC assembly is stable for more than 10000 cycles. The coloration efficiency values (CE) of these devices calculated at various film thicknesses comes out to be in the range of 200 cm^2/C. These are not as high (~500-1000 cm^2/C) as expected from polymer-based EC devices, but certainly much higher (10-100 cm^2/C) than the EC devices fabricated from metal oxides. Hammond et al.[52] have shown some good results in LbL film formation of single electrochrome LPEI/ PEDOT: SPS assembly as well as dual electrochrome PXV/ PEDOT: SPS, which is presented in Figure 2.27. This work from Hammond et al. has already been explained in detail in the polviologen section as an electrochromic material. The formation of redox peaks of LPEI/PEDOT: SPS assembly seems more distinguishable than the one investigated by Cutler and Reynolds [63(a)].

There are a few other organic materials like polypyrrole[216], polycarbazole[217], methoxybiphenyl[218], quinones[219], and diphenyl amines[220] which show promising results for being a high responsive EC material, but no work has been done regarding LbL film fabrication. Thus, a detailed discussion of these materials is not present in this review chapter.

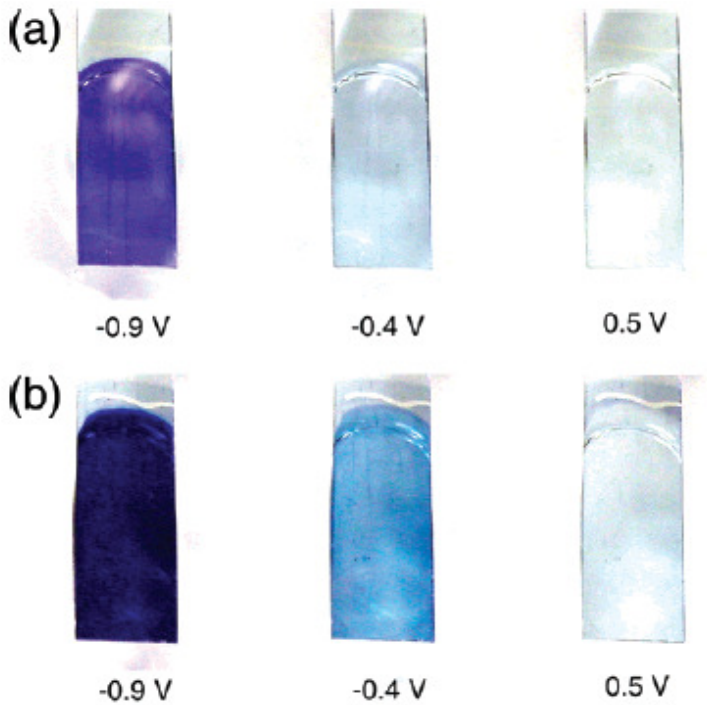

Figure 2.28 Digital photographs of the coloration and bleaching of (a) (PXV/PEDOT: SPS) $_{40}$, and (b) (PXV/PEDOT: SPS)$_{50}$.[Reprinted with permission from D. M. DelongChamp, M. Kastantin, P. T. Hammond, *Chem. Mater*. **2003**, *15*, 1575. Copyright 2003 American Chemical Society] [52]

2.6.3.2. Polyaniline (PANI)

Polyaniline (PANI), due to its simple and low-cost preparation, along with fast ionic conductivity and stability, has gained substantial attention in the recent past. Tamura et al.[221] showed stable repeated switching of PANI, which is far better than most of the other conjugated EC polymers available to date. The films were electrodeposited on the conductive ITO electrodes and have shown decent contrast between the three redox states. Being an EC polymer, PANI switches from a semi-transparent yellow reduced state known as leucomeraldine PANI, to a darker, oxidized green emeraldine salt or blue emeraldine base. [222] Huang et al. have done a detailed study on the optical properties of different redox states of the polyaniline and found that blue shift of the Π-Π* absorption band from 3.94 eV to 4.17 eV corresponds to conversion of luecoemeraldine base to its salt form.[222] The polaronic lattice structure of the polyaniline can be easily attained by protonating the emeraladine base form and it also accounts for the shift of 2.1

eV absorption peak to 1.5 eV. Bipolaronic lattice state can also be achieved by further protonating the polaronic state (emeraldine salt) form. Emeraldine, either in base or salt, is a highly conductive form of aniline. PANI has the ability to form both ionic and hydrogen bonding interacted LbL films; it depends upon the counter polyion whether it is a polyanion for ionic interactions or an H- bonding donor/acceptor. Hammond et al. have shown the fabrication of PANI/PAMPS and PEDOT/PAMPS films and observed the thickness/bilayers of 10.1 and 8.4 nm, respectively for 20 BL films; the roughness was less than 10% for both the systems. [223] Optical contrast reported for PANI/PAMPS films was high as well: 51.7 % at 748 nm for 20 and 40 bilayers. PAMPS enhances performance better than other polyions because of its strong acidity, which promotes low-level chemical doping of the PANI.[224] This occurs even in its normal insulating state, enhancing electrical conductivity and thus the speed of electron injection and withdrawal.[187,225] Figure 2.29 shows the 40-bilayer cell in the colored and bleached states, along with the UV spectra of both 20- and 40-bilayer cells. The below shown cell is a "solid-electrolyte" in which PAMPS polyelectrolyte gel is used instead of an electrolyte solution.

According to the referenced paper, the life span of unsymmetrical solid-state EC $Cell_{40}$ is more than 35,000 cycles with a bleaching time of less than 1sec and coloring time of more than 1.5 sec. Rubner et al.[226] were the first to demonstrate the LbL film fabrication method using PANI with a special method using DMAc[227] to ease the bilayer deposition, but further research work in the EC field by Hammond et al.[223] and Heflin et al.[93.94,100] has established PANI as an important EC material for the formation of robust, low roughness LbL films. Heflin et al.[93,94] have demonstrated the best response time (50 ms) to date of this kind of EC polymer formed by LbL assembly. The authors showed the LbL film assembly of PANI with PAMPS and also demonstrated that due to this technique, the precise nanoscale control of thickness can be possible with a reversible electrochromic switching of 50 ms for solid-state devices. Absorption spectra of 5, 10, 15 and 20 bilayer films of PANI/PAMPS showed that the initial light blue-gray color changes to dark blue on application of 1V or higher. H-bonding interaction of PANI with weak polyelectrolytes such as Poly AcrylicAcid (PAA), Poly Acrylic Acrylamide (PAAm), PEO, ethoxylate Poly(ethylamine) (ePEI) has shown decent results[223], but the LbL films are not stable enough for fast ionic conduction. This is due to the small resistance to the counterion diffusion created by very thick H-bonded LbL assembled films. It is important to mention that the mobile

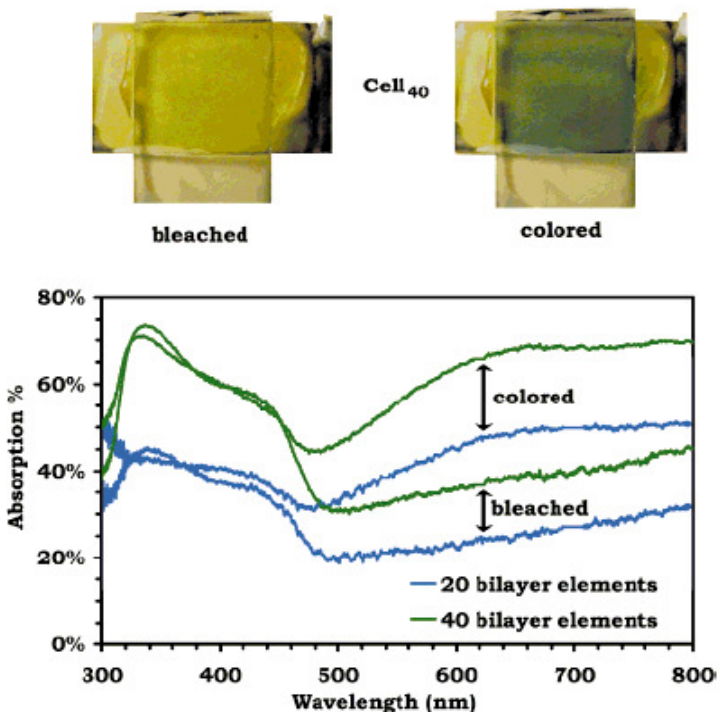

Figure 2.29 Demonstration of colored and bleached $Cell_{-40}$, with UV-Vis absorption spectra of $Cell_{-20}$ and $Cell_{-40}$. [D. M. Delongchamp, P. T. Hammond, Layer-by-Layer Assembly of PEDOT/Polyaniline Electrochromic Devices, *Adv. Mater.* **2001**, 13, 1455. Copyright Wiley-VCH Verlag GmbH & Co. KGaA. Reproduced with permission.][223]

species in H-bonded LbL films are anions, not small cations (H^+ ions in most of the cases).[30,41] This is one of the reasons that there is severely restricted ion permeation in highly charged LbL assembled films, due to intrinsic charge compensation and a lack of free ion-exchanged sites.[228] But Delongchamp et al. have shown that higher ionic conductivity can be achieved by carefully designing a unique assembly mechanism and have demonstrated the highest reported ionic conductivity (10^{-5}S/cm) for LbL films of linear poly(ethylene imine)(LPEI) and PAMPS of low concentrations.[167] Conductivity can be further improved by the addition of small amounts of lithium triflate salts to fully constructed LbL films.

2.6.4. Semiconductor Colloid Quantum Dots (QDs)

Colloidal semiconductor nanocrystals combine the physical and chemical properties of molecules with the optoelectronic properties of semiconductors.[229] Along with the advantage of high monodispersity and fluorescence efficiency, the absorption range of colloidal II-VI, III-V, and IV-VI QDs covers the spectrum from the UV to the mid-infrared. The advantage related with the use of QDs as an EC material is the ability to control the color, which is a direct consequence of quantum confinement on the electronic state.[230] Guyot-Sionnest et al.[231, 232] have shown special EC characteristics of some of the QDs. In brief, Guyot-Sionnest et al.[233] illustrate the effect that quantum confinement shifts the energy levels of the conduction band higher, which is typically less than 1eV for most sizes of the QDs. Hence, it is feasible to have electron injection into semiconductor nanocrystals, along with alkali metals, which is similar to that of organic polymers.

A drop of n-type conducting CdSe nanocrystal solution was placed on the surface of the working electrode (ITO) and allowed to dry slowly to form an optically clear film with a thickness of 0.5 μm.[233] However, the scheme adopted to form QD films didn't give high enough conductivity and fast switching speed. Figures 2.30 and 2.31 show the UV/Vis spectra and switching speed results, respectively. Figure 2.31 clearly shows a decrease in the maximum visible absorbance after a switching time of more than 5 minutes; this is because of the slow injection and ejection process in less homogeneous and ordered film of CdSe nanocrystals. As explained by Wang et al., the charging and the discharging rates are very dependent on the film quality and the existence of oxidative impurities, so charge trapping often happens when the film deposition is inhomogeneous, finally affecting the optical contrast as ions don't get access to all of the electroactive sites.[233]

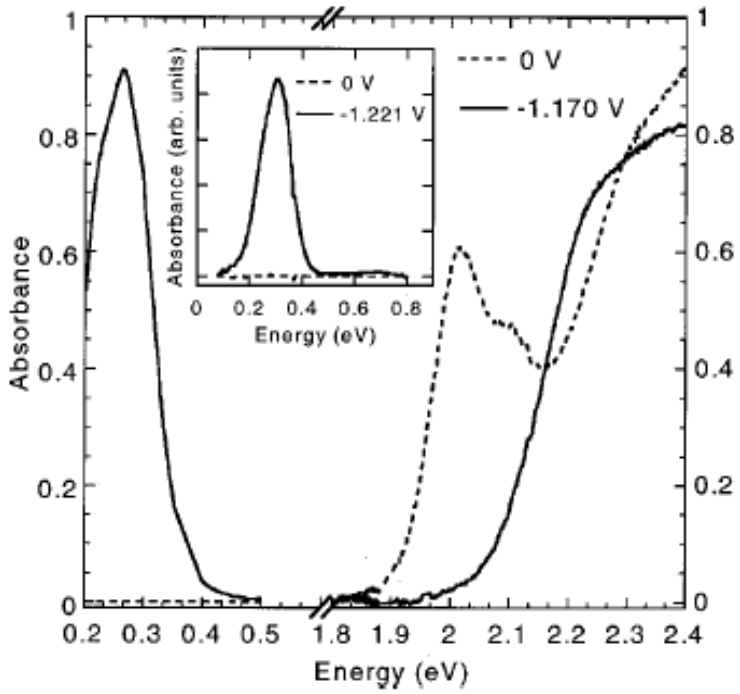

Figure 2.30 IR and UV/Vis spectra of 5.8 nm diameter CdSe nanocrystal film at different potentials. [Reprinted with permission from C. Wang, M. Shim, P. Guyot-Sionnest, Electrochromic semiconductor nanocrystal films, *Appl. Phys. Letters*, **2002**, 80, 4. Copyright 2002, American Institute of Physics.] [233]

Incorporating EC nanocrystals into LbL films has given a very good approach to working towards homogenous film formation technique. Kotov et al.[234-235] have shown good formation of LbL films of QDs, so this systematic technique can be used with the EC QDs to fabricate robust, homogenous, ordered, thickness-controlled films which can be readily adapted for commercial applications.

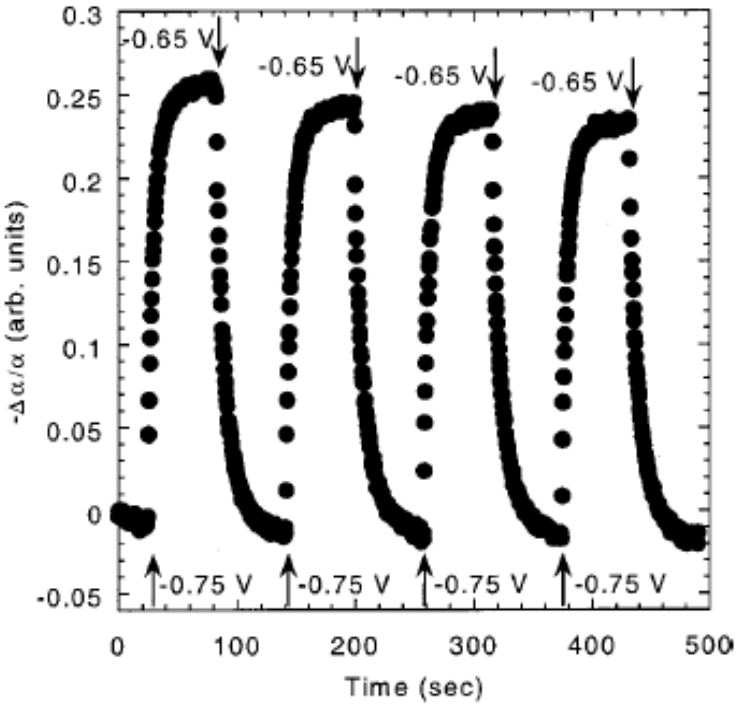

Figure 2.31 Visible absorbance at 1.97 eV of 6.8 nm CdSe film at different potentials. The applied potentials are switched between -0.65 and -0.75 V. The visible absorption of the film responds rapidly to the changes of applied potential. The arrows indicate the points where the potential is switched. [Reprinted with permission from C. Wang, M. Shim, P. Guyot-Sionnest, Electrochromic semiconductor nanocrystal films, *Appl. Phys. Letters*, **2002**, 80, 4. Copyright 2002, American Institute of Physics.] [233]

2.6.5. Polyoxymetalates (POMs)

Beyond the materials discussed above, the other EC materials that have not been given enough attention and are the some of the newest members in the EC materials library are Polyoxymetalates (POMs). Kurth et al. showed the ability of POMs to act as an electron reservoir which gives rise to colored mixed-valence state species while retaining their structural intergrity.[236] Although the authors have demonstrated the electrochromic behavior of these POMs, the results still do not show that these materials can achieve high contrast and fast switching times. Surface-encapsulated POMs are big molecules and have at least three to four redox pairs, and hence the authors have chosen the appropriate POM clusters, in which the structural and elctrochemical properties can be easily controlled. POMs show discrete electrochromic behavior, comparable to QDs and other conjugated polymers, as the cluster of

metal oxides provides a wide range of structures and properties. Instead of using LB assembly, electropolymerization or compressing POM solids, Kurth et al. have used the LbL film fabrication method to form stable films. The POM used by Kurth et al. was the Europium (III) derivative of the preyssler-type[237] hetropolytungstate $[Eu\text{-}(H_2O)P_5W_{30}O_{110}]^{12-}$(Eu-POM), the structure of Eu-POM along with the schematic of the LbL film is given in Figure 2.32.

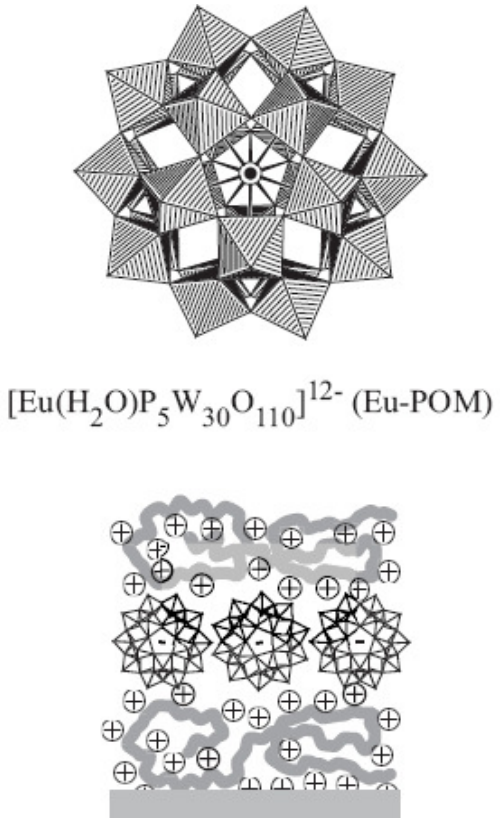

Figure 2.32 Top: Structure of the Eu-POM. Bottom: Schematic representation of the LbL film. [Reprinted with permission from M. H. Alizadeh, S. P. Harmalker, Y. Jeannin, J. Martin-Frere, M. T. Pope, *J. Am. Chem. Soc*. **1985**, *107*, 2662.Copyright 1985 American Chemical Society] [237]

The polycation used in the LbL films is PAH and the assembly formed by alternate deposition of PAH, PSS, PAH and Eu-POM on ITO coated glass slides. The bottleneck associated with the electrochromic effect in POM LbL films is the slow response time for coloration and bleaching, which is 4.2 and 4.4 s [237]. This may be because thick LbL films make the path longer for ions to transfer charge from one electrode to another during coloration and bleaching.

Another approach which has gained recent attention has been adopted by Ntera Inc., Ireland [238]. They have explored the possibility of incorporating semiconducting nanoparticles onto the electrode surface. The devices fabricated by Ntera Ltd have been given the name "nanochromics" because of the ability of nanomaterials to form electrodes with modified porous nanocrystalline films[239]. The pore size of n-type semiconducting materials like anatase TiO_2 ranges from 5-20 nm, and the surface of these pores is modified by chemisorbing, specially synthesized viologens, which behave as a phosphonic-type SAM and bind irreversibly to the oxide. The switching material is in direct contact with both the nanostructured electrode and liquid electrolyte, so it reduces the possibility of charge transfer and makes the switching speed as fast as 100-200 ms. In addition, the advantage of the utilization of the mesoporous films is that an amount of molecular modifier will give a perceptible color change in a working device and enhance the contrast of the viologen monolayer 10-100 times as compared to a flat monolayer that would not exhibit contrast visible to the human eye.[239] Figure 2.33 shows the schematic of a nanochromics reflective device. Material characteristics and display fabrication of these kinds of devices were explained in detail in the section on polyviologen as an electrochromic material of this chapter. One drawback that can be associated with nanochromic technology is that it is metastable (the device discharges its color over a period of hours). This prevents fast bleaching as there are no redox-active additives present in the electrolyte that can mediate the discharge of the device.

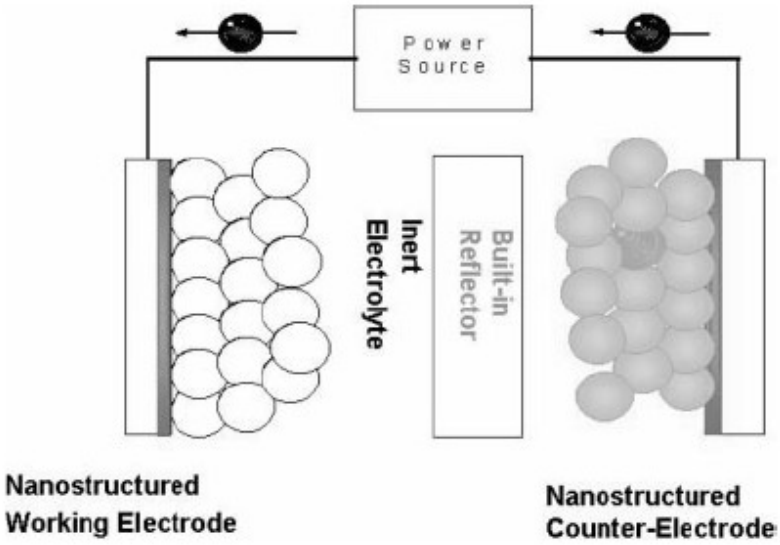

Figure 2.33 Schematic drawing of a nanochromics reflective device. [U. Bach, D. Corr, D. Lupo, F. Pichot, M. Ryan, Nanomaterials-Based Electrochromics for Paper-Quality Displays *Adv. Mater.* **2002**, 14, 845. Copyright Wiley-VCH Verlag GmbH & Co. KGaA. Reproduced with permission.][238]

Despite these drawbacks, the commercial availability of nanochromic device technology from Ntera, Ltd has shown great promise and performance that challenges liquid crystal displays (LCD), which has captured a large share of the current display market.

References

[1] R. D. Rauh, *Electrochim. Acta*, **1999**, 44, 3165.

[2] P. M. S. Monk, R. J. Mortimer, D. R. Rosseinsky, "*Electrochromism and Electrochromic Devices*", Cambrdige University Press, Cambridge, **2007**.

[3] C. G. Granqvist, *Handbook of Inorganic Electrochromic Materials*, Elsevier, Amsterdam, **1995**.

[4] R. J. Mortimer, A. L. Dyer, J. R. Reynolds, *Displays* **, 2006**, 27, 2.

[5] R. J. Mortimer, N. M. Rowley, in J. A. McCleverty, T.J. Meyer, eds., *Comprehensive Coordination Chemistry – II: From Biology to Nanotechnology*, Elsevier, Oxford, **2004**, Volume 9.2, M. D. ward., pp. 581.

[6] M. D. Ward, J. A. McCleverty, *H. Chem. Soc. Dalton Trans*., **2002**, 275.

[7] Z. C. Wu, Z. H. Chen, X. Du, J. M. Logan, J. Sippel, M. Nikolou, J. R. Reynolds, D. B. Tanner, A. F. Hebard, A. G. Rinzler, *Science*, **2004**, 305, 1273.

[8] P. M. S. Monk, R. J. Mortimer, D. R. Rosseinsky, *"Electrochromism: Fundamentals and Applications,"* VCH, Weinheim, 1995, pp 5-23.

[9] G. Decher, J. D. Hong, J. Schmitt, *Thin Solid Films* **1992**, 210/21 I, 831.

[10] H. Haas, G. Decher, H. Mohwald, A. Kalacbevt, *J. Phys. Chem.* **1993**, 97, 12835.

[11] G. Decher, J. D. Hong, *Makromo., Chem., Macromol. Symp*.**1991**, 95, 46, 321.

[12] G. Decher, *Science*, **1997**, 277, 1232.

[13] K. Ariga, J. P . Hill, Q. Ji, *Phys. Chem.Chemi. Phys*. **2007**, 9, 2319.

[14] P. Brent, K. Kurihara, T. Kunitake, *Langmuir*, **1992**, 8, 2486.

[15] D. L. Feldheim, K. C. Grabar, M. J. Natan, T. C. Mallouk, *J. Am.Chem. Soc.* **1996**, *118*, 7640.

[16] K. Ariga, Y. Lvov, M. Onda, I. Ichinose, T. Kunitake, *Chem.Lett.* **1997**, 125.

[17] Y. Lvov, K. Ariga, M. Onda, I. Ichinose, T. Kunitake, *Langmuir* **1997**, *13*, 6195.

[18] E. R. Kleinfeld, G. S. Ferguson, *Science* **1994**, *265*, 370.

[19] Y. Lvov, G. Decher, G. Sukhorukov, *Macromolecules* **1993**, *26*, 5396.

[20] Y. Lvov, Z. Lu, J. B. Schenkman, J. F. Rusling, *J. Am. Chem. Soc.* **1998**, *120*, 4073.

[21] Y. Lvov, J. Haas, G. Decher, H. Möhwald, A. Mikhailov, B. Mtchedlishvily, E. Morgunova, B. Vainshtein, *Langmuir* **1994**, *10*, 4232.

[22] S. Watanabe, S. L. Regan, *J. Am. Chem. Soc*. **1994**, *116*, 8855.

[23] J. H. Cheung, A. F. Fou, M. Ferreira, M. F. Rubner, *Polym. Prepr. ACS Proc.* **1993,** 34, 757.

[24] M. Ferreira, J. H. Cheung, M. F. Rubner, *Thin Solid Films* **1994**, *244*, 806.

[25] J. H. Cheung, A. F. Fou, M. F. Rubner, *Thin Solid Films* **1994**, *244*, 985.

[26] J.R. Heflin, M.T. Guzy, P.J. Neyman, K.J. Gaskins, C. Brands, Z. Wang, H.W. Gibson, R.M. Davis, K.E. Van Cott, *Langmuir,* **2006**, 22, 5723.

[27] K. Van Cott, M. Guzy, P. Neyman, C. Brands, J.R. Heflin, H.W. Gibson, R.M. Davis, *Angew. Chem. Int. Ed.*, **2002**, 41, 3236.

[28] P. T. Hammond, G. M. Whitesides, *Macromolecules* **1995**, *28*, 7569.

[29] Y. Sun, X. Zhang, C. Sun, B. Wang, J. Shen, *Macromol. Chem. Phys.* **1996**, *197*, 147.

[30] D. Laurent, J. B. Schlenoff, *Langmuir* **1997**, *13*, 1552.

[31] D. G. Kurth, J. P. Lopez, W. Dong, *Chem. Comm*. **2005**, 2119.

[32] J. Stepp, J. B. Schlenoff, *J. Electrochem. Soc.* **1997**, *144*, L155.

[33] M. Onoda, K. Yoshino, *Jpn. J. Appl. Phys.* **1995**, *34*, L260.

[34] S.E. Yancey, W. Zhong, J.R. Heflin, A.L. Ritter, *J. Appl. Phys*., **2006**, 99, 034313:1-10.

[35] M. Onda, Y. Lvov, K. Ariga, T. Kunitake, *Biotech. Bioeng.* **1996**, *51*, 163

[36] D. Yoo, S. S. Shiratori, M. F. Rubner, *Macromolecules*, **1998**, 31, 4309.

[37] S. S. Shiratori, M. F. Rubner, *Macromolecules* **2000**, 33, 4213.

[38] Y. Lvov, G. Decher, H. Mohwald, *Langmuir*, **1993**, 9, 481.

[39] A. Krozer, S. A. Nordin, B. Kasemo, *J. Colloid Interface Sci*. **1995**, 176, 479.

[40] K. Glinel, A. Moussa, A. M. Jonas, A. Laschewsky, *Langmuir* **2002**, 18, 1408.

[41] M. A. C. Stuart, H. Tamai, *Langmuir*, **1988**, 4, 1184.

[43] J. B. Schlenoff, H. Ly, M. Li, *J. Am. Chem. Soc.* **1998**, 120, 7626.

[44] S. Y. Yang, M. F. Rubner, *J. Am. Chem.Soc*. **2002**, 124, 2100.

[45] S. A. Sukhishvili, S. Garnick, *J. Am.Chem. Soc*. **2000**, 122, 9550.

[46] Z. Wang, X. Hu, *Thin solid films*, **1999**, *352*, 62.

[47] Y. Ikenoue, Y. Saida, M. Kira, H. Tomozawa, H. Yashima, M. Kobayashi, *J. Chem. Soc., Chem. Commun.* **1990,** 1694**.**

[48] S. Papaefthimiou, G. Leftheriotis, P. Yianoulis, *Ionics* **1998**, 4, 321.

[49] J. Stejskal, M. Trchova, S. Fedorova, I. Sapurina, J. Zemek, *Langmuir* **2003**, 19, 3013.

[50] C. L. Curtis, J. E. Ritchie, M. J. Sailor, *Science* **1993**, 262, 2014.

[51] E. Punkka, M. F. Rubner, *J. Electronic Mater.* **1992**, *21*, 1057.

[52] D. M. DelongChamp, M. Kastantin, P. T. Hammond, *Chem. Mater*. **2003**, *15*, 1575.

[53] N. A. Kotov, I. Dekany, J. H. Fendler, *J. Phys. Chem,* **1995**, 99, 13065.

[54] A. A. Mamedov, N. A. Kotov, *Langmuir* **2000**, 16, 5330.

[55] C. Jiang, S. Markutsya, V. V. Tsukruk, *Adv. Mater*. **2004**, 16, 157.

[56] C. Jiang, V. V. Tsukruk, *Adv. Mater*. **2006**, 18, 828.

[57] F. Caruso, R. A. Caruso, H. Mohwald, *Science* **1998**, 282, 1111.

[58] D. L. Feldheim, K. C. Grabar, M. J. Natan, T. E. Mallouk, *J. Am. Chem. Soc*. **1996**, 118, 7640.

[59] Y. Lvov, K. Ariga, M. Onda, I. Ichinose, T. Kunitake, *Langmuir* **1997**, 13, 6195.

[60] G. Zotti, S. Zecchin, A. Berlin, G. Schiavon, G. Giro, *Chem. Mater*. **2001**, 13, 43.

[61] J. Lukkari, M. Saloma1ki, A. Viinikanoja, T. Aa1ritalo, J. Paukkunen, N. Kocharova, J. Kankare, *J. Am. Chem. Soc.* **2001**, *123*, 6083.

[62] D. M. Welsh, L. J. Kloeppner, L. Madrigal, M. R. Pinto, B. C. Thompson, K. Schanze, K. A. Abboud, D. Powell, J. R. Reynolds, *Macromolecules* **2002**, *35*, 6517.

[63] (a) C. A. Cutler, M. Bouguettaya, J. R. Reynolds, *Adv. Mater.* **2002**, *14*, 684.

(b) J. Park, Y. Kwon, T. Lee, *Macromol. Rapid Comm*. **2007**, *28*, 1366.

[64] S. Ravaine, C. Lafuente, C. Mingtoaud, *Langmuir* **1998**, 14, 6347.

[65] H. Q. Xiang, K. Tanaka, A. Takahara, T. Kajiyama, *Langmuir* **2002**,18, 2223.

[66] J. Livage, *Chem. Mater*. **1991**, 3,578.

[67] A. E. Aliev, H. W. Shin, *Solid State Ion*. **2002**, 154, 425.

[68] C. G. Granquist, *Appl. Phys. A*, A57, **1993**, 19.

[69] D. R. Rosseinsky, R. J. Mortimer, *Adv. Mater.* **2001**, 13, 783.

[70] P. R. Somani, S. Radhakrishnan, *Mater. Chem. Phys.* **2002**, *77*, 117.

[71] A. A. Argun, P. H. Aubert, B. C. Thompson, I. Schwendeman, C. L. Gaupp, J. Hwang, N. J. Pinto, D. B. Tanner, A. G. MacDiarmid, J. R. Reynolds, *Chem. Mater.* **2004**, *16*, 4401.

[72] J. Roncali, Chem. Rev. 1997, 97, 173.

[73] G. A. Sotzing, J. L. Reddinger, A. R. Katritzky, J. Soloducho, R. Musgrave, J. R. Reynolds, *Chem. Mater*. **1997**, *9*, 1578.

[74] G. A. Sotzing, J. R. Reynolds, *Chem. Mater*. **1996**, *8*, 882.

[75] C. L. Gaupp, J. R. Reynolds, *Macromolecules* **2003**, 36, 6305.

[76] C. G. Granqvist, E. Avendano, A. Azens, *Thin Solid Films*, **2001**, 442, 201.

[77] C. J. Schoot, J. J. Ponjee, H. T. van Dam, R. A. van Doorn, P. T. Bolwjin, *Appl. Phys. Lett.,* **1973**, 23, 64.

[78] D. J. Barclay, D.H. Martin, In *Technology of Chemicals and Materials for Electronics*: E. R.Howells, Ed.: John Wiley and Sons: New York, **1984**, pp 266 - 276.

[79] P M. S. Monk, C Turner, S. P. Akhtar, *Electrochim. Acta*, **1999**, 44, 4817.

[80] R. J. Mortimer, C. P. Warren, *J. Electroanal. Chem.* **1999**, 460, 263.

[81] J. P. Coleman, A. T. Lynch, P. Madhukar, J. H. Wagenknecht, *Solar Energy mater. Solar cells*, **1999**, 56, 395.

[82] M.O.M. Edwards, G. Boschloo, T. Gruszecki, H. Petterson, R. Sohlberg, A. Hagfeldt, *Electrochim. Acta*, **2001**, 46, 2187.

[83] M. Wigginton, "Glass in Architecture," Phaidon, London, UK, 1996.

[84] C. M. Lampert, *SPIE*, **1999**, 3788, 2.

[85] C. M. Lampert, *SPIE*, **2001**, 4458, 95.

[86] C. G. Granqvist, *Int. Glass Rev*., **2001**, 2, 67.

[87] A. Azens, C. G. Granqvist, *SPIE*, **2001**, 2258, 104.

[88] R. L. Puterbaugh, A. G. Mychkovsky, R. Ponnappan, N. Kislov, *AIP conf. proc.,* **2005**, 746, 90.

[89] A. Azens, E. Avendaño, J. Backholm, L. Berggren, G. Gustavsson, R. Karmhag, G.A. Niklasson, A. Roos C.G. Granqvist, *Mater. Sci. Eng. B*, **2005**, 119, 214.

[90] I. Schwendeman, R.Hickman, G. Sonmez, P. Schottland, K. Zong, D. M. Welsh, J. R. Reynolds, *Chem. Mater.* **2002**, *14*, 3118.

[91] A. A. Argun, A. Cirpan, J. R. Reynolds, *Adv. Mater*. **2003**, *15*, 1338.

[92] D. Mercerryes, P. Marcilla, E. Ochoteco, H. Grande, J. P. Pomposa, R. Vergaz, J. M. S. Pena, *Electrochim. Acta* **2004**, *49*, 3555.

[93] J. A. Janik, J. R. Heflin , D. Marciu, M. B. Miller, H. Wang, H. W. Gibson, R M. Davis, *SPIE Proc.* **2001**, *4458*, 146.

[94] C. Brands, T. Piok, P. J. Neyman, A. Erlacher, C. Soman, M. A. Murray, R. Schroeder, J. R. Heflin, W. Graupner, D. Marciu, A. Drake, M. B. Miller, H. Wang, H. Gibson, H. C. Dorn, G. Leising, M. Guzy, R. M. Davis, *SPIE Proc*. Vol. **2000**, 3937, 51.

[95] G. Sonmez, I. Schwendeman, P. Schottland, K. Zong, J. R. Reynolds, *Macromolecules* **2003**, *36*, 639.

[96] (a) I. Schewendeman, J. Hwang, D. W. Welsh, D. B. Tanner, J. R. Reynolds, *Adv. Mater.* **2001**, *13*, 1753, (b) R. B. Bennett, R. B.; W. E. Kokonasky, M. J. Hannan, L. G. Baxall, US Patent 5,446,577, 1995.

[97] A. Kumar, D. M. Welsh, M. C. Morvant, F. Piroux, K. A. Abboud, and J.R. Reynolds, *Chem. Mater*. **1998**, 10, 896.

[98] D. M. Welsh, A. Kumar, E. W. Meijer, and J. R. Reynolds, *Adv. Mater*., **1999**, 11, 1379.

[99] K. Doblhofer, K. Rajeshwar, in *Handbook of Conducting Polymers*, 2nd ed. (Eds: T. A. Skotheim, R. L. Elsenbaumer, J, R. Reynolds), Marcel Dekker, New York, **1998**, pp 531.

[100] J. R. Heflin, J. A. Janik, K. Kuroda, M. Drees, S. Cho, D. Marciu, M. B. Miller, H. Wang, H. W. Gibson, R. M. Davis, 223rd ACS National Meeting, 4/**2002**, 369.

[101] K. Doblhofer, K. Rajeshwar, in *Handbook of Conducting Polymers*; 3rd ed.; Skotheim, T. A. Elsenbaumer, R. L. and Reynolds, J.R. Marcel Dekker ; New York, **1998**.

[102] A. Cirpan, PhD Thesis – The Middle East Technical University, Turkey, **2004**.

[103] H. Abruna, *Coord. Chem. Rev.* **1998**, 86, 135.

[104] R. F. Lane, A. T. Hubbard, *J. Phys. Chem*. **1973**, 77, 1401.

[105] E. J. Laviron, *Electroanal. Chem.* **1972**, 39, 1.

[106] D. M. Delongchamp, PhD Thesis, MIT, 2003.

[107] M. Vidotti, C. Greco, E. A. Ponzio, S. I. C. de Torresi, *Electrochemistry Communications*, **2006**, 8, 554.

[108] V. Jain, H. Yochum, H. Wang, R. Montazami, M.A.V. Hurtado, A. Mendoza-Galvan, H.W. Gibson, J.R. Heflin, *Macromol. Chem. Phys.,* **2008**, 209, 150.

[109] P. W. Atkins, *Physical Chemistry*, 5th edn., Oxford University Press, Oxford, **1994**, 545.

[110] C.A. Thomas, Ph.D. Thesis, Department of Chemistry, University of Florida, **2001**.

[111] P. M. S. Monk, R. J. Mortimer, D. R. Rosseinsky, *"Electrochromism: Fundamentals and Applications,"* VCH, Weinheim, 1995, pp 52-70.

[112] S. A. Sapp, G. A Sotzing, J. R. Reynolds, *Chem. Mater*. **1998**, *10*, 2101.

[113] G. Sonmez, H. Meng, F. Wudl, *Chem. Mater.* **2004**, *16*, 574.

[114] R. Cinnsealach, G. Boschloo, S. N. Rao, D.Fitzmaurice, *Solar Energy Mater. Solar Cells* **1998**, *55*, 215.

[115] W. C. Dautermont-Smith, *Displays I* **1982**, 3.

[116] M. T. Riou, C. Clarisse, *J. Electroanal. Chem.* **1988**, *249*, 181.

[117] G. A. Corker, B. Grant, N. J. Clecak, *J. Electrochem. Soc.* **1979**, *126*, 1339.

[118] E. W. Tsai, S. Basok, J. P. Ruiz, J. R. Reynolds, K. Rajeshwar*, J. Electrochem. Soc*. **1989**, *126*, 3683.

[119] G. Sonmez, *Chem. Commun*. **2005**, *42*, 5251.

[120] P. M. S. Monk, *The Viologens,* Wiley & Sons; West Sussex, U.K., **1998**.

[121] D. Bongard, M. Moller, S. N. Rao, D. Corr, L. Walder, *Helv. Chim. Acta* **2005**, *88*, 3200.

[122] M. O. M. Edwards, *Appl. Phys. Lett.* **2005**, *86*, 073507.

[123] D. F. Qi, K. Varahramyan, S. Selmic, *Mater. Res. Soc. Symp. P* **2004**, *814*, 311.

[124] R. J. Mortimer, C. P. Warren, *J. Electroanal. Chem.* **1999**, *460*, 263.

[125] H. C. Ko, S. Kim, H. Lee, B. Moon, *Adv. Funct. Mater.* **2005**, *15*, 905.

[126] J. Y. Lim, H. C. Ko, H. Lee, *Synthetic Metals* **2006**, *156*, 695.

[127] P. M. S. Monk, In *The Viologens. Physicochemical Properties, Synthesis and Applications of the Salts of 4, 4'-Bipyridine*, ed.; "Ed.' John Wiley and Sons: New York, **1998**, 239.

[128] D. C. Bookbinder, M. S. Wrighton, *J Electrochem Soc* **1983,** *130*, 1080.

[129] J. A. Barltrop, A. C. Jackson, *J Chem Soc Perk 2* **1984**, 367.

[130] U. Bach, D. Corr. D. Lupo, F. Pichot, M. Ryan, *Adv. Mater.* **2002**, 14, 845.

[131] J. H. Ryu, D. O. Shin, K. D. Suh, *J Polym. Sci. Part A-Poly. Chem.* **2005**, *43*, 6562.

[132] L. Cen, K. G. Neoh, E. T. Kang, *Adv. Mater.* **2005**, 17, 1656.

[133] J. H. Ryu, Y. H. Lee, K. D. Suh, *J. Appl. Poly. Sci*., **2008**, 107, 102.

[134] J. H. Ryu, Y. H. Lee, S. H. Han, K. D. Suh, *Macro. Rapid. Commn.* **2007**, 27, 1156.

[135] M. Khiterer, K. J. Shea, *Nano Lett* **2007**, 7, 2684.

[136] S. Santra, R. P. Bagwe, D. Dutta, J. T. Stanley, G. A. Walter, W. Tan, B. M. Moudgil, R. A. Mericle, *Adv Mater* **2005,** *17*, 2165.

[137] C. B. Barbe, K. John, F. Linggen, L. Kim, H. Qiang, L. Michael, C. Sandrine, A. Bush, G. Calleja, *Adv Mater* **2004,** *16*, 1959.

[138] D. C. Bookbinder, M. S. Wrighton, *J. Electrochem. Soc.* **1983**, *130*, 1080.

[139] K. J. Shea, D. A. Loy, *Chem Mater* **2001,** *13*, 3306.

[140] K. J. Shea, D. A. Loy, O. Webster, *J Am Chem Soc* **1992,** *114*, 6700.

[141] K. J. Shea, D. A. Loy, *Polym. Mater. Sci. Eng.* **1990,** *63*, 281.

[142] K. J. Shea, J. Moreau, D. A. Loy, R. J. P. Corriu, B. Bour, *Bridged Polysilsesquioxanes. Molecular - Engineering Nanostructured Hybrid Organic-Inorganic Materials. In Functional Hybrid Materials, ed.; 'Eds. Wiley Interscience: New York,* **2004**, pp 50.

[143] K. M. Choi, K. J. Shea, *Photonic Polymer Synthesis*. ed., Marcel Dekker: New York, 1998; 437-480.

[144] P. Innocenzi, B. Lebeau, *J Mater. Chem.* **2005,** *15*, 3821.

[145] C. R. Kagan, D. B. Mitzi, C. D. Dimitrakopoulos, *Science* **1999,** *286*, 945.

[146] H. W. Oviatt, K. J. Shea, S. Kalluri, Y. Q. Shi, W. H. Steier, L. R. Dalton, *Chem Mater* **1995,** *7*, 493.

[147] K. J. Shea, S. T. Hobson, Tran, *J. Hybrid Organic/Inorganic Absorbents.* 2003.

[148] J. Liu, X. D. Feng, G. E. Fryxell, L. Q. Wang, A. Y. Kim, M. L. Gong, *Adv Mater* **1998,** *10*, 161.

[149] L. Mercier, T. J. Pinnavaia, *Adv Mater* **1997,** *9*, 500.

[150] G. T. Huang, *Technol. Rev* **2005,** *108*, 64.

[151] M. Khiterer, D. A. Loy, C. J. Cornelius, C. H. Fujimoto, J. H. Small, T. M. McIntire, K. J. Shea, *Chem Mater* 2006, *18*, 3665.

[152] I. Honma, Y. Takeda, J. M. Bae, *Solid State Ionics* **1999,** *120*, 255.

[153] S. Xiong, Y. Xiao, J. Ma, L. Zhang, X. Lu, *Macro. Rapid. Commn.* **2007**, 28, 281.

[154] J. H. Ryu, J. H. Lee, *Macromol. Rapid Comm.* **2004**, *27*, 1156.

[155] J. Y. Lim, H. C. Ko, H. Lee, *Synthetic Metals* **2006**, *156*, 695.

[156] D. Corr, U. Bach, D. Fay, *Solid State Ionics* **2003**, *4*, 315.

[157] R. Cinnsealach, G. Boschloo, S. N. Rao, D. Fitzmaurice, *Solar Energy Mater. Solar Cells* **1999**, *57*, 107.

[158] M. Moller, S. Asaftei, D. Corr, M. Ryan, L. Walder, *Adv. Mater*. **2004**, *16*, 1558.

[159] N. Vlachopoulos, J. Nissfolk, M. Moller, A, Briancon, D. Corr, M. Ryan, A. Hagfeldt, *Electrochim. Acta*, **2008**, 53, 4065.

[160] C. G. Granqvist, *Sol. Energy Mater*. **2000**, 60, 201.

[161] R. Sato, N. Ishii, N. Kawamura, H. Tokumara, *European Phase Change and Ovonics Science Symposium*, **2004**.

[162] M. Green, *Chem. Ind.*, **1996**, 17, 641.

[163] F. Huguenin,V. Zucolotto, A. J. F. Carvalho, E. R. Gonzalez, O. N. Oliveira, Jr, *Chem. Mate*. **2005**, 17, 6739.

[164] I. Moriguchi, J. H. Fendler, *Chem. Mater*, **1998**, 10, 2205.

[165] R. J. Mortimer, *Chem. Soc. Rev*. **1997**, 26, 147.

[166] P. R. Somani, S. Radhakrishnan, *Mater. Chem. Phys*. **2003**, 77, 117.

[167] D. M. Delongchamp, P. T. Hammond, *Adv. Funct. Mater.*. **2004**, *14*, 224.

[168] D. M. Delongchamp, P. T. Hammond, *Chem. Mater*. **2003**, 15, 1165.

[169] K. Rajeshwar, N. De Tacconi, C. R. Chentahmaramakrishnan , *Chem. Mater*., **2001**, 13, 2765.

[170] I. Carpani, M. Giorgetti, M. Berrettoni, P.L. Buldini, M. Gazzano, and D. Tonelli, *J. Solid State Chem.*, **2006**, 179, 3981.

[171] K. Itaya, I. Uchida, U.D. Neff, *Acc. Chem. Res.* **1986**, 19, 162.

[172] A. Jaiswal, J. Collins, B. Agricole, P. Delhaes, and S. Ravaine, *J. Colloid Interface Sci.*, **2003**, 261, 330.

[173] R. C. Milward, C. E. Madden, I. Sutherland, R.J .Mortimer, S. Flecher, and F. Marken, *Chem. Comm*., **2001**, 19, 1994.

[174] D. R. Rosseinsky, and A. Glide, *J. Electrochem. Soc.* **2003**, 150, C641.

[175] D. M. DeLongchamp P.T. Hammond, *Chem. Mater*. **2004**, 16, 4799.

[176] S. Chen, and S. Hsueh, *J. of Electroanal.l Chem.* **2004**, 566, 291.

[177] T. Ito, H. Shirakawa, S. J. Ikeda, *Polym. Sci. Chem. Ed.* **1974**, *12*, 11

[178] C. K. Chiang, C. R. Fincher, Y. W. Park, A. J. Heeger, H. Shirakawa, E. J. Louis, S. C. Gau, A. G. Macdiarmid, *Phys. Rev. Lett.* **1977**, *39*, 1098.

[179] H. Shirakawa, E. J. Louis, A. G. Macdiarmid, C. K. Chiang, A. J. Heeger, *J. Chem. Soc., Chem. Commun.* **1977**, 578.

[180] C. K. Chiang, M. A. Druy, S.C. Gau, A. J. Heeger, E. J. Louis, A. G. Macdiarmid, Y. W. Park, H. Shirakawa, *Phys. Rev. Lett.* **1977**, *39*, 1098.

[181] J. Roncali, *Chem. Rev*. **1992**, 92, 711.

[182] J. Roncali, *Chem. Soc. Rev.* **2005**, *34*, 483.

[183] Rabindra Sahoo, PhD Thesis, Chemistry, IIT-Mumbai, **2008**.

[184] G. Inzelt, Conducting Polymers, A New Era in Electrochemistry, Springer-Verlag Berlin 2008.

[185] S. Brady, K. T. Lau, W. Megill, G. G. Wallace, D. Diamond, *Synth Met.* **2005,** *154,* 125.
[186] M. Matsuguchi, J. Io, g. Sugiyama, Y. Sakai, *Synth. Met.* **2002,** *128,* 15.

[187] J. S. Yang, T. M. Swager, *J. Am. Chem. Soc.* **1998,** *120*, 11864

[188] K. Maksymiuk, K. Doblhofer, *Synth Meth.* **1993,** *55,* 1382.

[189] K. Maksymiuk, K. Doblhofer, *Electrochim. Acta,* **1994**, *39,* 217.

[190] C. C. Chen, C. S. S. Bose, K. Rajeshwar, *J. Electroanal Chem.,* **1988,** *350,* 161.

[191] G. Tourillon, F. Garnier, *J. Phys. Chem.* **1984,** *88,* 5281.

[192] A. F. Diaz, J. Crowley, J. Bargon, G. P. Gardini, J. B. Torrance, *J. Electroanal. Chem.* **1981**, *121*, 355.

[193] G. Tourillon, F. Garnier, *J. Electroanal. Chem.* **1982**, *135*, 173.

[194] A. G. MacDiarmid, J. C. Chiang, W. S. Huang, B. D. Humphrey, N. L. D. Somasiri, *Mol. Cryst. Liq. Cryst***. 1985**, *125*, 309.

[195] P. Novak, K. Muller, K. S. V. Santhanam, O. Haas, *Chem. Rev.* **1997**, *97*, 207.

[196] G. E. Collins, L. J. Buckley, *Synth. Met.* **1996**, *78,* 93.

[197] G. W. Yoon, P. R. Berger, *Appl. Phys. Lett.* **2008**, 92, 013306.

[198] P. Novak, K. Muller, K. S. V. Santhanam, O. Haas, *Chem. Rev.* **1997**, *97*, 207.

[199] J. H. Burroughes, D. D. C. Bradley, A. R. Brown, R. N. Marks, K. Mackay, R. H. Friend, P. L. Bum, A. B. Holmes, *Nature* **1990**, *347*, 539.

[200] R. N. Marks, J. J. M. Halls, D. D. C. Bradley, R. H. Friend, A. B. Holmes, *J.Phys: Condens. Matter.* **1994**, *6,* 1379

[201] T. A. Skotheim, J. R. Reynolds, "Handbook of Conducting Ppolymers, 3rd Ed.", CRC press , Boca Raton, Fl, 2007.

[202] F. Garnier, G. Tourillon, M. Gazard, J. C. DuBois, J. Electroanal. Chem. 1983, 148, 299.

[203] M. Gazard, J. C. DuBois, M. Champagne, F. Garnier, G. Tourillon J. Phys C 1983, 3, 537.

[204] M. Aizawa, S. Wantabe, H. Shinohara, H. Shirakwa, *J. Chem Soc Chem Comm*, **1985**, 25, 264.

[205] C. Wang, J. L. Schindler, C. R. Kannewurf, M. G. Kanatzidid, *Chem. Mater.* **1995**, *7,* 58.

[206] P. Blanchard, A. Cappon, E. Levillain, Y. Nicolas, P. Frere, J. Roncali, *Org. Lett.* **2002**, *4*, 607.

[207] E. Aqad, M. V. Lakshmikantham, M. P. Cava, *Org. Lett.* **2001**, *3*, 4283.

[208] F. Jonas, L. Schrader, *Synth. Met.* **1991**, *41-42*, 831.

[209] G. Heywang, F. Jonas, *Adv. Mater.* **1992**, *4*, 116.

[210] Bayer AG, *Eur. Patent* 440 957.

[211] F. Jonas, W. Krafft, B. Wuys, *Macromol. Symp.* **1995**, 100, 169.

[212] F. Jonas, W. Krafft. **1990**. EP 440 957.

[213] S. Kirchmeyer, K. Reuter, *J. Mater. Chem*., **2005**, *15*, 2077.

[214] I. Schwendeman, R. Hickman, J. R. Reynolds, D. M. Welsh, *Chem. Mater*. **2002**, 14, 3118.

[215] D. M. Welsh, A. Kumar, E. W. Meijer, J. R. Reynolds, *Adva. Mater*.**1999**, 11, 1379.

[216] S. I. Yaniger, D. W. Vidrine, *Appl. Spectros*., **1986**, 40, 174.

[217] Y. J. Qui, J. R. Reynolds, *J.Electrochem. Soc.* **1990**, 137, 900.

[218] B. Grant, N. J. Clecak, M. Oxsen, A. Jaffe, G. S. Keller, *J. Org. Chem*. **1980**, 45, 702

[219] A. Desbene-Monnvernay, P. C. Lacaze, A. Cherigui, *J. Electroanal. Chem*., **1989**, 260, 75.

[220] A. Wantabe, K. Mori, Y. Iwasaki, Y. Nakamure, S. Niizuma, *Macromolecules*, **1987**, 20, 1793.

[221] T. Kobayashi, H. Yoneyama, H. Tamura, *J. Electroanal. Chem*. **1984**, 161, 419.

[222] W. S. Huang, A. G. Macdiarmid, *Polymer* **1993**, 34, 1833.

[223] D. M. Delongchamp, P. T. Hammond, *Adv. Mater*. **2001**, 13, 1455.

[224] M.-C. Bernard, A. H.-L. Goff, W. Zeng, *Electrochim. Acta* **1998**, 44, 781.

[225] R. D. Giglia, G. Haacke, in Vol. IS 4 (Eds: C. M. Lampert, C. G. Granqvist), *SPIE*, Hamburg **1988**, 41.

[226] W. B. Stockton, M. F. Rubner, *Macromolecules* **1997**, 30, 2717.

[227] J. H. Cheung, A. F. Fou, M. F. Rubner, *Thin Solid Films*, **1994**, 244, 985.

[228] T. R. Farhat, J. B. Schlenoff, *Langmuir* **2001**, 17, 1184.

[229] M. Shim, P. Guyot-Sionnest, *Nature*, **2000**, 407, 981.

[230] C. B. Murray, D. J. Norris, M. G. Bawendi, *J. Am. Chem. Soc*. **1993**, 115, 8706.

[231] M. Shim, C. Wang, P. Guyot-Sionnest, *J. Phys. Chem B*., **2001**, 105, 2369.

[232] D. Yu, C. Wang, P. Guyot-Sionnest, *Science* **2003**, 300, 1277.

[233] C. Wang, M. Shim, P. Guyot-Sionnest, *Appl. Phys. Letters*, **2002**, 80, 4.

[234] A. A. Mamedov, A. Belov, M. Giersig, N. Mamedova, N. A. Kotov, *J. Am. Chem. Soc*. **2001**, 123, 7738.

[235] N. A. Kotov, *MRS Bulletin*, Dec **2001**, 992.

[236] S. Liu, D. G. Kurth, H. Mohwald, D. Volkmer, *Adv. Mater.* **2002**, 14, 3, 225.

[237] Heteropolytungstates comprising the D_{5h}-symmetric P-W-O framework with composition $P_5W_{30}O_{110}]^{15-}$were first synthesized by Preyssler: C. Preyssler, *Bull. Soc. Chim. Fr.* **1970**, 30. The correct structural assignment, however, was achieved later by Jeannin, Pope et al.: M. H. Alizadeh, S. P. Harmalker, Y. Jeannin, J. Martin-Frere, M. T. Pope, *J. Am. Chem. Soc*. **1985**, *107*, 2662.

[238] U. Bach, D. Corr, D. Lupo, F. Pichot, M. Ryan, *Adv. Mater.* **2002**, 14, 845.

[239] N. Vlachopoulos, J. Nissfolk, M. Möller, A. Briançon, D. Corr, C. Grave, N. Leyland, R. Mesmer, F. Pichot, M. Ryan, G. Boschloo, A. Hagfeldt, *Electrochim. Acta*, **2008**, *53*, 4065.

Chapter 3

Solid-State Electrochromic Devices via Layer-by-Layer Assembly of a Polyviologen

This chapter presents electrochromic studies of a polyviologen (PV) that was synthesized by polymerization of N,N'-bis(-δ-aminopropyl)-4,4'-bipyridinium bromide hydrobromide (APD) and isophthaloyl chloride (ISP). The PV was completely soluble in water as well as in organic solvents. The spectroelectrochemical and electrochromic properties of the resulting Layer-by-Layer (LbL) films of PV/poly (2-acrylamido 2- methylpropanesulfonic acid) (PAMPs) were examined by cyclic voltammetry, Fourier transform infrared (FTIR) spectroscopy, UV–vis spectroscopy, optical switching and current density measurements. Solid state devices made of PV films sandwiched with polyaniline (PANI) as a counter electrode have switching times of 100-250 ms. 40-bilayer films of PV/PAMPs show high contrast (ΔT = 61%) in 0.1 M $NaClO_4$ liquid electrolyte solution and coloration efficiency (CE) as high as 57 cm^2/C, one of the highest reported so far for any bipyridinium salt system.

3.1 Introduction

Since the first major report on electrochromism, there has been much work done in the field of inorganic[1] and phthalocyanine[2,3] compounds as possible electrochromic materials, while the work with conducting polymeric[4,5] electrochromic devices has gained significant attention in the last decade or so. Other electrochromic materials have been studied, but polyviologens (which are bipyridinium systems) and their derivatives have been widely investigated for more than thirty-five years because of their electrical and electrochromic properties and good environmental stability.[6] A great amount of work has been done for dialkyl bipyridinium units, but significant efforts have also been made from time to time on the modification of their chemical structures to improve the electrochromic properties[7] and film-forming abilities.

Bipyridinium salts exhibit three redox states: the colorless dication (+2), colored radical cation (+1) and neutral. Out of all these states, the colorless dication is the most stable, followed by the radical cation, whose stability depends upon the delocalization of the radical electron in the π-framework. Electrochromism in bipyridinium species occurs due to the interconversion of these three species. Manipulation of the substituents at N and N' modifies the color by attaining the appropriate molecular orbital energy levels. Suitable substitution not only results in "fine color tuning" of the polyviologen system, but also results in the alteration of the redox and other physical properties without disturbing the electroactivity. Attached groups (aryl or alkyl) influence the reduction potential (E°), but further substitution of the aromatic system helps in tuning the rate of electron transfer between the redox species and influences the contrast, switching speed and coloration efficiency. Recently polyviologens have been applied in liquid crystalline devices, [8] light emitting diodes,[9] printing[10] and frozen food monitoring.

Several groups have previously reported[11,12,13,14] polyviologen electrochromic devices on mesoporous electrodes for display purposes, but the major breakthrough in this field came from the work done by Ntera Inc. [15] Continuing towards the same aim, our group has assembled and fabricated fast-switching solid-state devices of polyviologen with very high coloration efficiency, high contrast and long life, making them viable candidates for active-matrix displays.

In this work, we discuss the electrochromic properties of a polyviologen (PV)[16] LbL films with poly(2-acrylamido-2-methylpropanesulfonic acid) (PAMPs). Sammells et al.[17] incorporated PAMPs (10% w/w in water) within a heptylviologen system by suspending the latter with simple mixing; this brings higher contrast into the system with long-term write-erase efficiency, but slows the response time to a significant extent. To improve the contrast in the system we preferred PAMPs at a very low weight percentage [4.125 x 10^{-2} % w/w (2 mM) in water] as a polyanion in the LbL film assembly because of its natural ability to transfer ions, and the fact that it provides less bulk resistance and faster color change. The bilayers were characterized by cyclic voltammetry, Fourier transform infrared (FTIR) spectroscopy, UV–vis spectroscopy and current density and coloration efficiency (CE) measurements. In this study, we measured the electrochromic response of PV films in liquid electrolyte as well as solid state devices composed of PV/PAMPs slides sandwiched with films of polyanilne (PANI)/PAMPs.

3.2 Experimental

3.2.2 Equipment

^{1}H and ^{13}C NMR spectra were acquired on a VARIAN 400 MHz spectrometer, with $CDCl_3/D_2O$ as the solvent, and chemical shifts (δ) are given relative to tetramethylsilane as the internal standard. Mass spectra were obtained on a Fisons VG Quattro instrument. The melting point was obtained on a Mel-temp II instrument. An EG & G 273 A potentiostat/galvanostat was used for cyclic voltammetry (CV) studies. For electrochemical characterization, an indium tin oxide (ITO) coated glass slide was used as a working electrode, a Pt wire as the counter electrode, and a standard calomel electrode (SCE) as the reference electrode. Potential step chrono-amperometry was performed using a Voltalab 40 (Radiometer Analytical) instrument. An automated dipping machine from Nanostrata Inc. was used for deposition of the multilayer films. ITO-glass substrates with dimensions 3" x 1" were bought from Delta technologies. SEM images of the coated surface were taken on a LEO 1550 field emission scanning electron microscope (FESEM) at an accelerating voltage of 5 kV. Film thickness measurements were performed using a J. A.Woollam VB-2000 ellipsometer.

3.2.3 Fourier Transform Infrared – Attenuated Total Reflectance (ATR) Spectroscopy

Fourier transform IR analysis of the PV in powder form was performed on a Midac M2004 FTIR system. A SensIR "DurasamplIR" single bounce diamond ATR accessory was used to investigate the Mid-IR range (4000 to 650 cm^{-1}). The resolution used for the IR analysis was 4 cm^{-1}. Mirror velocity, aperture settings, and signal gain were set to 4 and a DTGS (tellurium-germanium selenide) room temperature IR detector was used in the setup. Every absorbance spectrum was created by averaging a total of 64 scans.

3.2.4. N,N'-bis(δ-aminopropyl)-4,4'-bipyridinium bromide hydrobromide (APD)

(Synthesis of this compound was performed by Dr. Hong Wang in Prof Gibson's Lab, Chemistry, Virginia Tech)

Under the protection of N_2, to a solution of 24.63 g (112.5 mmol) of 3-bromopropylamine hydrobromide in 62 mL of anhydrous ethanol at 45 ºC was added 8.25 g (52.8 mmol) of 4,4'-bipyridyl and 50 mL of anhydrous ethanol. After the solid was dissolved, the solution was heated at reflux. After about 5 h, the reaction solution became a yellow suspension. After 45 h, the hot thick yellow suspension was filtered, and the solid was washed 3 times with hot ethanol, and then 3 times with acetone. After drying in vacuum, the pale-yellow solid was dissolved in a small amount of water, and then precipitated by slow addition to ethanol while vigorously stirring. After it was collected by filtration and dried in vacuum, APD was obtained as a pale yellow powder (30%), mp 320 ºC (dec), lit. m.p 325 ºC. [23] ^{1}H NMR (ppm): δ 2.60 (m, 4H), 3.37 (t, *J*=7, 4H), 4.97 (t, *J*=7, 4H), 8.72 (d, *J*=8, 4H), 9.34 (d, *J*=8, 4H). ^{13}C NMR (ppm): δ 28.5, 36.3, 59.4, 127.2, 146.0, 150.3. The ^{1}HNMR and ^{13}C NMR spectra of APD (Figures 3.1 and 3.2) are consistent with its structure.

The molecular ion of APD is not observed in its mass spectrum (Figure 3.3); the fragment at m/z 272 is due to loss of HBr and 2 Br. The m/z 215 fragment results from loss of one of the aminopropyl groups along with one HBr and three Br.

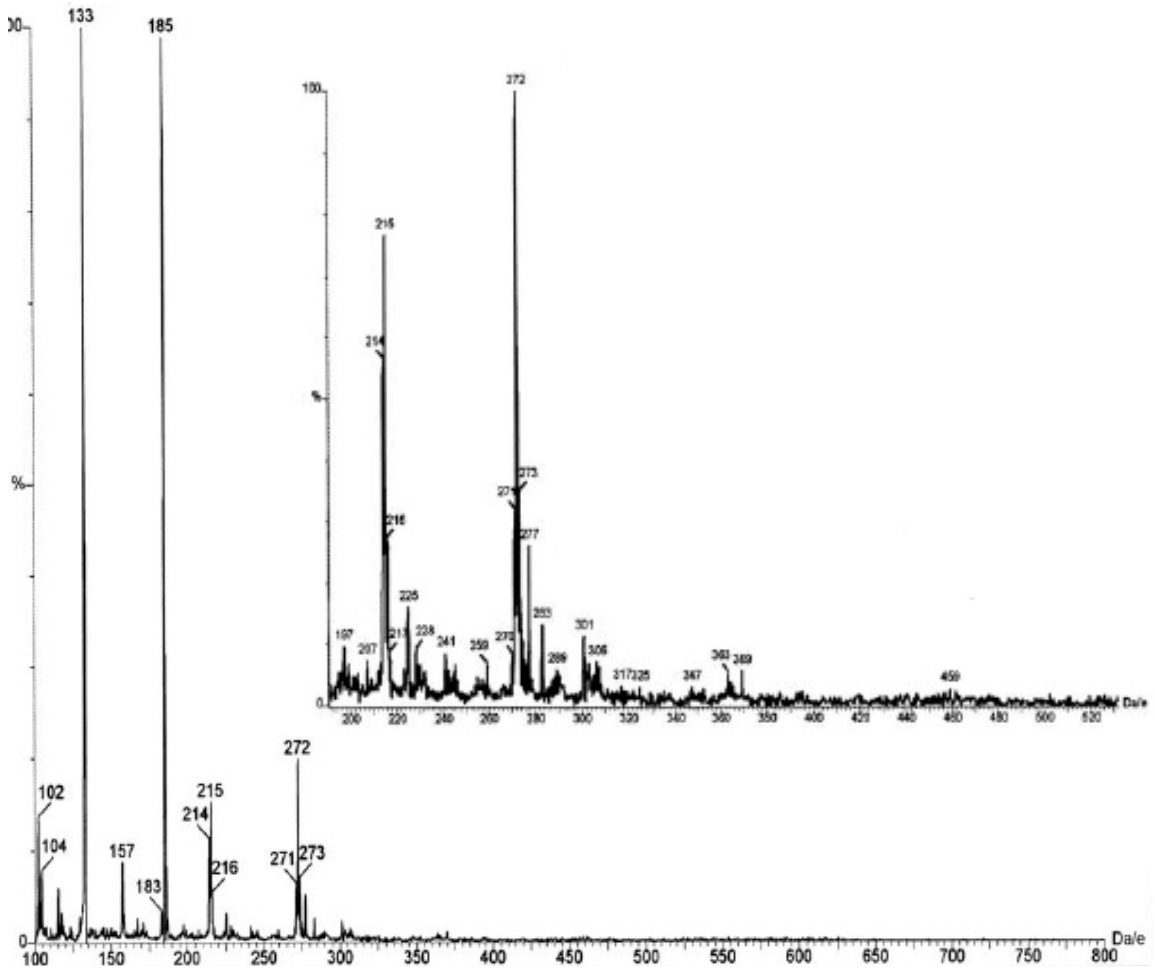

Figure 3.1 Positive ion FAB mass spectrum of the pyridinium monomer APD.

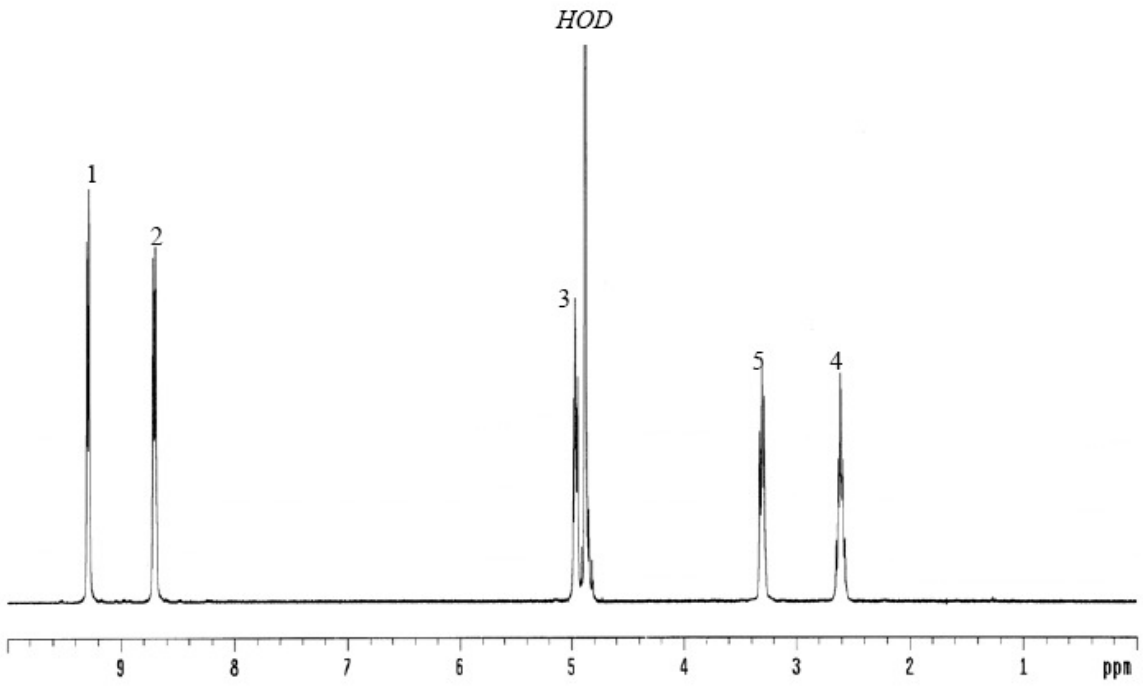

Figure 3.2 400 MHz ^{1}HNMR spectrum of the pyridinium monomer APD in D_2O.

3.2.5. Polymerization of APD and isophthaloyl dichloride

(Synthesis of this compound was performed by Dr. Hong Wang in Prof. Gibson's Lab, Chemistry, Virginia Tech)

To a vigorously stirred solution of 1.19 g (2.00 mmol) of APD and 0.42 g (4.0 mmol) of Na_2CO_3 in 10 mL of water was added a solution of 0.45 g (2.2 mmol) of isophthaloyl dichloride in 5 mL of dichloromethane. After about 15 min, a transparent gel was observed on the wall of the reaction flask. After 2 h, water was added to dissolve the gel by stirring overnight. The suspension was filtered. The filtrate was dropped into a large amount of acetone with vigorous stirring. After stirring overnight, the yellow solid was collected and dried in vacuum, 0.73 g (46%). ^{1}H NMR (ppm): δ 2.50 (m, 4H), 3.22 (m, 0.19H), 3.6 (4H), 4.97 (t, *J*=7, 4H), 7.5-8.6 (m, 8H), 9.20 (d, *J*=8, 4H). In the infrared spectrum the peak at 1525 cm^{-1} is due to the C=C

stretching of the aromatic ring of the bipyridinium moiety, the shoulder at 1507 cm^{-1} may be attributed to the C=C stretching of the isophthaloyl group. Moreover, the weak peak at 1690 cm^{-1} may be attributed to C=O stretching. The absorption bands at 1267, 1230 and 1169 cm^{-1} show the presence of C-N stretching vibrations of the amine bond, which are the characteristic functional group of the monomer. Peaks at 808 and 843 cm^{-1} arise from the in-phase out of plane aromatic C-H bending.

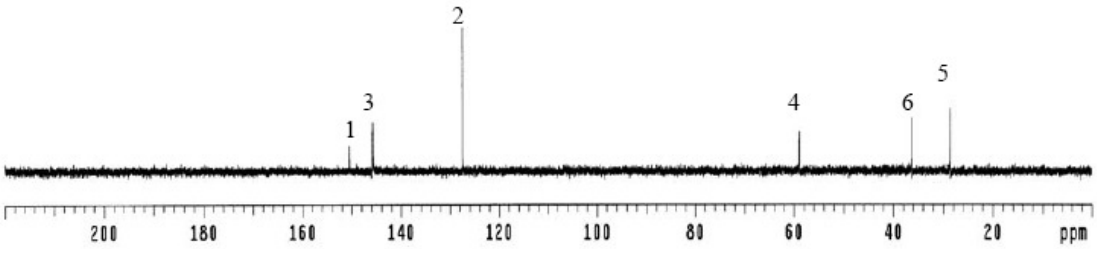

Figure 3.3 100 MHz ^{13}C NMR spectrum of the monomer APD in D_2O.

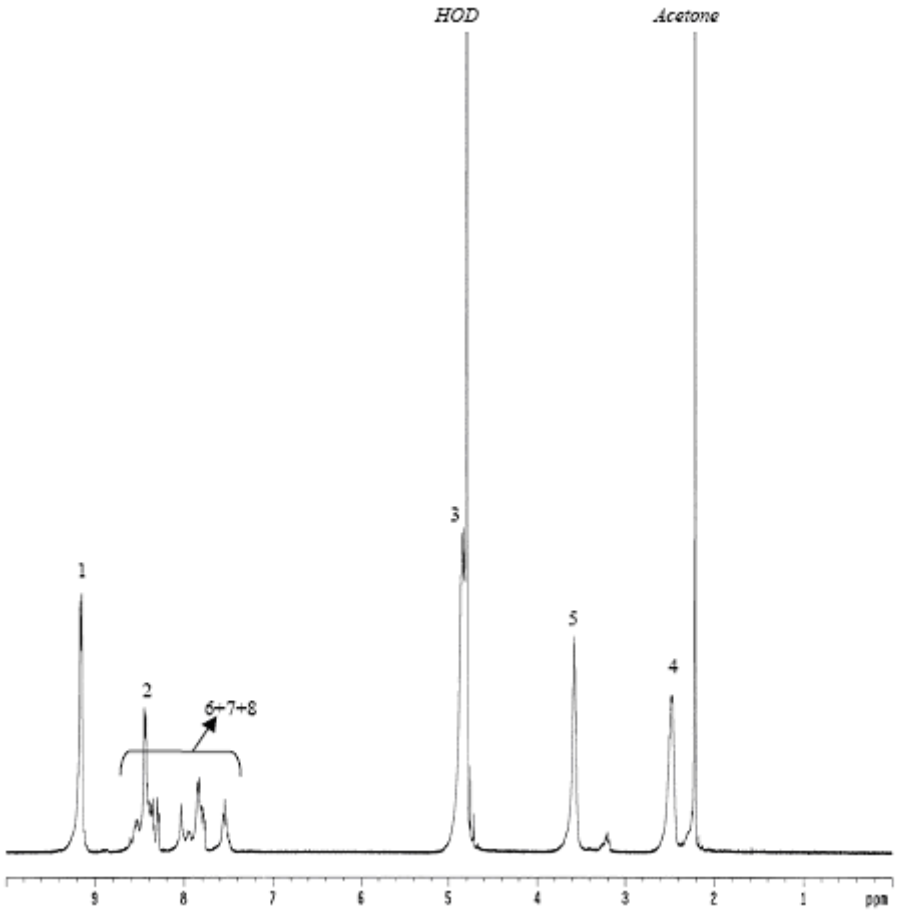

Figure 3.4 400 MHz ^{1}HNMR spectrum of the PV in D_2O.

Assuming one amino end group and one acid end group, the number average molecular weight (M_n) of the PV was estimated to be 3.0 kDa by end group analysis using ^{1}HNMR (Figure 3.4); the integral of the terminal methylene unit of the amine end at 3.2 ppm was compared to those of the main backbone signals.

3.2.6 Film Fabrication

LbL film fabrication was performed with the help of an automated slide stainer. The ITO slides were washed with water to develop some negative charge and then exposed to PV (pH 4, 2 mM) solution for 6 min, followed by 3 steps of rigorous rinsing with de-ionized water for 45 sec. Finally, the substrates were exposed to PAMPs (pH 4, 2 mM) solution for 6 min and again rinsed

with water for 45 sec each in three consecutive water baths. This cycle was repeated 40 times to get the desired number of bilayers. The pH of the solutions was adjusted with sodium hydroxide or hydrochloric acid.

For solid state devices, as shown in the Figure 3.5, the PV/PAMPs multilayer film described above was sandwiched with another film with a few drops of PAMPs gel placed in between. The other film was fabricated as above with PANI instead of PV. The PAMPs component of these films is not electrochromic.

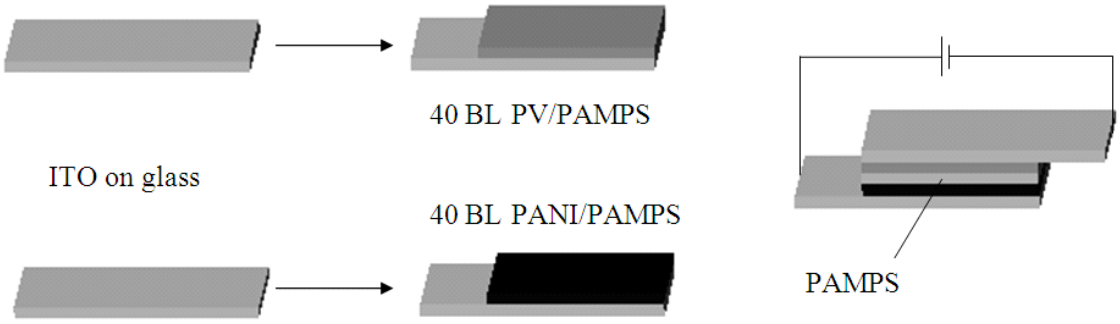

Figure 3.5 Solid-state dual ECD device from LbL films of PV/PAMPs and PANI/PAMPs.

It was found that a PV/PAMPs-PV/PAMPs sandwich did not have any color change with applied voltage, while the PV/PAMPs-PANI/PAMPs sandwich showed the same color change with an absorption peak at ~515nm as the PV/PAMPs in liquid electrolyte solution. This is distinguishable from the electrochromism of devices consisting of two PANI/PAMPs films, which we have shown in previous work to exhibit a peak absorption at 500 nm.[18]

3.3 Results and Discussion

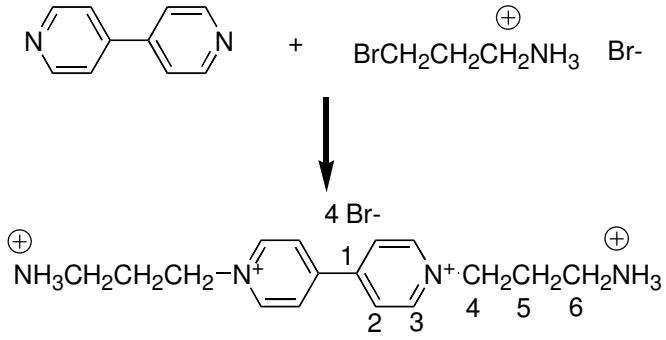

Scheme1: Synthesis of APD.

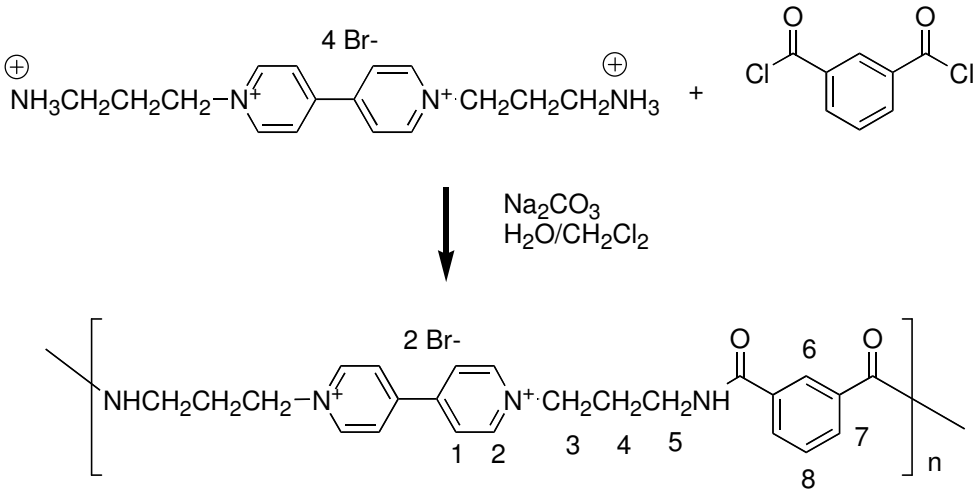

Scheme 2: Polymerization of APD and isophthalolyl chloride.

3.3.1 Film Thickness:

Figure 3.6 shows the cross sectional view of the 40 bilayer film of PV/PAMPs; with little surface roughness, the thickness of the film varies between 190-210 nm. The total film thickness increases linearly with the number of bilayers according to the equation $t = 4.537b$ (Figure 3.7), where t is the total film thickness in nm and b is the number of bilayers. The overall variation in

the actual film thickness from the reported values is ± 2% of the total film thickness. The linear increase in the thickness by 4.5 nm per layer pair is true for the first few bilayers as well as for higher numbers of bilayers. The film thicknesses were confirmed by ellipsometry.

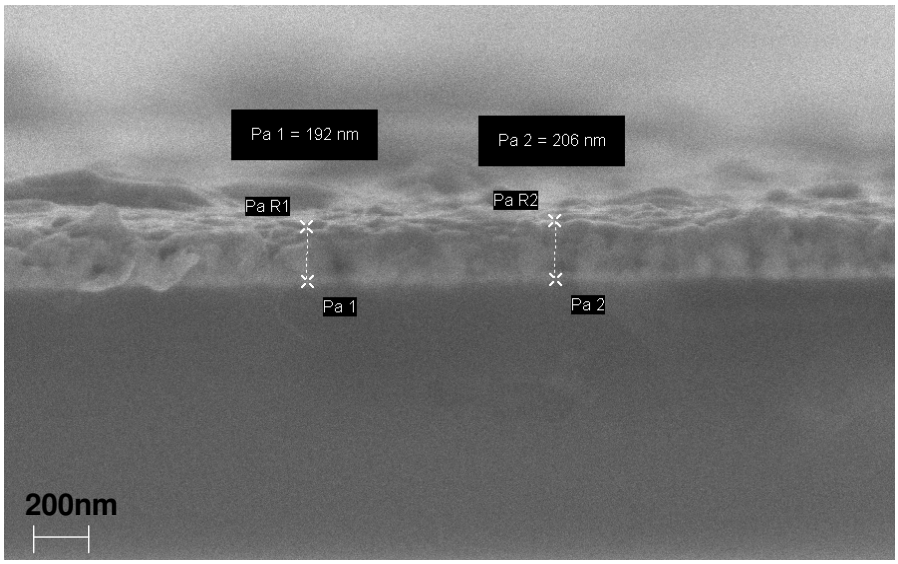

Figure 3.6 An SEM image of the cross section of a 40-bilayer film of PV/PAMPs done at 5kV shows the measurements of 192 nm and 206 nm.

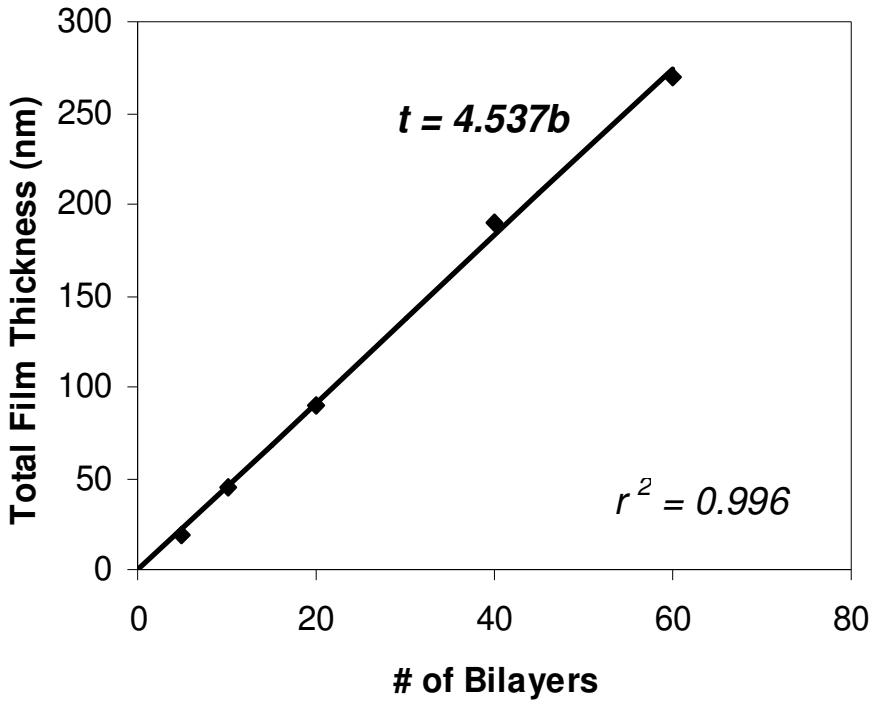

Figure 3.7 Total thickness of PV/PAMPs films with increasing number of bilayers.

The thickness of LbL films formed by several other groups[7, 13] did not increase in a linear fashion; one of the possible sources for that phenomenon is the relative concentration of the polyanion and polycation solutions. If the polyanion concentration is higher than the polycation concentration, the films develop a globular morphology and increased roughness, which results in a super-linear or exponential increase in the film thickness with the number of bilayers. In our study, special care was taken to keep the same concentration (2 mM) for both the PV and PAMPs solutions. Atomic force microscopy (AFM) images (not shown here) also confirm the extremely smooth and homogenous films of RMS surface roughness (Rq) of less than 2 nm for films with as many as 100 bilayers.

3.3.2 Coloration efficiency (η)

For electrochromic materials to be employed in fast-switching and efficient display operations, the value of the coloration efficiency η should be as high as possible. There has been a report of η as high as 1400 cm^2/C in the case of a conducting polymer-based electrochromic

device. [19,20] The best coloration efficiency value of any polyviologen system reported to date is 170 cm^2/C. [21]

Change in the transmittance state from colorless to dark violet gives an optical density of

$$\Delta OD(\lambda) = \log [T_b(\lambda)/T_c(\lambda)] \quad (1)$$

$$= 0.49$$

$$\eta(\lambda) = \Delta OD(\lambda)/Q_d \quad (2)$$

in which $Q_d = 8.8$ $mC.cm^{-2}$ for the reduction step and is calculated as the area under the CV curve for the reduction peak for a scan rate of 100 mV/s. The active working area of the film on the ITO electrode was 10 cm^2.

$$\eta(\lambda) = 57 \text{ cm}^2/\text{C}$$

The absence of a second reduction peak in the CV curve, even at low scan rates, makes it difficult to calculate the charge required for the second reduction step from monocationic to the completely reduced state. As explained by Cinnsealach et al.,[16] the extinction coefficient (ε) of the reduced PV, assuming that every electron injected into the ITO electrode reduces a viologen moiety, can be expressed as:

$$\varepsilon(\lambda) = \eta(\lambda) F/1000 = 96.5\, \eta(\lambda) \quad (3)$$

in which F is the Faraday constant (96.5 x 10^3 C/mol).

The value of ε for the reduced PV film at 515 nm was 5.3 x 10^3 $M^{-1}cm^{-1}$, which falls within the range of values reported by Monk et al. [1] for bipyridinium systems.

3.3.3 Cyclic Voltammetry (CV)

A CV measurement was applied to a 40-bilayer film of PV/PAMPs (Figure 3.8). The results are similar to those of the PV-containing LbL films studied by Delongchamp et al.[13] A

sharp peak appears at -0.6 V, corresponding to fast first reduction, and the resulting monocationic radical shows dark violet color in the visible region. The redox activity and color changes reported here are representative of the wide class of viologens, so the color change observed is due to the change in the redox state of bipyridinium moiety. The phthalic acid diamide unit in the PV is electroactive, but does not undergo any redox process within the voltage range employed. The dark violet color remains during the reduction scan between -0.6 to -0.85 V, but changes to pale yellow due to the doubly reduced viologen at potentials higher than -0.9 V. The second reduction peak, which corresponds to the yellow color, was not observed in the current CV scan of potential window from 0 to -1.0V, but has been observed by several other groups at -1.0 V or higher for scan rates of 10mV/s or slower.[22]

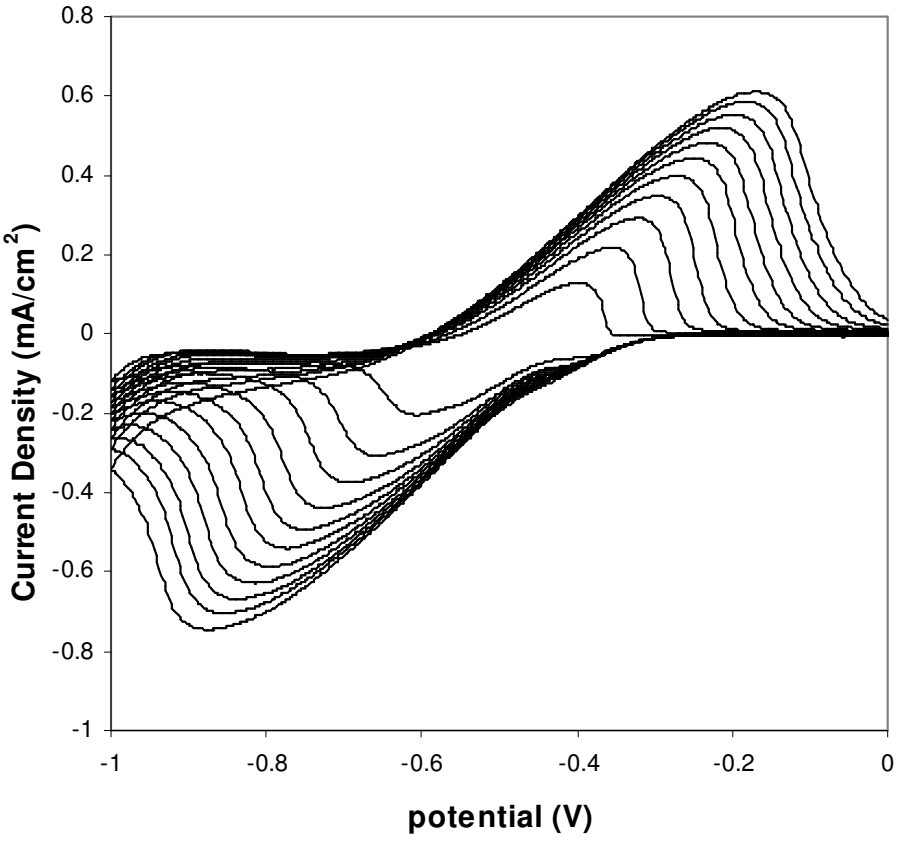

Figure 3.8 Cyclic voltammogram for the 40-bilayer film of PV/PAMPs in aqueous 0.1 M $NaClO_4$; reference was SCE. Active electrode of the film was $10cm^2$. Scan rate varies from 10 mV/s to 110 mV/s.

During the oxidation scan, the color changes from pale yellow to dark violet and finally back to the original transparent state. Both reduction and oxidation peak current densities increase with the scan rate; this confirms that the reaction is diffusion controlled but slow (Figure 3.9). The PV/PAMPs films formed by the LbL fabrication technique are quite thin and display an increase in hysteresis for both peaks because of the internal resistance of the bulk film. As explained by Bird et al.,[23] the CV experiment of polyviologens in a wide potential window from 0 to -1.0V or higher is chemically irreversible and the film degrades easily after a couple of scans with no peak, thus we limited the number of scans more negative than -1.0 V.

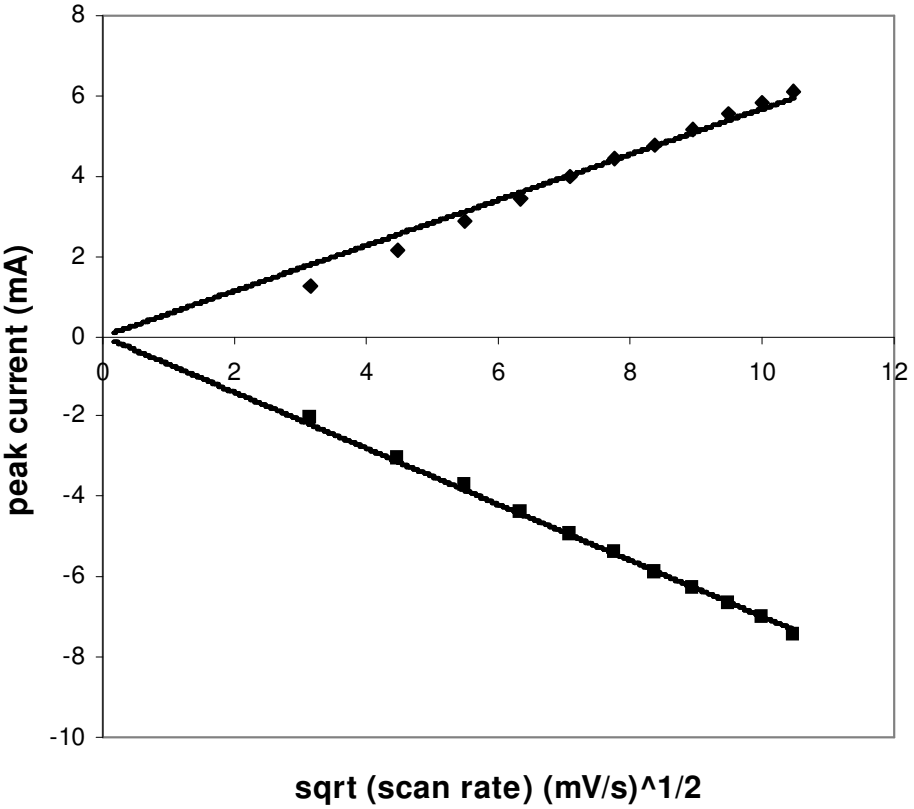

Figure 3.9 Peak current vs. square root of scan rate for oxidation and reduction peaks of a 40-bilayer film of PV/PAMPs in aqueous 0.1 M $NaClO_4$; reference was SCE. Active electrode area of the film was 10 cm^2.

Peak current density varies linearly with the square root of scan rate for both oxidation and reduction, which confirms that the redox process is diffusion controlled and the whole film contributes to the change in color. Although the peaks skewed away from the potential, the peak current density linearly fits best with the square root of scan rate with an R^2 value of over 0.996 as compared to scan rate, which has a value of 0.72. This is one of the primary reasons that we observe such a high color contrast from the contribution of PV alone.

Diffusion controlled redox is significant for the long-term stability of EC devices as it prevents charge trapping and film degradation with time, as observed with surface controlled redox processes. The whole thin LbL film is accessible in this case and it also brings out the maximum contrast possible for PV. Cyclic voltammetry was done for films of different numbers of bilayers, and for all multilayer films upto 100 bilayers the diffusion-controlled rate of redox process remained constant.

3.3.4 Chrono-Amperometry

Chrono-amperometry was performed by stepping between -0.9 V and 0.1 V (vs. Hg/HgO) with 30 seconds per step and 60 seconds per cycle. 40 and 100 bilayer films (Figure 3.10) coated on ITO electrodes were used as working electrodes in a supporting electrolyte of aqueous 0.1 M KBr with a platinum wire as the counter electrode. For all the films, several cycles were performed sequentially before the data was measured. The current wave was invariant for at least 200 complete cycles. The maximum current density increased with increased bulk film thickness and shows a slower response time with increasing numbers of bilayers. The reduction step shown in Figure 3.10 (a) has the final charge density (area under the current density trace) at 5 s of 70 mC/cm^2 and 22 mC/cm^2 for 100 and 40 bilayers respectively.

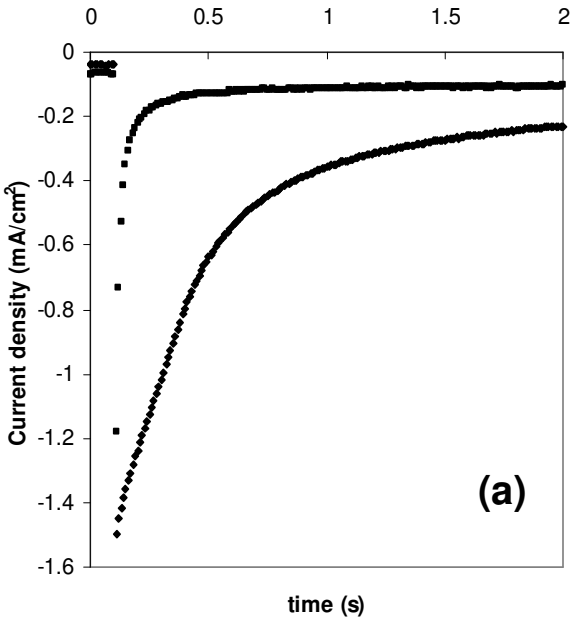

Figure 3.10 Reductive (a) and oxidative (b) current profile during switching from -0.9 V to 0.1 V for PXV/PAMPS films of 40 and 100 bilayers. Active electode surface areas of the 100 and 40 bilayer LbL film were 8.25 cm^2 and 5.75 cm^2 respectively. Electrolyte was 0.1M KBr and the reference was Hg/HgO.

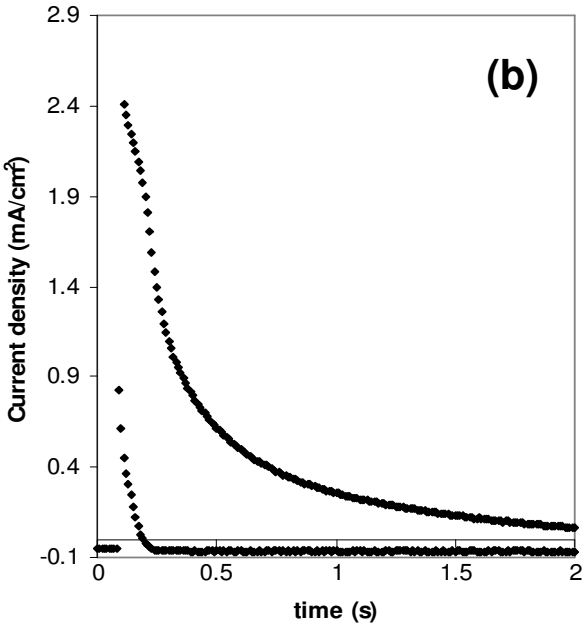

This ratio is not consistent with the increase in the number of bilayers; this phenomenon has also been observed by other groups studying the EC film properties of LbL films of polyviologen system.[13,24] Although a detailed explanation of this phenomenon is not clear, it is tentatively attributed to the charge trapping in the case of the thicker films.

3.3.5 Spectroelectrochemistry of electrochromic devices

3.3.5.1 Single-type electrochromic devices

Spectroelectrochemical studies of a 40-bilayer PV/PAMPs film in 0.1 M $NaClO_4$ (aq) were performed to study the transmission spectral changes with applied voltages at 0 V and from -0.6 V to -1.0 V (Figure 3.11).

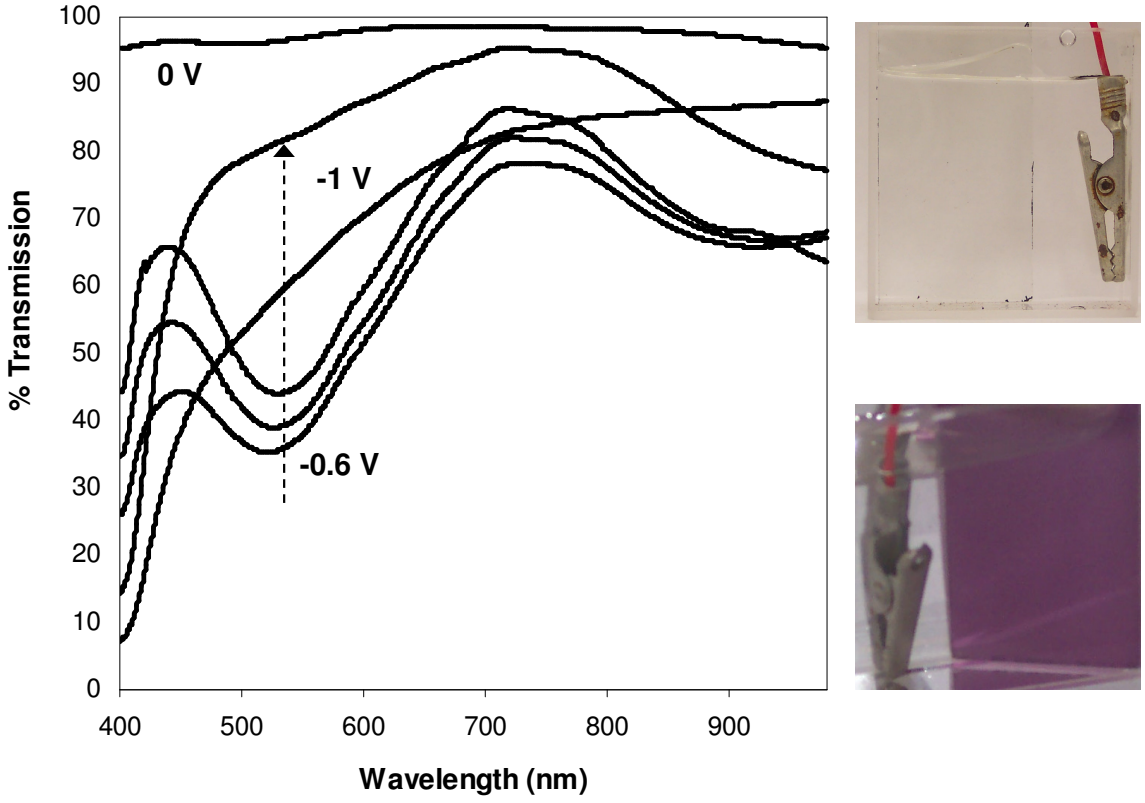

Figure 3.11 Transmission spectra of 40 bilayers of PV/PAMPs in 0.1 M $NaClO_4$ (aq) solution with an active electrode surface area of 10 cm^2. Applied voltage in direction of arrow is -0.6 V, -0.7 V, -0.8 V, -0.9 V, and -1.0 V. Digital photographs of bleached (colorless) and colored states (dark violet) of a 40-bilayer PV/PAMPs film.

The film changed from the colorless state of the +2 oxidation state to the violet of the reduced +1 state to the transparent pale yellow of the completely reduced state. At λ_{max} 515 nm, a maximum transmission change of 61% was observed between the color states at 0 V and -0.6 V of the mono-cationic state. On stepwise increase in the voltage from -0.6 V to -1.0 V, the observed change was 42% between dark violet and pale yellow color states. The second reduction peak was not observed in the CV experiment in the potential window from 0V to -1V, but the yellow color attributed to this state was observed by spectroelectrochemistry during the application of -0.9V and higher. It is important to note that the film changes color to yellow, which is an unstable state for an extended period of time. For the long-term stability, the device should mainly work in the dicationic-monocationic transition. At -0.6 V, the transmission spectrum remained unchanged, indicating that all the viologen moieties were reduced to the +1 oxidation state. Application of voltage higher than -1.5 V resulted in irreversible degradation to a permanently brown color. The contrast observed here for single electrochromic devices was on a par with results reported for polyviologens by other groups.[7, 12]

3.3.5.3 Dual-type electrochromic devices

A dual-type ECD device was fabricated with PANI as an anodically-coloring material and PAMPs as the polyelectrolyte gel. PAMPs in diluted form (2 mM) was used as the polyanion for LbL film fabrication and in gel form (15% w/w in water) as the polyelectrolyte. The solid-state device was made up of 40 bilayers of cathodically coloring PV/PAMPs and 40 bilayers of anodically coloring PANI/PAMPs. The contrast of the 40-bilayer dual-type electrochromic device was 25% at 515 nm (Figure 3.12) on application of +2 V with respect to the PANI/PAMPs electrode.

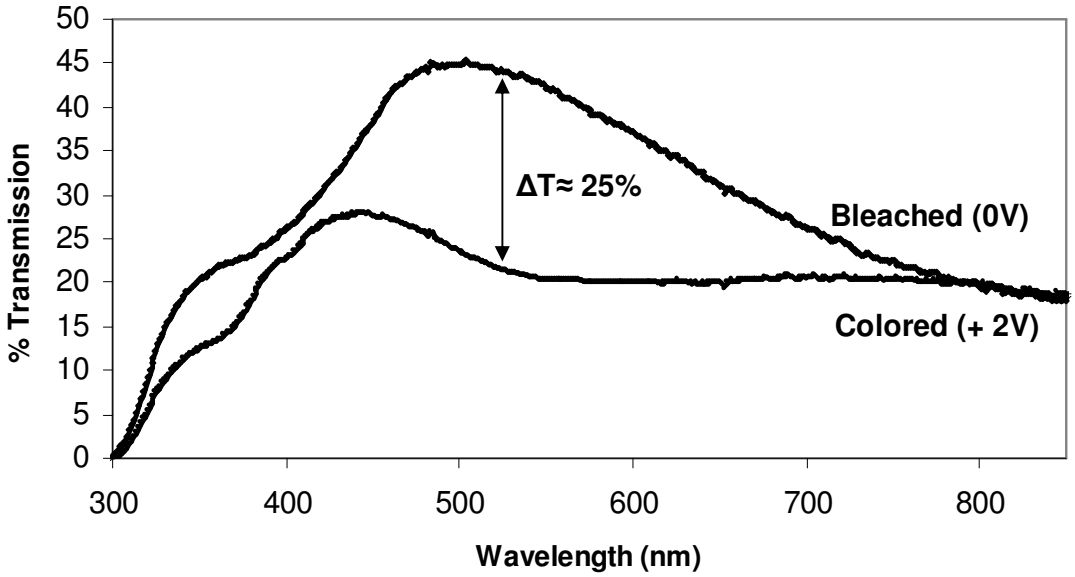

Figure 3.12 Transmittance change in the solid-state device of 40 bilayers PV/PAMPS and 40 bilayers of PANI/PAMPS on application of + 2V.

The maximum color change was observed at a wavelength similar to the one observed in salt solution (Figure 3.11). The contrast change for a 40-bilayer solid-state device is also on a par with the results shown by Lee et al.[25] for polythiophene-based devices.

3.3.6 Switching speed in solid-state

Switching of our devices was monitored over time with a He-Ne laser (633 nm) and photodiode as the square wave voltage (+2.0 to -2.0 V) was applied to the electrochromic film. The solid-state device changed color from light green to dark violet and yellow at different voltages. As seen in Figure 3.9, the device had a switching time of 100 ms for coloration and a de-coloration time of 250 ms at 70% overall change in transmittance at switching voltages of 2.0 V to -2.0 V; the optical switching reported is for the color change from light green to dark violet. As explained by Baioni et al., the difference in coloration and de-coloration time of the device is because of the different time constants for ejection/insertion of ions from/to the PV/ PAMPs matrix.[26] The area of the color-changing pixel in the solid-state device was 2 cm^2. To the best of

our knowledge, this is the fastest polyviologen switching ever reported. For better understanding of the coloration and decoloration times, an expanded view of the switching curve is also presented. For one of the best electrochromic displays of size 2.5 cm^2, Pettersson et al. reported coloration and de-coloration times of 300 ms and 400 ms, respectively.[27]

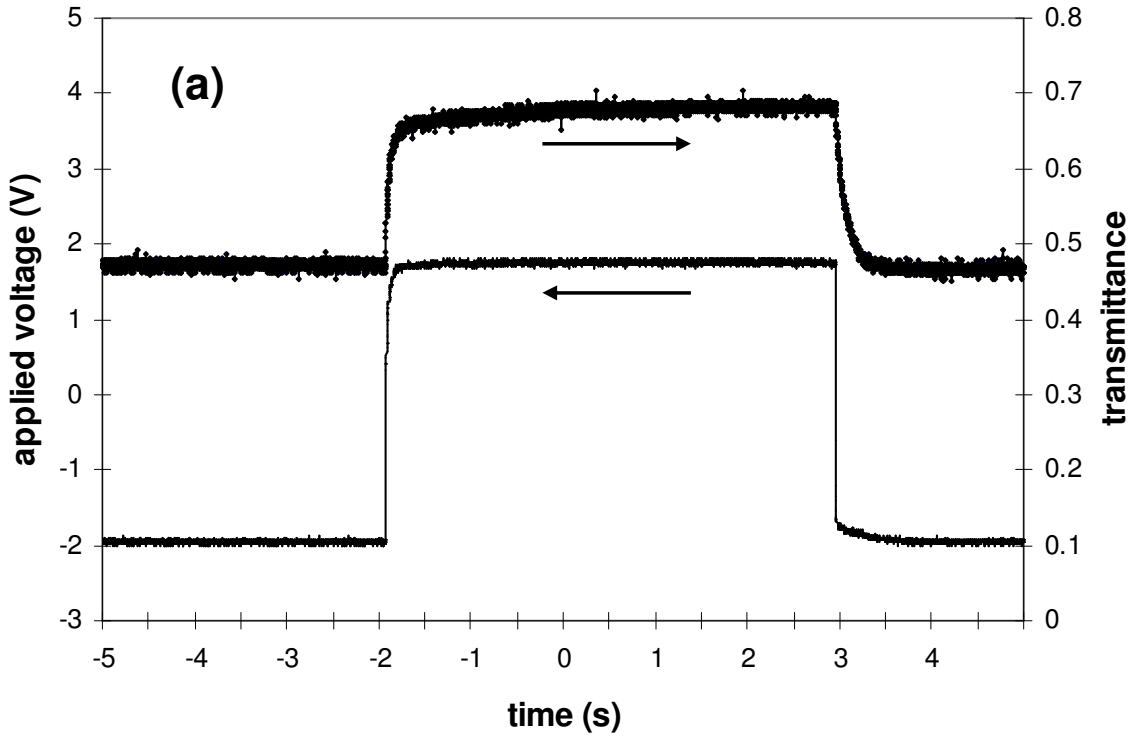

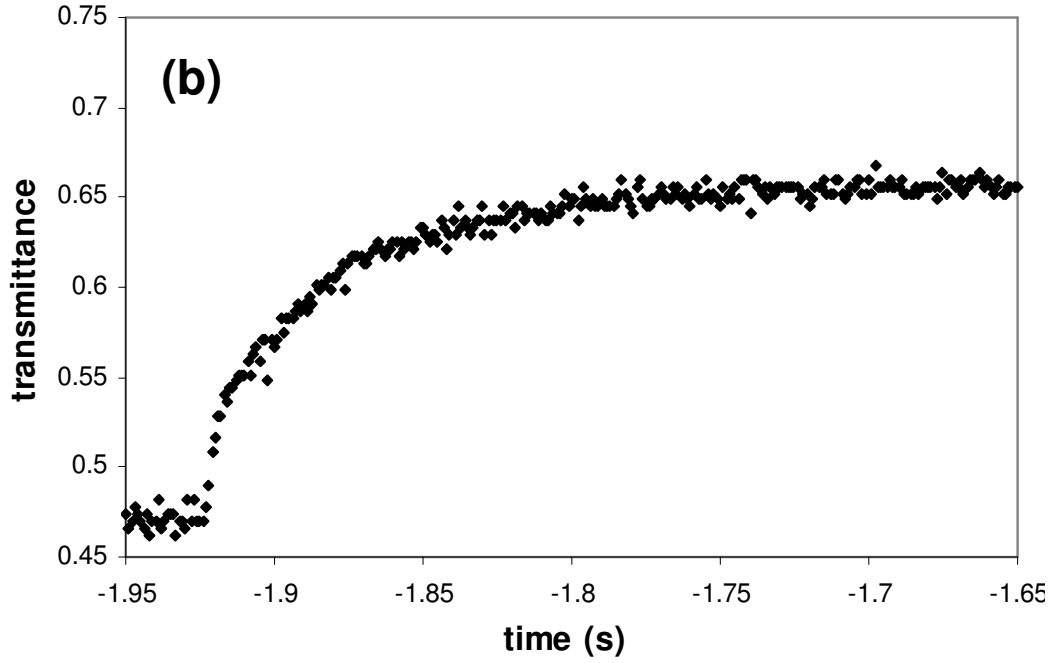

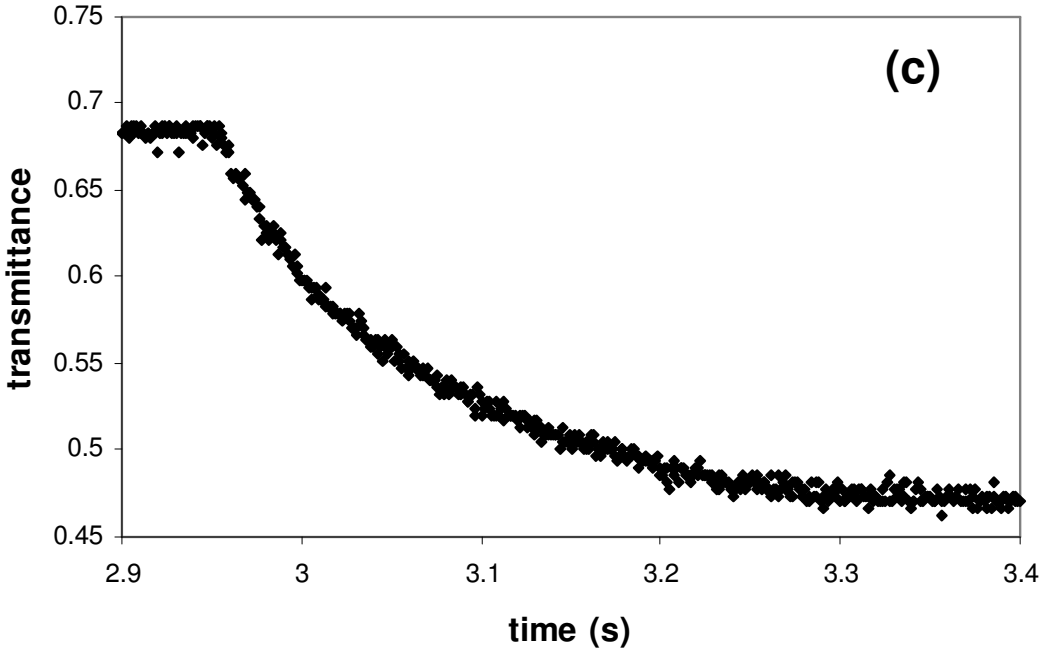

Figure 3.13 a) Switching speed curve for 40 bilayer solid-state device of PV/PAMPS and PANI/PAMS, transmittance as a function of time b) expansion of the coloration phase and c) expansion of the de-coloration phase.

3.4 Summary

The use of the PV as an electrochromic material provides a low reduction potential, good film forming ability and color tuning (colorless to dark violet to transparent yellow). Its solubility in water provides the advantage of easy processability using the LbL film assembly method with PAMPs and the flexibility to incorporate other electrochromic materials that increase the overall contrast or develop multi-hue electrochromic devices. The high coloration efficiency (57 cm^2/C) at low switching voltage (-0.2 V) and the ability to control the thickness of the bulk layer makes this approach unique. 40 bilayers of PV/PAMPs on an ITO electrode show a contrast of 61% at 515 nm as the color changes from a highly transmissive colorless state to a dark violet to a transparent yellow.

Integrated PV-PANI dual EC devices produce more plentiful switching colors (blue, dark violet and yellow) than the simple PV device in electrolyte solution. The switching times for coloration and decoloration were 100 ms and 250 ms, respectively, at low switching voltages (- 2.0 to +2.0 V) under ambient conditions.[28]

References

[1] W. C. Dautermont-Smith, *Displays I* **1982**, 3.

[2] M.-T. Riou, C. Clarisse, *J. Electroanal. Chem.* **1988**, *249*, 181.

[3] G. A. Corker, B. Grant, N. J. Clecak, *J. Electrochem. Soc.* **1979**, *126*, 1339.

[4] E. W. Tsai, S. Basok, J. P. Ruiz, J. R. Reynolds, K. Rajeshwar, *J. Electrochem. Soc*. **1989**, *126*, 3683.

[5] G. Sonmez, *Chem. Commun*. **2005**, *42*, 5251.

[6] P. M. S. Monk, "*The Viologens",* John Wiley & Sons; West Sussex, U.K., 1998.

[7] D. Bongard, M. Moller, S. N. Rao, D. Corr, L. Walder, *Helv. Chim. Acta* **2005**, *88*, 3200.

[8] M. O. M. Edwards, *Appl. Phys. Lett.* **2005**, *86*, 073507.

[9] D. F. Qi, K. Varahramyan, S. Selmic, *Mater. Res. Soc. Symp. P* **2004**, *814*, 311.

[10] R. J. Mortimer, C. P. Warren, *J. Electroanal. Chem.* **1999**, *460*, 263.

[11] J. H. Ryu, J. H. Lee, *Macromol. Rapid Comm.* **2004**, *27*, 1156.

[12] J. Y. Lim, H. C. Ko, H. Lee, *Synthetic Metals* **2006**, *156*, 695.

[13] D. Corr, U. Bach, D. Fay, *Solid State Ionics* **2003**, *4*, 315.

[14] R. Cinnsealach, G. Boschloo, S. N. Rao, D. Fitzmaurice, *Solar Energy Mater. Solar Cells* **1999**, *57*,107.

[15] M. Moller, S. Asaftei, D. Corr, M. Ryan,L. Walder, *Adv. Mater*. **2004**, *16*, 1558.

[16] M. S. Simon, P. T. Moore, *J. Poly. Sci, Poly. Chem. Ed.* **1975**, *13*, 1.

[17] A. F. Sammells, and N. U. Pujjare, *J. Electrochem. Soc.* **1986**, *133*, 1270.

[18] J. A. Janik, J. R. Heflin , D. Marciu, M. B. Miller, H. Wang, H. W. Gibson, R M. Davis, *SPIE Proc.* **2001**, *4458*, 146.

[19] S. A. Sapp, G. A Sotzing, J. R. Reynolds, *Chem. Mater*. **1998**, *10*, 2101.

[20] G. Sonmez, H. Meng, F. Wudl, *Chem. Mater.* **2004**, *16*, 574.

[21] R. Cinnsealach, G. Boschloo, S. N. Rao, D.Fitzmaurice, *Solar Energy Mater. Solar Cells* **1998**, *55*, 215.

[22] H.K. Jheong, Y.J. Kim, J. H. Pan, T. Won, W.I. Lee*, J. Electroceram.* **2006**, *17*, 929.

[23] C. L. Bird, *Chem. Soc. Rev.* **1981,** *10*, 49.

[24] J. B. Schlenoff, H. Ly, M.Li, *J. Am. Chem. Soc.* **1998**, *120*, 7626.

[25] H. C. Ko, S. Park, H. Lee, *Synthetic Metals* **2004**, *143*, 31.

[26] A. P. Baioni, M. Vidotti, P.A. Fiorito, E.A. Ponzio, S. I. Cordoba de Torresi, *Langmuir* **2007**, *23*, 6796.

[27] H. Pettersson, T. Gruszecki, L. H. Johansson, M. O. M. Edwards, A. Hagfeldt, T. Matusczczyk, *Displays* **2004**, *25*, 223.

Chapter 4

Millisecond Switching in Solid State Electrochromic Polymer Devices Fabricated from Layer-by-Layer Assembly

The electrochromic switching times of solid state conducting polymer devices fabricated by the layer-by-layer (LbL) technique has been investigated. The devices were composed of bilayers of poly(3,4-ethylenedioxythiophene): poly(styrenesulfonate) and poly(allylamine hydrochloride) on indium tin oxide substrates. Devices fabricated from 40-bilayer-thick films have coloration and decolaration switching times of 31 ms and 6 ms, respectively, with low applied voltage (1.4 V) for an active area of 0.6 cm^2. The switching times have been shown to decrease with the active area of the electrochromic device suggesting that even faster electrochromic switching times are possible for devices with smaller areas.

4.1 Introduction

Tungsten oxide electrochromic devices have been used in smart windows, automotive rear-view mirrors, and thin passive displays for more than a decade, but electrochromic materials have not yet been employed in fast displays because of their slow color-switching response time, typically on the order of seconds. A large number of conducting polymers exhibit electrochromic behavior, including polyaniline, polyviologens, and polypyrrole, but poly(3,4-ethylenedioxythiophene:poly(styrenesulfonate) (PEDOT:PSS) has been preferred in electrochromic studies because of its easy processability, high conductivity (300 S/cm), high contrast at low voltage, and long term stability without degradation as compared to other conducting polymers.[1,2,3,4] Here, we demonstrate fast switching response times (<10 ms) of electrochromic devices consisting of PEDOT: PSS and poly(allyamine hydrochloride) (PAH) multilayered films fabricated by the layer-by-layer (LbL) approach.

The electrochromic properties of PEDOT: PSS have been studied by several groups. Delongchamp et al. fabricated solid-state dual electrochromic PEDOT and polyaniline (PANI) LbL films which had switching speeds ($t_{75\%}$) of 0.37 s for decoloration and 1.22 s for coloration. Kumar et al. found that PEDOT: PSS films made by electropolymerization have switching speeds of several seconds for thicknesses of ~ 300 nm.[5] Cho et al. have shown that PEDOT nanotubes fabricated in an intricate process of laying out an array structure on ITO with a silica template have very fast reflectivity changes of 8.8 ms coloration and 3.5 ms decoloration for nanotubes of 20 nm wall thickness with -1 V to +1 V applied for a reflectivity change of 25%.[6] We report PEDOT electrochromic devices that operate at switching rates comparable to those reported by Cho and can be made with the fairly simple and inexpensive LbL approach with readily available conducting electrodes and materials.

4.2 Experimental

The LbL technique involves dipping a charged substrate alternately in aqueous polycation and polyanion solutions. We have used glass slides coated with ITO as our substrate, PAH as the cationic polymer, and PEDOT: PSS as the anionic polymer. Symmetric solid-state devices were fabricated by sandwiching together two ITO slides coated with PEDOT/PAH bilayers using a transparent conducting gel poly (2-acylamido 2-methyl propane sulfonic acid) (PAMPS). The device structure is shown in the insert of Figure 4.1.

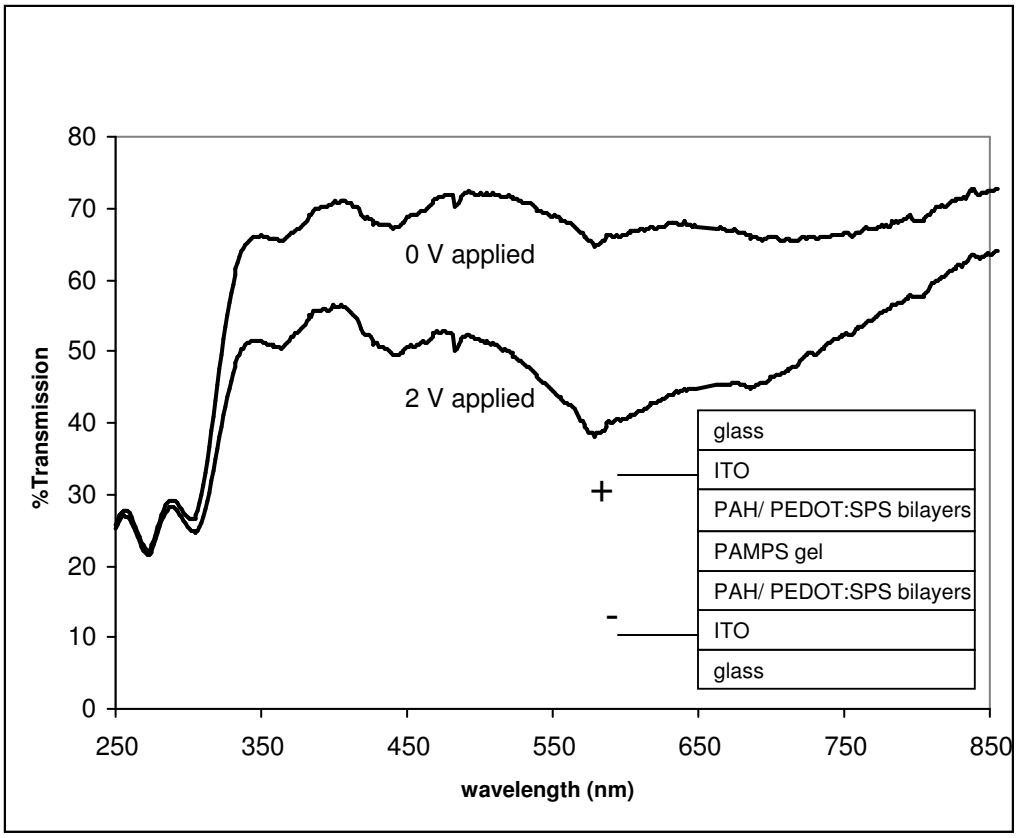

Figure 4.1 Percentage transmission v/s. wavelength of an electrochromic device consisting of two PAH/PEDOT 80 bilayer films with 2.0 V and 0 V applied.

10 mM PAH (Sigma-Aldrich) at pH 4 and PEDOT: PSS (BaytronP) prepared by the method described by Delongchamp et al. have been used.[2] The area of the electrochromic device was controlled by appropriately etching the ITO substrates to create stripes or pixels of the desired size.

4.3. Results and Discussions

Cyclic voltammetry of a (PAH/PEDOT: SPS) $_{40}$ film shows a broad reduction peak of the PEDOT and is consistent with the measurements of Tang.[3] The diffusion coefficient (D_e ~ 2.82 x $10^{-8}cm^2/s$) value calculated by Randles-Sevick equation,

$$Ip = (2.69 \times 10^5)\, n^{3/2}\, A\, D_e^{1/2}\, C\, \nu^{1/2}$$

in which Ip = 321mA is the cathodic peak current, n = 1 is the electron stoichiometry, A = 1 is the electrode area (cm^2), C = 0.01 is the concentration of electrolyte (mol/cm^3), ν = 0.5 is the scan rate (V/s).

Symmetric PEDOT EC devices in which one of the PEDOT layers acts as a conductive electrode material have been demonstrated by Mecerreyes et al.[7] In the present work, a completely symmetric and reversible PEDOT EC device has been demonstrated on ITO electrodes such that, dependent upon the polarity of the applied voltage, only the PEDOT film connected to the negative terminal exhibits a color change.

The transmission spectrum of the (PAH/PEDOT: SPS) $_{80}$ (consisting of two 80 bilayer films) device is presented in Fig. 1 at 0 V and with 2 V applied, as measured with a Filmetrics F20 UV-Vis spectrometer. The color change is between very pale blue and dark blue. The maximum change in transmittance between 0 V and 2 V is 35 % at 580 nm. The temporal response of the devices was monitored with a He-Ne laser and photodiode as a square wave voltage (0 -1.4 V) was applied to the electrochromic device. Figure 4.2 shows the electrochromic film response as well as the applied square wave voltage signal for a 40-bilayer (two 40-bilayer films) 1-cm^2 area PAH/PEDOT device.

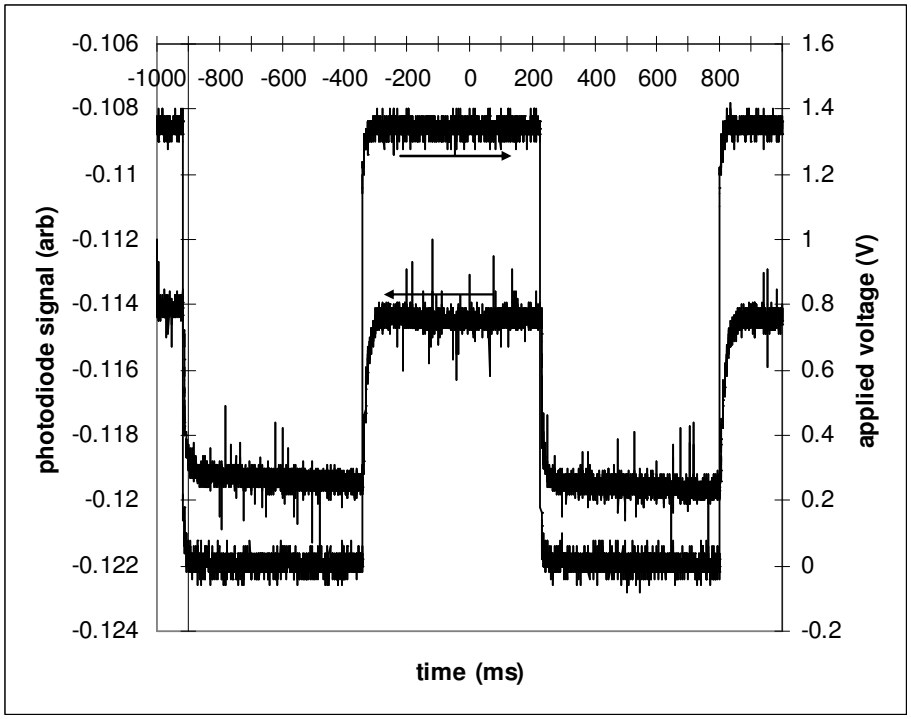

Figure 4.2 Photodiode signal vs. time with square wave voltage applied for a device consisting of two 40 bilayer films with 1 cm^2 area.

Figure 4.3 shows the fast electrochromic time response of coloration and decoloration of the 0.6 cm^2 (PAH/PEDOT: SPS)$_{40}$ device. The coloration and decoloration times (to 90% of equilibrium value) are 31 ms and 6 ms, respectively. We note that the decoloration time is shorter than the coloration time for these devices, as has been previously observed.[1] In addition, the coloration and de-coloration times of a 20 bilayer 1 cm^2 device are approximately 20 ms and 8 ms, respectively, indicating that thinner devices switch faster, as would be expected due to the decreased transit time for the ionic motion. The contrast associated with our switching experiments at 633 nm, which is not the wavelength of maximum contrast, is approximately 8 and 5% for 40-bilayer and 20-bilayer devices, respectively.

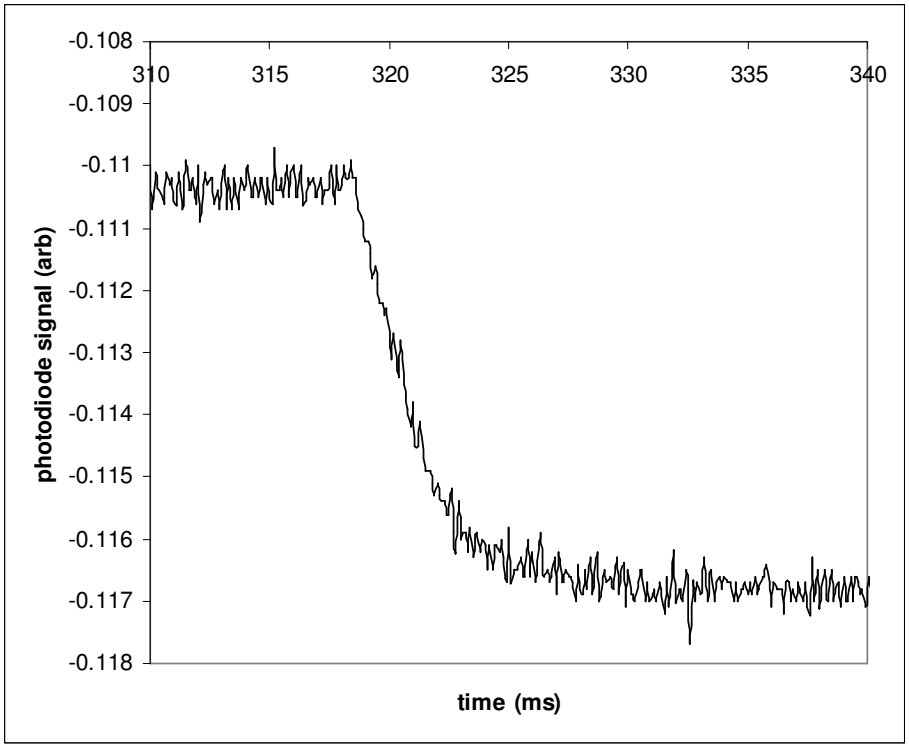

(a)

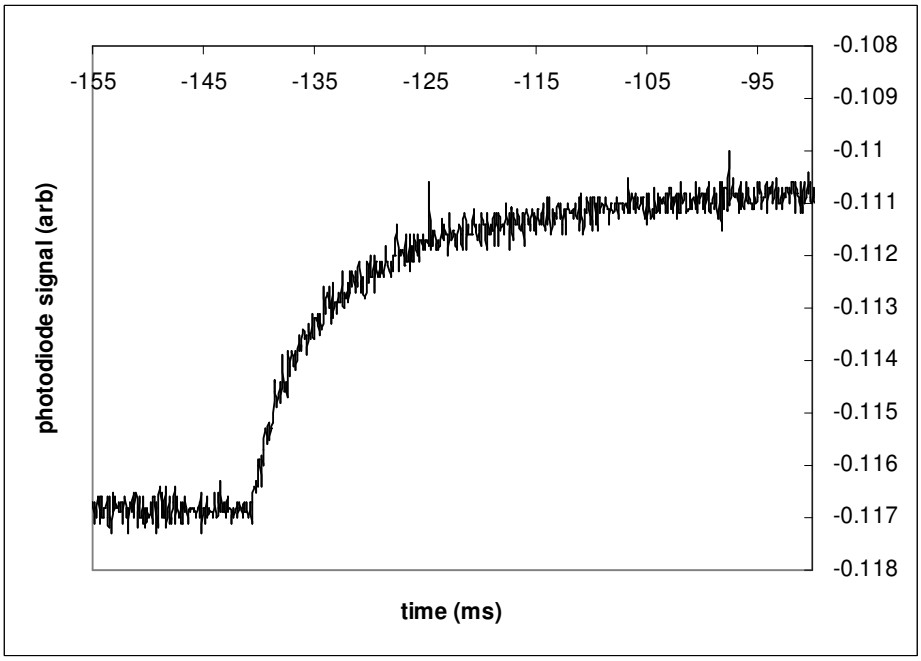

(b)

Figure 4.3 Decoloration and coloration of a 0.6 cm^2 device consisting of two 40 bilayer PAH/PEDOT films with applied voltage of 0 - 1.4 V.

In Figure 4.4, we show the relationship between switching speed ($t_{90\%}$) and the area of device; $t_{90\%}$ is the time for the film to achieve 90% of its full electrochromic response. The film response time decreases linearly with the active area of the device, similar to the response of an RC circuit. Pixel areas associated with active displays are often < 0.05 cm^2. The relationship in Fig. 4 suggests that switching times for 0.05 cm^2 area devices should be on the order of 3 ms for coloration and 0.6 ms for decoloration. It is anticipated that a combination of smaller area and increased polymer thickness can thus provide for very fast switching and significantly higher contrast than that measured here.

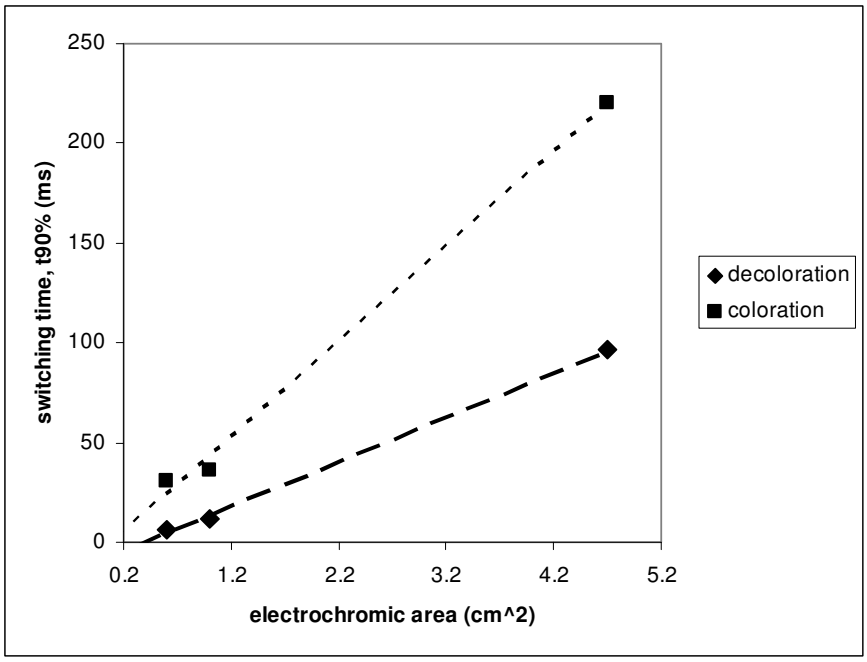

Figure 4.4 Decoloration and coloration switching times vs. electrochromic device area for devices consisting of two 40-bilayer PEDOT films. Lines shown to guide the eye.

4.4. Summary

We have demonstrated the fast switching of an ionic self-assembled multilayer solid-state polymer electrochromic device compatible with flat-panel display rates. Devices consisting of

two 80-bilayer PAH/PEDOT films display a maximum contrast of 35% at 580 nm. Devices with an active area of 0.6 cm^2 made from two 40-bilayer (400 nm thick) films show coloration and decoloration times of 31 ms and 6 ms, respectively, with a linear scaling of the switching speed with the active area of the device. The fast switching is attained through a combination of a number of factors: fabrication of thin, homogeneous films by self-assembly that have a large diffusion coefficient and short distance required for ionic motion, use of the symmetric quasi-solid state geometry with a thin layer of electrolyte gel, and recognition of the dependence of the response time on device area. These results suggest that LbL electrochromic devices are potential candidates for next-generation flat-panel displays.

References

[1] D.M. Delongchamp, M. Kastantin, and P.T. Hammond, *Chem. Mater*. **2005,** *15,*1575.

[2] D. M. Delongchamp, and P.T. Hammond, *Adv. Mater*. **2001,** *13,* 1455.

[3] Z. Tang, S.T. Donohoe, J.M. Robinson, P.A. Chiarelli, and H. Wang, *Polymer* **2005**, *46,* 9043.

[4] A.L. Holt, J.M. Leger, and S.A. Carter, *Appl. Phys. Lett*. **2005,** *86,*123504.

[5] A. Kumar, D.M. Welsh, M.C. Morvant, F. Piroux, K.A. Abboud, and J.R. Reynolds, *Chem. Mater*. **1998,** *10,* 896.

[6] S.I. Cho, W.J. Kwon, S.-J. Choi, P. Kim, S.-A. Park, J. Kim, S.J. Son, R. Xiao, S.-H. Kim, and S.B. Lee, *Adv. Mater*. **2005,** *17,*171.

[7] D. Mecerreyes, R. Marcilla, E. Ochoteco, H. Grande, J.P. Pomposoa, R. Vergaz, and J.M. Sánchez Pena, *Electrochim. Acta* **2004,** *49,* 3555.

Chapter 5

Synthesis and Characterization of Regiosymmetric Water Soluble 3, 4-Propylenedioxythiophene Derivative and its Application in the Fabrication of High Contrast Solid State Electrochromic Devices

A regiosymmetric water-soluble sulfonated monomer based on 3,4-propylenedioxythiophene (ProDOT-Sultone) was synthesized and characterized, via the *O*-alkylation of the corresponding unreactive β,β-disubstituted hydroxyl group with propane sultone in the presence of catalytic amount of diazabicyclooctane 1,4-diazabicyclo[2.2.2]octane (DABCO). This new monomer was oxidatively polymerized to get a regiosymmetric water-soluble conjugated anionic polyelectrolyte, which was then used for the fabrication of solid-state electrochromic devices using the Layer-by-Layer (LbL) deposition method. These solid state devices were found to exhibit better electrochromic properties in terms of color contrast, switching time, coloration efficiency (CE), surface control electroactivity and conductivity in thin films compared to the corresponding water soluble regiorandom 3,4-ethylenedioxythiophene (EDOT) derivative. For the 40 and 80 bilayer solid-state electrochromic devices, the electrochemical contrast was observed to be 31% and 40% at 570 nm with fast solid-state switching times of 100 and 220 ms, respectively, indicating faster movement of the ions in and out of the films. Furthermore, the coloration efficiency was found to be as high as 250 cm^2/C for 80 bilayer devices and independent of device thickness, indicating the full accessibility of all the ionic sites even in thicker films. Four-point probe conductivities of the LbL films and *in situ* conductivity of solution cast films were found to be in the range of 10^{-4} S/cm and 10^{-3} S/cm, respectively.

5.1 Introduction

Polymers based on 3,4-alkylenedioxythiophenes are an important class of conjugated polymers due to their widespread application in the area of electrochromic devices, sensors, hole transport layers in OLEDs and antistatic coatings.[1,2] Functionalization of these polymers to achieve the desired properties, while maintaing ease of processability is still a challenging task. Functionalization of EDOT-OH is relatively difficult due to the tedious synthetic pathways, whereas monomers like ProDOT-OH can be synthesized from easily available starting materials. Mishra et al. are the first to have reported the successful functionalization and electropolymerization of ProDOT-OH, which opens up many opportunities in the area of functional conducting polymers.[3]

In this chapter we discuss the electrochromic properties of a new water-soluble regiosymmetric monomer and conjugated polymer based on sulphonated 3,4-propylenedioxythiophene (ProDOT-Sultone). This polymer exhibits better electrochromic properties in terms of color contrast, switching time, coloration efficiency (CE), surface control electroactivity and conductivity in thin films, formed by LbL technique, compared to the corresponding water soluble regiorandom 3,4-ethylenedioxythiophene (EDOT) derivative. The advantage of the water-soluble polymer is that it can be processed using a wide range of deposition techniques like spin coating,[4] solution casting,[5] Langmuir-Blodgett (LB)[6] and Layer-by-Layer (LbL)[7]. Furthermore, the introduction of regiosymmetric nature improves the material properties as observed for other regioregular polymers based on thiophene.[8,9]

Zotti et al.[10] deposited water-soluble polyelectrolyte polymers using the LbL technique. The thin film deposition of polythiophene-based multilayers which were characterized in aqueous media was reported by Lukkari et al as well.[7] Recently Reynolds et al. and others[9,11] reported the LbL deposition studies on a similar polymer, but regiorandom, based on 3-4-ethylenedioxythiophene (PEDOT-Sultone) for electrochromic devices and also as hole transport layers in OLEDs. We felt that the device characteristics and the polymer properties can be significantly improved by the design of corresponding regiosymmteric water-soluble polymer.

Therefore, in this chapter, we report the synthesis of a new monomer ProDOT-Sultone and its polymer PProDOT-Sultone using an oxidative polymerization route. Studies on electrochemical and spectroelectrochemical properties and conductivity measurements of the films were carried out by depositing the films using the solution cast method and the LbL method. The films formed by the LbL method were characterized in organic and aqueous media, whereas the solution cast film was characterized in organic media due to the solubility of the polymer in aqueous media. This polymer shows an unusual acid doping phenomenon similar to those reported by the Reynolds group.[12] The films formed by the LbL method using polyallylamine hydrochloride (PAH) as the cationic polyelectrolyte were used in the fabrication of solid-state electrochromic devices which exhibit fast switching times. Synthesis and characterization of this new water-soluble regiosymmetric polymer along with the studies on solid-state electrochromic devices is reported here in this chapter.

5.2 Experimental

(Synthesis of this compound was performed by Prof. Kumar's group in Chemistry department, IIT-Mumbai)

Tetrabutylammonium perchlorate (TBAP) and lithium perchlorate ($LiClO_4$) were purchased from Fluka and used without further purification. The monomer PProDOT-Sultone was synthesized from ProDOT-OH. Poly (allylamine hydrochloride) (PAH) with M_w ca. 70,000 was purchased from Aldrich and used without further purification; all the other chemicals were of reagent grade and used without further purification. HPLC grade acetonitrile was used for electrochemical studies and was dried over calcium hydride prior to use. Indium doped tin oxide (ITO) coated glass slides with dimensions of 3" x 1" (12Ω/□) were obtained from Delta Technologies, USA. Solid-state devices are fabricated by pressure laminating LbL coated ITO electrodes with the help of binder clips for 20 minutes and then sealing the ends with the epoxy so that the transparent conducting gel poly(2-acrylamido-2-methylpropane sulfonic acid) (PAMPS) (15 wt% in H_2O; Sigma-Aldrich) does not degrade from over-exposure to air; the overall device configuration is shown in the schematic. Fabrication of the symmetrical solid-state devices made up of conducting electrochromic polymer has been shown previously by

Mecerreyes et al.[18], and in our case this symmetrical configuration utilizes similar PAH/PProDOT-Sultone LbL films as electroactive layers on each of the two ITO-coated substrates.

All electrochemical experiments were carried out in a EG&G PAR model 362 potentiostat/galvanostat or a PINE AFCBP1 bipotentiostat controlled by Pine Chem. software using a three electrode cell with Ag/Ag^{+}(0.01 M $AgNO_3$/ACN) as the reference electrode and a platinum flag as the counter electrode. For spectroelectrochemistry experiments, indium-doped tin oxide (ITO) coated glass slides from Delta Technologies, USA were used as the working electrodes and a silver wire was used as a quasi-reference electrode. For *in situ* conductance measurements, Ag/Ag^{+} was used as the reference electrode. UV-vis spectra were recorded either on a Perkin Elmer Lambda 25 or Filmetrics UV-vis spectrophotometer. ^{1}H NMR, and ^{13}C NMR, spectra were recorded on a VXR 400 NMR spectrometer. The chemical shifts are referenced to TMS. ES-MS analysis was carried out on a Waters Q Tof micro-YA-105 instrument. Thermogravimetric analysis (TGA) of the polymer PProDOT-Sultone was carried out under nitrogen atmosphere using Metler-Toledo TGA/SDTA 851 equipment.

5.2.1 Synthesis of (sodium 3-((3-methyl-3,4-dihydro-2H-thieno[3,4-b][1,4]dioxepin-3-yl)methoxy)propane-1-sulfonate(ProDOT-Sultone)

Sodium hydride (228 mg, 9.5 mmol) was mixed in a two-necked round bottom flask with 20 mL of dry THF under argon atmosphere. To this suspension, ProDOT-OH (2 g, 10 mmol) was added dropwise, followed by the addition of 1 mol % of DABCO. The mixture was allowed to stir for 20 minutes. A THF solution of propane sultone (1.15 g, 9.5 mmol in 10 mL THF) was added dropwise to this suspension while maintaining the temperature below 10 °C using an ice bath. After the addition, the reaction mixture was allowed to stir at room temperature for 15 h and then quenched by adding methanol. The precipitated product was collected by centrifugation, washed several times with chloroform, ethyl acetate and vacuum dried to get a pale white solid.

Yield: 356 mg (91 %); ^{1}H NMR ($CDCl_3$, δ, ppm): 0.94 (s, 3H), 1.99-2.04 (m, 2H), 2.95-3.00 (m, 2H), 3.60 (s, 2H), 3.61-3.66 (m, 2H), 3.76 (d, *J* = 12 Hz, 2H), 4.03 (d, *J* = 12 Hz, 2H), 6.69 (s, 2H). ^{13}C NMR ($CDCl_3$): 16.13, 24.22, 42.63, 47.91, 68.69, 72.71, 76.82, 106.79, 148.62; FT-IR (NaCl): 3103, 2963, 2869, 1641, 1558, 1486, 1449, 1380, 1186, 1110, 1046, 1019, 968, 850, 775, 612 cm^{-1}; ES-MS: 367.13 $(M + Na)^{+}$; HR-MS: 345.04 $(M + 1)^{+}$.

5.2.2 Polymerization of ProDOT-Sultone

For oxidative chemical polymerization, ProDOT-Sultone (1 g, 2.90 mmol) was suspended in 100 mL of chloroform in presence of 3.3 equivalent of iron (III) chloride and the reaction mixture was stirred at room temperature under argon atmosphere for 24 h. The color of the reaction mixture changed to blue after 2 h, indicating polymer formation. After 24 h, the polymer was isolated by centrifugation after adding methanol to reaction mixture. The polymer was first washed with methanol, and then stirred with methanolic solution of hydrazine hydrate for 24 h followed by 1% methanolic solution of sodium hydroxide to get the final undoped polymer as a dark blue powder with sodium as counter ions in 65% yield.

5.2.3 Layer-by-Layer Deposition of PProDOT-Sultone/PAH Films

The polymer films were formed by the alternate deposition on ITO glass slides, R_s= 10-12 Ω (Delta Technologies) first in 10 mM of PAH solution and then in 2 mM solution of PProDOT-Sultone for 6 minutes, followed by rigorous rinsing in Milli-Q water for 2 minutes after every step. LBL film assembly was done in an automated slide stainer (Nanostrata Inc.) ITO substrates were cleaned first by acetone and then by Milli-Q; to ensure a strong LbL template, the ITO slides are dipped in 1M NaOH for 15 minutes to provide enough negative charge so that the first layer of PAH deposited well on the ITO slides. ITO slides of a desired design were etched by masking the non-etched area by 3M electrical tape followed by deposition in 1:1 mixture of water and HCl for 1 h. Following that, the electrical tape was removed and the slides were

cleaned with acetone and then ultrasonicated in the base solution (70%H_2O:20% NH_4OH:10% H_2O_2) for 30 minutes prior to use.

5.2.4 Film Thickness measurement

Film thickness measurements were performed with a J.A.Woollam VB-2000 ellipsometer and also confirmed by use of an LEO 1550 Field Emission Scanning Electron Microscope (FE-SEM) at accelerating voltage of 5 KV Profilometer (AMBIOS TECH XP-2). Although measured values from all the three techniques agree with a variation of ± 5%, the results presented are of the ellipsometry measurements. The thicknesses of 40 and 80 bilayer films of PAH/PProDOT-Sultone were approximately 145 and 300 nm respectively. A Lorentz Oscillator best fit model was used to calculate the thickness of the LbL films. Overall the films were quite smooth and homogenous; film roughness after various bilayer measurements was estimated to be typically less than 5% of the film thickness.

5.3 Results and Discussions

ProDOT-Sultone monomer was synthesized by *O*-alkylation of ProDOT-OH with propane sultone in presence of DABCO as a catalyst as shown in Scheme 1. The monomer was fully characterized for its molecular structure using NMR, FTIR and HR-MS. ProDOT-OH was first reported by Kros et al.[13] in 2002 and caught the attention of various researchers around the globe, as this was one of the easiest ways to introduce hydroxyl functionality as side chain in the class of monomers based on 3,4-alkylenedioxythiophenes. Interestingly, it turned out that this excitement was short-lived as most of the efforts to functionalize this hydroxyl group, with various alkylating agents such as alkyl halides, allyl halides, propargyl halides and propane sultone etc., were futile due to the β,β-disubstituted nature of the hydroxyl group. However, limited success to functionalize this type of β,β-disubstituted hydroxyl group via benzylation was reported by Kumar[3] and via alkylation by Reynolds and coworkers[14]. It should be noted here that though the benzylation does happen in most solvents, alkylation only happens in DMF. This

was confirmed by the fact that alkylation in solvents other than DMF were unsuccessful. Furthermore, use of other alkylating agents such as allyl or propargyl halides or propane sultone in DMF as solvents was also unsuccessful. The presence of catalytic amounts of DABCO or (1,8-Diazabicycloundec-7-ene) DBU results in successful *O*-alkylation of ProDOT-OH with various alkylating agents such as allyl halides, propargyl halides, propane sultone etc. However, the exact role of DABCO as a catalyst is not clear at this stage and work is in progress to understand its role. It is sufficient to say here that use of DABCO is essential for the success of *O*-alkylation of the hydroxyl group of ProDOT-OH and it opens up various avenues for the simple one step syntheses of regiosymmetric functional monomers based on ProDOT-OH. It should also be mentioned here that success of DABCO as a catalyst is independent of the solvent used as well as the alkylating agent used.

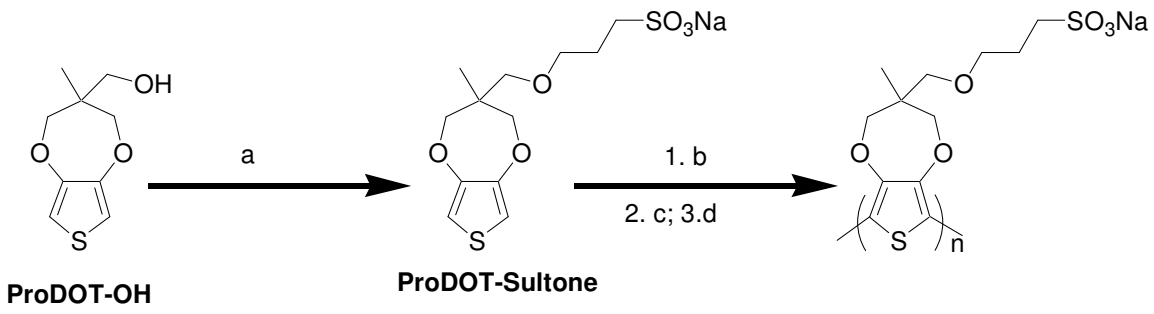

ProDOT-OH **ProDOT-Sultone**

a) NaH, THF, DABCO, propane sultone, room temp. 24h; b) $FeCl_3$, $CHCl_3$, room temp.24h; c) hydrazine hydrate, 24h d) 1% methanolic solution of NaOH, 24h

Scheme 1. Synthesis of monomer and polymer

The monomer ProDOT-Sultone was then oxidatively polymerized using iron (III) chloride in chloroform by stirring at room temperature. It should be mentioned here that the monomer was insoluble in chloroform, but the oxidizing agent was soluble and hence the polymerization effectively happened in solid state. The polymerization proceeded in usual fashion wherein color change from light yellow to light green to dark blue with time was observed. The polymer was isolated by precipitating the reaction mixture in methanol followed by stirring with hydrazine hydrate to undope the polymer and finally with 1% methanolic solution of sodium hydroxide to

convert all the counter ions back to sodium. The resulting undoped polymer was isolated as a dark blue powder and was found to be insoluble in common organic solvents but was soluble in water. The chemical polymerization of ProDOT-Sultone is supported by an observed red shift of the π-π^* transition upon polymerization.

The polymer showed an absorption at λ_{max} 554 nm (2.2 eV) with a band gap of 1.78 eV. In the FT-IR spectra, the band at 3097 cm^{-1} is characteristic of the ProDOT C-H (end group) vibration of the ProDOT-Sultone, which disappears completely upon polymerization. The presence of absorption due to the symmetric and asymmetric S=O stretching mode at 1045 cm^{-1} and 1190 cm^{-1} in both monomer and polymer is consistent with the proposed structures and stability of the pendant chains to the polymerization conditions.[8] The polymeric nature of the material is also evident from the low optical band gap (1.78 eV) compared to the corresponding monomer. The MALDI-TOF MS analyses confirmed the presence of chains of molecular weights of up to 6500 $gmol^{-1}$ which is no way limiting or average due to the inability of longer chains with a sulfonate group to be volatized.[8] Surprisingly, all the attempts to get well defined solution ^1H NMR with reasonable resolution were not successful due to poor resolution of the spectrum in D_2O, which is in agreement with other cases of conjugated polyelectrolytes.[8] The thermogravimetric analysis of the polymer PProDOT-Sultone was carried out under nitrogen at a heating rate of 10 °C per minute which showed that the polymer remains stable up to 290 °C, after which rapid weight loss is observed due to the degradation of the polymer. It was interesting to note that a solution of the polymer in water would result in precipitation on storage. Initially we thought that the polymer has a low shelf life in water, which results in decomposition on storage. However, careful examination of the polymer structure revealed that the precipitation from the water solution results from the ionic crosslinking of the backbone on partial self-doping due to the sulfonated side chains. The backbone forms cationic species on self-doping, which then forms ionic crosslinks with the anionic sulfonate group in the side chain. This ionic crosslinking was found to be reversible as confirmed by the re-dissolution of the precipitated polymer on addition of few drops of any reducing agent such as hydrazine hydrate.[15] This phenomenon of reversible crosslinking, due to self-doping, has technological advantage in self and reversible curing of the thin films as the doped thin films were found to be insoluble in water though water was used as the solvent to cast these thin films.[12]

5.3.1 Electrochemical Studies on PProDOT-Sultone

The scan rate dependence of the polymer thin films deposited using LbL method was studied both in aqueous and organic media by recording cyclic voltammograms. In organic media, 0.1 M $LiClO_4$/ACN, the thin films showed a well-defined oxidation peak, whereas a broad peak was obtained when TBAP was used as an electrolyte. This is in agreement with the data reported by Reynolds and co-workers in the case of regiorandom PEDOT-Sultone.[8] However, in aqueous media, 0.1 M $LiClO_4$ in water, the thin films exhibited a sharp oxidation peak centered around 0 mV at a scan rate of 50 mV/s. The sharp oxidation peak changes to a broad peak when the electrolyte is switched to 0.1 M $NaClO_4$. This is attributed to the size of the cation, which plays an important role in the redox behaviour of the polymer due to its inclusion and expulsion during potential cycling.[16] The scan rate dependence of polymer deposited by LbL method in 0.1 M $LiClO_4$/water suggests that the polymer redox response is non-diffusion-limited up to 1000 mV/s as the current varies linearly with scan rate, though there is an anodic shift of oxidation peak at higher scan rate. Also, as Hammond and co-workers[17] explained, a surface controlled non-diffusion limited redox process corresponds to open morphology of the multilayers; and provides faster movement of the ions in and out of the film required for rapid electrochromic switching. However, a surface controlled redox process also lowers the contrast, because the whole film thickness is not utilized. In this work, the films were formed to obtain a good combination of high contrast and fast switching speed to avoid the trade-off between these two values. This is one of the most significant advantages of the LbL film formation technique: the film thickness and morphology can be easily controlled by a slight variation of the ionic strength of the polyelectrolytes, through the salt concentration and pHs of the deposition solutions.[18] The cathodic shift of the peak potential in the cyclic voltammogram comes from the internal resistance of the bulk film[19], and arises primarily from the slow electron transfer from the ITO electrode to the PProDOT-Sultone via the resistive inactive polycation, PAH.

In order to study the effect of thin film formation on electrochemical properties, studies were carried out on thin films formed by drop casting from solution. For this purpose, 10 mg of the polymer was dissolved in 1 mL of water and was used for drop casting the thin film on ITO coated glass electrodes. These thin films were then studied for its electrochemical properties in

0.1 M $LiClO_4$ /ACN (5% water) (Figure 5.1) as the films used to fall out from the electrode in pure water during electrochemical scanning. Well-defined redox peaks were observed up to a scan rate of 25 mV/s which then broadens on increasing the scan rates up to 200 mV/s. The oxidation peak potential of the polymer was centered at 0.1 V vs Ag/Ag^+ at 25 mV/s. It is interesting to note that the LbL films of PProDOT-Sultone/PAH deposited from water were found to be electroactive in both organic and aqueous media; the films deposited by the solution cast method were only electroactive in an organic medium. Furthermore, the porous nature of the well-adhered film to the electrode surface deposited by LbL method allowed greater cation mobility.[20]

For spectroelectrochemistry, a thin film of the polymer was drop-cast (from a 10 mg/mL solution of polymer in water) on ITO coated glass, and the spectra of the polymer were recorded at different applied potentials in 0.1M $LiClO_4$/ACN, as shown in Figure 5.2. At -1 V, the polymer showed a λ_{max} of 557 nm due to π-π^* transition. On stepwise oxidation, the absorption due to the π-π^* transition decreases and the polymer absorbs at longer wavelength in the near- IR region (900 nm) due to the polaronic transitions. At higher oxidation levels, the bipolaron band absorption (>1100nm) dominates the spectra, while π-π^* and polaronic transitions remain relatively constant. In the neutral state, PProDOT-Sultone absorbs throughout almost the entire visible region with deep purple-blue color. An optical band gap (E_g) of 1.78 eV was calculated from the onset of π-π^* transition. The polymer shows a well-defined isosbestic point around 667 nm, which implies that only two chromophoric species (PProDOT-Sultone) are involved.

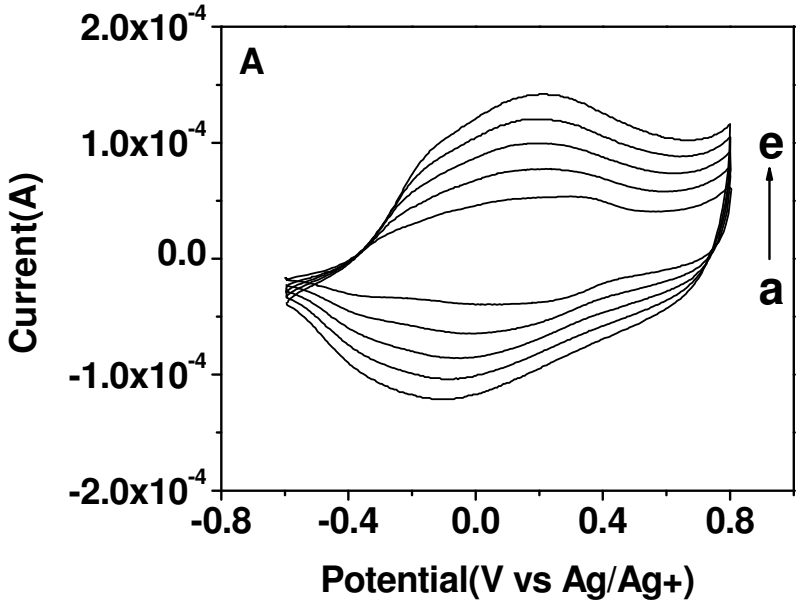

Figure 5.1 Cyclic voltammogram of chemically synthesized PProDOT-Sultone deposited on ITO coated glass at scan rates of (a) 5, (b) 10, (c) 15, (d) 20, (e) 25 mV/s in 0.1 M $LiClO_4$/ACN (5% water).

The spectroelectrochemistry of 40 and 80 LbL films was carried out in 0.1 M TBAP/ACN at different applied potential following the procedure mentioned above. The multi-layered films were first reduced with hydrazine hydrate followed by repeated washing in acetonitrile before the spectroelectrochemical experiment. The spectroelectrochemistry of the LbL films is essentially identical to that of the solution cast films. In the case of the LbL films, the polymer also has a maximum absorption at 557 nm due to π-π^* transition at -1.0 V. Upon stepwise oxidation of the film, the absorption due to π-π^* transition decreases with an increase in charge carrier absorbance bands at longer wavelengths centered around 900 nm. The films deposited by LbL method also undergo a transition to the oxidized state through an isosbestic point upon oxidation like the solution casted film.

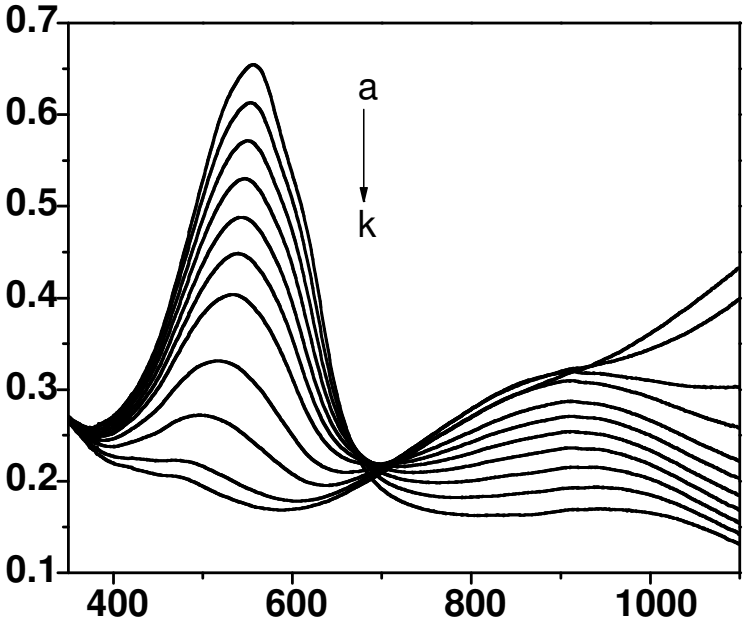

Figure 5.2 Spectroelectrochemistry of PProDOT-Sultone casted on ITO coated glass electrode in 0.1 M TBAP/ACN. Where (a) -1.0; (b) 0.1; (c) 0; (d) 0.1; (e) 0.15; (f) 0.2; (g) 0.3; (h) 0.4; (i) 0.6; (j) 0.8; (k) 1.0 V.

Fabrication and transmission spectral measurements of the symmetrical solid-state devices made up of conducting electrochromic polymer (PEDOT) have been shown previously by Mecerreyes et al.[21] In our case, this symmetrical configuration utilizes PAH/PProDOT-Sultone LbL films as electroactive layers on each of the two ITO-coated substrates similar to our recent work for PEDOT.[22] In brief, a potential of 1.5 V is applied to the two PProDOT-Sultone layers and the device changes color from light blue to dark purple-blue. The change in color occurs because of the neutral state of only one of the PProDOT-Sultone layers, while the other PProDOT-Sultone layer remains oxidized and does not contribute to the color change. The device goes back to the original light blue color once the potential is switched back to 0 V, showing no degradation or memory effect. An important thing to note here is that PProDOT-Sultone, being a conjugated polymer, can form symmetrical devices and hence does not need a reduction partner for

switching. This also results in fast switching of the symmetrical solid-state devices as compared to non-symmetrical solid-state devices in which both cathodically and andoically coloring material is required for device switching.

Electrochromic switching speed measurements of PProDOT-Sultone were performed both in liquid electrolyte solution as well as in solid state. For electrochromic switching studies in solution, polymer films were deposited by both the solution casting method as well as the LbL method on ITO coated glass and each polymeric film was stepped between its reduced (-1.0 V) and oxidized (+1.0 V) state in 0.1 M TBAP/ACN. As the films were switched, the $\%T$ at λ_{max} (557 nm) was monitored as a function of time. The contrast is given as the difference between $\%T$ in the reduced and oxidized states and reported as $\%\Delta T$. The film deposited by the solution casting method gave an electrochromic contrast of ~ 40 % with a switching time of 1.2 s. Films with 40 and 80 bilayers gave an electrochromic contrast of 40% and 46% respectively under static conditions (Table 1). The switching time was calculated from the time taken to reach 95% of the full contrast while switching the polymer from its fully oxidized to fully reduced state. Surprisingly, the film with 80 bilayers (Figure 5.3) demonstrated equally fast switching time (1.1 s) as compared to the 40 bilayer film (1.2 s). This indicates the easy movement of ions in and out of the film, which is independent of film thickness. This is in sharp contrast to earlier reports on solid state electrochromic devices wherein switching times were found to be inversely related to film thickness.[14,23] The composite coloration efficiencies for 40 and 80 bilayer films were found to be 165 and 250 mC/cm^2 which are very high as compared to other EC materials deposited by LbL method.[7,8, 24, 25, 26, 27]

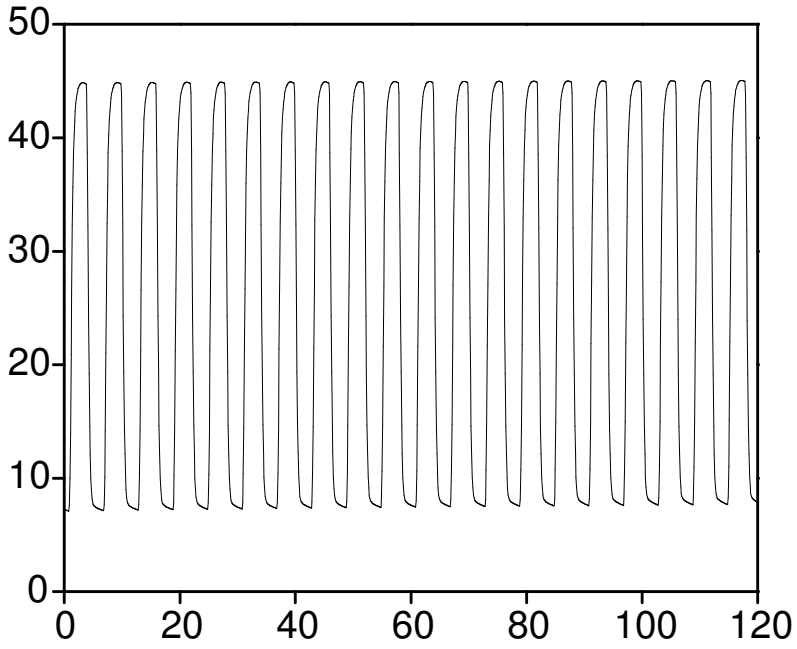

Figure 5.3 Optical switching studies for 80 bilayer LbL film as monitored by the %T at 557 nm when it was stepped between its reduced (-1.0 V) and oxidized (1.0 V) state.

Table 5.1. Physical properties of the PProDOT-Sultone films deposited using solution casting method and LbL methods.

Polymer PProDOT-Sultone		λmax (nm)	Optical Band Gap (eV)	Contrast (%ΔT)	Switching time(s)
In Water		554	1.78	--	--
Solution Cast Thin Films		557	1.78	40	1.2
LbL Thin Films	40 Bilayers	557	1.78	40	1.2
	80 Bilayers	557	1.78	46	1.1
Solid State Devices	40 Bilayers	570	--	31	0.1
	80 Bilayers	570	--	42	0.22

5.3.2 Switching Studies of Solid State Devices

The transmission spectra of solid-state PAH/PProDOT-Sultone devices made from two 20-bilayer and 40-bilayer PAH/PProDOT films are presented in Figure 5.4 at a constant potential of 0 V and 1.5 V. On switching the device between 0 V and 1.5 V, the 40 bilayer (2 films of 20 bilayers on ITO sandwiched together) and 80 bilayers (2 films of 40 bilayers on ITO sandwiched together) devices (Figure 5.5) showed maximum contrasts of 31% and 42%, respectively, at 570 nm. The change in transmittance is much higher than that of devices with a similar number of bilayers reported by Hammond and co-workers[28] for PEDOT and polyaniline (PANI) solid-state devices. The spectra in the solid-state are similar to the spectra in the liquid electrolyte solution for 40 bilayers of PAH/ PProDOT-Sultone.

The switching speed of the 40 bilayer devices was monitored over time with a He-Ne (633 nm) laser and photodiode as the square wave voltage (~1.5 V) is applied to the solid-state device (Figure 5.6). First, the switching speed curve shows the complete switching cycle, while the other two are the blow up for coloration and decoloration time. The device has coloration and decoloration times of 100 ms and 50 ms, respectively. It is interesting to note that this is one of the fastest switching speeds reported to date for solid-state electrochromic devices deposited using the LbL technique.[19] Therefore, polymers based on ProDOT-Sultone have the potential to be used as valuable electrochromic materials for next generation flat-panel display prototype devices with high contrast and long term stability.[29,30,31]

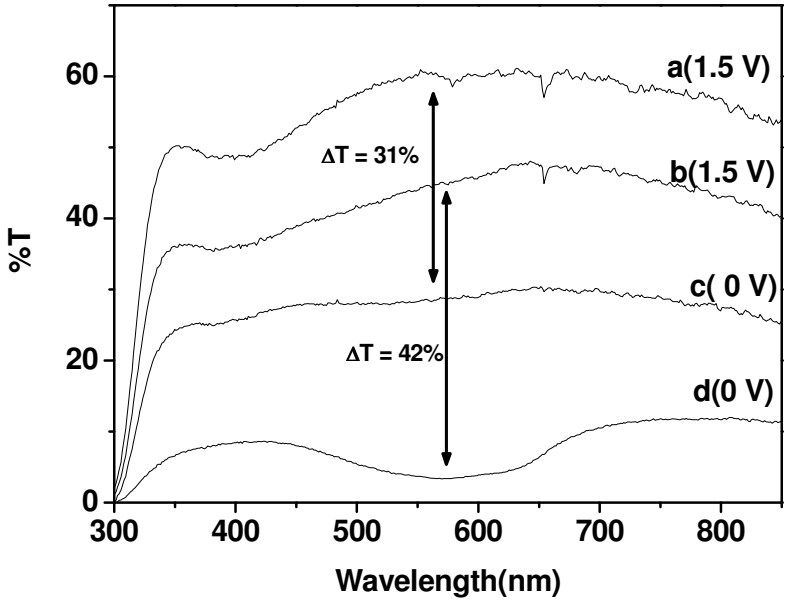

Figure 5.1 Transmission spectra of solid-state device of 40 (curve 'a' and 'c') and 80 (curve 'b' and'd') bilayer PAH/ PProDOT films at 0 V (a and b) and 1.5 V (c and d).

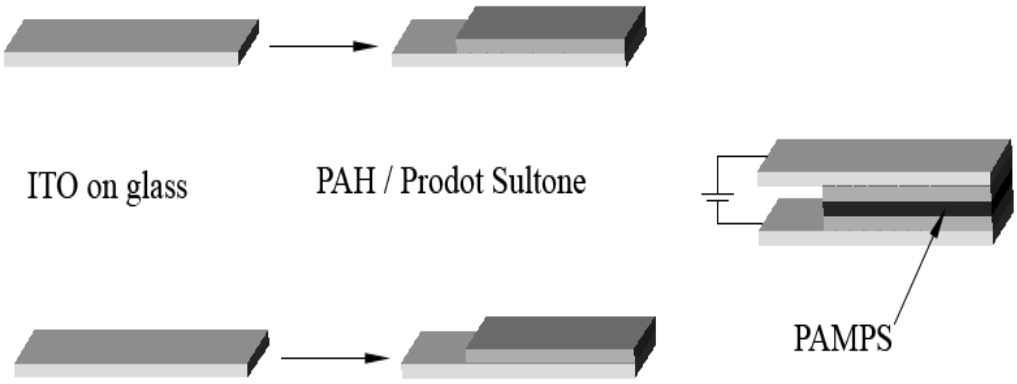

Figure 5.2 Schematic of a solid-state device.

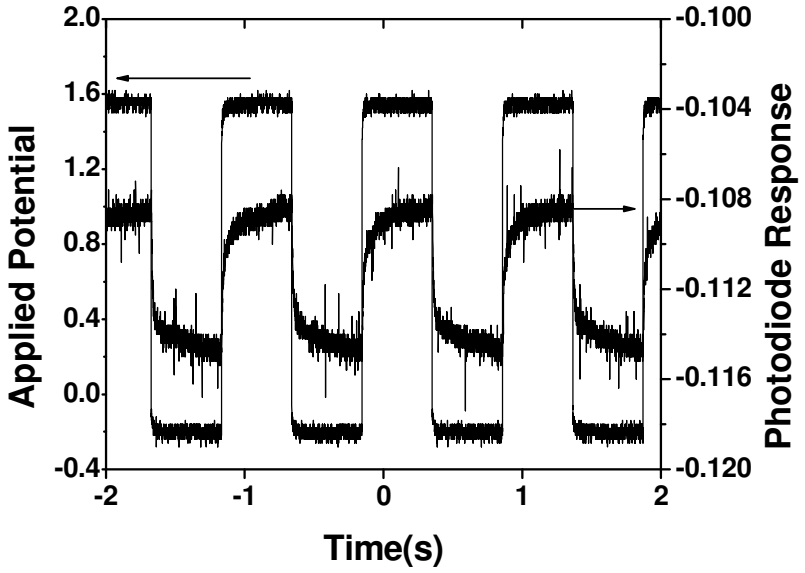

Figure 5.3 Photodiode signal vs time with square wave voltage applied for a 40-bilayer device with 1cm^2 area.

5.4 Summary

In summary, we have discussed a successful synthetic methodology for the *O*-alkylation of unreactive β,β-disubstituted hydroxyl group of ProDOT-OH using DABCO as a catalyst. This synthetic methodology is independent of the alkylating agent as well as the solvent used. Use of propane sultone as the alkylating agent resulted in the syntheses of a regiosymmetric water-soluble sulfonated monomer and polymer based on 3,4-propylenedioxythiophene. It was interesting to note the improvement in electrochemical propoerties due to regiosymmetric nature of the polymer based on PProDOT-Sultone as compared to that of regiorandom PEDOT-Sultone. The presence of a substitutent with a sulfonic acid alkyl group on the ProDOT ring gives a regioregular polymer which improves the film morphology without affecting the electronic properties. The fast switching speed of the solid-state devices, fabricated by LbL deposition, makes PProDOT-Sultone a potential candidate for ultrafast flat-panel displays. Because of the flexibility of the LbL assembly method, it should be noted that it has the potential to be used for the fabrication of multi-hue electrochromic devices by combining with cationic electrochromic materials (such as polyviologen, polyaniline etc).

References

[1] L. B. Groenendaal, F. Jonas, D. Freitag, H. Pielartzik, J. R. Reynolds, *Adv. Mater.* **2000**, 12, 481.

[2] L. B. Groenendaal, G. Zotti, P. Aubert, S. M. Waybright, J. R. Reynolds, *Adv. Mater.* **2003**, 15, 855.

[3] S. P. Mishra, R. Sahoo, A. V. Ambade, A. Q. Contractor, A. Kumar, *J . Mater. Chem*., **2004**, 14,1896.

[4] Z. Wang, X. Hu, *Thin solid films*, **1999**, *352*, 62.

[5] Y. Ikenoue, Y. Saida, M. Kira, H. Tomozawa, H. Yashima, M. Kobayashi, *J. Chem. Soc., Chem. Commun.* **1990**, 1694.

[6] E. Punkka, M. F. Rubner, *J. Electronic Mater.* **1992**, *21*, 1057.

[7] J. Lukkari, M. Saloma1ki, A. Viinikanoja, T. Aa1ritalo, J. Paukkunen, N. Kocharova, J. Kankare, *J. Am. Chem. Soc.* **2001**, *123*, 6083.

[8] (a) R. S. Loewe, R. D. McCullough, *Chem. Mater.* **2000**, *12*, 3214. (b) R. S. Loewe, P. C. Ewbank, J. Liu, L. Zhai, R. D. McCullough, *Macromolecules* **2001**, *34*, 4324.

[9] D. M. Welsh, L. J. Kloeppner, L. Madrigal, M. R. Pinto, B. C. Thompson, K. S. Schanze, K. A. Abboud, D. Powell, J. R. Reynolds, *Macromolecules* **2002**, *35*, 6517.

[10] G. Zotti, S. Zecchin, A. Berlin, G. Schiavon, G. Giro, *Chem. Mater*. **2001**, 13, 43.

[11] (a) C. A. Cutler, M. Bouguettaya, J. R. Reynolds, *Adv. Mater.* **2002**, *14*, 684. (b) Park, J. ; Kwon, Y.; Lee, T. *Macromol Rapid Comm*. **2007**, *28*, 1366.

[12] C. A. Cutler, M. Bouguettaya, T. Kang, J. R. Reynolds, *Macromolecules* **2005**, *38*, 3068.

[13] A. Kros, R. J. M. Nolte, N. A. J. M. Sommerdijk, *J. Poly. Sci: Part A:Polym. Chem.* **2002**, *40*, 738.

[14] R. M. Walczak, J. S. Cowart, K. A. Abboud, J. R. Reynolds, *Chem. Commun*. **2006**, 1604.

[15] (a) B. S. Kim, L. Chen, J. Gong, Y. Osada, *Macromolecules* **1999**, *32,* 3964. (b) R. D. McCullough, P. C. Ewbank, R. S. Loewe, *J. Am. Chem. Soc.* **199**7, *119,* 633.

[16] S. Chen, S. Hsueh, *J. Electroanal. Chem.* **2004**, *566*, 291.

[17] D. M. Delongchamp, M. Kastantin, P. T. Hammond, *Chem. Mater.* **2003**, *12*, 1575.

[18] G. Decher, *Science* **1997**, *227*, 1232.

[19] (a) C. L. Bird, A. T. Kuhn, *Chem. Soc. Rev*. **1981**, *10*, 49. (b) D. Laurent, J. B. Schlenoff, *Langmuir* **1997**, *13*, 1552.

[20] (a) T. R. Farhat, J. B. Schlenoff, *Langmuir* **2001**, *17*, 1184. (b) S. T. Dubas, J. B. Schlenoff, *Macromolecules* **1999**, *32*, 8153.

[21] D. Mercerryes, P. Marcilla, E. Ochoteco, H. Grande, J. P. Pomposa, R. Vergaz, J. M. S. Pena, *Electrochim. Acta* **2004**, *49*, 3555.

[22] V. Jain, H. M. Yochum, R. Montazami, J. R. Heflin, *Appl. Phys. Lett*. **2008**, *92*, 033304.

[23] (a) D. M. Delongchamp, P. T. Hammond, *Adv. Funct. Mater.* **2004**, *12*, 224. (b) D. M. Delongchamp, P. T. Hammond, *Chem. Mater.* **2004**, *16*, 4799.

[24] J. Stepp, J. B. Schlenoff, *J. Electrochem. Soc.* **1997**, *144*, L155.

[25] V. Jain, H. M. Yochum, H. Wang, R. Montazami, M. A. V. Hurtado, A. M. Galvan, H. W. Gibson, J. R. Heflin, *Macro. Chem. Phys.* **2008**, *209*, 150.

[26] R. Cinnsealach, G. Boschloo, S. N. Rao, D. Fitzmaurice, *Sol. Energ. Mat. Sol. C.* **1998**, *55*, 215.

[27] Y. Ikenoue, A. O. Patil, F. Wudl, A. J. Heeger, *J. Am. Chem. Soc.* **1998**, *110*, 2983.

[28] D. M. Delongchamp, P. T. Hammond, *Adv. Mater*. **2001**, *13*, 1455.

[29] D. Corr, U. Bach, D. Fay, M. Kinsella, C. McAtamney, F. O'Reilly, S. N. Rao, N. Stobie, *Solid State Ionics* **2003**, *165*, 315.

[30] S. I. Cho, W. J. Kwon, S. Choi, P. Kim, S. Park, J. Kim, S. J. Son, R. Xiao, S. Kim, S. B. Lee, *Adv. Mater*. **2005**, *17*, 171.

[31] S. I. Cho, D. H. Choi, S. Kim, S. B. Lee, *Chem. Mater*. **2005**, *17*, 4564.

Chapter 6

High Contrast Solid State Electrochromic Devices based on Ruthenium Purple Nanocomposites Fabricated by Layer-by-Layer Assembly

Electrochromic Ruthenium purple/polymer nanocomposite films, fabricated by multilayer assembly, were found to exhibit sub-second switching speed and the highest electrochromic contrast reported to date for any inorganic material.

6.1. Introduction

In the last two decades, the only inorganic non-oxide materials that have attracted significant attention for incorporation in low power electrochromic displays are those belong to the metal hexacyanoferrate (HCNF) family.[1] In the HCNF family, Prussian Blue (PB) is by far the most studied electrochromic material. In contrast, Ruthenium Purple (RuP) has not been explored for electrochromic displays because the neutral form is insoluble in aqueous solution. Though nanocomposites incorporating polymer and inorganic materials have shown improved performance as compared to the separate constituents for mechanical stability, electrochemical activity, and solar energy conversion,[2] their use in electrochromic devices has not been well studied. In this chapter, the synthesis of stable ruthenium purple nanoparticles and the electrochromic and surface properties of ruthenium purple/polymer nanocomposites fabricated by the layer-by-layer (LbL) assembly approach are demonstrated.

RuP belongs to the class of well-defined zeolite-like polynuclear inorganic materials with fixed metal ionic redox centers (e.g., Ru (II) and Fe (III)) wherein the electroneutrality is maintained during the redox process by the movement of freely diffusing cations in and out of the lattice

structure.[3] As discussed by several groups and similar to PB, RuP is present *in two forms*: ionized water-soluble KFe^{III} $[Ru^{II}(CN)_6].xH_2O$ and a neutral insoluble compound, Fe^{III}_4 $[Ru^{II}(CN)_6]_3$.[4,5,6,7] The soluble RuP is present in a colloidal form and the inclusion of potassium makes it stable in aqueous media, bringing an overall negative charge, which allows LbL assembly using RuP colloids as the anions. As explained by Rosseinsky et al.,[8] the incorporation of K^+ as a 'supernumerary' cation in $Fe^{III}[Ru^{II}(CN)_6]$ makes it water-soluble. RuP ($Fe^{III}_4[Ru^{II}(CN)_6]_3$ / KFe^{III} $[Ru^{II}(CN)_6]$ $.xH_2O$) is present in its natural form as a deep purple color which changes to colorless ruthenium white (RW), $Fe^{II}_3[Ru^{II}(CN)_6]_2$ upon reduction.

6.2. Experimental

For the present studies, 5 mM solution of RuP were prepared by mixing equal concentrations of potassium rutheniumcyanide ($K_4[Ru(CN)_6]$), ferric chloride ($FeCl_3$) and potassium chloride (KCl). KCl was added to ensure an excess of potassium ions crucial for the solubility of RuP. This solution was ultrafiltered to remove insoluble RuP, following the procedure described by Delongchamp et al.[7]

An automated dipping machine from Nanostrata Inc. was used for deposition of the multilayer films. For LbL assembly, ITO substrates were first washed with water to develop some negative charge and then alternately dipped in a 10 mM solution of linear poly(ethylen imine) (LPEI) at pH 4 and 5 mM solution of RuP at pH 4 for 6 mins each, followed by 3-step of rigorous -rinsing with deionized water for 45 secs after each deposition step. The linear increase in absorbance with increased number of bilayers (Figure 6.1) demonstrated that an equal amount of material was deposited with every bilayer. Linearity in the absorbance was observed as high as 160 bilayers, showing that thick films can be easily formed without disturbing the overall morphology or surface coverage per bilayer.

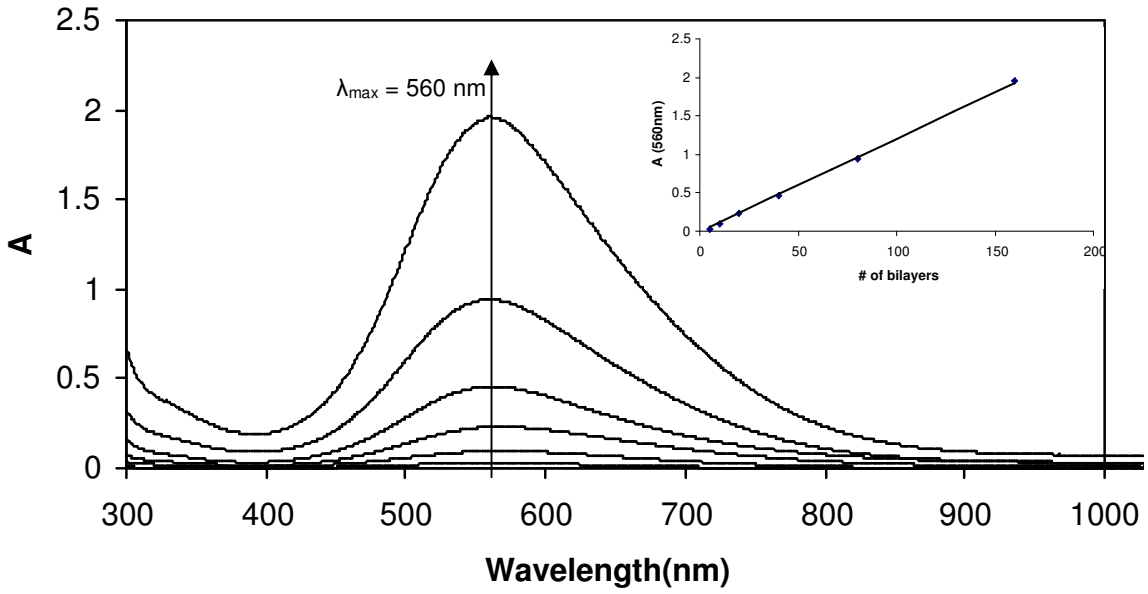

Figure 6.1 Absorbance versus number of bilayers of the LPEI/RuP nanocomposite film. Inset is the linear increase in the absorbance (at 560 nm) of LPEI/RuP film with number of bilayers.

High-resolution transmission electron microscope (HRTEM) images were obtained on a FEI Titan 300 at an accelerating voltage of 200 kV. Samples for TEM analysis were prepared by spreading a drop of dilute dispersion of as-prepared products on thin (3 nm) amorphous carbon-coated copper grids (Ted Pella Inc) and then dried in air. The average particle size and its standard deviation were estimated from HRTEM image analysis of 100 particles at 200 keV.

X-ray diffraction (XRD) patterns of the products were recorded using a Rigaku Ultrax 18 rotating anode X-Ray generator operating at 60 kV and 40 mA. A pyrolytic graphite monochromator was used to filter out all radiation except the CuKα doublet, with an average wavelength of λ = 1.5418 Å. No background corrections were applied. The powder form of the nanoparticles was obtained by drying the concentrated solution of RuP on a glass slide placed on a hot plate and then scraping the film. The DLS size and zeta potential measurements were performed with a Zetasizer nanoZS (Malvern Instruments) operating at a fixed angle of 173° and 633 nm wavelength. To remove the large nanoparticle agglomerates, the diluted ruthenium purple solution was passed through a 100 nm Teflon filter.

XPS spectra were obtained on a PHI Perkin-Elmer Model 5400 photoelectron spectrometer. The excitation radiation was a Mg Kα X-ray (hν = 1253.6 eV). The X-ray generator was operated at 14 kV and 300 watts. A PHI 10-360 hemispherical energy analyzer was used which operated in the constant pass energy (E_0) mode, where E_0 = 44.75 eV for survey scans and E_0 = 17.9 eV for high-resolution narrow scans. The vacuum was maintained below 5 x 10^{-7} torr during analysis. The XPS spectra were obtained at a take-off angle of 45° with respect to the surface of the sample unless otherwise noted. Initially a wide scan spectrum (survey scan) over a binding energy range of 1 to 1100 eV was obtained. First, all the elements were then identified from their binding energies, and then several narrow scans were carried out for each element identified in the survey scan. After correction of the sensitivity factor, the atomic ratio of the atoms in the LbL film was calculated from their relative peak areas. XPS spectra of the 40-bilayer LPEI/RuP film show nearly 1:1 atomic concentration of Fe and Ru.

UV-vis spectra were recorded in a Perkin Elmer Lambda 25 UV-Vis spectrophotometer.
Switching of the devices was monitored over time with a He-Ne laser (633 nm) and photodiode as the square wave voltage from -1.0V to +0.8 V was applied to the solid-state electrochromic device. The switching time for coloration and a de-coloration time is for 70% overall change in transmittance at switching voltages of -1.0V and +0.8 V.

6.3. Results and Discussions

6.3.1. X-ray diffraction (XRD)

The composition of the as-synthesized product in powder form was confirmed by the X-ray diffraction (XRD) pattern (Figure 6.2). The main peaks at 16.9° (200), 23.8° (220), 34.1° (400), 38.2° (420), and 44.3° (420) can be readily indexed as a pure face-centered cubic (fcc) phase of RuP [space group: Fm3m]. The broadening of the XRD is known to occur when the particle size reduces progressively below 200 nm.[9] The values are in good agreement with values reported by other groups for RuP and its analogues.[6,10,11]

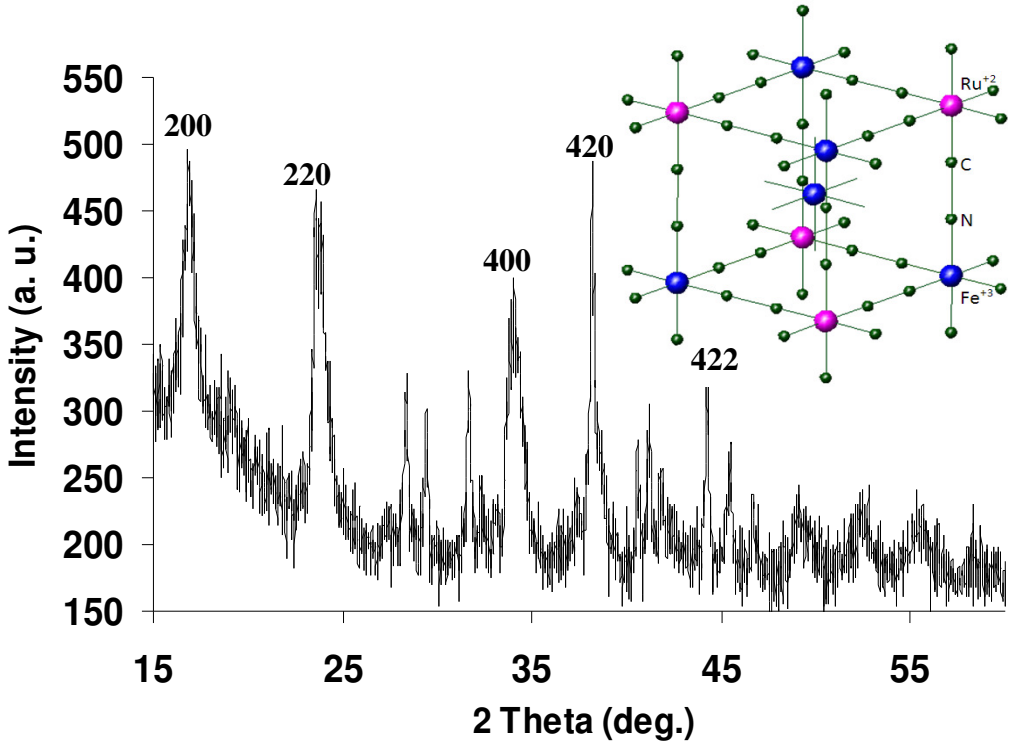

Figure 6.2 An XRD pattern of the powder form of the RuP sample, confirming the formation of pure fcc $Fe_4[Ru(CN)_6]_3$. The inset is the unit cell of $Fe_4[Ru(CN)_6]_3$.

6.3.2. Transmission electron microscopy (TEM)

TEM (Figure 6.3) and dynamic light scattering (DLS) (Figure 6.3(a)) of the sample were carried out from diluted RuP solutions and both techniques show that the average RuP nanoparticle size is 20-30 nm, which is in the range of the values reported for HCNF nanoparticles by other groups.[7,12] RuP possess a simple face-centered cubic (FCC) lattice structure;[13,14] the metal ion centers in the FCC structure are Ru (II) and Fe (III) with cyanide groups between these ions. The presence of (200) FCC structure is confirmed by FFT image (inset of Figure 2(a)) of the TEM diffraction pattern and is in agreement with the XRD results. The d-spacing value of 2.3 Å measured by TEM (Figure 6.3 (b)) for a crystal lattice (420) within the RuP nanoparticles with a lattice constant, a = 10.26 Å is in good agreement with the standard values for bulk cubic RuP.[15]

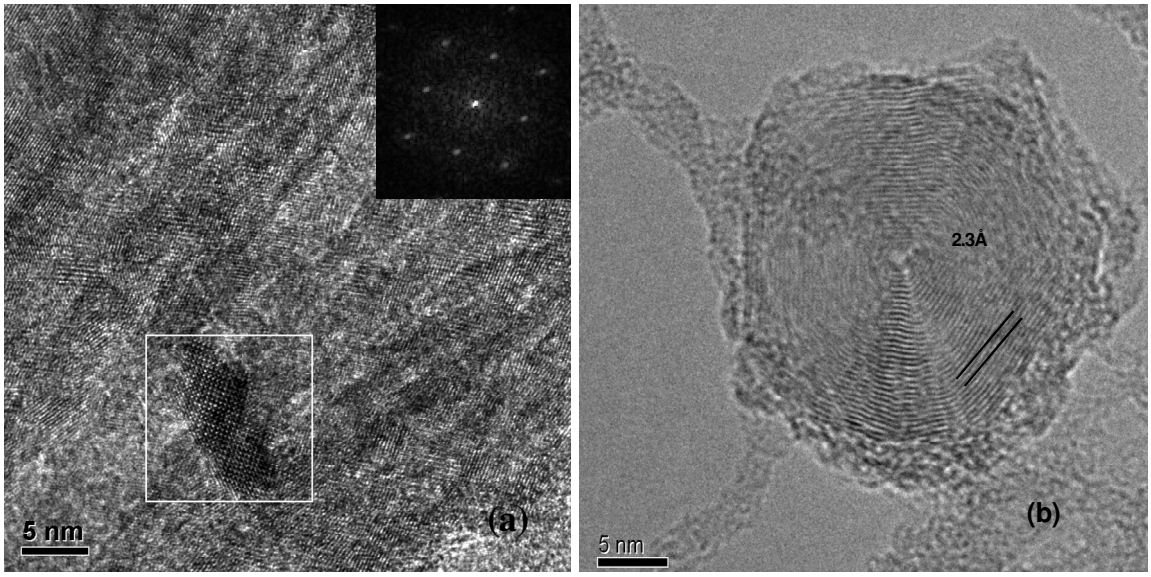

Figure 6.3 TEM image (a) of the nanoparticles and FFT diffraction pattern (inset) of one the marked nanoparticles, (b) shows the d-spacing values.

6.3.3 Zeta potential

Zeta potential measurements (Figure 6.4(b)) also confirmed the presence of two kinds of hexacyanoferrates, one of higher content (> 90%) with a negative potential value of -30.0 mV and the other low content insoluble part (< 10%) of value 2.5 mV. The amount of negative charge carried by soluble RuP nanoparticles is sufficient to fabricate films by LbL assembly. Though the colloidal dispersion of RuP nanoparticles was stable for months, sonication for 15-20 minutes before deposition resulted in better films due to breaking of the agglomerates.

Although the LbL approach has been used in the formation of (all-inorganic) PB and RuP multilayers onto electrode surfaces,[6] the application of this technique in the production of hybrid polymer/inorganic nanocomposites films has been so far reported only for PB combined with either LPEI[7] or polyaniline (PANI)[16] as the polymeric materials, but none has been

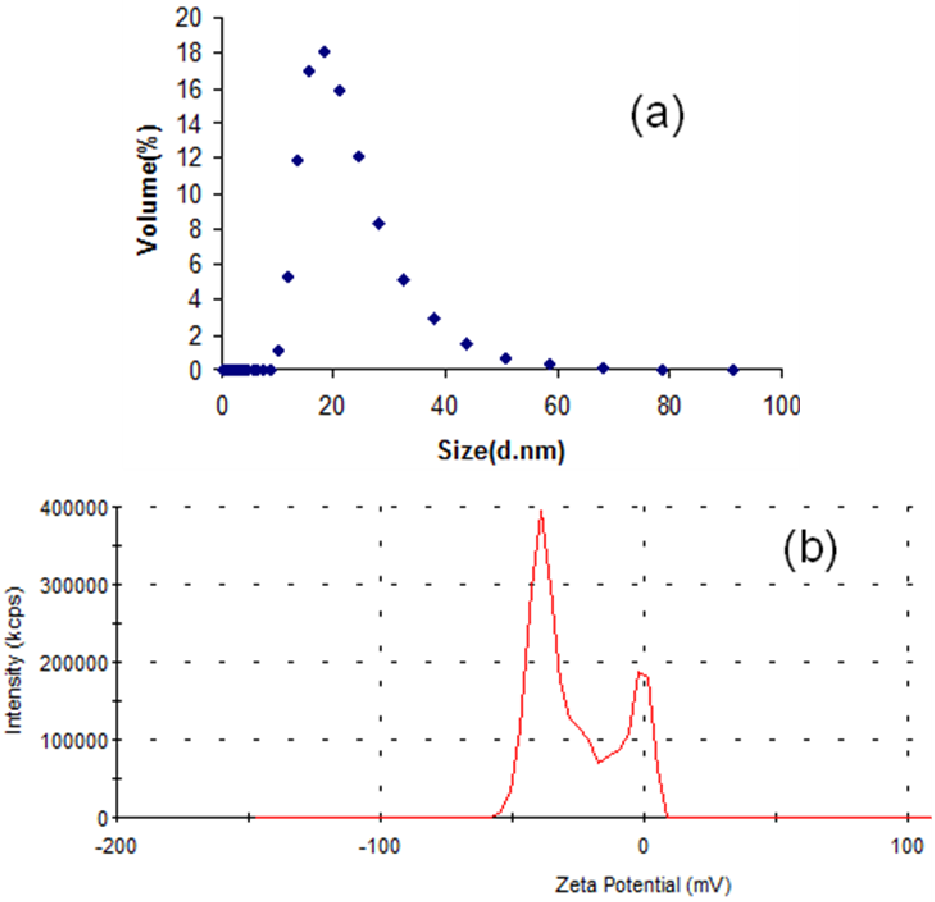

Figure 6.4 (a) Dynamic Light Scattering (DLS) and (b) zeta potential measurements of the aqueous dispersion of as-synthesized RuP nanoparticles.

reported for RuP. Herein, we show for the first time an adaptation of this approach to the formation of LPEI/RuP nanocpmposite multilayered films with improved electrochromic properties. The LbL assembly approach introduced by Decher et al.[17] provides nanoscale control of multilayer film thickness.

6.3.4. X-ray photoelectron spectroscopy (XPS)

XPS data (Figure 6.5) of the 40 bilayer LbL film (with outermost layer of the film of RuP nanoparticles) of LPEI/RuP further showed almost 1:1 atomic concentration of Ru and Fe, confirming the presence of soluble RuP nanoparticles in the films, while higher ratios of Ru to

Fe would have indicated the presence of extra Ru (II) occupying interstitial K^+ cationic sites in $[Ru^{II}(CN)_6]^{-4}$ lattice vacancies and making it insoluble.

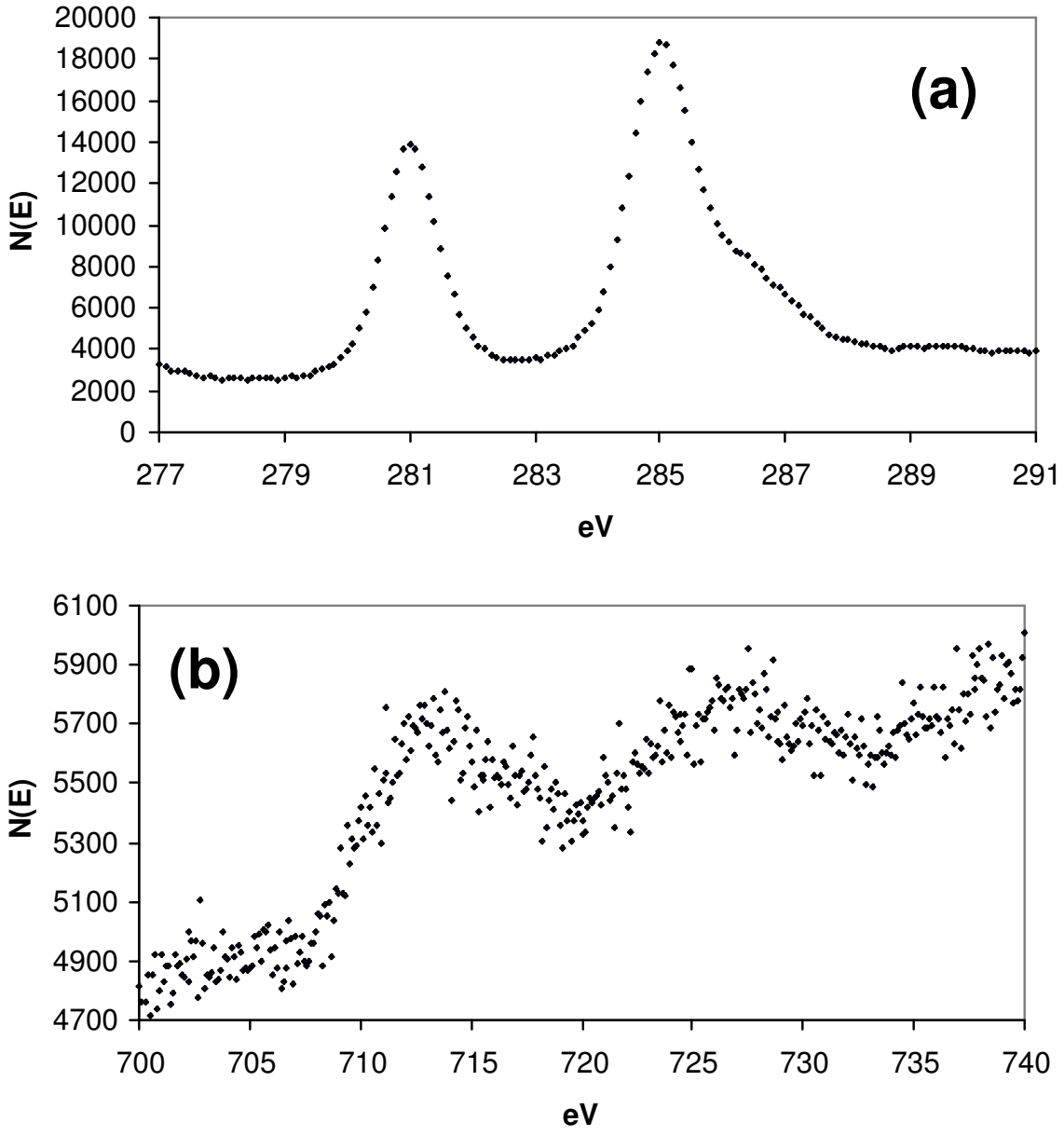

Figure 6.5 The a) Ru $3d^5$ and b) Fe 2p high-resolution X-ray photoelectron spectra (XPS) of a 20 bilayer LBL film of LPEI/RuP.

Spectroelectrochemistry studies of the RuP nanocomposite films in solution showed the color change from purple/violet color to transparent as a negative voltage was applied. The absorption

spectra from +1V to -1V, in 0.1V steps, of a 40-bilayer film of LPEI/RuP nanocomposite are presented in Figure 6.6. An exceptionally large change in transmittance of greater than 84% at a wavelength of 560 nm was observed as the film becomes transparent (RW) from the purple-magenta color (RuP). This is, to our knowledge, the highest contrast reported to date for any inorganic electrochromic material. The contrast values reported by Delongchamp et al. are 77% (60 bilayers) and 61% (30 bilayers) for LPEI/PB[7] and PANI/PB[16] respectively. There is no report of coloration efficiency or solid-state switching measurements in those publications.

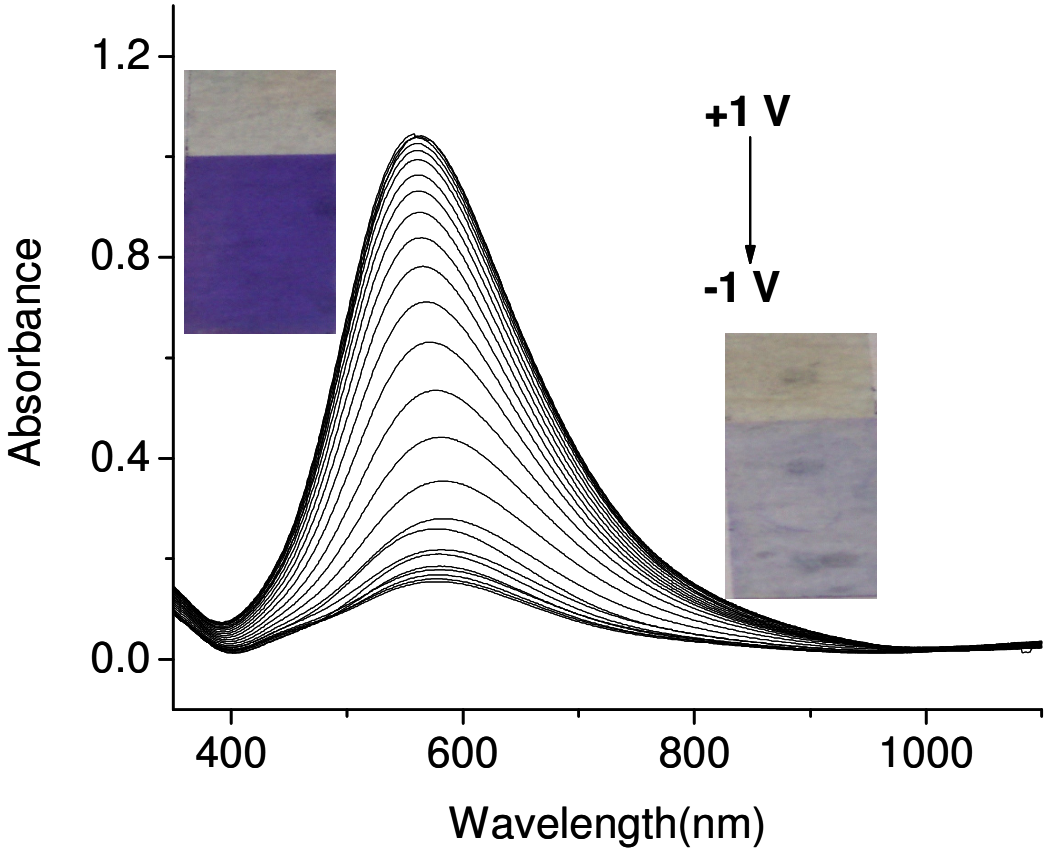

Figure 6.6 Spectroelectrochemistry data of the absorbance of a 40 bilayer RuP film in 0.1M LiClO4/ACN solution on increase of voltage from +1 V to -1 V in 0.1 V steps.

6.3.6 Cyclic voltammetry (CV)

CV was performed on the LPEI/ RuP nanocomposite between -0.5 V to 1.0 V, which is the potential range expected for the RuP to RW transition (Figure 6.7). LPEI is an inactive

polyelectrolyte, so the RuP controls the electrochemistry of the nanocomposite as confirmed by the agreement with the redox potential values of RuP found by other groups.[18] The reduction peak for RuP to RW was observed at 0.05 V is in agreement with the reported values.[5,7] The corresponding oxidation peak was observed at 0.23 V in the reverse scan. The electrochemical reaction for the 40 bilayer LPEI/RuP nano-composite film was completely reversible at low scan rates up to 50 mV/s, which showed that even thick films (>1μm) were fully electrochemically accessible.

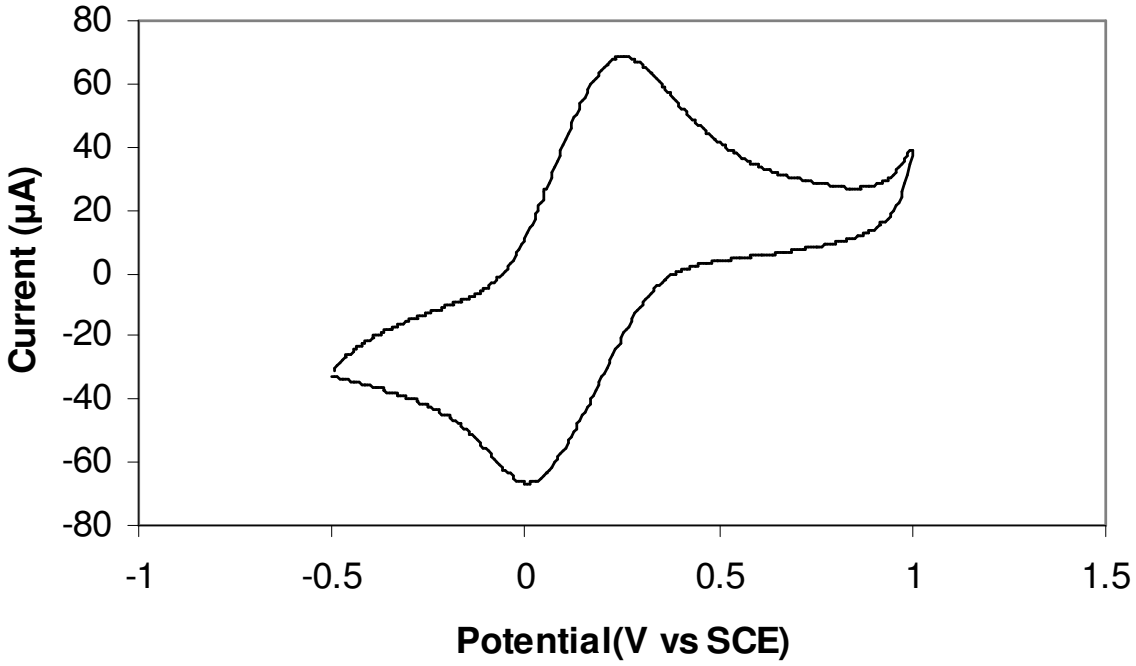

Figure 6.7 Cyclic voltammetry of a 40 bilayer LPEI/RuP film in 0.1M $LiClO_4$ /ACN electrolyte solution at 50 mV/s scan rate.

At higher scan rates the film was partially reduced and the sharp peaks of oxidation and reduction broadened and became flat. The broadening of the peaks is attributed to the presence of inactive LPEI present in the nanocomposite film; this increases the internal resistance of the film and the Li^+ ion insertion from the electrolyte to the electrochemical sites is more difficult. As explained by Ellis et al.,[19] at low scan rates the shape of the cyclic voltammogram is controlled more by the thermodynamic rather than the kinetic factors. The overall reaction mechanism does not change for different electrolytes, but as reported by Chen et al[20], the E^o values of the RuP seem to be affected by the type of cation (H^+, Li^+, Na^+, K^+, Rb^+) in the electrolytic solutions.

This could be due to the size of the cation, which plays an important role in the electrochemical behavior of the RuP films due to its inclusion and expulsion in the crystal lattice during potential cycling. According to the above discussion, the redox reaction of the RuP in the case of Li^+ cations can be written as:

$$KFe^{III}[Ru^{II}(CN)_6] + Li^+ + e^- \leftrightarrow LiKFe^{II}[Ru^{II}(CN)_6] \quad (1)$$

6.3.7 Calculation of the Coloration Efficiency (η)

The coloration efficiency was found to be 205 cm^2/C for the present LPEI/ RuP nanocomposites and is one of the highest reported for any inorganic electrochromic material. Coloration efficiency defined at the wavelength maximum λ_{max} (560nm in our case) is the relationship between the changes in optical density to the total injected/ejected charge as a function of the electrode area. Change in the transmittance state from colorless to dark purple gives an optical density of

$$\Delta OD = \log [T_b(\lambda)/ T_c(\lambda)]$$

$$= 0.853$$

$$\eta(\lambda) = \Delta OD/Q_d$$

in which Q_d = 4.16 mC/cm^2 for the reduction step and is calculated as the area under the CV curve for the reduction peak for the scan rate of 50 mV/s. The active working area of the film on the ITO electrode was 10 cm^2.

Hence, $\eta(\lambda) = 205\ cm^2/C$

The charge per unit area required for the reduction process of RuP to RW is 4.16 mC/ cm^2 for a 40 bilayer film, which is the same number of bilayers used for CV, optical switching and UV-vis absorption data. The Faradaic charge associated with one bilayer for the process is 105$\mu C/ cm^2$ and the surface coverage for each bilayer can be calculated by

$$\Gamma = Q/ nF$$

where F is the Faraday constant (96.5 x 10^3 sA/mol). The surface coverage calculated using the above equation was found to be 1.1 x 10^{-9} mol/ cm^2. This agrees well with the surface coverage expected for RuP nanoparticles of this size.[21]

6.3.8 Switching-Speed

Optical switching of RuP nanocomposite films was performed in both liquid electrolyte (Figure 6.8) and in solid-state (Figure 6.9) devices. Solid-state devices were fabricated by depositing the LbL film on ITO coated glass in the same way as described in our previous work.[22]

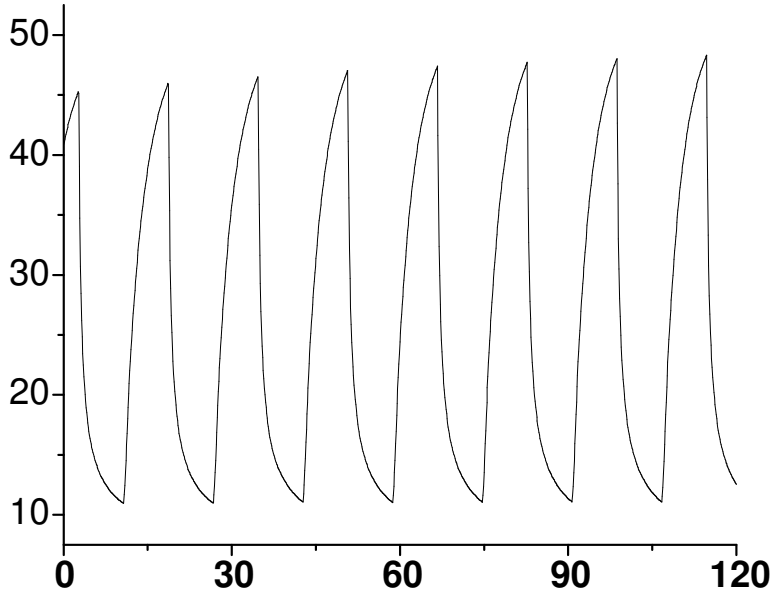

Figure 6.8 Liquid electrolyte optical switching of a single 40 bilayer LPEI/RuP film immersed in 0.1M LiClO4/ACN with delay time of 8 sec.

Two separate 40-bilayer films of PANI/Poly (2-acrylamido 2-methyl propanesulfonic acid) PAMPS and LPEI / RuP were taken as complementary anodically and cathodically coloring materials, respectively. The $LiClO_4$/PC gel polyelectrolyte used for the solid-state device was prepared as described by Sonmez et al.[23] The solid-state device switches from light blue to dark-purple with coloration and decoloration times in the range of 600 ms and 300 ms, respectively, as shown in Figure 6.9.

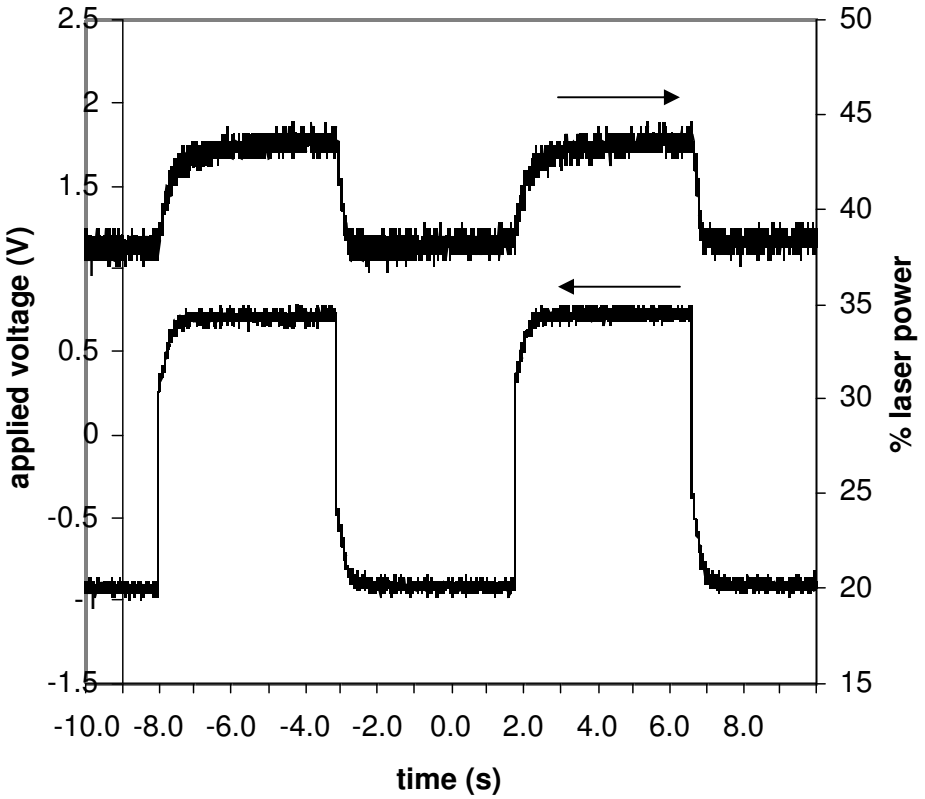

Figure 6.9 Solid-state switching of a device consisting of a 40 bilayer LPEI/RuP film as a cathodically coloring material and a 40 bilayer PANI/PAMPS film as the anodically coloring material at -1V to +0.8V.

The switching speed can potentially be improved by replacing LPEI with a cationic conducting polymer such as PANI, Poly(phenylenevinylene) (PPV) etc. This is one of the first nanocomposite solid-state electrochromic devices reported in the literature.

6.4. Summary

In conclusion, RuP nanoparticles with spherical morphology were synthesized and thin film polymer/ RuP nanocomposites were fabricated by the LbL technique. The absorbance of the film increased linearly with the number of bilayers deposited indicating that thick nanocomposite films can be easily fabricated without sacrificing the individual contributions of the constituents. The 40-bilayer nanocomposite films showed a very high contrast of around 84% with a high coloration efficiency of 205 cm^2/C. The change in color from purple-red (magenta) to transparent and switching in solid-state devices also filled in the gap in tri-color space of cyan, magenta, yellow (CMY) reflective displays described by Delongchamp et al[7]. In this chapter, our aim was to show the synthesis of RuP nanoparticles and the electrochromic properties of the polymer/RuP nanocomposites. Detailed electrochemical and multi-chromic studies and the effect of other polyelectrolytes are good candidates for future work.

References

[1] C. G. Granqvist, "*Handbook of Inorganic Electrochromic Materials*" **1995**, Elsevier, Amsterdam.

[2] K. Rajeshwar, N. De Tacconi, and C. R. Chentahmaramakrishnan, *Chem. Mater.* , **2001**, *13,* 2765.

[3] I. Carpani, M. Giorgetti, M. Berrettoni, P.L. Buldini, M. Gazzano, and D. Tonelli, *J. Solid State Chem*., **2006**, *179*, 3981.

[4] K. Itaya, I. Uchida, U.D. Neff, *Acc. Chem. Res*. **1986**, *19*, 162.

[5] A. Jaiswal, J. Collins, B. Agricole, P. Delhaes, and S. Ravaine, *J. Coll. Interface Sci.*, **2003**, *261*, 330.

[6] R. C. Milward, C. E. Madden, I. Sutherland, R.J .Mortimer, S. Flecher, and F. Marken, *Chem. Comm*., **2001,** *19,* 1994.

[7] D. M. Delongchamp, P.T. Hammond, *Adv. Funct. Mat*., **2004**, *14,* 224.

[8] D. R. Rosseinsky, and A. Glide, *J. Electrochem. Soc.*, **2003**, *150(9)*, C641.

[9] A.R. West, *Solid State Chemistry and its applications*, John Wiley and Sons, Chicchester, 1990, pp. 173.

[10] M. Cao, X. Wu, X. He, and C. Hu, *Chem. Comm*., **2005**, *17*, 2241.

[11] Y. Song, W. Jia, Y. Li, X. Xia, Q. Wang, J. Zhao, and Y. Yan, *Adv. Funct. Mater*., **2007**, *17*, 2808.

[12] N. Bagkar, R Ganguly, S. Choudhury, P.A. Hassan, S. Sawant, and J. V. Yakhmi, *J. Mater. Chem.*, **2004**, *14*, 1430.

[13] H. Inoue, and S. Yanagisawa, *J. Inorg. Nucl. Chem*., **1974**, *36*, 1411.

[14] M.V. Bennett, L.G. Beauvais, M.P. Shores, and J. R. Long, J. *Am. Chem. Soc.,* **2001**, *123*, 8022.

[15] A. Ludi, and H.U. Gudel, in *Structure and Bonding*, ed. J. D. Dunitz, Springer-Verlag, New York, 1973, Vol.14, Ch. 1, pp.8.

[16] D. M. DeLongchamp P.T. Hammond, *Chem. Mater*. **2004**, *16*, 4799.

[17] G. Decher, *Science*, **1997**, *227*, 1232.

[18] K. Sone, and M. Yagi, *Macromol. Symp.,* **2006**, *235*, 179.

[19] D. Ellis, M.Eckhoff, and V.D. Neff, *J. Phys. Chem*., **1981**, *85*, 1221.

[20] S. Chen, and S. Hsueh, *J. Electroana. Chem.*, **2004**, *566,* 291.

[21] S. Liu, D. G. Kurth, H. Mohwald, and D. Volkmer, *Adv. Mater.* **2002**, *14*, 225.

[22] V. Jain, H.M. Yochum, H. Wang, R. Montazami, M. A. V.Hurtado, A. Mendoza- Galván, H. W. Gibson, J. R. Heflin, *Macromol. Chem. Phys*., **2008**, *209*, 150.

[23] G. Sonmez, H. Meng, and F. Wudl, *Chem. Mater*. **2004**, *16*, 574.

Chapter 7

Layer-by-Layer Self-Assembled Conductor Network Composites in Ionic Polymer Metal Composite Actuators with High Strain Response

In this chapter, we present an investigation of the electromechanical response of a conductor network composite (CNC) fabricated by the layer-by-layer (LbL) self-assembly method. The process makes it possible for CNCs to be fabricated at sub-micron thickness with high precision and quality. An electromechanical actuator fabricated with this CNC exhibits high strains of ~6.8% under 4 volts, whereas RuO_2/Nafion CNCs exhibit strains of ~ 3.3%. The high strain and sub-micron thickness of the LbL layers in an ionic polymer metal composite (IPMC) yield large and fast actuation. The response time of a 26 μm thick IPMC with 0.4 μm thick LbL CNCs to step voltage of 4 volts is 0.18 seconds. Investigation into the limiting factors for the actuation speed of ionomeric polymer conductive network composite (IPCNC) actuators, in which motion of the excess ions into and out of the conductive network composite (CNC) electrodes generates electromechanical transduction, is also shown in this chapter. It is demonstrated that the slow ionic transport of the mobile ions in the CNC electrode layer is what limits the actuation speed. It was found that the IPCNC actuator speed is proportional to $1/d_e^2$ as compared to neat ionomers in which the actuation speed is proportional to 1/d where d and d_e are the ionomer and the CNC electrode layer thickness, respectively.

7.1 Introduction

Electroactive polymers (EAPs), which generate large electromechanical actuation while operated under low voltage (~ a few volts), are attractive since they have the potential to be easily integrated with microelectronic controlling circuits to perform complex functions.[1,2,3,4,5,6,7] For several decades, electrical actuation has been provided by inorganic electromechanical actuator

(EMA) materials, including electroactive ceramics (EACs) and shape memory alloys (SMAs) and they can generate high forces and displacements, but tend to suffer from slow response times, large mechanical hysteresis and short lifetimes. These problems are not faced by EAPs of various kinds such as dielectric elastomers, conducting polymers, carbon nanotube actuators, molecular actuators and ionic EAPs.[8,9] Recently introduced ionic EAPs (*i*-EAPs) have gained significant attention due to their advantage of requiring low voltages (<10V) to exhibit large bending displacements. Being easy to fabricate, flexible, lightweight and able to form final structures that are low-voltage, low-power devices are a few of the advantages of ionomeric polymer metal composites (IPMC) among i-EAPs. IPMC usually consists of a perfluorintaed ionomeric memberane (Nafion™ (Dupont), Flemion™ (Asahi Glass) etc. (Figure 7.1)), a high surface area electrically conducting electrode and an ion conducting diluents. All of these components play very important roles in the efficient working of the IPMCs.

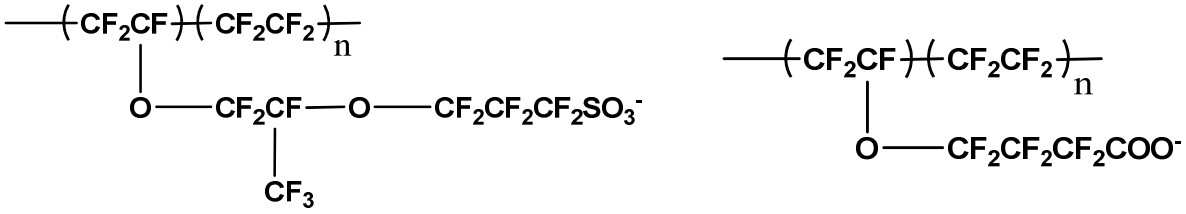

(a) (b)

Figure 7.1 Perfluorinated ionomers used in the fabrication of IPMC (a) Nafion™ (b) Flemion™.

Early work on the Pt-electroded Nafion is an example of EAPs exhibiting a relatively large bending actuation under a few volts applied, which attracted a great deal of attention.[4-7] Since then, much research effort has been devoted to this class of EAPs with the objective of further improving the electromechanical performance properties such as the actuation speed, strain level, and efficiency.[4,5,6,7,10,11,12,13,14,15,16]

Figure 7.2(a) illustrates schematically such an ionic polymeric bending actuator in which the accumulation and depletion of cations at the cathode and anode, respectively, create bending of the ionic polymer membrane under an electrical signal. Experimental results have indicated that a high population of the excess charges at the electrodes is highly desirable in order to generate high electromechanical actuation. To realize that, porous electrodes which offer large electrode areas in contact with ionomers are often utilized in this class of actuators.[4-14] One widely investigated IPMC uses a chemical reduction method to deposit precious metals onto Nafion (a perfluoro-sulfonated ionomer developed by DuPont) membrane surfaces, in which nanosized metal particles penetrate into the Nafion membrane to form porous electrodes.[5-7,11,14] More recently, a direct assembly method was developed in which conductive nanoparticles were mixed with a Nafion (or an ionomer) solution and the mixture was directly deposited on the Nafion (or an ionomer) membrane to fabricate the IPMC.[8,9,12,13]

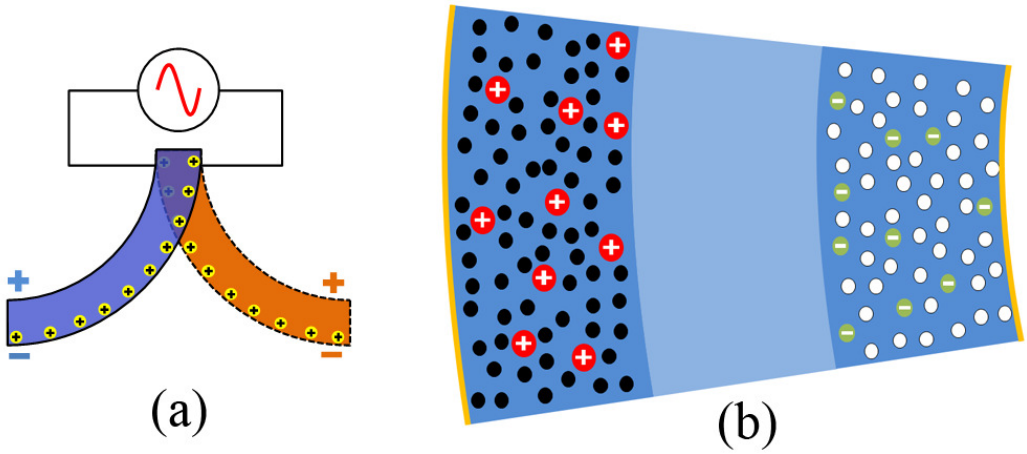

Figure 7.2 (a) Schematic of an ionomer bending actuator under an electric signal, (b) Schematic of a CNC/ionomer/CNC (C/I/C) three layer IPMC bimorph actuator (The Au electrode layers are also shown).

The direct assembly method to fabricate IPMCs is attractive because it allows for the use of a broad range of nanosized conductors for the electrodes such as carbon nanotubes.[13] It also simplifies the fabrication process of IPMCs and enhances actuator manufacturing

repeatability.[8,9,12,13] Illustrated in Figure 7.2(b) is a typical bimorph (bending) actuator thus developed, which in general has a three layer structure, i.e., two porous composite electrode layers, which are referred to as the conductor network composite (CNC) and generate strain under applied voltage, separated by a neat ionomer layer. Performance of Nafion-based IPMCs actuators is promising, but several disadvantages like hydration dependence and high cost discourage industry from using it at large scale. As explained by Lee et al., the rapid loss of water through evaporation and electrolysis at 1.23 V causes a reduced flux of metal cations and inner solvent, which damages the electrode and shortens the lifecycle of an actuator.[17] To avoid this problem, several research groups have tried to replace water as a solvent in IPMC, with less volatile or electrochemically stable compounds. For example, Nasser et al. used mixtures of ethylene glycol and glycerol as inner solvent[18] and Lee et al. reported that the use of a mixture of polar organic solvents and deuterated water can improve the electrolytic stability, but still actuator performance enhancement wasn't significant enough to seriously employ these solvent systems in the devices. Bennett and Leo were one of the first groups to explore the option of using ionic liquids as electrolytes in IPMCs.[19] Ionic liquids are mixtures of low-molar mass anions and cations and exhibit unique properties such as low vapor pressure, excellent electrochemical and thermal stability, high ionic/electrical conductivity and low viscosity. Along with Leo et al, several other groups have published some very interesting work on the applications of ILs in IPMCs. [20,21,22,23,24] Yoo et al. took this research a step further by analyzing structural factors that can affect the properties of ILs and also the performance of IPMCs containing them. It was observed that the larger the size difference between the cationic and an ionic species of the ILs the larger the tip displacement of the bending actuator.

Recently, the approach of using the advantages of ILs in IPMCs was applied in various different ways. Fukushima et al.[25,26,27] have designed a new kind of actuator known as "bucky-gel actuators" to get rid of the solvent dependency of the EAP actuators that operate at low voltages. Bucky gel was formed by grinding single walled carbon nanotubes (SWNTs) in ionic liquids at room temperature. It was observed that a gel is formed because of the cation-Π interactions between the SWNTs and ILs, which helped in exfoliating the heavily entangled carbon nanotubes. This mixture was added to a polymer-support solution (poly vinylidene fluoride-co-hexafluoropropylene (PVdF (HFP)), which was then heated at 80 ºC and cast on an

aluminium mold to cool to room temperature to form electrodes. Similarly, a polymer supported ionic liquid electrolyte mixture was made and cast onto the polymer-supported bucky gel electrodes. Lastly, one more layer of polymer-supported bucky gel electrode was deposited to form a three-layer dry actuator that has a bimorph configuration (Figure 7.3(a)).

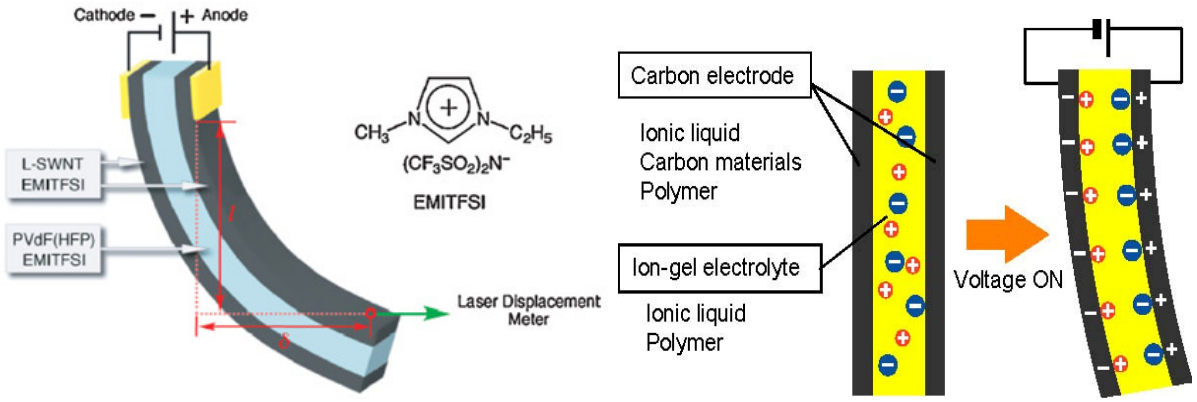

(a) (b)

Figure 7.3 Schematic structure of (a) Bucky-gel-based bimorph actuator (b) Ionic-gel actuator.

Watanabe et al. have worked on developing an ionic gel from a polymer-ionic liquid (polymer-salt system) to improve the ionic conductivity of the system, which in turn results in faster actuation speed of the bending actuator ("ionic gel actuators" (Figure 7.3b)[28]). [29,30] The same research group has also demonstrated the successful synthesis of a special kind of photocurable ionic gel, which was prepared by addition of an ionic liquid to a photocurable polymer. Irradiation with UV light forms a miscible system, which is then hot-pressed between two carbon-based electrodes to make a soft actuator device. The main ambition of using the photocurable ionic gel is to rapidly produce soft actuators using a photolithographic approach.

Another quest in the field of IPMCs is to look for an alternative material that can replace the expensive nafion membrane. A recent review article by Duncan et al. provided a very good background.[31] A few ionomers have ionic conductivity and water uptake ratio at par or better than Nafion. Some of these ionomers synthesized by standard step-growth polymerization are

sulfonated and carboxylated version of poly(aryleneether sulfone)s, poly(ether ketones), polyimides, polybenzimidazoles, and polyphosphazenes.[32 33] However, poor melt processability and low elastic modulus makes them unfavorable materials for lightweight bending actuators. This area is only briefly mentioned here, as it is a very broad topic and it is difficult to obtain an ionomer that contains all the critical properties at par with nafion.

In this chapter, we investigate a class of CNC fabricated by a direct assembly method to form IPMC bimorph actuators in which the CNC electrodes were deposited onto the Nafion membrane via a layer-by-layer (LbL) self-assembly process. The CNC made of the LbL composite exhibits a very large strain (~ 6.8%) as deduced from the bending actuation. Furthermore, an LbL CNC allows for precise control of the CNC thickness on the nanometer scale. By utilizing this LbL CNC, IPMC bimorph actuators with the CNC layer thickness ~ 0.4 μm (one side) display a large bending actuation with a short actuation time (~ 0.18 seconds). For comparison, we also fabricated IPMC bimorph actuators using RuO_2/Nafion nanocomposite as the CNCs by the direct assembly method. RuO_2/Nafion nanocomposite IPMCs have been investigated extensively and have shown high strain response among the IPMCs developed.[4-13] We also show the relation of the thickness of either the ionic membrane (d) or the thin CNC electrode (d_e) deposited on it with the actuation speed of IPCNC actuators. It was observed that decreasing electrode thickness was accompanied by faster actuation speed of the actuator

7.2. Experimental

For the IPCNCs investigated in this chapter, the commercial Nafion film NR-211 of thickness 25 μm was chosen as the ionomer layer in Figure 7.2(b). The LbL composite electrodes were fabricated by immersing the Nafion film into two oppositely-charged solutions alternately, which contained anionic gold nanopaticles (~2 nm diameter, Purest Colloids, Inc.) and the polycation poly(allylamine hydrochloride) (PAH), respectively.[343536] The composites grew via the electrostatic attraction between the polyelectrolyte or nanoparticles in solution and the oppositely-charged substrate. The LbL CNCs, comprising 100 and 200 LbL bilayers, had electrode thicknesses of 0.4 μm and 0.8 μm, respectively. For each IPCNC, there were CNC electrodes on each of the two surfaces and hence the total IPCNC thickness was 25.8 μm and

26.6 μm, respectively. The IPMCs with these two CNC layer thicknesses are referred to as LbL1 and LbL2 in the chapter. For comparison, RuO_2/Nafion composites were prepared using the direct assembly method.[13] RuO_2 nano-particles purchased from Alfa Aesar with 13-19 nm diameters were mixed with 20% Nafion dispersion from Aldrich. The mixture was sonicated before being sprayed onto the Nafion film surface. After spraying, films were transferred to a vacuum oven to rid them of solvent and were then ready for actuator fabrication. The RuO_2/Nafion ionomer composite thickness was 3 μm and hence the total thickness of the IPMC is 31 μm. The samples identified as RuO_2/Nafion and RuO_2 1 were similar, and are just identified differently in sections 7.3.1 and 7.3.3. Neat Nafion 2 is a commercial Nafion film NR-212 of thickness 50 μm and was chosen as the ionomer layer in Section 7.3.3.

Table 7.1 summarizes the thicknesses of the composite electrode layer d_e and the total thickness d of the bending actuators investigated in this chapter *

IPCNCs	Composite electrode Thickness d_e	Total thickness of the actuator
Neat Nafion 1	0	25 μm
LBL 1	0.4 μm	25.8 μm
LBL 2	0.8 μm	26.6 μm
RuO_2 1	3 μm	31 μm
RuO_2 2	10 μm	45 μm
Neat Nafion 2	0	50 μm

* All actuators have lateral dimensions of 1 mm x 8 mm (width x length).

After composites were deposited on the neat Nafion membrane, actuators were fabricated by soaking samples with 40 wt% ionic liquid 1-ethyl-3-methylimidazolium trifluoromethanesulfonate (EMI-Tf) and depositing 50 nm thick gold leaves as external electrodes on the two sides of the samples. Several other room temperature ionic liquids were also tested, and it was found that IPCNCs with EMI-Tf generate the highest strain response. The lateral dimensions of all the actuators were 1 mm in width and 8 mm in length.

The actuators were sent to the laboratories of Dr. Qiming Zhang at Penn State University for characterization. The bending of these actuators was characterized by two optical methods. For large bending actuation under greater than 1 volt, the time resolved bending strain of the actuators was recorded by a CCD video camera attached to a probe station with frame rate of 2000 frames/second (Pulnix TM-6740CL) to record the photographic images of the bending actuation. A step voltage was applied to generate bending strain and the maximum applied voltage was 4 volts. For small bending actuation (applied voltage < 0.4 volt) the tip displacement of the bending actuators as a function of frequency was characterized using a laser vibrometer (Polytec OFV3001 controller and OFV511 fiber interferometer). The electric impedance of the actuators was measured by both a precision LCR meter (Hewlett Packard 4284A) and a lock-in amplifier (Stanford Research Systems SR 830) under 0.1 Volt AC signal. The elastic modulus of each layer along the film surface direction in the IPCNC was characterized using a set-up specifically designed to measure the elastic modulus of soft materials. In this set-up, the specimen was fixed at two ends and a displacement transducer was used to generate strain in the specimen and the corresponding stress (force/cross section area) was measured by a load cell.

7.3. Results and Discussions

7.3.1 Strain Measurements

In this study, the elastic modulus of the Nafion film with 40 wt% EMI-Tf was measured first (=50 MPa). Then the elastic modulus of the specimen with CNC deposited to Nafion membrane was characterized from which the elastic modulus of the CNC layer was deduced (Y=0.4 GPa for LbL CNCs and =0.3 GPa for RuO_2 nanocomposite CNCs). The elastic modulus of the five-layer IPCNC swollen with EMI-Tf was also measured from which the elastic modulus of the Au layer was deduced (=20 GPa). Presented in Figure 7.4 are the bending actuation of the LbL1, LbL 2, and RuO_2/Nafion IPCNC.

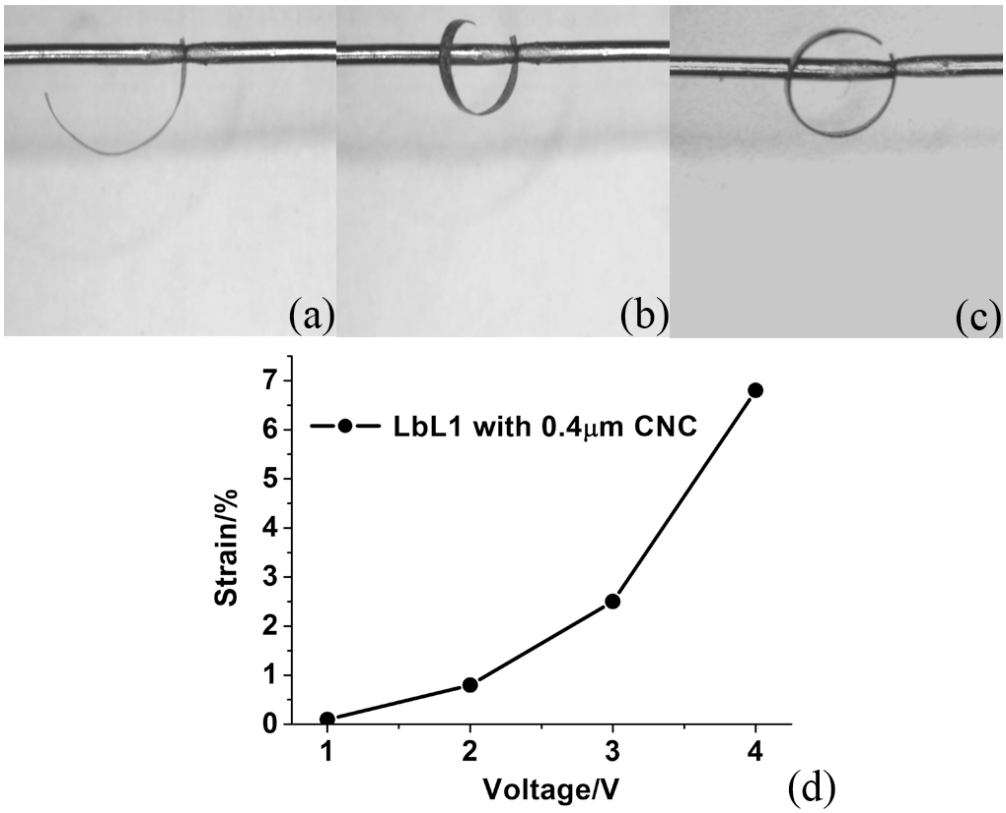

Figure 7.4 Photographic images of the bending actuation under 4 volts. a) the 100 bilayers LbL composite actuator; (b) the 200 bilayers LbL composite actuator; (c) the 3μm RuO_2/Nafion composite actuator; (d) the 100 bilayers LbL CNC strain S_{10}^{c} versus applied voltage.

In general, for such a bending actuator, a thicker CNC layer will generate larger bending if the intrinsic strain in the CNC layer (S_{10}^{c}) is the same. In these bimorph actuators, the bending actuation is generated by the strains in the CNC layers. In order to extract the intrinsic strain in the CNC layer (S_{10}^{c}) which is a material property of CNC layers, we derive the relationship between the bending radius of curvature R and the strain S_{10}^{c} along the film surface in the CNC layers (see Figure 7.5). In the bending actuators, the actual strain S_{1}^{c} is reduced from S_{10}^{c} due to the stresses from the ionomer layer and Au film, i.e., where s^{c}_{11} is the elastic

$$S_1^c = S_{10}^c + s_{11}^c T_1^c \quad (1)$$

compliance and T^c_1 is the stress along the film surface(see Figure 7.3). It is noted that S_{10}^c is a property of the CNC material and will not change, for example, with the various layer thicknesses in the bimorph actuators (Figure 7.2(b)). On the other hand, the actual strain in the CNC layers S_1^c will change with the bimorph configuration, ranging from near zero to S_{10}^c. For the bending actuator in Figure 7.5, it can be assumed that all the other stress components are very small compared with T_1^c and can be approximated as zero. [37,38] Further, it can be derived that the strain S_1 is related to the radius of the curvature R as, [19]

$$S_1 = \frac{L'-L}{L} = \frac{(y+R)\theta - R\theta}{R\theta} = \frac{y}{R} = \kappa y \quad (2)$$

From the equilibrium conditions, when there is no external force or moment, the total moment M and total force F of the bending actuator satisfy $\int dF = 0$ and $\int dM = 0$.

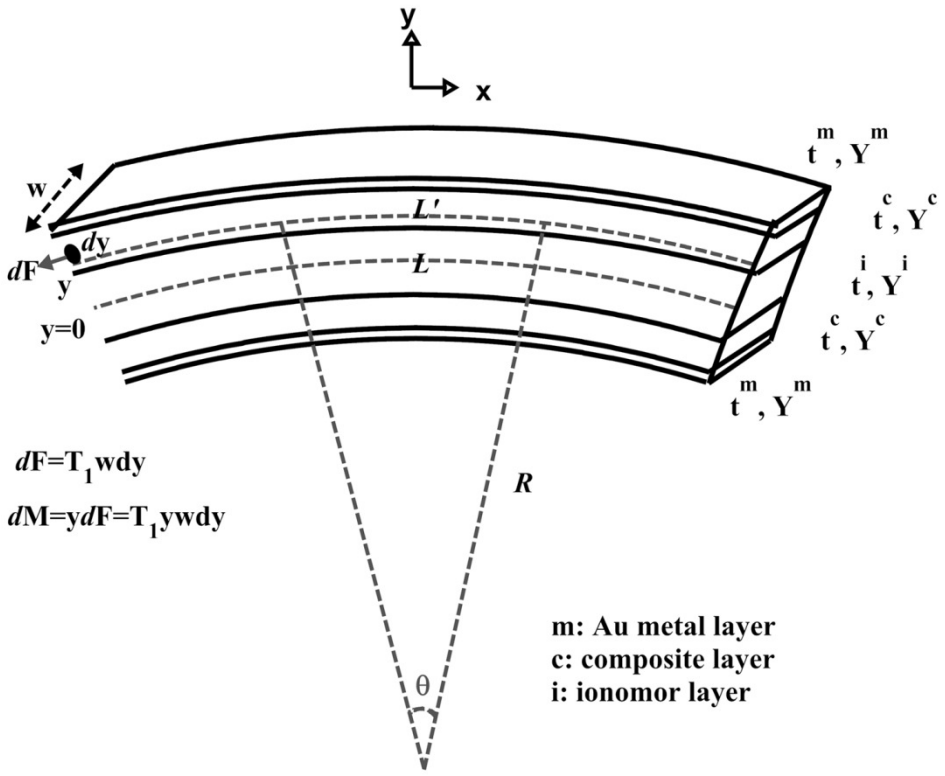

Figure 7.5 Schematic of the 5-layer bending actuator used for the derivation of the relation between the bending radius of curvature R and initial strain S_{10}^{c} in the CNC layers (eq. (3). Y is the Young's modulus, t is the layer thickness. Superscipts m, c, and i indicate Au metal layer, conductor composite, and ionomer layer, respectively.

Assuming the strain S_{10}^{c} in the two CNC layers in the bending actuator is the same in magnitude with opposite sign (one expanding and one contracting), $\int dF = 0$ is true for any S_{10}^{c} value. Therefore, integrating over the thickness for $\int dM = 0$, initial strain in the CNC layer S_{10}^{c} can be derived as

$$\frac{1}{R} = -\frac{Y^{c}(t^{i}t^{c} + t^{c^{2}})S_{10}^{c}}{Y^{m}(\frac{2t^{m^{3}}}{3} + 2t^{m}(t^{c} + \frac{t^{i}}{2})^{2} + t^{m^{2}}(2t^{c} + t^{i})) + Y^{c}(\frac{2t^{c^{3}}}{3} + t^{c}\frac{t^{i^{2}}}{2} + t^{c^{2}}t^{i}) + Y^{i}\frac{t^{i^{3}}}{12}} \quad (3)$$

The meaning of each parameter in eq. (3) is illustrated in Figure 7.5. From the radius of the curvature measured from several LbL1 and LbL2 bending actuators, the strain S_{10}^{c} is derived to be 6.8% under 4 volts step voltage. In comparison, the strain S_{10}^{c} in the RuO_2 CNC layer is 3.3% under the same voltage. In Figure 7.4(d), we present S_{10}^{c} of LbL CNCs as a function of applied voltage. The results here show that the LbL CNCs can generate much higher strain under low applied voltage compared with other electroactive polymers (EAPs) reported.[2,39]

7.3.2 Actuation Speed

The bimorph bending actuation speed was also characterized for these actuators. Presented in Figure 7.6 is the strain S_{10}^{c} (in reduced unit) as a function of time for the LbL1 and the IPMC with 3 μm RuO_2/Nafion nanocomposite as CNC. The data is fitted with $S = S_0 (1-\exp(-t/\tau))$, which yields a τ=0.18 seconds for the LbL1 and τ=1.03 seconds for the IPMC with 3 μm RuO_2/Nafion nanocomposite electrodes. The fast actuation speed of LbL1 is due to the thin CNC layer, which is 0.4 μm, compared with 3 μm for the RuO_2/Nafion composite electrodes.

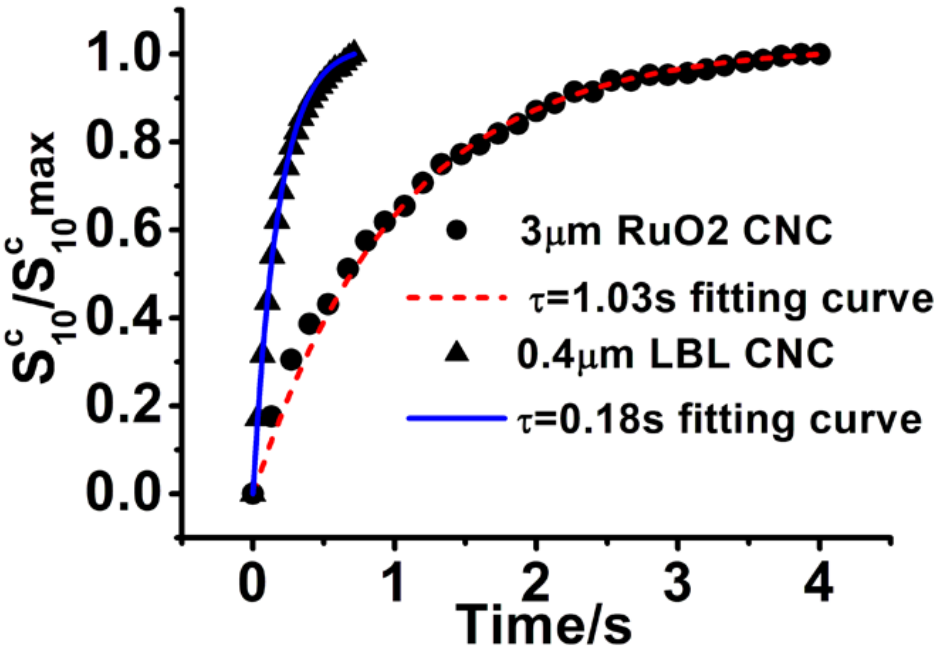

Figure 7.6 The actuator response as a function of time under a step voltage for the LbL1 (25.8 μm total thickness) and RuO_2/Nafion CNC based IPCNC (31 μm total thickness).

7.3.3. Limiting factors for the actuation speed

In a further detailed study into the actuation speed, we first studied the bending actuator performance without the composite electrode layer, i.e. neat Nafion film of 25 μm thickness with 40 wt% of ionic liquid EMI-Tf which functions as the solvent as well as provides mobile ions for the actuation. Figure 7.7(a) is a photographic image of the bending actuation of the neat Nafion actuator under a DC driving voltage of 4 Volts. The bending actuation is quite small due to the low electric double layer capacitance (EDL) from the flat electrodes of the neat ionomer films. Ionomeric polymer films such as Nafion with blocking electrodes form an electric double layer capacitor near the electrodes and have been modeled as an interface EDL capacitor C at the electrodes in series with a resistor R which accounts for the conduction in the bulk of the film, as illustrated in Figure 7.8(a).[40,41,42] The resistance is given by $R=L/(A\sigma)$ where L is the Nafion film thickness, A is the area, and σ (=qnμ, where q is the charge carried by the mobile ion) is the conductivity which is a product of mobile ion density n and mobility. To take into account the

leakage current at the electrode, a resistor (R_{in} >> R) is often added in parallel with the EDL capacitor C. The excess charges accumulated in the EDL capacitor C generate local strain near the electrodes and, for the case investigated here, create a bending actuator when the strains at the cathode and anode are not the same.

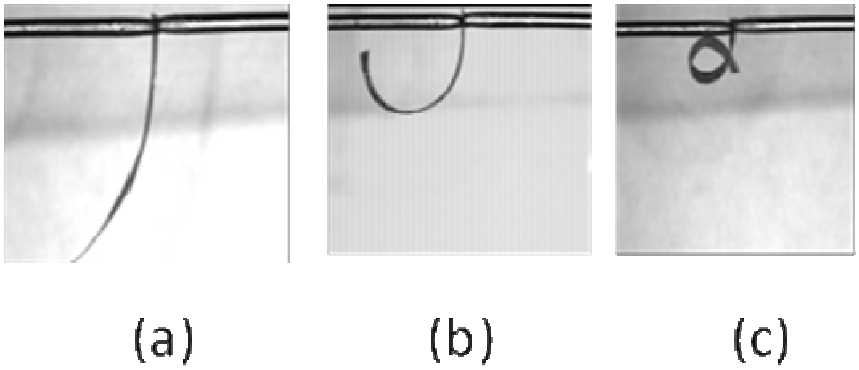

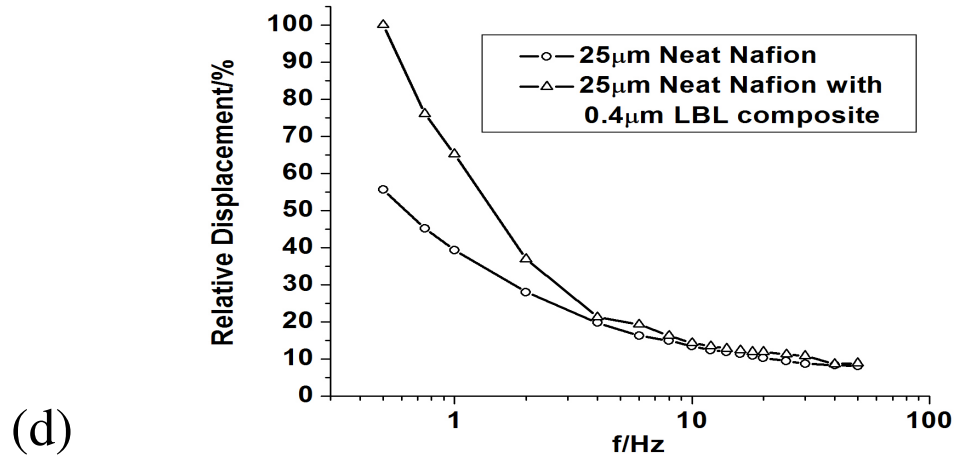

Figure 7.7 Photographic images of the bending actuation under 4 volts DC voltage for (a) The neat Nafion actuator; (b) LBL 1; (c) RuO_2 1; (d) The tip displacement (in reduced unit, i.e., all divided by the respective deflections at 0.5 Hz) as a function of frequency for the neat Nafion layer actuator (open circles) and LBL 1 actuator (open triangles).

With the composite electrodes (which raise the electrode capacitance and hence the total excess charges at the electrodes of the actuators), the bending actuation is markedly increased, as presented in Figures 7.7(b) and 7.7(c) in which all the actuators are activated under a DC voltage of 4 Volts. As presented in Figure 7.7(b), even with only 0.4 μm LBL composite on each side of Nafion (hence the total thickness of the actuator is 25.8 μm), a very large bending can be achieved for LBL 1, which

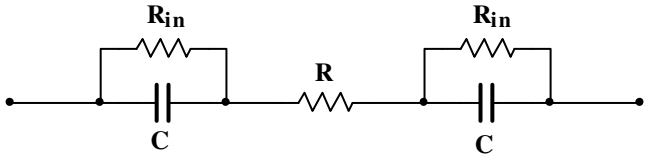

(a)

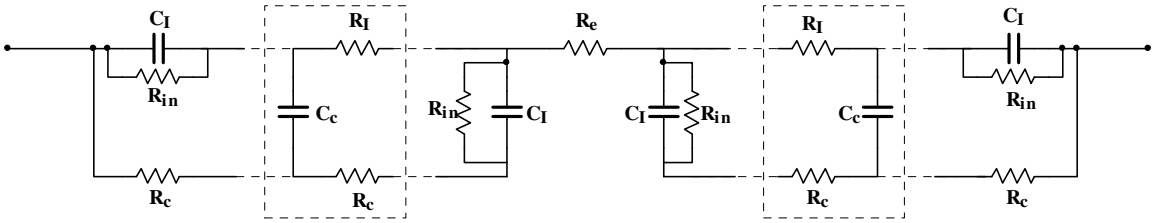

(b)

Figure 7.8 (a) Equivalent electric circuit of neat Nafion film under the blocking electrodes (forming EDL C); (b) An equivalent electric circuit for Composite electrode/Ionomer/Composite electrode system. The ion transport in the composite electrode layer is modeled as a transmission line. Number n of RC blocks in the composite electrode is determined by the operation frequency and analysis details. C_c is the EDL capacitor formed at the conductive network surface, R_I is the resistance for the ion transport in the ionomer matrix, and R_c is the resistance for the electronic conduction in the conductive network. C_I represents the EDL capacitors between the composite electrode and neat ionomer spacer (see (a)) and C_{II} represents the EDL capacitors between the external Au electrodes and the ionomers in the CNC.

illustrates the superior strain generation capability of the LBL composite films. As expected, the bending actuation increases with increased electrode capacitance as the composite layer thickness is increased. It is deduced from the bending actuation that the composite electrode

layer in the LBL 1 and LBL 2 actuators exhibit large strain (~ 6.8 %), which is much higher than that in the RuO_2 composite electrode layer in the RuO_2 1 and RuO_2 2 actuators (strain ~ 2.5%) as well as in other composite electrodes as reported earlier.[10]

Since the actuation is caused by the excess charges stored in the electrode capacitors, it is expected that the actuation speed will be reduced due to increased charging time as the electrode capacitance increases. Figure 7.7(d) presents the tip displacement under 0.4 volt AC signal of a LBL composite actuator (LBL 1) as a function of frequency and its comparison with that of a neat Nafion film (25 μm thick). Even though the LBL composite electrode thickness is only 0.4 μm, its tip displacement and, hence, the strain in the composite electrode layer, drops with frequency at a much faster rate compared with the neat Nafion film of 25 μm. This result suggests that the composite electrode layer is the major factor in limiting the actuator speed. In fact, as will be shown in the following, the ion transport in the composite layer is orders of magnitude slower than that in the neat ionomers.

For the neat Nafion layer (Fig. 7.7(a) and 7.8(a)), the actuator speed is limited by the capacitor charging time, which is determined by the RC time constant. For the equivalent electric circuit in Figure 7.7(a), the electric impedance is written as

$$Z = R_s + \frac{1}{j\omega C_s} \tag{4}$$

where $R_s = R + \frac{2R_{in}}{1+(\omega\tau_1)^2}$, $C_s = \frac{1+(\omega\tau_1)^2}{2(\omega\tau_1)^2}$, and $\tau_1 = R_{in}C$ and ω is the angular frequency.

Eq. (4) can quantitatively describe the change of R_s and C_s with frequency in Figures 7.9(a) and 7.9(b). At frequencies when $\omega R_{in}C \gg 1$, the electric impedance of Figure 7.8(a) is $Z = R + 1/(j\omega C)$ and it is this RC time constant that determines the charging time of EDL capacitor. For neat ionomers such as the Nafion films, it is well known that the EDL capacitor does not change while R will increase with film thickness.[33, 34, 35] Indeed, Figures 7.9(a) and 7.9(b) show that the capacitance of the neat Nafion films of 25 μm (C ~4.9×10^{-8} F) is nearly the same as that of 50

μm thick (C ~ 4.5×10^{-8} F), while R increases from 52 Ω for the 25 μm thick film to 97.5 Ω for the 50 μm thick film. The small variations in the R and C values are caused by the experimental uncertainties (± 5%). All these values are taken at 10 kHz where both C_s and R_s become nearly independent of frequency and equal to C and R, respectively, because $\omega\tau_1 >> 1$ at that frequency range. Here, a neat Nafion film of 50 μm was used for comparison purpose. From the resistance value R, the conductivity of the Nafion film with IL at 10 kHz can be deduced as $\sigma = 6 \times 10^{-4}$ Scm^{-1}. The linear increase of the RC time constant with the Nafion film thickness indicates that the actuation speed (high frequency response) of the neat Nafion film is inversely proportional to the film thickness.

The increased R in the 50 μm thick neat Nafion film reduces the actuator speed as also reflected by the phase angle plot of Figure 7.9(c), where the phase angle is the phase difference between the applied voltage and current, which is $\tan\phi = \frac{1}{\omega R_s C_s}$. A $\phi = 90°$ corresponds to a pure capacitor and $\phi = 0°$ to a pure resistor (which would indicate the electrical impedance of the resistor is much larger than that of the capacitor which is $1/(\omega C)$. Here again, 10 kHz as the reference frequency was taken which is approximately the intersection of the phase angle plot (see Figure 7.9(c)). At this frequency, $\phi = 81^o$ for 25 μm Nafion film and ϕ is reduced to 75^o for 50 μm thick Nafion film.

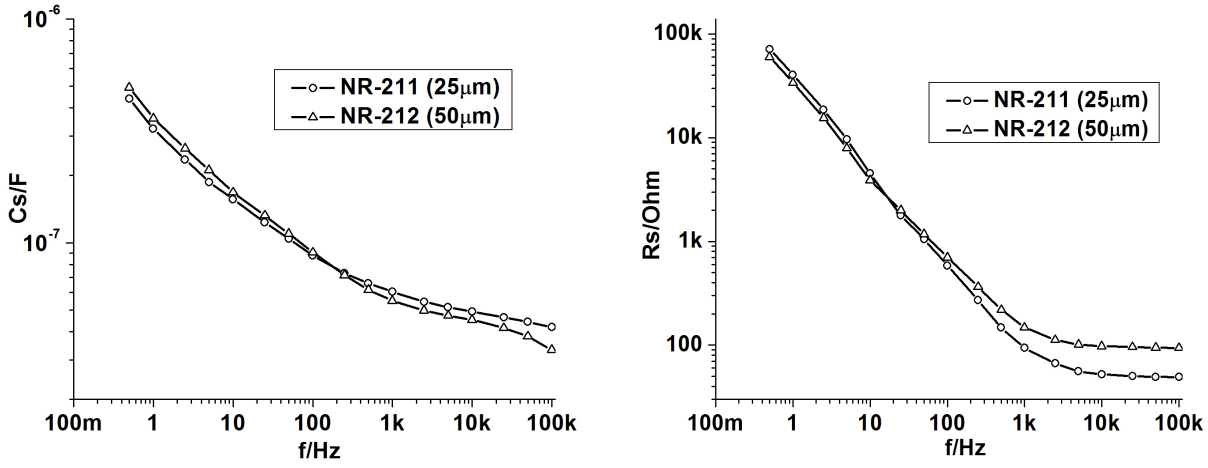

(a) (b)

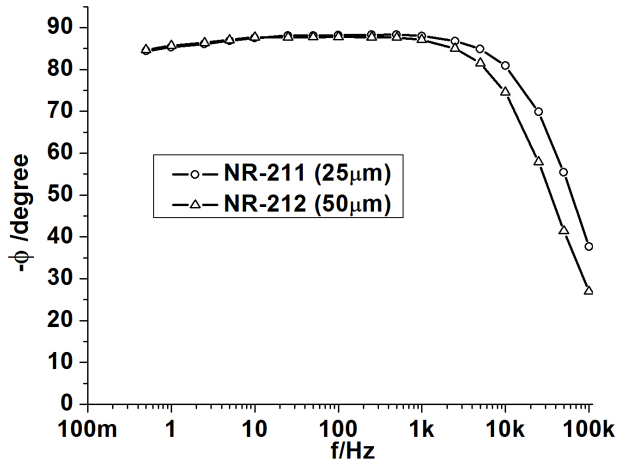

(c)

Figure 7.9 Electric impedance as a function of frequency for the neat Nafion films (circle for 25 μm thick and triangle for 50 μm thick Nafion films): (a) the capacitance C_s; (b) the resistance R_s, and (c) the phase angle a between the current and voltage. At high frequencies, R_s ~ R and C_s ~ C (see Figure 7.8(a)).

Figure 7.10 presents the electrical impedance for the IPCNC actuators of LBL 1 and LBL 2 and Figure 7.11 for RuO_2 1 and RuO_2 2. The CNC electrode layers increase the capacitance of these actuators. Besides the increase of capacitance with the composite electrode layer thickness d_e, the resistance of these actuators is increased at a much faster rate compared with the neat Nafion films. Consequently, the phase angle ϕ of the actuator films becomes much closer to the resistive side, indicating that in addition to the reduction of the actuation speed, the actuator loss is also increased markedly.

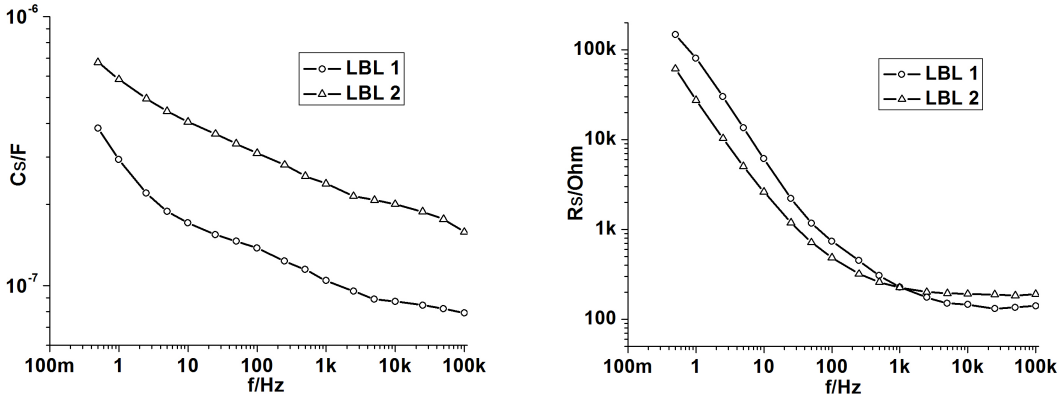

(a) (b)

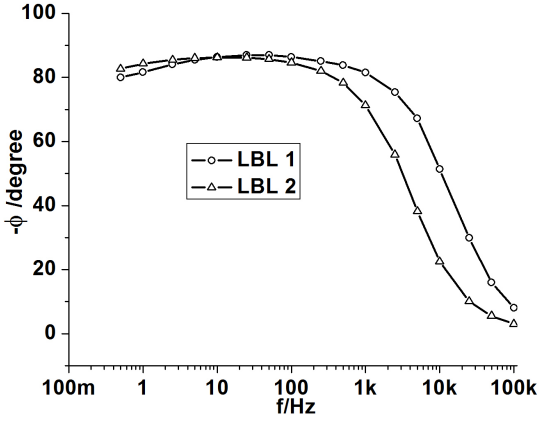

(c)

Figure 7.10 Electric impedance as a function of frequency for LBL composite actuators: (a) the capacitance C_s, (b) the resistance R_s, and (c) the phase angle α. For the composite electrodes, both C_s and R_s are functions of R_I, R_c, C_c, C_I, C_{II}, and R (see Figure 7.8(b)).

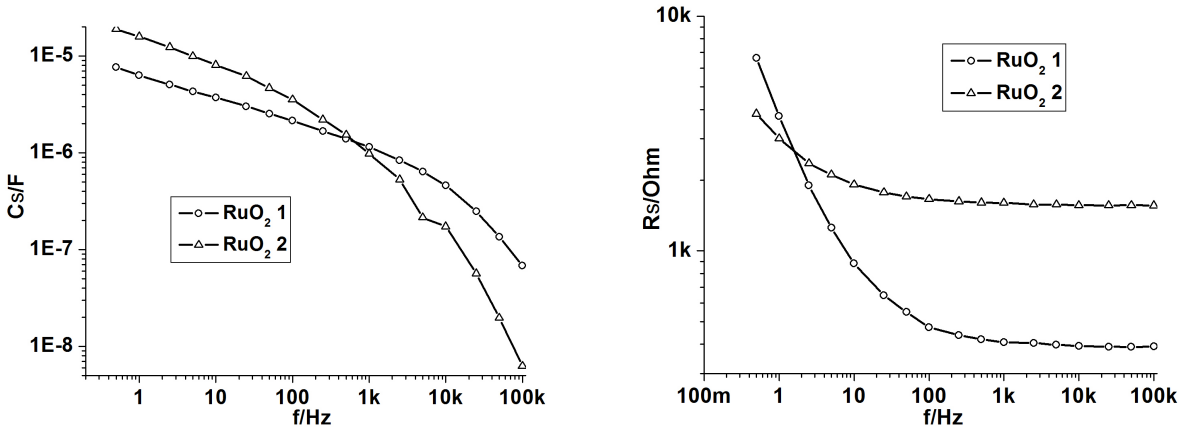

(a) (b)

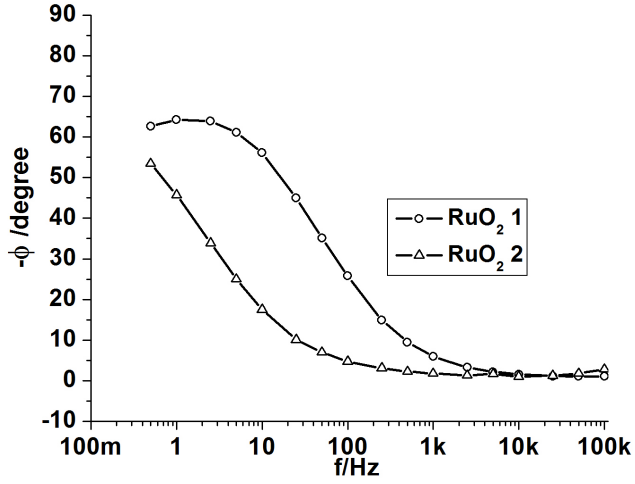

(c)

Figure 7.11 Electric impedance vs. frequency of RuO_2/Nafion composite actuators: (a) the capacitance C_s, (b) the resistance R_s, and (c) the phase angle α. For the composite electrodes, both C_s and R_s are functions of R_I, R_c, C_c, C_I, C_{II}, and R (see Figure 7.8(b)).

For comparison, the capacitance and resistance values of the LBL 1 and LBL 2 actuators at 10 kHz, the same frequency as that considered for the neat Nafion films: R = 146 Ω and 191 Ω and $C=8.7\times10^{-8}$ F and 2.0×10^{-7} F for LBL 1 and LBL 2 actuators, respectively was taken. Even though both actuator films (25.8 μm and 26.6 μm, respectively) have very similar thickness to

that of 25 μm neat Nafion film, the resistance value is increased markedly and is much higher than that of the 50 μm thick Nafion films. In general, the composite electrode layer, which is very much similar to the porous electrodes used in supercapacitors, should be modeled as a transmission line as illustrated in Figure 7.8(b).[43,44,45] The resistance obtained at 10 kHz is in fact a lower bound of the total resistance in the RC networks. The high resistance values indicate that the transport of ions in the composite electrode layer is very different from and is much slower than that in the neat Nafion film. For comparison, we subtracted of the neat Nafion film resistance value (R=52 Ω) from the total resistance for LBL 1 and LBL 2 and took the difference as that of the composite electrode layer resistance R_e =92 Ω and 142 Ω for the two actuators. The conductivity deduced from $R_e=2d_e/(\sigma A)$ was $\sigma=1.1x10^{-5}$ Scm^{-1} and $\sigma= 1.4x10^{-5}$ Scm^{-1}, respectively. Since the R_e used here is the lower bound of the total resistance in the composite layer, these conductivity values are the upper bound of the conductivity of ions in the composite electrodes, which in fact contain both the electronic conductivity from the conductive network and ionic conductivity from the ILs in the ionomers. The results indicate that the "true" ion conductivity in the composite electrode layer is smaller than these values, which suggests that the ion transport in these composite electrodes is at least one order of magnitude slower than that in the neat Nafion ionomers.

As the composite electrode layer thickness d_e increases to 3 μm and 10 μm for the RuO_2 1 and RuO_2 2 actuators, both the capacitance and resistance increase, resulting in a much slower actuator response. At 10 kHz, the electric impedance of both actuators is dominated by the resistive component as seen in Figure 7.11. The high frequency resistance value of the two composites, which are very weakly frequency dependent, is increased to 450 Ω and 1660 Ω for RuO_2 1 and RuO_2 2, respectively, even though the total composite layer thickness in the actuator $2d_e$ is still smaller than 25 μm. The large increase in R is consistent with the data in Figure 7.10 for the LBL CNCs and the conclusion drawn in the proceeding paragraph that the ion transport in the composite electrode layer is much slower than that in the neat Nafion films. The large increase in R also results in a large increase in the electric loss, as revealed in Figure 7.12, for the RuO_2 1 and RuO_2 2 actuators. This partially explains why IPCNC actuators have generally shown very low efficiency since the composite electrode layer thickness used is usually larger than 10 μm.[4,46,47,48,49,50]

Furthermore, the equivalent circuit model in Figure 7.8 indicates that both the capacitance and resistance of the composite electrode layer increase with the composite electrode layer thickness d_e. If the actuator speed is mainly determined by the charging time of the composite electrode layer, the result here suggests that the actuator speed should be inversely proportional to the square of d_e (~ $1/d_e^2$). Indeed, for the LBL 1 actuator, the bending actuation speed is ~ 0.1 seconds to reach the state in Figure 7.7(b) due to the thinness of the composite electrode layer (d_e=0.4 μm). In contrast, the bending actuation speed is ~ 10 seconds for RuO_2 1 (d_e=3 μm), which is about 100 times slower than that of LBL 1. The result indicates that the actuator speed is determined by the ion transport in the CNC layers and will decrease with the CNC layer thickness d_e at a rate ~ $1/d_e^n$ with $n \geq 2$.

The change of the resistance and capacitance of the IPCNC actuator films with the film thickness is also reflected by the phase angle plots of Figures 7.9(c), 7.10(c), and 7.11(c), where the phase angle is the phase difference between the applied voltage and current, which is $\tan\phi = \frac{1}{\omega R_s C_s}$. A ϕ=90° corresponds to a pure capacitor and ϕ = 0° to a pure resistor (which would indicate the electrical impedance of the resistor is much larger than that of the capacitor which is $1/(\omega C)$).

The frequency position f_1 of these actuator films at ϕ=45°, at which the real (resistive) and imaginary (capacitive) parts of the electric impedance become equal, is taken for comparison. For the neat Nafion films, the increase of the thickness from 25 μm to 50 μm causes a reduction of f_1 from 79.3 kHz to 43.7 kHz, approximately a reduction of half in frequency. On the other hand, for LBL 1 which is only 25.8 μm thick (0.8 μm total CNC layer thickness), f_1 becomes 13.5 kHz. Further increasing total CNC layer thickness to 1.6 μm reduces f_1 of LBL 2 actuator films to 3.64 kHz, which is consistent with ~ $1/d_e^2$ dependence of the CNC electrode layer capacitor charging time on d_e. For RuO_2 1 and RuO_2 2, which have total thickness of CNC electrode layers of 6 μm and 20 μm, f_1 is reduced to 24.5 Hz and 1 Hz, respectively. These results further confirm that it is the slow ion transport process in the CNC electrode layer that

limits the actuator speed of the IPCNCs and the reduction in the actuator speed is at a rate of $\sim 1/d_e^n$ with $n \geq 2$.

The slow ion transport process in the CNC electrode layer also results in a large electric loss and sets limit on the IPCNC actuator electromechanical efficiency, which measures percentage energy conversion from the total input electrical energy to mechanical energy. Figure 7.12 summarizes the pure electric losses (D = tan (90-ϕ)) of these actuators and their comparison with the two neat Nafion films. The total input electric energy into the actuator films includes the energy stored in the capacitors and resistive loss. It is the former that will be converted to mechanical energy for actuation and this conversion process has an efficiency η_{ME} which is below 100%. This is very similar to that in piezoelectric materials in which only a fraction of the electric energy stored in the capacitor is converted into mechanical energy, as measured by the electromechanical conversion efficiency of piezoelectric materials.[51] If there is no other loss, the total electromechanical conversion efficiency η_T which is the ratio of the mechanical energy generated to the total input electric energy is

$$\eta_T = \eta_e \times \eta_{ME} \tag{5}$$

where η_e is the ratio of the electric energy stored in the capacitor component to the total input electric energy (= 1/(1+D)) and plots η_e as a function of frequency for various actuator films. The results indicate that a thicker CNC electrode layer will lead to lower efficiency.

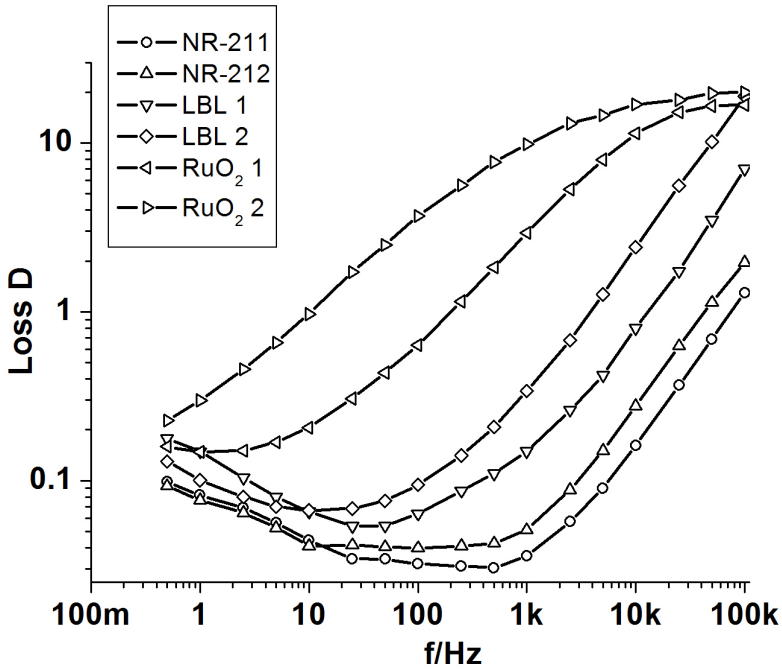

Figure 7.12 The electric loss for all the actuators investigated as a function of frequency. It can be seen that for actuators with the composite electrode layer thickness at 10 μm thick, the electric loss becomes very high, which limits the speed and efficiency of the IPCNC actuators.

These results indicate that the major limiting factor in the IPCNC actuator speed is the low transport speed of the mobile ions in composite electrodes. Furthermore, the slow ion transport in the composite electrode results in a high resistive loss when d_e becomes large (> a few microns) which also results in a low actuator efficiency. The increase of both the capacitance and resistance of the CNC electrodes with d_e indicates that the actuation speed is inversely proportional to the square of the composite layer thickness d_e (~ $1/d_e^2$). Hence by reducing the composite layer thickness, the actuator speed can be improved markedly. Indeed, for the LBL 1 actuator, the bending actuation speed is ~ 0.1 seconds to reach the state in Figure 7.7(b) due to the thinness of the composite electrode layer (d_e=0.4 μm). In contrast, the bending actuation speed is ~ 10 seconds for RuO_2 1 (d_e=3 μm).

7.4. Summary

In conclusion, the results presented indicate the potential of LbL self-assembled CNCs as a class of EAPs for large actuations under low applied voltage. It was also studied that a thin composite electrode layer, however, will generate lower total force output of the actuator. Hence, the actuator design should balance the trade-off between the speed and total actuation energy output. These results also demonstrate the potential for further optimizing LbL CNCs for IPCNCs which can generate even higher strain with improved ion transport speed.

References

[1] R. H. Baughman, C. Cui, *Science* **1999,** *284,* 1340.

[2] Y. Bar-Cohen and Q. M. Zhang, *MRS Bull.* **2008***, 33,* 173.

[3] E. W. H. Jager, E. Smela, and O. Inganas, *Science* **2000,** *290,* 5496.

[4] M. Shahinpoor, Y. Bar-Cohen, J. Simpson, and J. Smith, Int. *J. Smart Mater. Struct*., 1998, *7,* R15.

[5] K. Oguro, Y. Kawami, and H. Takenaka, *J. Micromachine Soc*., **1992,** *5,* 27.

[6] K. Onishi, S. Sewa, K. Asaka, N. Fujiwara, K. Oguro, *Electrochim. Acta,* **2000,** *46,* 737.

[7] M. Shahinpoor, *J. Intell. Mater. Syst. Struct*., **1995,** *6,* 3.

[8] J.D.W. Madden, N. A. Vandesteeg, P.A. Aquetil, P.G.A. Madden, A. Takshi, R.Z. Pytel, I. W. Hunter, *IEEE Oceanic Eng*. **2004**, 29, 706.

[9] T. Mirfakhari, J.D. W. Madden, R.H. Baughman, *Mater. Today* **2007**, 10, 30.

[10] B. J. Akle, M. D. Bennett, and D. J. Leo, *Sens. Actuators A: Phys* **2006,** *126,* 173.

[11] M. D. Bennett and D. J. Leo, *Sens. Actuators A: Phys* **2004,** *115,* 79.

[12] I. S. Park, K. Jung, D. Kim. S. M. Kim, and K. J. Kim, *MRS Bull*., **2008,** *33,* 3.

[13] S. Nemat-Nasser and Y. Wu, *J. Appl. Phys*., **2003,** *93,* 5255.

[14] B. J. Akle, D. Leo, M. Hickner, and J. McGrath, *J. Mater. Sci.*, **2005,** *40,* 3715.

[15] B. J. Akle and D. J. Leo, *J. Intell. Mater. Syst. Struct*., **2008***, 19,* 8.

[16] D. Kim, K. Kim, Y. Tak, D. Pugal, II-Seok Park, *Appl. Phys. Lett*., **2007,** *90,* 184104.

[17] Jang-Woo Lee, Young-Tai Yoo, *Sens. Actuators B* **2009,** *137(2)*, 539.

[18] S. N. Nasser*, J. Aply. Phys*. **2002**, 92, 2899.

[19] M. Bennett, D. Leo*, Sens. Actuators A: Phys* **2004**, 115, 79.

[20] B.J. Akle, D. J. Leo, M. A. Hickner, J. E. McGrath, *J. Mater. Sci.* **2005**, *4)*, 3715.

[21] B. J. Akle, M. D. Bennett, D. J. Leo, K. B. Wiles, J. E. McGrath, *J. Mater. Sci.* **2007**, *42*, 7031.

[22] M. D. Bennett, D. J. Leo, G. L. Wilkes, F. L. Beyer, T. W. Pechar, *Polymer* **2006**, *47*, 6782.

[23] J. Lee, Y. Yoo, *Sens. Actuators B* **2009,** *137(2)*, 539.

[24] F. Vidal, C. Plesse, D. Teyssie, C. Chevrot, *Synth. Metal.* **2004,** 142, 287.

[25] T. Fukushima, K. Asaka, A. Kosaka, T. Aida, *Angew. Chem. Int. Ed.* **2005**, *44*, 2410.

[26] K. Mukai, K. Asaka, K. Kiyohara, T. Sugino, I. Takeuchi, T. Fukushima, T. Aida, *Electrochim. Acta* **2008**, *53*, 5555.

[27] K. Mukai, K. Asaka, T. Sugino, K. Kiyohara, I. Takeuchi, N. Terasawa, D. N. Futaba, K. Hata, T. Fukushima, T. Aida, *Adv. Mater.* **2009**, *21*, 1582.

[28] S. Imaizumi, Y. Kato, H. Kokubo, M. Watanabe, Abstract - *214th Electrochem. Soc.Meeting, Honolulu*, HI, General Student Poster Session, **2008**, A1-117.

[29] M.A B. H. Susan, T. Kaneko, A. Noda, M. Watanabe, *JACS* **2005**, *127(13)*, 4976.

[30] S. Saito, Y. Katoh, H. Kokubo, M. Watanabe, S. Maruo, *J. Micromech. Microeng.* **2009**, *19*, 035005/1.

[31] A. J. Duncan, D. J. Leo, T. E. Long, *Macromolecules* **2008**, 41, 7765.

[32] M. A. Hickner, H. Ghassemi, Y. S. Kim, B. R. Einsla, J. E. Mcgrath. *Chem. Rev*. **2004**, 104, 4587.

[33] K. D. J. Kreuer, *J. Membr. Sci*. **2001**, 185, 29.

[34] G. Decher, *Science*, **1997,** *227,* 1232.

[35] P. T. Hammond, *Adv. Mater.*, **2004,** *16,* 15.

[36] V. Jain, H. M. Yochum, R. Montazami, and J. R. Heflin, *Appl. Phys. Lett*., **2008,** *92,* 033304.

[37] J.M. Herbert, *Ferroelectric Transducers and Sensors*. (Gordon and Breach, New York, 1982).

[38] Q. M. Wang and L. E. Cross, *Ferroelectr*., **1998,** *215,* 187.

[39] J. D. W. Madden, et al., *IEEE J. Oceanic Eng*., **2004,** *29,* 706.

[40] R. Coelho, *J. Non-Cryst. Solids* **1991,** *131,* 1136.

[41] R. J. Klein, S. H. Zhang, S. Dou, B. H. Jones, R. H. Colby, J. Runt, J. *Chem. Phys.* **2006**, *124,* 144903.

[42] J. R. MacDonald, *Phys. Rev.* **1953,** *92,* 4.

[43] J. Bisquert, A. Compte, *J. Electroanal. Chem.* **2001,** *499,* 112.

[44] B. E. Conway, *Electrochemical Supercapacitors,* Kluwer Academic/Plenum Publishers, **1999.**

[45] R. de Levie, *Electrochim. Acta* **1963,** *8,* 751.

[46] M. Shahinpoor, K. J. Kim, *Sens. Actuators A -Physical* **2002,** *96,* 125.

[47] K. J. Kim, M. Shahinpoor, *Smart Mater. Struct.* **2003,** *12,* 65.

[48] M. D. Bennett, D. J. Leo, *Smart Mater. Struct.* **2003,** *12,* 424.

[49] L. Cao, S. Mantell, D. Polla, *Sens. Actuators aAPhysical,* **2001,** *94,* 117.

[50] B. R. Donald, C. G. Levey, C. D. McGray, I. Paprotny, D. Rus, *J. Microelectromech. Syst.* **2006,** *15,* 1.

[51] IEEE Standard in Piezoelectricity, ANSI/IEEE Std 176-1987.

Chapter 8

Conclusions and Suggestions for Future Work

8.1 Conclusions

An in-depth study of the effect on the switching speed of EC electrochromic devices fabricated with layer-by-layer films of a wide variety of materials has been conducted and presented in this thesis. The motivation behind developing fast switching-speed EC devices is to employ them in flat panel displays as faster-responding and wider viewing angle alternatives to LCDs. Polyviologen, PEDOT (poly(3,4-ethylenedioxythiophene)), water-soluble sulfonated 3,4-propylenedioxythiophene (ProDOT-Sultone), and ruthenium purple were deposited by the LbL technique and their EC properties were measured along with several other key characterization methods. The results for PEDOT show that EC devices fabricated by LbL assembly with a switching speed of less than 30 ms for video displays are possible by carefully adjusting the film thickness, device area, and type of material. Contrast measurements through spectroelectrochemistry and Filmmetrics optical transmission (solid-state devices), amount of charge and the location of the redox peak measurement through cyclic voltammetry, and switching-speed measurements through potentiostat, laser and oscilloscope set-up were done to measure various EC properties to ensure the optimum performance of different materials. Successful synthesis and the complete characterization of two new electrochromic materials (polyviologen and ProDOT-Sultone) were carried out and these materials were synthesized in Prof. Gibson's group (Chemistry, Virginia Tech) and Prof. Anil Kumar's group (Chemistry, IIT-Mumbai), respectively. Furthermore, synthesis and characterization of ruthenium purple nanocolloids and the nanocomposites formed with it were also reported. The synthesis of these new materials has aided in creating an ever-expanding library of EC materials and also shows that the LbL technique is very much applicable and successful with materials beyond those commercially available.

This thesis has also described the application of LbL in the field of electromechanical bending actuators. A new class of conductive composite network (CNC) electrodes based on LbL self-

assembled conductive gold nanoparticle composites was fabricated and the strain and actuation speed of CNCs of different numbers of bilayers on an ionomer substrate (i.e. nafion) were calculated and compared with the already well-studied CNC material ruthenium oxide (RuO_2). This work was done in close collaboration with Prof. Qiming Zhang's group (Electrical Engineering, Penn State) who measured the strain value and actuation speed.

The conclusions of this thesis are presented chapter-wise, to provide an insight to the different applications and advantages of various materials for the EC and actuation properties.

Chapter 3 addresses the synthesis and characterization of a polyviologen (PV) and further characterization and surface properties of LbL films fabricated through PV and PAMPS. The polyviologen (PV) that was synthesized by polymerization of N,N'-bis(-δ aminopropyl)-4,4'-bipyridinium bromide hydrobromide (APD) and isophthaloyl chloride (ISP) is highly soluble in water as well as in organic solvents. Polymer identification was done through ^{1}H and ^{13}C NMR spectra and Fourier transform infrared – Attenuated Total Reflectance (ATR) spectroscopy. The synthesis and characterization of this polyviologen was performed by Dr. Hong Wang in Prof. Harry Gibson's group. The LbL films of PV and PAMPS were then characterized for film thickness and determined to be in the range of 190-210 nm for a 40-bilayer film. The same film on an ITO electrode shows a contrast of 61% at 515 nm as the color changes from a highly transmissive colorless state to a dark violet to a transparent yellow. The high coloration efficiency (57 cm^2/C) at low switching voltage (-0.2 V) and the ability to control the thickness of the bulk layer makes this approach unique. Unsymmetrical solid-state EC devices were fabricated with an oxidative EC material (Polyaniline (PANI)), because polyviologen is not a conductive material and doesn't support the fabrication of symmetrical solid-state EC device as explained in Section 2.4.1 and 2.4.2. Integrated PV-PANI dual EC devices produce more plentiful switching colors (blue, dark violet and yellow) than the simple PV device in electrolyte solution. The switching times for coloration and decoloration were 100 ms and 250 ms, respectively, at low switching voltages (- 2.0 to + 2.0 V) under ambient conditions. The use of the PV as an electrochromic material provides a low reduction potential, good film forming ability, and color tuning (colorless to dark violet to transparent yellow). Its solubility in water provides the advantage of easy processability using the LbL film assembly method with PAMPS

and the flexibility to incorporate other electrochromic materials that increase the overall contrast or develop multi-hue electrochromic devices.

In **Chapter 4**, the fast switching of a LbL assembled solid-state polymer electrochromic device compatible with flat-panel display rates is demonstrated. Devices consisting of two 80-bilayer PAH/PEDOT films display a maximum contrast of 35% at 580 nm. Similar devices with an active area of 0.6 cm^2 made from two 40-bilayer (400 nm thick) films show coloration and decoloration times of 31 ms and 6 ms, respectively, with a linear scaling of the switching speed with the active area of the device. After careful study of the solid-state devices of different numbers of bilayers, it was found that the fast switching is obtained through the combination of a number of factors: fabrication of thin, homogeneous films by self-assembly that have a large diffusion coefficient and short distance required for ionic motion, use of the symmetric quasi-solid state geometry with a thin layer of electrolyte gel, and recognition of the dependence of the response time on device area. These results suggest that LbL electrochromic devices are potential candidates for next-generation flat-panel displays. This study is one of the first fundamental studies of its kind demonstrating that the switching speed varies with the size of the device. This is because the solid-state EC device is considered primarily as an 'RC' circuit and the contribution of the capacitance value depends on the area of the device, while the area contribution for the resistance value is that of the cross section area which stays constant when the device size varies for the same number of bilayers.

Chapter 5 addresses the successful synthesis, for the first time, of a new regiosymmetric water-soluble sulfonated monomer based on 3,4-propylenedioxythiophene (ProDOT-Sultone), via the *O*-alkylation of the corresponding unreactive *β,β*-disubstituted hydroxyl group with propane sultone in presence of catalytic amount of diazabicyclooctane 1,4-diazabicyclo[2.2.2]octane (DABCO). The work on Prodot and its derivatives in the field of synthesis and fabrication of EC devices through electropolymerization, spin casting, solution casting, etc. has been extensively studied by Prof. John Reynold's group in the Department of Chemistry, University of Florida. Some very interesting analysis of EC devices are presented in several publications that came out of his group in the last decade on this topic. Still, a successful synthesis of the water-soluble Prodot derivative is a void that his group was unable to fill. Water solubility of a conducting

polymer opens up a new avenue of research and certainly makes the compound a fit candidate for LbL assembly, in which combination of other compounds can be brought in as well. The synthesis and characterization of this polymer was conducted in Prof. Kumar's lab in the Chemistry Department at IIT-Mumbai, while the LbL film fabrication and EC property characterization was done by the author of this thesis. The synthesis has shown that this methodology is independent of the alkylating agent as well as the solvent used. Use of propane sultone as alkylating agent resulted in the synthesis of regiosymmetric water-soluble sulfonated monomer and polymer based on 3, 4-propylenedioxythiophene, which is important for the high conductivity of this polymer. Four-point probe conductivity of the LbL and *in situ* conductivity of solution cast films was found to be in the range of 10^{-4} S/cm and 10^{-3} S/cm, respectively.

An interesting observation was made that an improvement in electrochemical properties due to the regiosymmetric nature of the polymer based on PProDOT-Sultone as compared to that of regiorandom PEDOT-Sultone was found. The presence of a substituent with a sulfonic acid alkyl group on the ProDOT ring gives a regioregular polymer which improves the film morphology without affecting the electronic properties. For the 40 and 80-bilayer solid-state electrochromic devices, the electrochemical contrast was observed to be 31% and 40% at 570 nm with fast solid-state switching times of 100 and 220 ms, respectively, indicating faster movement of the ions in and out of the films. The work so far reported by Prof. Reynold's group on Prodot and its derivatives did not show such a fast switching speed, which could be because of deposition of these materials by conventional techniques and also of not giving significant attention towards fabricating symmetrical solid-state devices. The fast switching speed of the solid-state devices, fabricated by LbL deposition, makes PProDOT-Sultone a potential candidate for flat-panel displays if it can be improved to less than 40 ms. The coloration efficiency was found to be as high as 250 cm^2/C for 80-bilayer devices, and independent of device thickness indicating the full accessibility of all the ionic sites even in thicker films. Because of the flexibility of the LbL assembly method, it should be noted that it has the potential to be used for the fabrication of multi-hue electrochromic devices by combining PProDOT-Sultone with cationic electrochromic materials (such as polyviologen, polyaniline etc).

Chapter 6 addressed synthesis of Ruthenium Purple (RuP) nanocolloids with spherical shape and the fabrication of a thin film polymer/ RuP nanocomposite by the LbL technique was presented. Equal concentrations of potassium rutheniumcyanide ($K_4[Ru(CN)_6]$), ferric chloride ($FeCl_3$), and potassium chloride (KCl) were mixed for the synthesis. A systematic study was done, and it was found that the presence of the excess of potassium ions through KCl is crucial for the solubility of RuP. Inorganic nanocolloids have a tendency of settling when not agitated, but the presence of excess potassium ions made the RuP dispersion stable for months. Complete particle characterization of these RuP nanocolloids through powder XRD for crystal lattice structure, DLS and TEM for size, and zeta potential for the charge of the surface groups have been done. Particle size in the range of 20-30 nm was confirmed by both TEM and DLS measurements. The zeta potential value of -30.0 mV carried by RuP nanocolloids is sufficient to fabricate films by LbL assembly for this typical size. LbL films deposited of LPEI/RuP show a linear increase in the absorbance of the film with an increase with the number of bilayers indicating that thick nanocomposite films can be easily fabricated without sacrificing the individual contributions of the constituents. The 40-bilayer nanocomposite films show a very high contrast of around 84% with a high coloration efficiency of 205 cm^2/C. Irrespective of the switching speed that RuP LbL films shows, this high value of contrast for RuP suggests that these films can be used for electronic paper displays, digital billboards, etc. where fast switching is not as important as the contrast along with low power consumption. A small amount of voltage and current is required to turn on displays fabricated with RuP materials and a reverse voltage to switch it off whenever required.

Successful synthesis of RuP nanocolloids, fabrication of LbL films of it, and the change in color from purple-red (magenta) to light blue during switching in solid-state devices fills a gap in the cyan-magenta-yellow (CMY) color scheme. Two separate 40-bilayer films of PANI/ PAMPS and LPEI / RuP were taken as complementary anodically and cathodically coloring materials, respectively and an unsymmetrical solid-state EC device was fabricated that showed coloration and decoloration times in the range of 600 ms and 300 ms, respectively.

A new application of LbL in the field of electromechanical bending actuators from ionic polymer metal composites (IPMCs) was addressed in **Chapter 7**. Ionic membranes (nafion) were

deposited with LbL films of polymer/gold nanoparticles to fabricate porous conductive network composite (CNC) electrodes. This is the first time a nanoscale thickness controlled CNC for the application of bending actuators has been reported. The electrolyte solvent used for the actuation study is a commercially available ionic liquid, EMI-Tf because there are several advantages of using an ionic liquid that were discussed in Section 7.1. The thickness of the CNC varies in size from 100-800 nm on both sides of the membrane for bilayers ranging from 20 to 200 bilayers. DLS and zeta potential measurements of commercially available Au NPs were performed to ensure the size and surface group charges are favorable for LbL deposition. The earlier work reported in this field for CNCs have typical thickness of about 3-5 μm and that leads to actuators that show low strain values at higher voltage. An electromechanical actuator fabricated with this CNC of 100-bilayer PAH/Au NPs film exhibits high strain ~ 6.8% under 4 volts, whereas the RuO_2/Nafion CNCs exhibit strain ~ 3.3%. CNCs and 200 bilayers of PAH/AuNPs composite showed strain value of ~5.8% at 4 V. The strain value and actuation speed measurements were performed by Dr. Zhang's group at Penn State. An important thing to note here is that the strain values presented for LbL fabricated CNCs and RuO_2/nafion composite is an intrinsic value and the reason for using that instead of an actual overall strain for the composite is because the thickness of the ionic membrane used for these calculations is similar of every sample and also that it is beneficial to study the individual strain contribution of these CNCs to study the contribution effect of different materials on them. Till now, the major issue in using IPMCs is the presence of a low viscosity electrolyte and the actuation speed. The problem with the electrolyte has been fixed by replacing it with a viscous ionic liquid that also provides higher ionic conductivity and the actuation speed of a 0.18 seconds for a 26 μm thick IPMC with 0.4 μm (on one side of nafion) thick LbL CNCs to a step voltage of 4 volts has shown significant improvement in that as well.

8.2 Future Work

This thesis has presented a significant amount of work on developing solid-state EC devices. Several different commercially available and specially synthesized materials have been used after carefully reviewing the recent literature and their advantages and disadvantages. Still, it is only a first step towards using EC devices for flat-panel displays. This work has created an

impetus and interest in the research community to pursue this work with new ideas and applications. There are a few suggestions that should be made to improve this work and also to go into further detail with the individual EC systems presented here. First of all, the system with PEDOT needs to be very carefully studied in terms of the effect of the number of bilayers on switching speed, contrast, and lifecycle. A detailed study of lifecycle is one of the important aspects that was not very carefully studied in this thesis, since the research focus was more on developing new fast-switching devices with good contrast. But it is very important that these EC devices switch for at least a million cycles to be used for commercial application of displays. PEDOT is a very promising material and has shown significant development in other areas of optoelectronics, but to take advantage of its high conductivity it is also important to develop a new electrolyte gel for faster movement of ions in and out of the films. This will bring a significant jump in the already-reported values of switching speed for PEDOT and other materials. Till now, the electrolyte gel based system, which is either polymer-based (H^+ ions from PAMPS) or contains inorganic salt (Li^+ ions from $LiClO_4$ as explained in Chapter 6) have been used extensively, but for a new gel it is important to eliminate either water or low boiling point solvent based systems. Gels made from ionic liquids can be a very important progress in this field. Some groups have shown this recently,[1] but the ionic liquid is not carefully chosen and that results in shuttling of large ions in and out of the film. A new design for this IL-based system can definitely help in overcoming some of the weakness in the EC system in terms of lifecycles and switching-speed.

This thesis presented work on several new electrochromic materials, but the search for new electrochromic materials should continue. More collaboration between synthetic chemists and device fabrication teams is required to use these materials for the EC displays. Other than PEDOT and PANI, a few other conducting polymers that show promise are PRODOT, polypyrrole and their derivatives. If the displays need to be based on Red, Blue, Green (RGB) colors then it is necessary to look for a material that can switch fast between red and green colors along with keeping high contrast. Work started by Sonmez et al. was in that direction,[2 3] but the synthesis of the polymers is very cumbersome and there should be an easier way to synthesize these new materials.

Taking these EC fast-switching EC devices towards fabrication of displays ultimately is also necessary. Here, careful steps should be taken to choose whether the approach needs to be passive-matrix (generally uses one transistor for each row and one for each column) or active-matrix (there is a separate circuit for each pixel and thin film transistor (TFT)) technology should be used. Both approaches have their own advantages and disadvantages, but active-matrix has high contrast along with being difficult to fabricate.

Work on fabricating thin porous CNCs for elecromechanical actuators by LbL is just in the initial phases, and there is much that needs to be done to understand its effect on the fundamental properties of the IPMC. Much more detailed study of the effect of the number of bilayers on the actuation speed and strain is required. Till now in this study, we have only used Au NPs, but a detailed study of different kinds of metal NPs like Pt, Cu, Zn, Ag etc should be done in detail along with their effect on strain values and actuation speed. Choice and replacement of EMI-Tf ionic liquid should also be kept in mind for larger size difference between the cation and anions of the ionic liquid. The large size difference creates higher strain because of larger volume differential at the electrodes of the IPMC. A size variation study of similar kind of NPs should be done along with checking the morphological properties of the LbL films deposited by them. A porous surface at the ionic membrane is highly desirable and the LbL technique provides the flexibility of depositing larger NPs close to the membrane surface while keeping the smaller NPs more towards the metal electrode section of the IPMC. New materials like water-dispersed single-walled nanotubes (SWNTs) and conducting polymers should be deposited on their own along with combinations of other materials to achieve the optimum thickness, material, and actuation speed for IPMCs.

References

[1] S. Ahmad, M. Deepa, *Electrochem. Comm*. **2007**, 9, 1635.

[2] G. Sonmez, C.K.F. Shen, F. Wudl, *Adv. Mater*. **2004**, 16, 1905.

[3] G. Sonmez, C.K.F. Shen, Y. Rubin F. Wudl, *Angew. Chemie. Int. Ed*. **2004**, 43, 1498.